Mineralogy and geochemistry of the lower and middle magbesian limestone of county Durham

Jones, K.

MINERALOGY AND GEOCHEMISTRY OF THE LOWER AND MIDDLE MAGNESIAN LIMESTONE OF COUNTY DURHAM.

By

K. Jones, B.Sc. (Dunelm)

A thesis submitted for the degree of Doctor of Philosophy in the University of Durham.

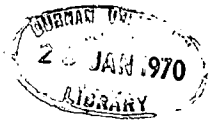

Grey College

December, 1969.

ABSTRACT.

The Magnesian Limestone is of Permian age. In Durham, shelf and basin facies can be recognized within the Lower division while lagoon, reef and basin facies occur within the Middle division. Calcite, dolomite, gypsum and anhydrite form the main mineralogical components, although minor amounts of limonite, quartz, pyrite and an illitic clay mineral are common. Gypsum and anhydrite are characteristic of the two basin facies but are also associated with the shelf and lagoon facies in South-East Durham. In North-East Durham, the three shallow-water facies are predominantly dolomitic; calcite occurs most commonly as void filling, but also replaces dolomite and occurs in a "felted" texture which is believed to have been formed by replacement of a sulphate mineral. Extremes of carbonate composition are found within the two basin facies. Sulphates only occur in abundance where dolomite is the predominant carbonate. Calcite is believed to have formed at depth by the reaction of dolomite with locally derived, sulphate-rich solutions. The process might still be occurring. Differences in pore-size distribution make the shallow-water

facies more porous and permeable than the basin facies. The relationship between porosity and permeability is discussed. Strontium occurs as a solid-solution impurity in dolomite and calcite and, to a much greater extent in gypsum and anhydrite. Dolomite also contains considerable manganese. During dedolomitization by the "sulphate-agent" mechanism, strontium is incorporated into, and manganese largely excluded from, the lattice of the replacement calcite. Rubidium and at least some barium, lead, boron and nickel are considered to occur as detrital constituents within the illitic clay material. Copper, in part at least, is associated with organic carbon. Zinc, lead and barium are enriched in rocks of the three shallow-water facies. The elements are considered to have been introduced into porous and permeable rocks by metal-bearing solutions. The mode of occurrence of these elements and the source of the "mineralizing" solutions is discussed.

ACKNOWLEDGEMENTS.

I wish to thank Professor G. M. Brown, Head of Department, for granting the use of research facilities and technical assistance and Professor K. C. Dunham, now Director of the Institute of Geological Sciences, for originally suggesting the project.

I am especially grateful to Dr. D. M. Hirst for supervision throughout the course of study and for critically reading the manuscript, and to Mr. D. B. Smith of the Institute of Geological Sciences for help in obtaining sample material and for many hours of useful discussion on Permian stratigraphy. Thanks are also due to Dr. J. G. Holland, Mr. R. Phillips and Mr. R. K. Taylor for advice on various aspects of the project.

I should like to thank the following persons for helpful discussion and for granting access to sample material and confidential information:-

Mr. L. S. Phillips and Dr. H. G. Davies (formerly) of Imperial Chemical Industries Limited,

Dr. D. Magraw of the National Coal Board,

Mr. U. T. Burston and Dr. T. Cairney of the Northumbrian River Authority,

Mr. J. Clough of the Hartlepools Water Company,

Mr. G. M. Thompson of The Tees Valley and Cleveland Water Board and

Mr. R. A. Pepper of the Sunderland and South Shields Water Company.

My thanks are also due to Mrs. P. B. Leggett for typing the thesis and to my wife for constant help and encouragement.

The award of a N.E.R.C. Research Studentship is gratefully acknowledged.

CONTENTS.

Page.

Page.

LIST OF FIGURES.

LIST OF TABLES.

LIST OF PLATES.

CHAPTER 1.

INTRODUCTION.

General Geology and Physiography.

The Permian of Eastern England forms a comparatively narrow outcrop stretching southwards for about 150 miles from South Shields in Durham, through Central Yorkshire and Eastern Derbyshire, to Nottingham.

In Durham, the Permian outcrop occupies the eastern part of the county (Figure 1-1). It is terminated in the east by the Durham coastline which trends approximately north-north-west. The western edge of the outcrop runs in a very approximate north-north-east direction from Piercebridge to South Shields. The Permian outcrop in Durham therefore has the shape of a steep-sided triangle, the apex of which lies at South Shields. However, very small outliers do occur farther north at Tynemouth and Cullercoats in Northumberland.

In Durham, the Permian rests unconformably on the Carboniferous. The rocks immediately beneath the surface of the unconformity range from high in the Barren Coal Measures at Sunderland to the lower part of the Millstone Grit Series at Piercebridge. In the south-east of the county, the Permian rocks pass gradually

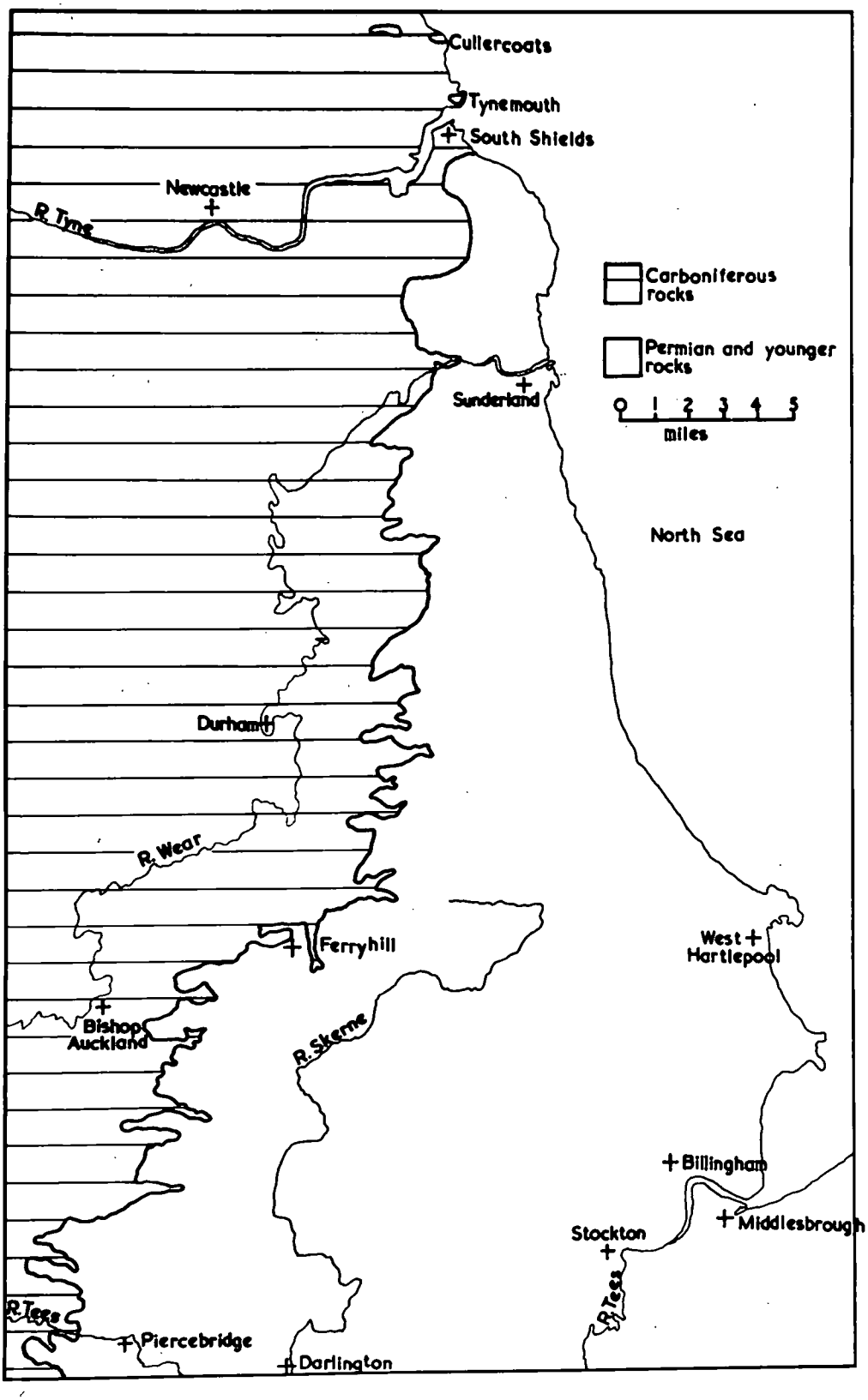

FIGURE 1-1. SIMPLIFIED GEOLOGICAL MAP OF NORTH-EAST ENGLAND.

upwards into Triassic Bunter Sandstone, the base of which is almost certainly diachronous in this area.

Over much of the Durham outcrop and particularly in the south, the Permian is obscured by superficial deposits, especially drift. North of an east-west line from Ferryhill to Hartlepool, drift is thin or absent along the western edge of the outcrop but it is often more than 60 ft thick nearer the coast and can locally become much thicker (up to 300 ft) along buried valleys (Smith and Francis, 1967). In this northern area, most exposures are in narrow belts along the western edge of the outcrop, along the coast and in narrow ravines in the eastern part of the area.

South of the Ferryhill to Hartlepool line, most of the area is overlain by thick drift, and buried valleys belonging to the River Tees system occur. Exposures are confined to narrow belts lying immediately south of this line and along the western edge of the outcrop but for the most part, information is derived from boreholes drilled during water, brine and anhydrite exploration and from the underground workings of the Imperial Chemical Industries' anhydrite mine at Billingham.

North of the River Wear at Sunderland and south of the River Tyne, the outcrop forms part of the physiographical area known as

the Wear-Tyne Lowlands and gives rise to a featureless land surface, for the most part less than 200 ft O.D., where drainage is somewhat indefinite.

From Sunderland south to the east-west line running from Ferryhill to Hartlepool, the outcrop underlies the East Durham Plateau, the western edge of which is a prominent, indented escarpment reaching a height of 400 - 600 ft O.D. Two major gaps, believed to be glacial overflow channels, breach the escarpment; one at Ferryhill which carries the Edinburgh - London railway and one at Sunderland through which flows the lower course of the River Wear. From the scarp edge, the land slopes gently to the east and gives rise to a fairly continuous 100 ft cliff-line along the coast. The Plateau is cut by several deep and narrow, wooded valleys or "denes" - Hawthorn Dene, Castle Eden Dene and Hesleden Dene - in which small streams drain eastwards to the North Sea. The "denes" locally cut down through the drift into the underlying Permian rocks.

The area from Piercebridge to the mouth of the River Tees forms the northern part of the Tees Basin. The area consists of undulating lowland 200 - 300 ft O.D. but in the east includes some reclaimed tidal flats. To the north, the area grades gently upwards into the East Durham Plateau while it merges with the foothills of the North Pennines to the west. The area is drained to the south

by the River Skerne - a tributary of the River Tees - and to the east by the River Tees and streams flowing into its estuary.

History of Research into the Permian of Durham.

The Permian rocks of Durham have attracted attention from as early as 1817 (Winch) and general accounts of Permian geology have since been given by Sedgwick (1835), Wilson (1881), Woolacott (1912, 1919B), Trechmann (1913, 1925, 1931) and more recently by Smith (in Magraw et al., 1963) and Smith and Francis (1967). More specific contributions to the geology of the Permian in parts of Durham have been given by Woolacott (1919A) and Trechmann (1932, 1942).

Classification of the Permian rocks was first attempted by Sedgwick (1835) and has since been successively refined by Howse (1848, 1857), King (1850), Kirkby (1860), Woolacott (1912) and Smith (in Magraw et al., 1963; in press). The nature of the Permian-Triassic boundary has been discussed by Sherlock (1926, 1948), Trechmann (1930), Hollingworth (1942) and Smith and Francis (1967).

Separate accounts of the Yellow Sands have been given by Hodge (1932) and Davies and Rees (1944) while Lebour (1905) and Burton (1911) paid special attention to both the Yellow Sands and Marl Slate.

Woolacott (1912) gave details of published contributions to the palaeontology of the Magnesian Limestone up to that time while Trechmann, in almost all of his papers, supplied further palaeontological information and in 1925 gave a faunal list which represented the results of 20 years collecting. Logan (1962) revised the palaeontology of the Magnesian Limestone and Smith and Francis (1967) have produced the most recent faunal list. Westoll (1941) has described fish from the Marl Slate while Stoneley (1958) has given an account of the plant remains from the Marl Slate and overlying beds. Algal structures from the Middle Magnesian Limestone reef have received special attention from Smith (1958) and Smith and Francis (1967).

The origin of the brecciated strata within the Magnesian Limestone has been discussed in detail by Lebour (1884), Abbot (1903), Woolacott (1909), Trechmann (1913), Hickling and Holmes (1931) and Smith (in press). Woolacott (1909) and Trechmann (1954) have paid special attention to the "thrusting" features observed in the Magnesian Limestone. The concretionary structures developed in the Upper Magnesian Limestone have been discussed by Garwood (1891), Holtedahl (1921) and Holmes (1931).

Much relevant information on Permo-Triassic stratigraphy in South Durham has come from Lebour (1887), Wilson (1888), Bird (1888), Howse (1890), Marley (1892), Sherlock (1921), Sherlock and Holling-

worth (1938), Hollingworth (1942), Robertson (1948), Napier (1948), Wood (1950), Raymond (1960) and an Internal Report of the Northumbrian River Authority.

Tentative correlation between the Permian successions north and south of the West Hartlepool Fault has been offered by Dunham (1960, plate 6), Smith and Francis (1967) and Smith (1968; in press). Smith and Francis (1967, p. 95) have suggested a correlation between the Permian deposits of Durham and Central Yorkshire which has been further supported by the evidence of Smith (1968) and extended to East Yorkshire and Germany by Smith (in press).

Correlation between the Permo-Trias of South Durham and other parts of the country has received much attention. Thus Sherlock (1926, 1948), Fowler (1944), Raymond (1953), Stewart (1954) and Dunham (1960) have supplied information which has facilitated correlation between the Permian of South-East Durham, Yorkshire and Nottinghamshire. Information on correlation between North-East England and North-West England has been given by Sherlock (1926, 1948), Hollingworth (1942), Stewart (1954) and Meyer (1965).

Accounts of the epigenetic minerals found in the Permian have been given by Fowler (1943, 1957), Westoll (1943) and Dunham *et al.* (1948).

Statement of Problem.

Although the mineralogy and geochemistry of the Marl Slate have received considerable attention (Deans, 1950; Love, 1962; Hirst and Dunham, 1963), no detailed mineralogical and geochemical investigation of any part of the overlying Magnesian Limestone in Durham has yet been attempted. Extensive analyses of various beds of Durham Magnesian Limestone have been provided by Browell and Kirkby (1866), Trechmann (1914) and Thomas et al. (1920, pp. 79 - 91) but these workers have been concerned principally with the relative proportions of calcite and dolomite and with the amount of insoluble residue. More recently, White (1966) has investigated the distribution of strontium in carbonates and sulphates from the Durham Magnesian Limestone.

Ideally, the mineralogical and geochemical characteristics of the three lithological divisions of the Durham Magnesian Limestone would be of great interest, particularly in view of the environmental model recently proposed by Smith and Francis (1967). Unfortunately, the Upper Magnesian Limestone is confined to a narrow coastal belt to the north of the West Hartlepool Fault and is known only from boreholes farther south. Much of this division is also either collapse-brecciated and foundered, or shows the development of concretionary structures, the origin of which is still largely enigmatic, and has obviously undergone severe chemical

alteration. On the other hand, as beds of the Middle and Lower Magnesian Limestone form the greater part of the Durham outcrop, these divisions are reasonably well exposed and have been intersected in numerous shafts and boreholes sunk in Durham and the adjacent offshore area. The stratigraphy of these two divisions is reasonably well understood and the Middle Magnesian Limestone is known to contain a reef complex and associated lagoon and basin facies while in the Lower Magnesian Limestone, shelf and basin facies can be recognized although no reef is developed on the basin rim.

In view of the foregoing, the mineralogical and geochemical investigation has been confined to the various facies of the Lower and Middle Magnesian Limestone of Durham. However, it must be emphasized that this investigation is in the nature of a reconnaissance study, the results of which might form the basis for more selective and detailed examination in the future.

CHAPTER 2.

STRUCTURE AND STRATIGRAPHY.

Within the Concealed Coalfield, the Butterknowle Fault forms a major structural feature (see Figure 2-1). This fault also displaces the overlying Permian and conveniently separates two areas of contrasted structural type. The area to the north of the fault has a comparatively simple structure while the area to the south has a more complex structure which is largely hidden beneath thick drift.

Structure North of the Butterknowle Fault.

The strike throughout most of this area is north and the beds dip to the east at an average rate of 110 - 150 ft per mile although, as the Permian rocks thicken downdip towards the coast, the dip of the higher beds is slightly less than those below. Most exposures of Permian beds contain low-amplitude rolls which frequently appear to have been caused by local variations in sedimentation rather than by tectonics. Similar structures are common to the east of the Middle Magnesian Limestone reef where they appear to be related to differential compaction and subsidence over strata which have suffered collapse-brecciation.

Three main trends of faulting are recognizable: easterly, north-easterly and north-north-westerly. The easterly trending faults include many minor fractures and some larger structures, while the north-easterly trending faults are small and straight. The north-north-westerly trending faults are generally short but occasionally faults of greater magnitude occur; pairs of these larger faults sometimes form troughs. The faults in this area are normal, appearing either as clean, simple fractures with a hade of about 20^{o} or as near-vertical shatter belts 20 - 30 ft wide.

The Permian in this northern area appears to have joints which are approximately parallel to the north-easterly and north-north-westerly fault trends (Dunham, in Spears, 1961). These joint trends are similar to those in the Permian near Mansfield where the same parallelism between fault and joint trends has been reported (Moseley and Ahmed, 1967).

Structure South of the Butterknowle Fault.

In the west near Ferryhill, the Butterknowle Fault downthrows the Permian 350 ft to the south whereas in the east, towards the coast, the throw is inferred to be only 100 ft (Smith and Francis, 1967, p. 196 and plate XV). At Ferryhill, the Permian strata to the south of the Butterknowle Fault form an anticline and complementary

syncline. To the east, these folds become less well-defined until south of the Fault in the Hartlepool area, the dip of the beds is to the east at a low angle, very similar to that farther north. The folds are weak manifestations of similar, but better developed, structures in the underlying Coal Measures and, like these, appear to be related to movement along the Butterknowle Fault.

Although information is limited, south of West Hartlepool the Permian appears to dip in a south-easterly direction at a greater angle than that observed north of the Butterknowle Fault. In the Billingham area, the base of the Permian dips to the south-east at 300 ft per mile while higher Permian strata, such as the Main Anhydrite (q.v.), dip at about 250 ft per mile (Raymond, 1960, p. 299, fig. 2). To the east of Billingham, the regional dip appears to increase (Sherlock, 1921, plate 2, section 2; Napier, 1948) while to the west, a rise in the Carboniferous floor produces a high local dip in the Permian (Wood, 1950; Raymond, 1960). At the western edge of the outcrop, the average dip appears to be about 300 ft per mile in a south-easterly direction (Anderson and Dunham, 1953, p. 25) although faulting, "cambering" and irregularities in the Carboniferous floor produce local variations in both amount and direction.

Downfaulting of the Permian to the south in the region of West Hartlepool has been long established. Trechmann (1913) estimated a

throw of 700 ft but because the fault is hidden by drift, its trend and nature have been largely conjectural. The fault was represented on early maps as a straight line extending from West Hartlepool to Darlington (Trechmann, 1925) and later (Fowler, 1945) as an arcuate fracture extending from West Hartlepool to Catterick. Robertson (1948) and Stewart (1954, p. 210) have suggested that the fault might be transcurrent. Recent information from Smith and Francis (1967) and the Internal Report of the Northumbrian River Authority reveals that this Hartlepool-Darlington fault is in fact a series of normal, southward throwing east-west faults arranged en échelon, approximately along the old line of the conjectural fault (Figure 2-1). In the Hartlepool region, two members of this fault system have been identified as the West Hartlepool Fault and the Seaton Carew Fault. The former has a downthrow of 300 ft in the Permian at its western end and 600 ft at its eastern extremity, and the latter a throw of around 600 ft. To the south-west, two other members of this system have been identified but the throw across each of these appears to be small.

The most numerous faults in the Permian of this area south of the Butterknowle Fault are those which have a general north-westerly trend. The faults of this group range in trend from north-north-westerly to west-north-westerly and in fact have a radial, fan-like arrangement. They are generally of short, linear extent and some-

times have fairly large displacements. There appear to be only a few north-easterly faults and these are short in length and small in throw.

The main trends in faulting in South Durham correspond with those observed to the north of the Butterknowle Fault. The large faults include the Butterknowle, West Hartlepool and Seaton Carew Faults and belong to the group with an easterly trend.

The Permian fracture trends observed throughout Durham are identical to those observed in the Carboniferous rocks of the exposed and concealed parts of the Durham Coalfield. This parallelism between fracture trends in the Permian and underlying Carboniferous has also been reported from Nottinghamshire by Moseley and Ahmed (1967). Where information is available, the faults can be seen to throw considerably less in the Permian than in the Carboniferous, although at least one fault in the Ferryhill area (Smith and Francis, 1967, p. 197) shows an equal amount of displacement in the rocks of both Systems.

The Permian fractures, as elsewhere in Eastern England, appear to have been inherited from the underlying Variscan features in the Carboniferous during the Alpine (Tertiary) earth movements (Moseley and Ahmed, 1967).

Stratigraphic Classification.

The classification of the Permian used here (Table 2-1) follows that adopted by Smith (in Magraw et al., 1963) and Smith and Francis (1967) and is based on the scheme proposed by Woolacott (1912). It also includes the amendments to the position of the collapse-brecciated strata lying to the east of the Middle Magnesian Limestone reef made by Smith (in press).

Table 2-1.

Classification of the Permian in Durham.

Upper Permian Marls and associated evaporites.	Upper Anhydrite
	Rotten Marl
	Billingham Main Anhydrite
Upper Magnesian Limestone.	Hartlepool and Roker Dolomites.
	Concretionary Limestone (including the Flexible Limestone)
Middle Magnesian Limestone.	Post-reef dolomites and Hartlepool Anhydrite
	Reef dolomite and lagoonal and off-reef equivalents
	Transitional beds
Lower Magnesian Limestone.	
Marl Slate.	
Basal Permian Sands and Breccias.	

Woolacott (op. cit.) defined the base of the Middle Magnesian Limestone as being coincident with the base of the reef which occurs within that division. This meant that the base of the Middle Magnesian Limestone could not be identified directly where the reef is absent. Also, the base of the reef is a variable horizon. To overcome these difficulties, Smith (in Magraw et al., 1963) has taken the base of the Middle division at a slightly lower, more consistent horizon - at the base of a loosely defined group of transitional beds which underlie the reef and which can also be recognized in non-reef areas. The boundaries between the other subdivisions are fairly clear-cut.

The lateral equivalence of the Marl Slate and the Upper Permian Kupferschiefer of Germany has long been recognized. However, opinion on the age of the underlying basal deposits appears to be divided. Authorities on the Zechstein of North-West Europe favour an Upper Permian age for the basal sands and breccias but Smith and Francis (1967, p. 92) suggest that both the Continental deposits and their Durham equivalents are more likely to be of Lower Permian age by comparison with the type area of Russia. By this reasoning, the base of the Marl Slate therefore represents the base of the Upper Permian (Thuringian).

A simplified differentiation of the Permian outcrop in Durham is shown in Figure 2-1.

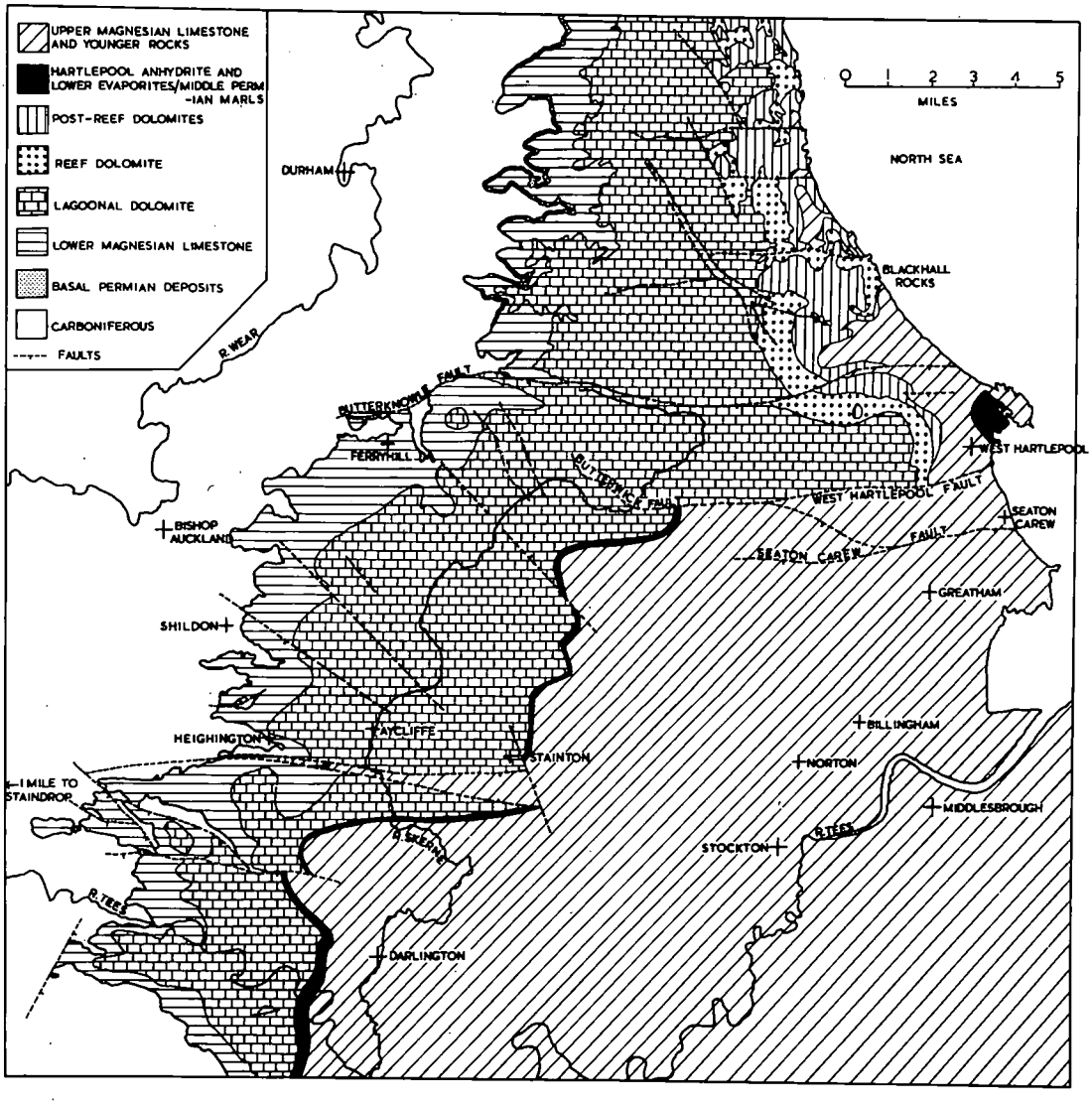

FIGURE 2-1. SIMPLIFIED DIFFERENTIATION OF THE PERMIAN OUTCROP IN DURHAM.

The Pre-Permian Surface.

Prior to the deposition of Permian sediments in Durham, the gently folded Carboniferous rocks in the area lying to the north of the West Hartlepool Fault appear to have been eroded to a low-lying plain. The evidence suggests that the plain had a gentle slope to the east and was broken only by a few areas of slightly higher ground. The inclination of the plane of the Carboniferous-Permian unconformity in borings and in surface exposures in this area suggests that the small-scale relief of the plain was also low (Smith and Francis, 1967).

To the south, the Carboniferous rocks were more strongly folded and the erosional remnants of the fold structures appear to have given rise to a series of east-west trending ridges. One large ridge lay just to the south of Durham at Middleton Tyas (Fowler, 1944, 1945) where it had been formed from the broad Howgill-Middleton Tyas anticline. A second, apparently smaller ridge lay near Billingham Village (Napier, 1948; Wood, 1950) from where it appears to have extended westwards through Stainton (Raymond, 1960) to Heighington (Internal Report of the Northumbrian River Authority). This ridge was probably formed from a structure which is manifested in the Carboniferous near Staindrop.

At the beginning of the Zechstein transgression, the ridges gave rise to an Atlantic-type coastline and appear to have remained above sea level (although in subdued form) until early Upper Magnesian Limestone times (Fowler, 1945; Raymond, 1960). As a consequence, the lower strata of the Permian show signs of overlap as the ridges are approached. Over the ridges, only the higher strata are present and the Permian is greatly reduced in thickness.

Pre-Permian weathering of the Carboniferous surface in Durham produced reddening at and below the surface by oxidation of pyrite and siderite *in situ* and by the introduction of red iron oxide into pore-space and joints (Anderson and Dunham, 1953). In the Concealed Coalfield, the reddening reaches a maximum recorded depth of 292 ft below the Carboniferous-Permian unconformity (Smith and Francis, 1967, p. 19). The phenomenon has also been recorded from South Durham and the Cleveland Hills (Fowler, 1944).

Lower Permian.

A sinuous east-north-east line extending from Shildon to Blackhall Colliery (see Figure 2-1) divides the basal Permian deposits into two distinct types. To the north and west of this line, the typical deposits are coarse, incoherent sands, traditionally known as the "Yellow Sands" although Smith (in Magraw *et al.*, 1963) and Smith and Francis (1967) have used and promoted the term

Basal Sands for these deposits. To the south and east of the line, breccias and sandstones predominate.

Basal Sands.

These deposits vary very rapidly in thickness and Smith and Francis (1967) report a range of 0 - 134 ft 6 in. The deposits have been shown to consist mainly of silica with small amounts of felspar and the suite of heavy minerals has led Hodge (1932) to suggest that the sands were derived from rocks in the immediate vicinity and partly from rocks exposed to the north.

The sands are generally yellow at outcrop although patches of white or light-grey sand can sometimes be seen. The yellow colour is due to an irregular coating of limonite on the quartz grains. At depth, the sands are grey and contain abundant pyrite while limonite is virtually absent. The oxidation of pyrite appears to have furnished the limonite (Anderson and Dunham, 1953) and the pyrite appears to have formed diagenetically, probably during deposition of the overlying Marl Slate.

Size analyses and the presence of frosted, well-rounded, "millet-seed" grains show the sands to have an aeolian origin. It was formerly thought that the sands accumulated in hollows on the eroded Carboniferous floor (Woolacott, 1912) but there is strong evidence to suggest that they formed positive features resting on the Carboniferous surface. Smith and Francis (1967, pp. 97 - 98) consider them to have

originally been elongate seif dunes formed by constant east-north-east winds, although they realize that partial sub-aqueous redistribution is likely to have taken place subsequently.

Basal Breccias and Sandstones.

These deposits do not outcrop in Durham and are known only from boreholes and shafts where the maximum recorded thickness appears to be 44 ft 6 in (Magraw et al., 1963, p. 197). The usual range in South Durham is 0 - 20 ft (Raymond, 1962; Smith and Francis, 1967), although unfortunately there is insufficient data to deduce the detailed distribution of the beds.

The breccias contain fragments of Coal Measure mudstones and sandstones and of Carboniferous Limestone. The fragments are embedded in a matrix consisting mainly of angular sand grains, together with some aeolian grains and small rock fragments. Sometimes breccia fragments are absent and the beds consist almost entirely of sandstone, which is often micaceous.

The presence of "dreikanter" pebbles with "desert varnish" suggests that the breccias might have formed part of a stony desert pavement (Smith and Francis, 1967, p. 92).

Upper Permian.

The continental phase, represented by the Lower Permian basal sands, breccias and sandstones, was brought to a close by the transgression of the Zechstein Sea. This sea covered much of North-West Europe, including North-East England, for the duration of Upper Permian times (see Lees and Taitt, 1946, fig. 7).

In Durham, the Zechstein deposits comprise the Marl Slate and overlying Magnesian Limestone. At outcrop, the Magnesian Limestone falls naturally into three lithological divisions which have formed the basis of classification. The upwards impoverishment in shelly macrofauna within each of these divisions has recently led Smith and Francis (1967, p. 92) to suggest that each lithological division represents the carbonate unit of a complete evaporite cycle. Thus, the Magnesian Limestone sequence at outcrop in Durham consists of the superimposed carbonate phases of three main evaporite cycles (see Table 2-2). To the south, beneath Tees-side, a possible fourth evaporite cycle is represented by the Upper Anhydrite.

Table 2-2.

Classification of the Permian in terms of Evaporite Cycles.

		Upper Permian Marls
4th Evaporite Cycle ?		Upper Anhydrite
		Upper Permian Marls (Rotten Marl)
3rd Evaporite Cycle	{	Billingham Main Anhydrite
	{	Upper Magnesian Limestone
2nd Evaporite Cycle		Middle Magnesian Limestone
1st Evaporite Cycle	{	Lower Magnesian Limestone
	{	Marl Slate

It is thought that the full cycle of carbonate, followed in lateral and vertical succession by sulphate, halite and eventually the highly soluble potassium and magnesium salts, was nowhere developed in Durham because most of this area lay in the shelf zone of the Zechstein Sea.

In North-East Durham, the margin between shelf and basin in the lowest cycle appears to have lain at about the longitude of West Hartlepool, but in subsequent cycles it followed the outer slope of the Middle Magnesian Limestone reef. In South-East Durham,

the margin appears to have lain at about the longitude of Billingham for all three main cycles. To the east of Billingham and also in the offshore area adjacent to the Durham coastline, the evaporite cycles show the development of more saline deposits as the main basin of deposition is approached.

Marl Slate.

The Marl Slate, together with the overlying Lower Magnesian Limestone, is considered to represent the first evaporite cycle in Durham.

In the central part of the Permian outcrop, the Marl Slate is thickest at the western edge where it reaches a maximum proved thickness of 18 ft. However, its thickness is generally of the order of 2 ft or less and at the coast and in the offshore area, it appears to be absent (Smith and Francis, 1967, p. 102 and fig. 19).

The Marl Slate is also known to occur in South Durham (Robertson, 1948) where it is best developed and thickest in the west. However, there has been a suggestion (Robertson, op. cit.) that in this area it may represent a facies feature.

In lithology, the Marl Slate is typically a finely laminated, bituminous, argillaceous dolomite which is yellow-brown in colour at outcrop and alternately black and grey at depth. The deposit

has an uneven base and locally penetrates the underlying breccia. It is usually overlain sharply by the Lower Magnesian Limestone, although in the south, it commonly passes upwards by alternation into that division. Near the base, aeolian sand grains are common and penecontemporaneous slump structures have also been reported. Pyrite, galena and sphalerite frequently coat bedding-planes and joints. The Marl Slate is well known for its fauna of fossil fish (Westoll, 1941) and for its unusual geochemistry (Deans, 1950; Hirst and Dunham, 1963). Plant remains occur throughout.

Deposition of the Marl Slate is thought to have taken place in euxinic conditions free from bottom scavengers, in water estimated by Love (1962) to be 300 - 600 ft deep. The time for deposition is thought to have been about 17,000 years (Oelsner, 1959).

Lower Magnesian Limestone.

Exposures of Lower Magnesian Limestone are restricted to a relatively narrow belt along the western edge of the Permian outcrop from the River Tyne to the River Tees. From Sunderland to Ferryhill, the Lower Magnesian Limestone is exposed along a prominent escarpment while to the north of Sunderland, beds of

the division are commonly exposed at the coast. However, over most of Durham, and particularly in the south, rocks of the division are known only from shafts and boreholes.

The division is thickest in the central part of the area where it reaches 245 ft near Easington (Smith and Francis, 1967, fig. 19). North and south of Sunderland, the thickness originally appears to have been about 80 - 90 ft (personal communication, D. B. Smith) but over much of this area, the thickness is greatly reduced owing to the action of submarine slides at the end of Lower Magnesian Limestone times. In the offshore area, most records show the division to be about 70 ft thick, but in the National Coal Board Offshore Borehole No. 1, it appears to be only about 40 ft (Smith and Francis, 1967).

In South Durham, the situation is complicated by the fact that until the recognition of the transitional beds, the carbonate sequence lying beneath the Lower Evaporite Bed (q.v.) was termed the "Lower Magnesian Limestone" (e.g. Robertson, 1948; Raymond, 1962). Although information is limited, it seems likely that the thickness of Lower Magnesian Limestone (sensu stricto) is very variable over much of South Durham owing to the presence of Carboniferous ridges in this area. Locally, as near Billingham (Raymond, 1960, fig. 2), the division is absent together with higher strata. In the Aycliffe - Darlington area, the Lower

Magnesian Limestone usually varies from 40 - 70 ft in thickness (Internal Report of the Northumbrian River Authority).

At outcrop in the central part of the area, the Lower Magnesian Limestone is divisible into three lithological units distinguished by colour, texture and bedding characteristics (Smith and Francis, 1967, p. 106).

The lowest unit reaches up to 12 ft in thickness and comprises medium-bedded, granular or finely crystalline dolomites and limestones. At some localities, laminated argillaceous layers are widespread in the lower part of the unit, and immediately above the Marl Slate the beds contain small amounts of pyrite, galena and sphalerite.

The middle unit consists of up to 120 ft of very thinly bedded, grey to buff, finely crystalline dolomitic limestone. However, at some localities (e.g. Raisby Hill and beneath Sheraton - Smith and Francis, 1967, p. 107), beds of this unit become more calcitic. Many bedding-planes are argillaceous and/or carbonaceous and when seen in the unweathered state, show development of sub-parallel stylolites and a fine nodular structure. These features are believed to be due to pressure-solution as are the steeply inclined stylolites which sometimes occur. However, there does not appear to be any general relationship between stylolite frequency and thickness of the unit. Brown, leathery, often bituminous clay

films are found in the lower beds of the group, while at higher levels, widespread autobrecciation showing different stages of development occurs. Collapse-brecciated horizons due to the removal of interbedded sulphates have also been reported from near the top of the unit, particularly in the area to the south of the Butterknowle Fault. In some places, especially at Raisby Hill and Thickley (Smith and Francis, 1967, p. 107), the beds of this middle unit pass laterally into lenticular masses of shelly limestone which are believed to have escaped dolomitization.

The upper unit varies in thickness from 40 - 100 ft and consists of thick, uneven or lenticular beds of buff-brown, granular calcitic dolomite. The bedding-planes are more regular, while stylolites and autobrecciation are less common than in the middle unit. Veins and cavities containing barite and fluorite are widespread in the topmost beds of the unit.

Smith and Francis (1967) state that the three-fold subdivision of the Lower Magnesian Limestone can be traced eastwards for up to 6 miles from the scarp edge. Farther east, it is not recognizable and in the offshore area, the Lower Magnesian Limestone is represented by fairly uniform, grey and brown, fine-grained dolomitic limestone. The limited evidence available suggests that it is also not possible to recognize the units in the Lower Magnesian Limestone of South Durham. In the Aycliffe-

Darlington area, the division consists of thickly bedded, buff to grey, fine-grained, saccharoidal dolomite containing thin, slightly stylolitic, black, clayey laminae. To the north-east of Billingham, the division is much reduced in thickness and is comprised of fine-grained, buff dolomite containing black, micaceous, shaley partings.

In parts of South Durham, especially near Billingham, and in the offshore area, gypsum and/or anhydrite occur in the Lower Magnesian Limestone as disseminated porphyroblastic blebs, acicular crystals and thin veins.

The fauna of the Lower Magnesian Limestone is very limited and in places beds of the division are almost entirely barren. Less than 40 invertebrate species have been reported from the whole of Durham, with brachiopods, polyzoa and lamellibranchs being most common. In the central part of the area, shelly fossils are in general concentrated in the lowest 20 - 30 ft of the division, although they do occur up to 100 ft above the base. Amphibia and fish have been reported from some areas in Durham while plant remains are common, particularly in the lower beds of the division.

Middle Magnesian Limestone.

Smith and Francis (1967) consider the beds of this division to represent the deposits of a single major evaporite cycle, although they realize that chemical precipitation probably began in Durham only at a fairly late stage.

Beds of the division occupy most of the Permian outcrop north of the West Hartlepool Fault, a circumstance arising mainly from a combination of low easterly dip and the gradual easterly fall of the land surface.

The earliest deposits of the Middle Magnesian Limestone are the transitional beds. They are a relatively thin group of beds present over almost the whole of the area and form the base of the division. After the deposition of the transitional beds, an elongate shell-bank appears to have formed in the east of the area and this became the locus of formation of a barrier reef which can be traced for 20 miles from West Boldon (near Sunderland) to West Hartlepool. The development of the barrier reef defined the margin between shelf and basin more clearly than in Lower Magnesian Limestone times and brought about a fundamental change in depositional environments on its eastern and western sides. Consequently, north of the West Hartlepool Fault, three distinct and contrasting facies can be recognized above the transitional beds, a lagoonal facies in the west separated by the reef from a basin facies in the east.

South of the West Hartlepool Fault, knowledge of the Middle Magnesian Limestone comes mainly from borehole information and is less thorough than farther north. The reef does not appear to extend farther south than Seaton Carew (Trechmann, 1942) and consequently the margin between shelf and basin is more difficult to locate in South Durham. Nevertheless, the evidence at present available suggests that it lay in the vicinity of Billingham.

Transitional Beds:- In the shelf area north of the West Hartlepool Fault, the transitional beds reach a maximum thickness of 40 ft (Smith in Magraw et al., 1963). In South Durham where they have been recognized in most recent boreholes, they are usually less than 10 ft thick (personal communication, D. B. Smith). They are coarse-grained, granular calcitic dolomites, commonly buff or cream in colour and contain a limited shelly fauna characterized by the lamellib-ranch Astartella vallisneriana (King).

As the beds contain comparatively few stylolites and lack the colouring typical of the beds below, the junction between the Lower and Middle divisions in the shelf area is quite sharp. In the basin area however, the junction is usually indistinct as the lithological change is less marked and the boundary is usually placed at the incoming of a shelly fauna above the barren beds

of the underlying Lower Magnesian Limestone. Except where overlain by the reef, the transitional beds grade imperceptibly into the overlying strata.

Lagoonal Facies:- North of the West Hartlepool Fault, the lagoonal facies consists of a series of granular, oolitic and pisolitic dolomites which interdigitate with the uppermost deposits of the reef. The maximum recorded thickness of the lagoonal beds is 300 ft (in a borehole at Dalton Piercy waterworks, near West Hartlepool) but the top of the beds is not seen in this area.

The beds show widespread shallow-water depositional features, especially small-scale, low-angle cross-bedding. Oncolites, compound pisoliths believed to be of algal origin, occur throughout the lagoonal beds but are concentrated mainly in a belt a few hundred yards wide behind the reef. These features have led Smith and Francis (1967, p. 117) to suggest that the lagoon was a protected shallow-water environment in which sedimentation lagged behind the rapid upward growth of the reef.

Euryhaline gastropods and lamellibranchs form the chief fauna of the lagoonal beds although adjacent to the reef, and presumably derived from it, a wider variety of shelly fossils occurs.

Reef Facies:- The lower parts of the reef are composed of massive,

biohermal dolomitic limestones and dolomites, containing a prolific fauna of stenohaline brachiopods, lamellibranchs and polyzoa, together with poorly-preserved, scattered stromatolitic incrustations. The lower part of the reef appears to have been built mainly by cryptostome polyzoa, although marine calcareous algae are also thought to have contributed, while the upper parts are almost wholly of algal origin. Because of this vertical change, it is thought that as the reef was built upwards, the shallow water encouraged more rapid growth of calcareous algae while at the same time, increasing salinity first led to stunting and then to extinction of many of the earlier faunal elements.

The reef is the most fossiliferous part of the Durham Magnesian Limestone, both in terms of variety of species and number of individuals. The distribution of faunal assemblages within the reef appears to be similar to that found in the Capitan Reef of the Guadalupe Mountains (Newell et al., 1953). Smith and Francis (1967) have described the varied growth forms of stromatolites within the reef and have demonstrated how these reflect different reef environments.

During the early stages of reef formation, it appears that growth was predominantly upward , but later the reef grew seaward, presumably in response to the rate of subsidence (Newell et al., op. cit., p. 106).

Throughout the period of reef-growth, quantities of derived bioclastic material accumulated in the lagoonal deposits adjacent to the back-reef and formed a narrow belt of coquinas and calcarenites, while wedge-shaped talus fans accumulated at the base of the fore-reef slope. At times, reef-growth extended both backwards over lagoonal sediments and forwards over reef talus. Interdigitation at the margins of the reef, particularly on the lagoonal side, suggests that reef formation might not have been continuous, and that the reef is, in fact, a composite structure built up of a succession of reefs formed generally at much the same place. At least one debris-filled channel has been recognized and it is not known whether the reef is a continuous mass or whether it is divided wholly or partly by channels of varying depth and width. The course of the reef is typical of many present-day barrier reefs with wide embayments and, in some cases, prominent spurs projecting seawards (Smith, in press).

In the area around and to the north of Sunderland, the reef rests on a much reduced thickness of older Permian deposits. This controversial situation appears to result from submarine sliding occurring late in Middle Magnesian Limestone times and locally removing considerable quantities of sediment (personal communication, (D. B. Smith). Reef formation may have continued longer in the

central and southern parts of the area than in the north. This may have been the result of a gentle southerly tilting of the whole area, bringing about a gradual emergence of the northern parts of the reef, with continuing subsidence of central and southern parts. The extent of the reef southwards from West Hartlepool is uncertain, but it appears that it may continue as far south as Seaton Carew where it has a more subdued relief and where it interdigitates with normal carbonate sediments.

As a result of the different rates of sedimentation behind and in front of the reef, a sharply asymmetrical form was produced with back-reef and lagoonal deposits of low surface-relief being separated from a steeply plunging reef-front by a reef-top platform up to a mile wide. Smith and Francis (1967, p. 122) have inferred that the reef-front was eventually over 200 ft high with a slope between 30° and 85°. It effectively limited subsequent major sediment deposition to the basin area to the east until over 200 ft of sediment had accumulated.

Basin Facies:- Beds of Middle Magnesian Limestone lying east of the reef-front fall into two groups - those that are the same age as the reef, and therefore equivalent to it, and those that are younger.

The basinal equivalents of the reef decrease in thickness and coarseness towards the basin. In a borehole at Hartlepool Lighthouse, immediately east of the reef, these beds are represented by 75 ft of bedded dolomites, buff, brown and grey in colour, containing shells and bioclastic debris. Finely crystalline, mottled stylolitic dolomite is interbedded with breccias containing reef-derived blocks in a matrix of bioclastic debris.

Farther east in the National Coal Board Offshore Borehole No. 1 (3 miles from the reef), the reef equivalents are 37 ft thick and consist of mottled, grey-brown, stylolitic, thinly bedded, fine-grained calcareous dolomite. There is no evidence of derived rock fragments or bioclastic debris and the most common fossils are chonetid brachiopods and foraminifera which are believed to represent the indigenous fauna of the basin.

The fauna in these boreholes indicates an equivalence with the early and middle period of reef-growth, but the basinal bed(s) equivalent to the end of reef-growth cannot be identified owing to the absence of index fossils and "marker" horizons. However, it is possible that the last stages of reef-growth are represented in the basin by chemically precipitated carbonates or even sulphates.

The post-reef beds in the basin area comprise fine-grained, barren dolomites overlain by the Hartlepool Anhydrite. The

Anhydrite outcrops at the surface only at Hartlepool where in boreholes it is over 250 ft thick. It reaches a maximum recorded thickness of 500 ft in the National Coal Board Offshore Borehole No. 2, but in the offshore area north of this locality, the Anhydrite thins until it is absent off Sunderland and South Shields (Smith, in press). It is apparent that in some places (e.g. Hartlepool) the Anhydrite must have been deposited close to the reef-wall and that it thickened rapidly to the east. In other places, a lenticular deposit of oolitic dolomite up to 65 ft in thickness lies between the lower part of the Anhydrite and the reef-wall.

The lithology of the anhydrite varies very little. It is a hard, blue-grey, translucent rock, finely to coarsely crystalline, in which fine-grained, grey or brown dolomite forms an extensive, delicate mesh of stringers which usually form less than 10 per cent. of the volume of the rock. Dolomite also forms beds which reach up to 14 ft in thickness and which are usually spaced at wide intervals, except towards the base of the deposit where they sometimes become very common. At the top and bottom of the Hartlepool Anhydrite, the rock has been hydrated to gypsum, and tabular selenite crystals occur throughout the mass, replacing both dolomite and anhydrite.

While accepting that replacement of dolomite by anhydrite has taken place, Smith and Francis (1967, p. 123) consider this

to be a relatively minor process and regard the Anhydrite as a largely primary deposit. The top of the Hartlepool Anhydrite is defined by the smooth, sharp base of the Upper Magnesian Limestone. The lower surface of the deposit was originally considered to be transgressive (Smith in Magraw et al., 1963) but the presence of a characteristic nodular bed at the base of the Anhydrite at widely scattered points shows that the lower junction is not diachronous (Smith, in press).

The absence of the Anhydrite in coastal sections north of Hartlepool and in the northern part of the offshore area is believed to be secondary and to be due to removal by solution - the horizon of the Anhydrite now being represented by a solution residue (Smith, in press). The thickness and character of the residue vary considerably and reflect the content of dolomite and insoluble material originally present in the anhydrite. Thus, where dolomite beds were rare or absent, the residue is 2 - 4 in thick and consists of a brown-grey, mushy mixture of carbonates and clay minerals. Where dolomite beds were originally more common, the residue is thicker (reaching a maximum of 30 ft) and consists of disarticulated carbonate beds separated by mushy, carbonate/clay material.

The recognition of the solution residue has necessitated the reclassification of the collapse-brecciated strata exposed to the east of the reef as Upper Magnesian Limestone (Smith, in press). Previously, these beds were considered to form part of the Middle Magnesian Limestone and in early classifications had been quoted as a stratigraphic unit of this age (e.g. Woolacott, 1912).

While the Hartlepool Anhydrite was being deposited in the east, granular and oolitic carbonates were accumulating on the submerged reef-platform. These beds are identical with, and therefore indistinguishable from, the highest lagoonal beds west of the reef and because of this it is not possible to recognize the three facies in the highest beds of Middle Magnesian Limestone in Durham north of the West Hartlepool Fault.

Middle Magnesian Limestone in South Durham:- The southerly downthrow of the West Hartlepool Fault, and of other faults in the east-west series to which it belongs, contributes significantly towards the preservation of the whole of the Middle Magnesian Limestone beneath the Upper Magnesian Limestone in South Durham. Over much of this area, the Middle Magnesian Limestone lying above the transitional beds has characteristics very similar to beds of the lagoonal facies which are

exposed farther north and the conditions of deposition are assumed to have been very similar. However, the upper part of the division is very different from the highest lagoonal beds seen to the north.

Smith and Francis (1967, p. 132) report that in a borehole 1½ miles west of Greatham, the upper part of the lagoonal dolomites contains several beds of anhydrite. Farther south, anhydrite becomes increasingly important at this level and forms the bulk of the lagoonal deposits, together with subordinate beds of dolomite and red mudstone, in a borehole at Norton. At Billingham, and farther east at Wilton, about 60 ft of anhydrite occurs at this level and forms part of the Lower Evaporite Bed (e.g. Robertson, 1948; Raymond, 1953).

Hollingworth (1942) has shown that the Lower Evaporites undergo a striking change in character and composition when traced across a line trending north-north-west through Billingham. To the east of this line, the anhydrite is overlain by halite (Hollingworth, 1942, plate 7), while to the west, the sulphate becomes increasingly contaminated with clastic material and as a result is indistinguishable from the Middle Permian Marls of Yorkshire to which it is equivalent (Hollingworth, 1942, p. 144; Smith and Francis, 1967, p. 123; Smith, in press). This evidence, together with the fact that the Permian strata dip at an increased

rate to the east of Billingham (Sherlock, 1921, plate 2, section 2; Raymond, 1960, fig. 2), suggests that in South Durham, the margin between shelf and basin lay farther west than it did immediately north of the West Hartlepool Fault.

In South Durham, the Middle Permian Marls appear to reach about 150 ft in thickness (Hollingworth, 1942, plate 7) and consist of blue-grey gypsum-anhydrite rock which occurs in beds up to 50 ft thick, although generally they are much thinner (Smith, in press). The anhydrite : gypsum ratio increases with depth and the sulphate beds are separated by dull, red and grey silty mudstones ("marls") and thin beds of dolomite. The beds are often contorted owing to the mobility and solution of the sulphate and sometimes show signs of collapse-brecciation. Veins of satin spar are very common.

The top of the Middle Permian Marls/Lower Evaporites is terminated sharply by the Upper Magnesian Limestone, as is the top of the Hartlepool Anhydrite. The upper boundaries of both evaporite bodies would therefore appear to be equivalent. This is to be expected, as the influx of less saline water in which the lowest beds of the Upper Magnesian Limestone are believed to have been deposited, would bring evaporite deposition to an abrupt end. It is not possible to say if the lower boundaries of the two

groups of evaporites are equivalent, although Smith (1968) suggests that the beginning of evaporite deposition in directly connected areas of such close proximity is likely to be broadly synchronous.

Smith and Francis (1967, p. 123) have suggested that the shelf area in South Durham was probably open and that sulphates were deposited in alternation with carbonates. The red clastic deposits of late Middle Magnesian Limestone age represent a nearly complete infilling of this part of the Zechstein Sea so that by the end of this second cycle, the depositional surface was almost flat and emergent. However, it must be said that owing to erosion, the top of the lagoonal Middle Magnesian Limestone is seen nowhere north of the West Hartlepool Fault. It is possible, therefore, that evaporites and red beds were formerly present and that similar conditions prevailed in this area also at the end of Middle Magnesian Limestone times.

Upper Magnesian Limestone.

North of the West Hartlepool Fault, the Upper Magnesian Limestone is preserved only in the eastern part of Durham where the outcrop forms a narrow belt lying between, but in some places on, the Middle Magnesian Limestone reef and the coast. To the

north, the reef and the coast diverge, and between Sunderland and South Shields the outcrop of Upper Magnesian Limestone increases to about 3 miles in width. The preservation of the Upper Magnesian Limestone in this northern area is due almost entirely to a foundering of over 400 ft as a result of the complete solution of the underlying Hartlepool Anhydrite (Smith, in press).

The realization that the foundered and collapse-brecciated strata exposed in East Durham belong to the lower part of the Upper Magnesian Limestone means that the total thickness of Upper Magnesian Limestone at outcrop is likely to exceed the figure of 200 ft given by Smith and Francis (1967, p. 154). As the brecciated beds are not present in the National Coal Board Offshore Borehole No. 2, the thickness of 416 ft recorded there (Smith and Francis, 1967, p. 154) would still appear to represent the maximum proved thickness. The topmost beds of the division are not preserved in Durham north of the West Hartlepool Fault and have not yet been proved in the adjacent offshore area.

South of the Fault, the Upper Magnesian Limestone underlies much of South Durham and extends as far west as Darlington, but owing to the cover of younger rocks and drift, it is known only from boreholes. It is wholly preserved over much of this area but appears to be very much thinner than farther north. Thus, Smith and Francis (1967, p. 154) report that immediately south

of the West Hartlepool Fault the Upper Magnesian Limestone is about 80 ft thick and this figure corresponds with the general thickness of 75 ft given by Robertson (1948) for the South-East Durham area.

The Upper Magnesian Limestone of Durham has been subdivided on the basis of lithology into the Concretionary Limestone below and the Hartlepool and Roker Dolomites above. Smith and Francis (1967) have stated that the presumed alga Tubulites (formerly Filograna) permiana (King) is very common in the lower subdivision but has only been doubtfully recorded from the upper; there thus appears to be some palaeontological foundation for the subdivision.

The Upper Magnesian Limestone contains the least number of species of all three divisions of the Magnesian Limestone and the very limited fauna (apart from Tubulites) is found in both subdivisions. It consists mainly of euryhaline gastropods and lamellibranchs although foraminifera, ostracods and one possible brachiopod fragment have been recorded. Plant remains are also locally abundant.

The Concretionary Limestone is mainly composed of thinly bedded, granular dolomite. The lower beds are finely laminated, especially at the base, where they comprise the Flexible Lime-

stone which reaches up to 12 ft in thickness and contains fish at Fulwell, near Sunderland. Above the Flexible Limestone, the rock has locally undergone recrystallization and contains concretions. At the coast, the concretions are most abundant in the lower part of the subdivision and are generally absent above. The widest variety of concretions is found in the Sunderland area (Holtedahl, 1921), and farther south they usually take the form of subspherical aggregates of radially crystalline calcite. The thin-bedded, laminated strata lying beneath the level at which concretions become widely developed are most affected by brecciation (Smith, in press).

The brecciation itself shows a wide range of development. At its simplest, gentle sagging of the beds has caused the rock to fracture into large blocks which are only slightly separated and disoriented. In such cases, the dolomite, the fossils and any sedimentary structures present in the beds are preserved. In the most extreme case, the beds have been completely disrupted into disordered, angular fragments which are recrystallized, dedolomitized and hardened, and in which almost all fossils and sedimentary structures have been destroyed. Intermediate stages of development can be recognized.

In boreholes away from the outcrop, the Concretionary Limestone is represented by hard, grey, impure, foetid, often bituminous dolomitic limestone in which the characteristic structures can seldom be recognized.

The Hartlepool and Roker Dolomites have a maximum proved thickness of 366 ft in Offshore Borehole No. 2, but inland, this division appears to be much thinner. The beds of this subdivision undergo very little lateral variation in lithology and consist almost entirely of soft, granular and oolitic, cross-bedded, ripple-marked dolomites which contain multiple ooliths and pisoliths at some levels.

Immediately south of the West Hartlepool Fault, it is still possible to recognize the two-fold subdivision of the Upper Magnesian Limestone. It does not seem possible to do this farther south, and in the Billingham area the Upper Magnesian Limestone is a fine-grained dolomitic limestone, often colour-banded in shades of buff and grey, which contains thin, dark, carbonaceous and bituminous, often stylolitic laminae. Sometimes the laminae are replaced by black shaley partings which have a nodular and even botryoidal form. Smith (in press) has recognized foundering and collapse-brecciation in the Upper Magnesian Limestone of South Durham, although it appears much less intense and extensive than farther north and does not have

any associated widespread mineralogical changes.

Sulphates occur in the Upper Magnesian Limestone throughout Durham. In granular beds, the gypsum occupies the interstices while elsewhere it takes the form of scattered porphyroblastic blebs, replacement patches, joint and bedding-plane coatings and thin, fibrous beds, secondary in origin. At outcrop, the gypsum has been dissolved out, leaving cavities, while at depth, some of the sulphate is in the form of anhydrite.

At the close of Middle Magnesian Limestone times, the Zechstein Sea in Durham had probably become almost filled. The widespread inundation of this low-relief surface by less saline waters brought an end to evaporite deposition in the east and south, and deposition of the Upper Magnesian Limestone began. The presence of overlap within the Upper Magnesian Limestone deposited in the vicinity of the Middle Magnesian Limestone reef suggests that the reef had been incompletely buried and continued to exercise some local control over sedimentation at the beginning of Upper Magnesian Limestone times. The reduced thickness of Upper Magnesian Limestone south of the West Hartlepool Fault has led Smith and Francis (1967, p. 154) to suggest pene-contemporaneous movement along the fault.

Upper Permian Marls.

The Upper Permian Marls and their associated evaporites are preserved only south of the West Hartlepool Fault. However, the presence of fragments of red and green mudstones of Upper Permian Marls lithology in collapse-brecciated Upper Magnesian Limestone in coastal sections (King, 1850; Smith and Francis, 1967) proves their former development north of the Fault.

Smith (in Magraw et al., 1963) made no suggestion as to the relative position of the evaporites within this group, but Smith and Francis (1967) consider that the Billingham Main Anhydrite lies at the base of the division and thus directly overlies the Upper Magnesian Limestone.

To the east of Billingham, the Main Anhydrite is overlain by up to 100 ft of halite while to the west, the Anhydrite decreases in thickness and becomes associated with marl (Sherlock, 1921; Hollingworth, 1942; Robertson, 1948). In the far west, near Darlington, the Upper Permian Marls appear to contain no anhydrite and are undifferentiated. The Main Anhydrite is 33 ft thick at Billingham (e.g. Wood, 1950), but a thickness of 62 ft has been recorded in a borehole just south of the West Hartlepool Fault (Bird, 1888). Sherlock (1921, plate 2, section 3) used this information to show that the Main Anhydrite thickened to

the north, but there is evidence to suggest that the figure of 62 ft might be anomalous and include some Upper Magnesian Limestone which has been replaced by anhydrite (Smith and Francis, 1967, p. 165).

In South Durham therefore, the evaporites lying above the Upper Magnesian Limestone show lateral and vertical changes which are very similar to those observed in the evaporites lying beneath the Upper Magnesian Limestone. Hollingworth (1942, p. 145) believed that a change in depositional environment from basin to shelf adequately explained the variations in both cases.

The Main Anhydrite is separated from the Upper Anhydrite by a variable thickness (15 - 30 ft) of red, gypsiferous silty mudstone, sometimes known as the Rotten Marl. The Upper Anhydrite is a thin (6 - 20 ft), but very persistent, sulphate bed which decreases in thickness to the west where it also contains more dolomite (Wood, 1950). The persistence of the bed leads to its use as a datum in evaporite correlation in North-East England. It is overlain by 190 - 390 ft of red silty mudstone containing abundant sulphate near the base and becoming interbedded with red sandstone towards the top. The sandstone increases in abundance until the rocks assume the appearance

of Bunter Sandstone. The Permian-Triassic junction is therefore somewhat arbitrary and almost certainly diachronous.

The Upper Permian Marls represent the final silting up of the Zechstein Sea in Durham and include portions of two evaporite cycles. The Billingham Main Anhydrite, together with the Upper Magnesian Limestone, represents the third evaporite cycle, while the Upper Anhydrite, although not associated with a well-developed carbonate phase in the Durham area, appears to represent a fourth, partial cycle. Smith and Francis (1967, p. 93) suggest that the Upper Anhydrite may have been deposited in the shelf areas following a relative rise in sea level during a cycle whose carbonate and later phases are restricted to the centre of the basin.

CHAPTER 3.

SAMPLING AND ANALYTICAL PROCEDURE.

Sampling Scheme.

Weathering effects make samples taken from outcrop less desirable for analysis than samples collected from the sub-surface. Consequently, for the purposes of mineralogical and geochemical analysis, samples of Lower and Middle Magnesian Limestone were obtained from one adit and from the cores of fourteen boreholes sunk in Durham and the adjacent offshore area in recent years.

The sampling locations are identified by the numbers 1 - 15 and prefixed by the symbol ML. Abridged geological sections, together with other significant details, are given in Appendix 1 and the distribution of the sampling locations is shown in Figure 3-1. Samples from the adit ML 1 were collected by the writer, while those from borehole ML 8 were obtained from the collections of the Geology Department of Durham University. Specimens from boreholes ML 2, 3, 4, 5, 6 and 9 were taken from the collections of the Institute of Geological Sciences at Leeds and, by request, the original numbers on these samples were retained. Specimens from boreholes ML 7 and 10 were obtained

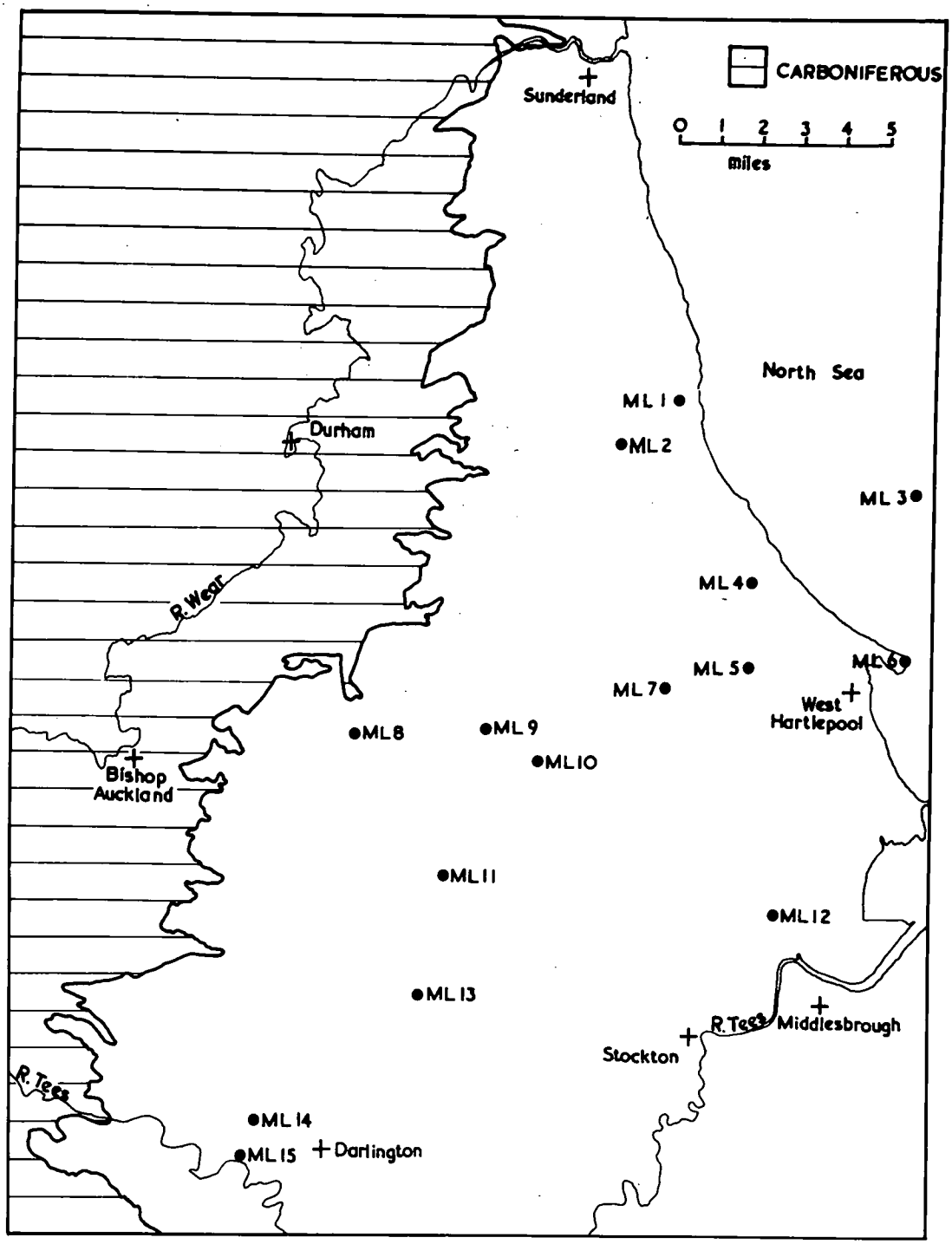

FIGURE 3-1. DISTRIBUTION OF SAMPLING LOCATIONS.

from the Hartlepools Water Company, those from ML 11, 12 and 13 were presented by Imperial Chemical Industries Ltd. and samples from ML 14 and 15 were provided by the Tees Valley and Cleveland Water Board. In addition, samples were taken from outcrop and other borehole cores in order to obtain information for use in conjunction with the analytical data.

The samples were chosen carefully in an attempt to obtain an even representation of the shelf and basin facies of the Lower Magnesian Limestone and the lagoon, reef and basin facies of the Middle Magnesian Limestone. Nevertheless, there is a sampling bias in favour of the shelf facies of the Lower Magnesian Limestone and the lagoon facies of the Middle Magnesian Limestone. This arises from the fact that these facies form the greater part of the Permian outcrop in Durham.

The identification of facies in the sinkings is based on geological sections provided by the Institute of Geological Sciences, the National Coal Board and Imperial Chemical Industries Ltd. The designation of samples to a particular facies of the Lower or Middle Magnesian Limestone is complicated by the fact that the junction between these two divisions is sometimes difficult to place. This is particularly true in the basin area where failure of the usual criteria for recognizing the junction makes it less definite than elsewhere. Samples from the trans-

itional beds are classed as belonging to the immediately overlying facies of the Middle Magnesian Limestone, while samples taken from the reef-lagoon "transitional beds", found between 81 and 90 ft in borehole ML 2 (see Appendix 1), are included in the lagoonal facies as they have more in common with that facies than with the reef.

The Permian stratigraphy in borehole ML 12 has already received attention from Raymond (1962, borehole B 18). He followed the older scheme of classification and designated the carbonate sequence lying beneath the Lower Evaporites as "Lower Magnesian Limestone". Revision of the stratigraphy in South Durham has revealed that most of the "Lower Magnesian Limestone" in this borehole is in fact Middle Magnesian Limestone and that the Lower Magnesian Limestone (sensu stricto) is only 18 ft 6 in thick (see Appendix 1). The thin development of Lower Magnesian Limestone (sensu stricto) in this borehole appears to be related to the presence of the Carboniferous ridge which lies to the west (Raymond, 1960). The thickness of the overlying Middle Magnesian Limestone suggests that this division is unaffected by the ridge.

Raymond (1962) places the base of the Lower Evaporites in this borehole at 678 ft 11 in although beds of dolomite altogether occupy over three-quarters of the interval from 655 ft 6 in to 692 ft. Hence, it can be seen that the junction between the

Middle Magnesian Limestone and the overlying Lower Evaporites is indefinite, unlike the equivalent junction in boreholes ML 3 and ML 6 (see Appendix 1). In this investigation, 3 samples (B 5, 7 and 9) taken from dolomite beds lying between 655 ft 6 in and 678 ft 11 in are designated as Middle Magnesian Limestone basin samples. Raymond would have categorized them as Lower Evaporites.

It is not completely certain that the Lower and Middle Magnesian Limestone intersected by borehole ML 12 was formed in a basin environment, although the borehole is located just to the eastern, and hence basinward side of the line (Hollingworth, 1942) dividing shelf from basin in South-East Durham. Raymond (1962, p. 50) has reported oolitic dolomite from the "Lower Magnesian Limestone" in a borehole at Kirkleatham, about 8 miles south-east of the location of borehole ML 12. Unless Raymond actually observed "pseudo-ooliths" (see Dunham, 1948, p. 221), this suggests that the Lower Magnesian Limestone in the Kirkleatham borehole was deposited in a shallow-water (shelf) environment. However, this is far beyond the eastern extent of the shelf in Durham and the occurrence of oolitic dolomite in this borehole would appear to be anomalous. The general lithology of the Lower and Middle Magnesian Limestone in borehole ML 12 appears to have

much in common with the basin facies seen elsewhere; ooliths were not observed, nor are they recorded in the borehole log. The carbonate sequence lying beneath the Lower Evaporites in ML 12 is therefore classed as basinal in this investigation; this interpretation was confirmed by the mineralogical and geochemical examination described subsequently.

As stated in the previous chapter, it is not possible to correlate any bed in the basin facies of the Middle Magnesian Limestone with the end of reef-growth. Consequently, carbonate beds of post-reef age cannot be separated from those which are equivalent to the main phase of reef-growth. Hence, samples classed as belonging to the basin facies of the Middle Magnesian Limestone in boreholes ML 3, 6 and 12 very likely include specimens which are younger than any other rocks examined and which have no equivalents in the reef and lagoon facies.

Petrography.

The individual borehole samples used for analysis were usually quite small and only occasionally were sufficiently large to allow thin sections to be taken. However, where possible, thin sections were also obtained from larger samples of characteristic and representative lithologies taken from outcrop and from other borehole cores.

The thin sections of Magnesian Limestone were stained with acidulated solutions of potassium ferricyanide and alizarin red - S, following the scheme proposed by Dickson (1965), in order to distinguish between calcite, dolomite and the ferroan varieties of these minerals. The quantitative measurement of $Fe(Mn)^{2+}$ substitution in selected crystals of ferroan dolomite and ferroan calcite was made by determining the ordinary ray refractive index in monochromatic light. Reference to the charts of Smythe and Dunham (1947) and Kennedy (1947) then enabled the molecular composition of the chemically complex carbonates to be estimated.

Analysis.

Sample Preparation.

Drill cuttings were not used for analysis because of contamination and selective sampling effects (Cameron, 1966). Only samples of carbonate rocks taken from borehole cores were analysed. In this account, a carbonate rock is defined as one which contains at least 50 per cent. by weight of calcite plus dolomite; consequently, severely stylolitized material and beds and laminae of marl and sulphate were avoided.

Samples collected for analysis from the adit ML 1 were trimmed with a hammer to remove the dust-covered rind. Borehole

samples showing the drillers' depth-markings, or obvious signs of rust from the drill bit, were rejected, or if sufficiently large, scraped clean with a knife-blade. Samples which had been hammered or scraped with a knife-blade were sand-papered to remove any possible steel-streaks. All samples were then scrubbed, rinsed in distilled water and dried for 3 days in an oven maintained at a steady temperature of 40°C. After drying, the samples were stored in sealed manilla envelopes until required for grinding.

Prior to grinding, the larger samples were reduced to small fragments by a Sturtevant roll jaw crusher with manganese steel jaws. Grinding of all samples was carried out in a Tema laboratory disc mill which produced a powder of less than 50μ in approximately 5 minutes. Grinding for a longer time caused excessive binding and "balling", which resulted in poor powder recovery without producing a significantly smaller mean grain-size. After grinding, the powders were stored in screw-top plastic bottles.

X-ray Diffraction Analysis.

X-ray diffraction was used to identify the mineralogical components and to make rapid estimations of their relative amounts. The technique proved particularly useful for samples which were too

small to allow thin sections to be taken and also for rocks of fine grain-size.

Attempts were made to develop a modal X-ray diffraction technique which would give rapid, but accurate, analyses of the mineralogical components calcite, dolomite, gypsum, anhydrite, quartz and illite. The development of such a technique was considered to be highly desirable, especially in view of the work of Kaye et al. (1968) which showed that "quantitative X-ray diffraction provides the most reliable mineralogical abundance data, particularly if this data is to be used in correlation studies with the chemistry".

X-ray diffraction techniques for the quantitative estimation of calcite and dolomite in carbonate rocks of widely different composition have been described by Tennant and Berger (1957), Gulbrandsen (1960), Weber and Smith (1961), Diebold et al. (1963) and Bromberger and Hayes (1966). However, the above workers mostly investigated systems of relatively simple mineralogy; none worked with carbonate rocks containing significant amounts of calcium sulphate in either or both of its two most common forms. Weber and Smith (op. cit.) have discussed the effects of other minerals on the main spectra of calcite and dolomite and have concluded that in sedimentary rocks, only albite, polyhalite and gypsum are likely to give

interfering reflections.

Albite and polyhalite have not been observed or detected in any of the specimens examined in this investigation, but gypsum is frequently present, particularly in samples from the basin facies of the Lower and Middle Magnesian Limestone. The information presented in Table 3-1 shows how minor gypsum reflections are likely to interfere with the strongest reflections of calcite and dolomite.

Table 3-1.

Interference by Gypsum on Calcite and Dolomite.

Reflection.		dÅ	2θ° (Cu Kα)
Calcite	104	3.035	29.43
Gypsum	$14\bar{1}$	3.059	29.19
Difference		0.024	0.24
Dolomite	104	2.886	30.99
Gypsum	002	2.867	31.20
Difference		0.019	0.21

In view of the small separation between the strongest reflections of calcite and dolomite and the respective reflections of gypsum, it was decided to investigate the possible effects of interference more thoroughly.

A series of mixtures in the binary mineralogical systems calcite-gypsum and dolomite-gypsum were made from the following pure end-members:-

(a) calcite - a large crystal of Iceland spar,

(b) gypsum - a large selenite crystal,

(c) dolomite - U.S. National Bureau of Standards Sample No. 88.

The calcite and gypsum crystals were crushed in a Tema laboratory disc mill and sieved to pass 200 mesh, whereas the dolomite was already in fine powder form. The relevant powders were mixed and homogenized in a Spex mixer mill for 2 hours in order to make the series of mixtures listed below:-

Calcite-Gypsum Binary System	Dolomite-Gypsum Binary System
weight fraction of calcite in mixture	weight fraction of dolomite in mixture
0.25	0.25
0.50	0.50
0.65	0.65
0.80	0.80
0.90	0.90
0.95	0.95

Following the method of Klug and Alexander (1954, pp. 411 - 415), the theoretical intensity-concentration curves for the two series of binary mixtures were calculated using the following relationship:-

$$\frac{I_1}{(I_1)_o} = \frac{X_1 \cdot \mu_1}{X_1 (\mu_1 - \mu_2) + \mu_2} \qquad (3\text{-}1)$$

where μ_1 = the mass absorption coefficient of component 1 at the wavelength concerned,

μ_2 = the mass absorption coefficient of component 2 at the wavelength concerned,

X_1 = the weight fraction of component 1,

$(I_1)_o$ = the intensity of X-rays diffracted by the pure component 1,

and I_1 = the intensity of X-rays diffracted by the component 1 with weight fraction X_1 in the binary mixture.

The mass absorption coefficients of the components at the wavelength concerned are obtained from the following equation:-

$$\mu = \mu_a (x_a) + \mu_b (x_b) + ... \mu_n (x_n) \qquad (3\text{-}2)$$

where μ = the mass absorption of the component,

$\mu_a, \mu_b \cdots \mu_n$ = the mass absorption coefficients of the elements comprising the component at the wavelength concerned,

and $x_a, x_b ..... x_n$ = the weight fractions of the respective elements in the component.

At the wavelength of Cu Kα radiation (1.5418 Å), the mass absorption

coefficients of the components concerned are calcite - 75.62, gypsum - 63.10 and dolomite - 50.43.

The theoretical intensity-concentration curves for the two series of binary mixtures are shown in Figures 3-2 and 3-3. Also shown on the Figures are the experimentally determined curves for the binary mixtures obtained using the experimental method outlined in Table 3-2, from measurements on the strongest reflections of calcite on the one hand and dolomite on the other. Figure 3-2 shows how increased resolution (produced by a smaller slit system) causes the experimentally determined curve to move closer to the theoretical curve. However, it can be seen that even with the $\frac{1}{2}^{o}$ slit system, there is still a marked divergence between the experimental and theoretical intensity-concentration curves for the calcite-gypsum and dolomite-gypsum binary systems.

To check the practical validity of the analytical method used, a small number of calcite-quartz and dolomite-quartz mixtures were made up. A piece of Brazilian rock crystal was used to provide the quartz end-member in these mixtures. The mixtures were prepared, and the theoretical and experimental intensity-concentration values for the two series were obtained by following a procedure similar to that outlined above. At the wavelength of Cu Kα radiation, the mass absorption coefficient of quartz is 34.90. Figures 3-4 and 3-5 show that the experimental

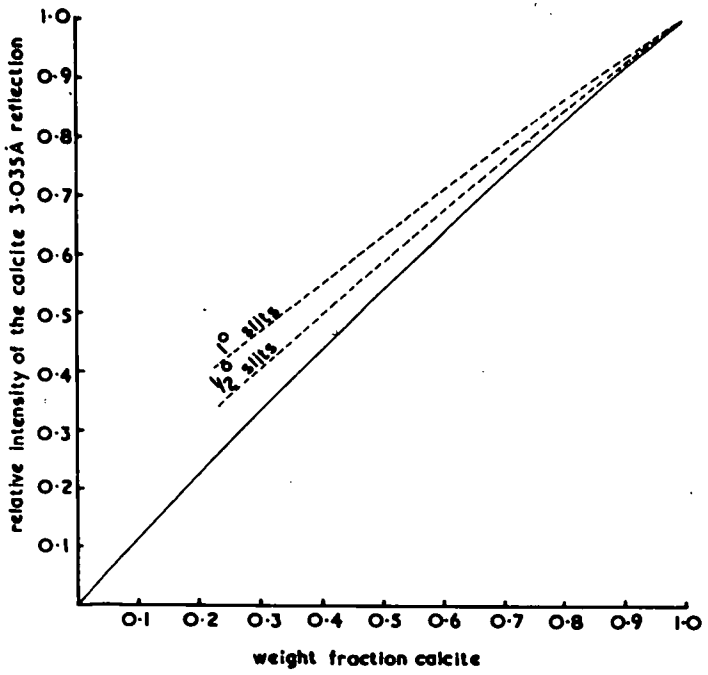

FIGURE 3–2. COMPARISON OF THEORETICAL (solid line) AND EXPERIMENTAL (broken lines) INTENSITY–CONCENTRATION CURVES FOR THE CALCITE–GYPSUM BINARY SYSTEM.

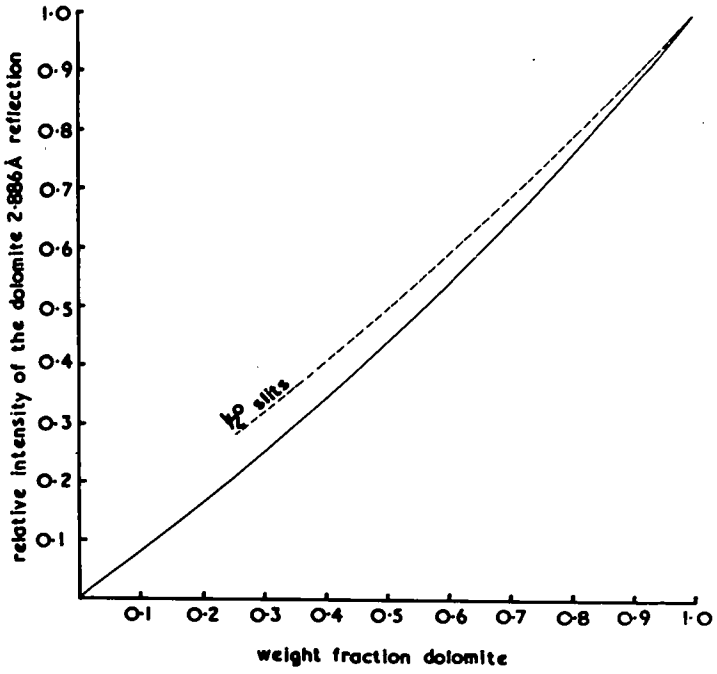

FIGURE 3–3. COMPARISON OF THEORETICAL (solid line) AND EXPERIMENTAL (broken line) INTENSITY–CONCENTRATION CURVES FOR THE DOLOMITE–GYPSUM BINARY SYSTEM.

values lie very close to the theoretical curves for both the calcite-quartz and dolomite-quartz binary systems. In these systems, line-line interference effects are absent.

Table 3-2.

X-ray Diffraction Experimental Method.

Apparatus:	Phillips 2 Kilowatt Diffractometer		
Conditions:	40 kV 20mA		
Radiation:	Ni filtered Cu Kα		
Slit System:	divergence	receiving	scatter
	1°	0.1 mm	1°
and	0.5°	0.05 mm	0.5°
Counter:	Sealed flow operated at 1.55 kV		
Discriminator:	attenuation factor	lower level	channel width
	2	62 voltage units	20 voltage units
Counting Method:	Fixed time of 100 seconds		
Analysis:	peak 2θ°	background 2θ°	
calcite	29.43	27.00	
dolomite	30.99	27.00	
Line Intensity:	expressed as peak intensity-background intensity.		
Mount:	rotating cavity		

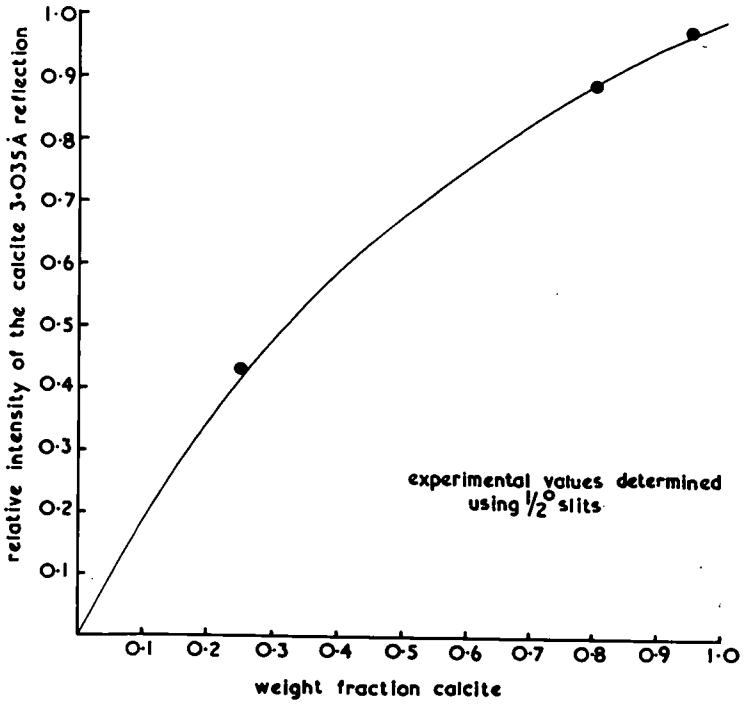

FIGURE 3–4. COMPARISON OF THEORETICAL INTENSITY–CONCENTRATION CURVE (solid line) WITH EXPERIMENTAL VALUES (closed circles) FOR THE CALCITE–QUARTZ BINARY SYSTEM.

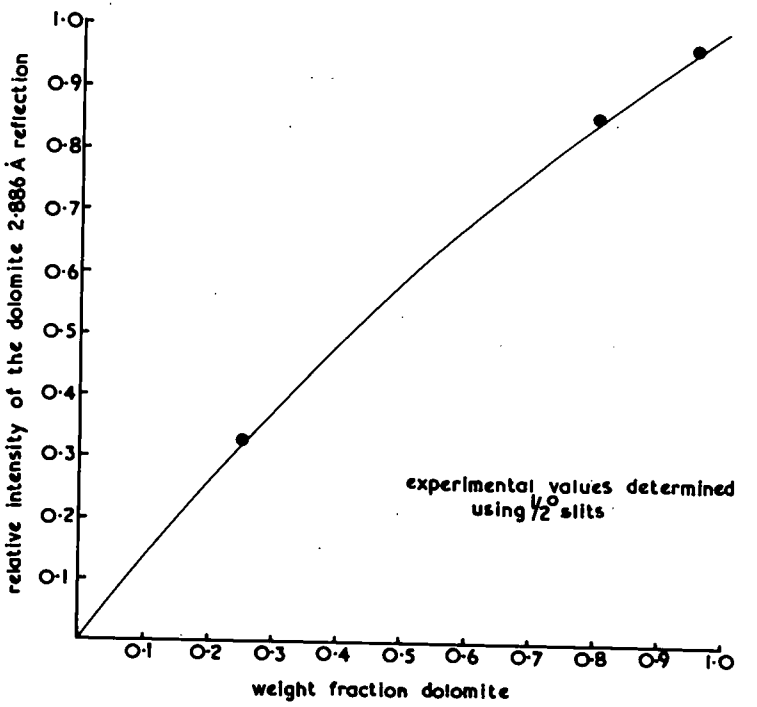

FIGURE 3–5. COMPARISON OF THEORETICAL INTENSITY–CONCENTRATION CURVE (solid line) WITH EXPERIMENTAL VALUES (closed circles) FOR THE DOLOMITE–QUARTZ BINARY SYSTEM.

The divergence between the experimental and theoretical intensity-concentration curves for the calcite-gypsum and dolomite-gypsum binary systems is attributed to the effects of interference from the minor gypsum reflections mentioned above. The experimental values in these systems are consistently higher than the theoretical values, as expected if the divergence is caused by interference.

In a simple two, or perhaps even three component carbonate-sulphate system, it is probable that corrections derived from data of the type given above could be developed for use in a quantitative X-ray diffraction technique for the analysis of unknown samples with equally simple mineralogy. However, the samples of Magnesian Limestone under investigation may be considered to consist of at least six basic mineralogical components, several of which vary considerably in quantity. It would be most difficult to make corrections for sulphate interference in such a variable, multicomponent, mineralogical system. Hence, it would appear that interference from gypsum renders the calcite 3.035 Å and dolomite 2.886 Å reflections unsuitable for the quantitative X-ray diffraction analysis of Magnesian Limestone.

Calcite and dolomite are of fairly high symmetry (trigonal) and hence give rise to a large number of reflections when diffracted. Unfortunately, there is a large decrease in relative

intensity between the strongest and next strongest reflections for both calcite and dolomite. Consequently, no other calcite or dolomite reflections appear sensitive enough for use in quantitative X-ray diffraction analysis. In addition, the next strongest reflections of both calcite and dolomite have interference problems of their own. As a result, the attempt to develop a modal X-ray diffraction technique was abandoned.

Chemical Analysis.

Using an analytical procedure based on that described by Shapiro and Brannock (1962), total chemical analyses were carried out on five natural end-members which were then utilized as standards for X-ray fluorescence major element analysis (q.v.).

Total water ($H_2O^+ + H_2O^-$) in these and in other samples was determined by the Penfield tube method. Hygroscopic or incidental water (H_2O^-) was determined by measuring the weight loss which occurred after heating the samples in an oven maintained at 40°C for 3 days. The usual procedure of heating overnight at 110°C could not be followed as some samples contained gypsum which begins to dehydrate at 50°C (Deer et al., 1962, p. 207). Using samples known to be free of gypsum, it was possible to show that the loss in weight which occurred after heating over-

night at 110°C was identical to that which occurred after heating for 3 days at 40°C. Diffractometer traces of pure, finely powdered gypsum showed that no mineralogical changes occurred after heating for 3 days at 40°C. The difference between the total and hygroscopic water values gave the structural water (H_2O^+) content.

Organic carbon and carbon dioxide were determined for some samples using an absorption train technique (Groves, 1951).

X-ray Fluorescence Spectrography.

X-ray fluorescence spectrography was used to analyse for both light elements in major amounts and heavy elements in minor and trace amounts. There are three major sources of error, often termed deviations from proportionality, inherent in this method of analysis. These have been listed by Liebhafsky and Winslow (1958) as:-

(1) instability in the spectrograph and in associated equipment,

(2) heterogeneity in the samples,

(3) absorption and enhancement effects related to the chemistry of the sample.

However, in the long wavelength region associated with the light elements, these fundamental sources of error have a relative

importance which is different from that in the short wavelength region associated with the heavy elements. Because of this, the technique used in the analysis of major elements is, of necessity, considerably different from that used for the minor and trace elements. The two techniques are described separately below.

Major Element Analysis:- Analyses of Si, Al, Fe, Mg, Ca, Na, K, Ti and S were obtained using a Phillips Automatic X-ray Spectrograph (PW 1212) and following a modification of the method described by Holland and Brindle (1966). The conditions under which the spectrograph was operated are given in Table 3-3. For the elements Mg, Na and S, the intensity of the analytical line was obtained from the difference between the peak and background intensities.

To overcome the errors arising from instability, the spectrograph was housed in a small constant-temperature laboratory. Constant-temperature conditions reduce fluctuations in the electronic circuitry and variations in the lattice spacing of the analysing crystal (Davies, 1958). However, a control standard (monitor) was used to correct for any instrument drift which did occur.

Table 3-3.

Operating Conditions for the Analysis of Major Elements by the Phillips Automatic X-ray Spectrograph (PW 1212).

Element and Line		Si Kα	Al Kα	Fe Kα	Mg Kα	Ca Kα	Na Kα	K Kα	Ti Kα	S Kα
Wavelength in Å		7.12	8.34	1.94	9.89	3.36	11.90	3.74	2.75	5.37
Tube		Chromium, 2 Kilowatt rating →								
Generator	kV	60	50	60	50	20	50	60	60	50
	mA	24	40	32	40	8	40	16	24	40
Crystal		P.E.	P.E.	LiF 110	Gypsum	P.E.	Gypsum	P.E.	P.E.	P.E.
Counter		Flow	Flow	Flow + Scint-illation	Flow	Flow	Flow	Flow	Flow	Flow
Counter Voltage		1800	1800	Flow 1800 Scint.1000	1800	1800	1800	1800	1800	1800
Collimator		Coarse →								
Discriminator		Automatic Pulse Height Selection →								
Path		Vacuum →								
Fixed Count		10^5	3×10^4	10^5	3×10^4	10^6	3×10^3	10^5	3×10^4	3×10^5
Sample State		Briquette →								
Rotation		Yes →								
Peak 2θ°		109.07	144.95	85.72	81.33	45.07	103.12	50.58	36.58	75.65
Background 2θ°		-	-	-	79.05	-	105.02	-	-	73.49

Heterogeneity in the samples arises from either segregation or surface effects. The effects of segregation have been investigated and summarized by Bernstein (1962). The powders obtained from the Tema disc mill were considered to be of such an homogeneity and fineness that segregation effects may be ignored. Liebhafsky et al. (1960, pp. 220 - 221) have pointed out that surface effects differ from segregation effects in that they are controlled by the wavelength of the analytical line. At the long wavelengths associated with the light elements, there is a small critical depth in the sample; hence, the relative contribution of the surface layer to the intensity of the analytical line is much greater than for the heavy elements. Consequently, it is necessary to have a very carefully prepared sample surface which is constant from sample to sample. This was achieved by forming a briquette from the sample powder as described by Holland and Brindle (1966, p. 2090). It was not possible to use the sample binder MOWIOL mentioned by these authors as it dissolves calcium sulphate. To compensate for the consequent loss of adhesion, the 1.25 in diameter briquettes were formed at a higher pressure of 7 tons maintained for 5 minutes.

Errors arising from absorption-enhancement effects are perhaps the most difficult to eliminate. The entire chemistry of a sample governs the absorption and emission of X-rays at each analytical wavelength; at a particular wavelength, the total mass absorption of a sample is determined by the following relationship:-

$$\mu_s = \mu_a(C_a) + \mu_b(C_b) + \ldots . \mu_n(C_n) \qquad (3\text{-}3)$$

where μ_s = the total mass absorption of the sample,

$\mu_a, \mu_b \ldots . \mu_n$ = the mass absorption coefficients of the elements comprising the sample at the wavelength concerned,

and $C_a, C_b \ldots C_n$ = the concentrations of the respective elements in the sample.

Many methods have been used to allow for, or to eliminate, the absorption-enhancement effects but most have proved to be of use only in limited circumstances. The method of Holland and Brindle (1966) however, appears to be of wider application because it achieves a complete solution to Equation (3-3) and thus predicts inter-sample differences in total mass absorption at each analytical wavelength. The method is rapid and enables a large number of specimens to be analysed in a relatively short time. It is for these reasons that the method was adopted in this investigation.

In view of the lack of a comprehensive set of international standard sedimentary rocks in the required chemical range, standards for the method were obtained by mixing together in varying proportions five chemically analysed natural end-members. They were used in conjunction with the U.S. National Bureau of Standards sample numbers 1A (Argillaceous Limestone) and 88 (Dolomite) to give a complete set of thirteen standards which adequately covered the range of all the elements of interest in the samples investigated.

Several modifications were made to the method of Holland and Brindle (op. cit.) to facilitate its use in the analysis of samples of Magnesian Limestone. The computer programme was adjusted so that H_2O^+ values, determined independently, could be included in the input data. Also, in order to effect the necessary matrix corrections, it was essential to make certain assumptions concerning the manner in which the elements were bonded. Thus it was assumed, as is customary in the analysis of silicate systems, that Si, Al, Fe, Na, K and Ti could be expressed in oxide form. Mg, Ca and S however, could not be realistically expressed in this form. Consequently, it was assumed that Mg was combined as $MgCO_3$, that Ca was in the form of $CaCO_3$ and $CaSO_4$ and that S, as the SO_4^{2-} radical, was combined entirely with Ca^{2+} in the $CaSO_4$. These assumptions

determined the correction factors made to the matrix block (Holland and Brindle, op. cit., p. 2091), but in turn posed certain practical problems. The most important arose from the fact that the total intensity reading of Ca Kα was compounded from two sources, Ca CO_3 and Ca SO_4. To overcome this problem, it was assumed that the S Kα count gave a direct measure of the quantity of Ca SO_4 in the system. The total calcium count was then partitioned between the two phases following the procedure outlined below:-

If I_{Ca} represents the total calcium intensity for a given sample and $I_{Ca}^{Ca\ CO_3}$ and $I_{Ca}^{Ca\ SO_4}$ respectively represent the contributions to the total calcium intensity from the Ca CO_3 and Ca SO_4 in the sample then

$$I_{Ca} = I_{Ca}^{Ca\ CO_3} + I_{Ca}^{Ca\ SO_4}.$$

Assuming that the sulphur intensity I_S gives a direct measure of the quantity of Ca SO_4 in the sample then

$$I_{Ca}^{Ca\ SO_4} = k.I_S$$

where k = a constant whose value may be obtained from the standards.

Hence $$I_{Ca} = I_{Ca}^{Ca\ CO_3} + k.I_S$$

and $$I_{Ca}^{Ca\ CO_3} = I_{Ca} - k.I_S \qquad (3\text{-}4)$$

The accuracy of the analyses from the X-ray fluorescence

method depends directly on the accuracy of the standards used. However, as the analyses are used for internal comparison only, high precision is one of the main objectives. The precision was found to be better than 0.5 per cent. of the analysed component.

Minor and Trace Element Analysis:- Analyses of Ba, Sr, Rb, Pb, Zn, Cu, Ni and Mn for some of the samples were obtained using a Phillips X-ray Spectrograph with universal vacuum attachment (PW 1540) and electronic timer (PW 4062). For the remainder of the samples, analyses of these elements were obtained using the Automatic Spectrograph (PW 1212). The operating conditions for both instruments are given in Table 3-4.

For both sets of apparatus, constant-temperature conditions and the use of a control standard are considered to have eliminated any errors arising from instrumental instability.

At the short analytical wavelengths involved, surface effects are negligible and it is possible to use the sample powders obtained from the Tema disc mill directly for analysis. The powders were lightly packed into sample holders fitted with a 6.25 μ mylar-foil window.

In the analysis of minor and trace elements, absorption-enhancement effects still constitute the major source of error. As Equation (3-3) still holds true at the short wavelengths involved, their analysis could therefore be carried out in a manner similar to that used for the major elements. Unfortunately, it would be necessary to know the concentration of the major elements in order to calculate the minor and trace element concentrations from Equation (3-3). For many samples, there may be no desire to determine the major element concentrations and otherwise unnecessary determinations would have to be made in order to use Equation (3-3) for the calculation of minor and trace element concentrations. Also, small errors in the major element concentrations could, when used in the equation, produce relatively significant errors in the values of the minor and trace constituents. These considerations render the use of such a method undesirable.

The technique adopted for the analysis of the minor and trace elements was based on that of Andermann and Kemp (1958) in which the coherently scattered radiation is used as an internal standard to correct for instrumental, sample and absorption effects. Following the recommendation of Kalman and Heller (1962), the background in the region of the analytical line in question was used as a measure of this scattered radiation.

Table 3-4.

Operating Conditions for the Analysis of Minor and Trace Elements by the Phillips PW 1540 and PW 1212 Spectrographs.

Element and Line			Ba Kα	Sr Kα	Rb Kα	Pb $L\beta_1$	Zn Kα	Cu Kα	Ni Kα	Mn Kα
Wavelength in Å			0.39	0.88	0.93	0.98	1.44	1.54	1.66	2.10
Tube		PW 1540	Tungsten, 1 Kilowatt rating →							
		PW 1212	Tungsten, 2 Kilowatt rating →							
Generator	kV	PW 1540	54	54	54	46	46	46	46	46
		PW 1212	80	80	80	60	60	60	60	60
	mA	PW 1540	16	16	16	20	20	20	20	20
		PW 1212	24	24	24	32	32	32	32	32
Crystal		Both	LiF 110 →							
Counter and Voltage		PW 1540	Scintillation Counter operated at 1000 volts →							
		PW 1212	Scintillation Counter operated at 900 volts →							
Collimator		PW 1540	Fine →							
		PW 1212	Coarse →							
Discrimin-ator		PW 1540	No discrimination →							
		PW 1212	Automatic Pulse Height Selection →							
Path		Both	Vacuum →							
Fixed Time (seconds)		PW 1540	60 →							
		PW 1212	20	40	40	40	40	40	40	20
Sample		Both	Powder →							
Rotation		PW 1540	No rotation →							
		PW 1212	Rotation →							
Peak $2\theta^\circ$		Both	15.62	35.87	37.99	40.34	60.60	65.56	71.26	95.19
Back-ground $2\theta^\circ$		PW 1540	18.12	37.41	37.41	41.24	59.60	68.06	70.26	93.69
		PW 1212	16.82	36.94	36.94	41.83	59.37	66.94	69.94	96.94

For the elements Zn, Ni and Mn, the analytical lines lie above a level background and it was sufficient to make a single background measurement close to, but clear of, the line concerned. The analytical lines of Ba, Sr, Rb and Pb appear above the sloping W continuous spectrum while Cu Kα lies on the flank of the W Lα_1 line. For these elements, an estimate of the background was obtained by making a correction to the background determined close to each line in order to allow for the effect of the slope. The individual correction factors were derived from information which had been obtained from an empirical solution to the equation defining the general slope of the background.

For Ba, Sr, Rb, Pb, Zn, Cu and Ni, the intensity of the analytical line was recorded as $\frac{\text{peak intensity-background intensity}}{\text{background intensity}}$. At the longer wavelength of Mn, the decrease in the intensity of the scattered radiation (Andermann and Kemp, 1958) invalidates the use of this relationship. For this element, the intensity of the analytical line was recorded as peak intensity-background intensity.

Johnson and Matthey "Specpure" compounds were added to one of the unknown samples in the correct proportions to make a series of addition standards containing 5, 10, 25, 50, 100, 200, 300, 500, 750, 1000 and 2500 ppm. of each element. Each standard

was shaken for 8 hours in a Spex mixer mill to ensure homogeneity.

A sample of Johnson and Matthey "Specpure" $CaCO_3$ was used to determine the amount of spectral contamination caused by the X-ray tube filament. The minor and trace element values were corrected for this source of contamination.

The minor and trace element concentrations of a selection of samples which had been analysed using the PW 1540 were redetermined using the PW 1212. The two sets of results were comparable for all elements.

The precision of the X-ray fluorescence analytical technique was determined by analysing a standard sample ten times at random. The results are presented in Table 3-5 and are considered to be satisfactory. The limit of detection for each element, taken as the concentration which produces a line intensity equal to three times the standard deviation of the background count, is also presented in Table 3-5. The Standard Diabase W-1 was analysed for the elements of interest to assess the accuracy of the analytical method. This is not entirely satisfactory in view of the matrix differences between W-1 and the Magnesian Limestone, but the results obtained (see Table 3-5) are comparable with those recommended by Fleischer (1965).

Table 3-5.

Precision, Limits of Detection and Accuracy of the X-ray Fluorescence Minor and Trace Element Technique.

	Ba	Sr	Rb	Pb	Zn	Cu	Ni	Mn
Mean Content of Standard Sample (ppm.)	95	553	26	45	62	53	35	873
Standard Deviation (ppm.)	±11	±7	±2	±2	±3	±2	±3	±63
Relative Deviation (%)	11.68	1.27	7.69	4.44	4.84	3.77	8.57	7.22
Limit of Detection (ppm.)	5	5	3	10	5	8	3	15
Recommended Values for W-1 (ppm.)	180	180	22	8	82	110	78	1320
Values for W-1 obtained in this investigation (ppm.)	220	195	30	<10	85	135	85	1450

Emission Spectrography.

The Emission Spectrograph was used to analyse for boron in 27 samples of Magnesian Limestone.

Spectrochemically, boron belongs to the involatile group of elements. The general principles for the analysis of elements

of this group have been outlined by Ahrens and Taylor (1961, pp. 189 - 190). Details of the experimental method used for the determination of boron in this investigation are given in Table 3-6. Standards were obtained by adding Johnson and Matthey "Specpure" boric acid ($H_3 BO_3$) to one of the unknowns to give a series of standard mixtures containing 25, 50, 100, 250 and 500 ppm. of added boron. The addition standards were shaken for 2-3 hours in a Spex mixer mill to ensure homogeneity. The inadequacies of addition standards in spectrochemical analysis have been pointed out by Ahrens and Taylor (1961, pp. 158 - 159). However, as international standards with known concentrations of boron were not available at the time of analysis, it was considered justifiable and necessary to use addition standards.

A special three step filter (with a step ratio of 2:1) was used with the standards to produce the emulsion calibration curve relating photographic response to intensity of spectral radiation. For the unknowns, it was necessary only to use one step to find the intensity of the boron and palladium lines. In this investigation, photographic response was recorded by the Seidel function, $\log\left(\frac{d_o}{d} - 1\right)$ where d_o is the clear glass galvanometer deflection and d the galvanometer deflection for

a particular spectral line. This function enables low photographic response (i.e. weak spectral lines) to be measured more accurately. A working curve relating the intensity ratio B:Pd to the total boron content for the standards was used to derive the boron content of the unknown samples.

Table 3-6.

Experimental Method for the Determination of Boron by Emission Spectrography.

Instrument.	Hilger and Watts Large Automatic Spectrograph E 742.
Charge Preparation.	
Internal Standard.	Johnson and Matthey "Specpure" Ammonium Chloropalladite $(NH_4)_2$ Pd Cl_4 .
Buffer.	National Carbon (SP - 2) grade Graphite.
Internal Standard /Buffer Mix.	Internal Standard and Buffer mixed together in a Spex mixer mill for 3 hours to give a mix containing 0.5% Palladium.
Total Sample Mix.	1 part sample mixed with 2 parts Internal Standard/Buffer mix in a Spex mixer mill for 30 minutes.
Electrode Assembly.	
Anode.	Johnson and Matthey Graphite rods (JM 2104). Diameter 4.5 mm. Boron content $\geq$ 0.01 ppm.
Dimensions of Crater.	Diameter 0.125 in (3.2 mm). Depth 2.5 mm.

Table 3-6 (Continued).

Cathode.	Johnson and Matthey Carbon rods (JM 1205). Diameter 5 mm. Boron content $\geq$ 3 ppm.
Analytical Gap.	4 mm.
Atmosphere.	Air.
Optical System.	Quartz Prism.
Wavelength Range.	2470 - 3510 Å.
Lens System.	F 1025 focussed on Collimating Lens and used in conjunction with a special three step filter.
Slit.	Height 8.5 mm (to allow for filter). Width 7μ
Camera Diaphragm.	10 mm.
Plate.	Kodak B-10 from the same batch.
Exposure.	
Source.	Hilger and Watts 10 amp. Triggered D.C. Arc Unit FS 141.
Current.	Short Circuit 10 amps. Burn 7 - 7.5 amps.
Time.	Pre-burn 0 seconds. Burn 30 seconds.
Comments.	Standards and unknowns arced in duplicate.
Photographic.	
Developer.	Kodak DX-80 for 2.5 minutes at 20°C.
Fixer.	Kodak Rapid Fixer for 5 minutes.
Washing.	45 minutes.

Table 3-6 (Continued).

Finish.	Kodak Photoflo Solution for 30 seconds.
Drying.	5 minutes on electric drier.
Lines.	
Analysis.	B 2497.7 Å.
Internal Standard.	Pd 2476.4 Å.
Microphotometry.	
Instrument.	Hilger and Watts Non-recording Microphotometer with a clear glass galvanometer deflection of 50 divisions.
Slit.	Height 12 mm. Width 0.2 mm.
Background Correction.	No correction for Si O band interference.

The precision of the analytical method was determined by arcing two standard samples, each for ten times, at random on the plates. The results are shown in Table 3-7, from which it can be seen that the precision is poor and that the boron analyses are really only semi-quantitative. The low precision would appear to be a result of uneven burning of the charges which can be attributed to the effects of incidental moisture and carbon dioxide. To remove incidental moisture (H_2O^-) from the charges, it is usual to heat the loaded electrodes in an oven at 110°C for 24 hours prior to arcing. As some of the samples

were known to contain gypsum, it was not possible to follow this procedure. Instead, the loaded electrodes were stored in a dessicator for 24 hours before arcing in an attempt to remove at least some incidental moisture. In order to prevent the evolution of carbon dioxide from extruding the charge from the electrode, a wide, shallow cavity was used. Nevertheless, the effect was not entirely eliminated and this is believed to have been the main cause of uneven burning.

Table 3-7.

Precision of the Emission Spectrographic Technique for Boron.

Mean Boron Content of the Standard Samples (ppm.)	111	572
Standard Deviation (ppm.)	± 17	± 72
Relative Deviation (%)	15.31	12.59

CHAPTER 4.

MINERALOGY.

In view of the failure to develop a quantitative X-ray diffraction technique for modal analysis, the mineralogical compositions of 162 samples taken from twelve of the fifteen sinkings were estimated by recalculation of the major element analyses obtained by X-ray fluorescence spectrography.

Method of Recalculation.

Recalculation schemes for computing the mineralogical compositions of sedimentary rocks have been proposed and discussed by Imbrie and Poldervaart (1959), Miesch (1962) and Nicholls (1962). Miesch (op. cit.) has stated that recalculation is highly accurate when the qualitative mineralogical composition of the rock system and the exact chemical composition of each mineral phase are known. The method of chemical analysis must also, obviously, be as accurate as possible.

Petrography and X-ray diffraction revealed that calcite, dolomite, gypsum and anhydrite form the main mineralogical components in the Magnesian Limestone, although minor quantities of quartz, limonite, clay minerals (predominantly illite) and pyrite are common. Magnesite was not detected in any sample;

paragenetically its occurrence seems unlikely in these rocks (e.g. Stewart, 1963), but Raymond (1962) has noted one probable occurrence in the Stainton area and Browell and Kirkby (1866) record $MgCO_3$ in excess of that required to form dolomite.

The main mineralogical components are of fairly rigid composition. Anhydrite and gypsum in particular show little variation in composition (see Deer et al., 1962). Calcite and dolomite do show some compositional variation owing to substitution by other divalent cations. Thus, Mg^{2+} and $Fe(Mn)^{2+}$ both commonly replace Ca^{2+} in calcite, while in dolomite, Ca^{2+} and $Fe(Mn)^{2+}$ are known to replace Mg^{2+}. In ancient calcites, the $MgCO_3$ content is usually of the order of 1-2 weight per cent. (Chave, 1954), although in calcite associated with dolomite, up to 9 mol. per cent. Mg^{2+} has been reported substituting for Ca^{2+} (Goldsmith et al., 1955). Calcian dolomites appear to be of limited occurrence. Both of these substitutions cause changes in the crystal structure which are readily detectable by X-ray diffraction. No such changes were detected in the calcites and dolomites of the Magnesian Limestone and these substitutions are therefore likely to be insignificant. $Fe(Mn)^{2+}$ substitution is well known in both calcite and dolomite, particularly in the latter. The staining technique of Dickson (1965), used in conjunction with the determination of

the ordinary ray refractive index, revealed that small quantities of slightly ferroan dolomite and, less commonly, slightly ferroan calcite occur only sporadically in the Magnesian Limestone samples. In general, the calcite and dolomite appear to be iron-free.

The X-ray fluorescence major element analysis appears to be theoretically accurate and to be subject only to the counting error inherent in all X-ray techniques. However, the assumption that all the calcium is bonded as $Ca\ CO_3$ and/or $Ca\ SO_4$ (see Chapter 3) does not allow for calcium combined with fluorine in fluorite or as phosphate in hydroxyapatite . Fortunately, fluorite is of very sporadic occurrence and low in amount, while the extremely low concentrations of phosphorus recorded from the Magnesian Limestone (e.g. Smith and Francis, 1967, p. 116) suggest that hydroxyapatite can only be present in traces, except in certain obvious cases (Dunham et al., 1948). Sulphur may also be present in barite in addition to gypsum and anhydrite; barite is known to occur in the Magnesian Limestone, although in small and sporadic amounts. Sulphur may also occur in pyrite as well as galena, sphalerite and chalcopyrite which have all been recorded from the Magnesian Limestone (e.g. Smith and Francis, 1967, p. 168). As the sulphur value is used to give a direct measure of the

$Ca\ SO_4$ in the system, the presence of other sulphates and/or sulphides will lead to errors in $Ca\ SO_4$ and low values for $Ca\ CO_3$ (see Equation 3-4). These complementary errors are unavoidable by the method of data processing employed, but are considered to be small as the quantities of pyrite, and especially the sporadic amounts of galena, sphalerite and barite, are low. The representation of total iron as an oxide is potentially the greatest source of error, for although iron is present in limonite and illite, it also occurs as the sulphide in pyrite and chalopyrite, and as the carbonate in ferroan varieties of calcite and dolomite. Fortunately, the iron content of the Magnesian Limestone is generally low and the errors involved are not serious.

Organic carbon contents were not determined for all of the 162 samples analysed by the X-ray fluorescence major element technique. As the computer programme of Holland and Brindle (1966) sums the major element analyses to 100 per cent., the absence of organic carbon values in the input data results in an error in the output values for the other components. Determination of organic carbon in 34 samples of Magnesian Limestone (see Appendix 2) showed that the content was less than 1 per cent. in every case. The resulting error in the major element analyses will therefore be very small.

The following procedure for recalculation of the major element analyses was adopted:-

(1) The $MgCO_3$ was combined with the stoichimetric amount of $CaCO_3$ to yield dolomite, $CaMg(CO_3)_2$, and any residual $CaCO_3$ was returned as calcite. Occasionally, there was a slight insufficiency of $CaCO_3$ for the formation of dolomite. This was not considered to be due to the presence of magnesite or high magnesian calcite, as a $CaCO_3$ deficiency was only observed in the analyses that contained $CaSO_4$. The insufficiency probably arose from a slight error in the partition of the calcium intensity data between $CaCO_3$ and $CaSO_4$. Whenever a $CaCO_3$ deficiency occurred, the $MgCO_3$ and $CaCO_3$ values were added together to give an approximate dolomite value.

(2) The H_2O^+ was combined with the stoichimetric amount of $CaSO_4$ to yield gypsum, $CaSO_4.2H_2O$, and any residual $CaSO_4$ was returned as anhydrite. Very occasionally, there was a slight insufficiency of $CaSO_4$ to satisfy the quantity of H_2O^+. The insufficiency was probably due to excess H_2O^+ being

contributed from clay minerals and/or limonite. Whenever a Ca SO_4 deficiency occurred, the H_2O^+ and Ca SO_4 values were added together to give an approximate gypsum value. Other sulphur-bearing minerals likely to occur in the Magnesian Limestone are anhydrous; consequently, their presence would produce errors in the recorded values of anhydrite rather than gypsum. Low anhydrite values are therefore regarded with more suspicion than low gypsum values, especially when recorded in rocks from relatively shallow depths.

(3) The remainder of the major element analyses were left in oxide form because carbonates and sulphates together frequently account for over 95 per cent. of the mineralogy of the samples. The concentrations of the remaining elements were generally so low that any calculation of such a compositionally variable group as the clay minerals would very likely have been inaccurate.

The recalculation procedure outlined above gave, therefore, only partial mineralogical analyses. This was satisfactory as the main interest was the variation in the type and amount of carbonate and sulphate minerals in the various facies of the Magnesian Limestone. However, while suitable for the comparative studies made in this investigation, the data should not be used for extrapolation to other areas, except in a very general way. The partial mineralogical analyses of the 162 samples are presented in Appendix 3.

Kaye et al. (1968) have pointed out that using major element chemistry to calculate mineralogical composition makes it no longer possible to correlate the two, as they are not independent variables. While this is certainly true, it must be borne in mind that in an essentially carbonate-sulphate system of the type investigated here, the comparatively rigid composition of the component minerals very strongly and obviously controls the major element geochemistry.

Lower Magnesian Limestone - Shelf Facies.

Partial mineralogical analyses were calculated for 37 samples taken from the six boreholes tabulated below:-

Borehole	ML 2	ML 7	ML 8	ML 11	ML 13	ML 14
Thickness of Facies (ft in)	246	76 6 (proved)	?129 10	61 11	c.36 2 (proved)	c.45 (proved)

The shelf Lower Magnesian Limestone was only completely intersected in three boreholes, ML 2, ML 8 and ML 11. Boreholes ML 7, ML 13 and ML 14 only penetrated the upper part of the Lower Magnesian Limestone beneath the transitional beds. Five of the boreholes are situated to the south of the Butterknowle Fault and the sampling locations are therefore unevenly spaced over the Permian outcrop.

Sulphates.

Five analyses show the presence of gypsum and 7 the presence of anhydrite. Gypsum ranges in content from 0.05 per cent. (UP 35) to 0.82 per cent. (UP 55), while the anhydrite values vary from 0.11 per cent. (UP 155) to 1.21 per cent. (UP 55). The combined concentrations of gypsum and anhydrite reach a maximum recorded value of 2.03 per cent. in sample UP 55. Sulphates were not detected in samples from ML 2 and ML 8 and were only recorded (mainly as anhydrite) in occasional samples from ML 13 and ML 14. Bore-

holes ML 7 and ML 11 show the most frequent development of sulphates which decrease in content towards the top of the sequence in both boreholes.

Sulphates were not observed in thin section or detected by X-ray diffraction but their occurrence is not inconsistent with the findings of other workers. Trechmann (1914, pp. 247 - 248) reported small quantities of sulphur trioxide in samples of Lower Magnesian Limestone from the shelf area. Although small amounts of barite are known to occur sporadically in the Lower Magnesian Limestone, the consistent presence of sulphur trioxide suggests that small quantities of gypsum and/or anhydrite may also be present. Recalculated total chemical analyses of samples of (shelf) Lower Magnesian Limestone from a borehole near Embleton (Smith and Francis, 1967, p. 116) all show the presence of small quantities of gypsum, and Woolacott (1919B, p. 456) reported gypsum crystals from cavities in the Lower Magnesian Limestone at Raisby Hill Quarries, near Coxhoe. Gypsum is more common within the shelf "Lower Magnesian Limestone" of South-East Durham where Raymond (1962) has also reported the occurrence of anhydrite, but only in beds lying at more than 500 ft from the surface. Even at this depth, gypsum is still the most common form of sulphate, the anhydrite occurring as relics within the gypsum. Consequently, the detection

of anhydrite, particularly in amounts in excess of gypsum, in samples from relatively shallow depths in this investigation must be regarded with suspicion. The small quantities of anhydrite probably reflect the amount of pyrite in these samples. In borehole ML 7, the 3 samples which are reported to contain significant amounts of anhydrite also have comparatively high values of $Fe_2 O_3$ and from thin section are known to contain pyrite.

Carbonates.

Dolomite is the predominant carbonate in all the samples, the lowest recorded content being 88.22 per cent. (YG 4690); many values, particularly in samples from ML 2, exceed 99 per cent. Calcite was recorded in 17 samples and ranges in content from 0.13 per cent. (UP 162) to 7.52 per cent. (UP 185). All but one of the samples from ML 7 and ML 8 contain calcite but generally the occurrence of calcite is sporadic. When expressed in terms of the three "components" calcite, dolomite and total sulphate (gypsum plus anhydrite) in Figure 4-1, the 37 analyses cluster in the dolomite corner of the triangular diagram, emphasizing the very limited mineralogical composition of the samples examined.

In thin section, the dolomite occurs as subhedral grains 10 - 50μ in diameter, although individual sections tend to be

of uniform grain-size. Calcite, when present usually occurs in discrete areas as sparry crystals very much larger than the adjacent dolomite grains and commonly showing well-developed cleavage (e.g. Plate 4-2). It is interpreted as void filling (Bathurst, 1958, p. 20) and as such infills cavities and hair-line fractures, but also occupies intergranular pores as cement. In one sample (UP 51), a calcite mosaic occurs in the form of laths arranged in a semi-radial manner (see Plates 4-9, 4-10). This mode of occurrence is characteristic of the lagoonal facies of the Middle Magnesian Limestone, and the nature and origin of this texture are discussed fully in the relevant section of this chapter.

No beds of calcitic Lower Magnesian Limestone, similar to that found in masses at Raisby, Thickley and beneath Sheraton, were sampled in this investigation. The calcite in these apparently isolated masses of limestone is considered to be "primary" (e.g. Trechmann, 1914, 1921; Dunham, 1960), having escaped dolomitization for some reason; this form of occurence is in direct contrast to the clearly late-diagenetic calcite described here.

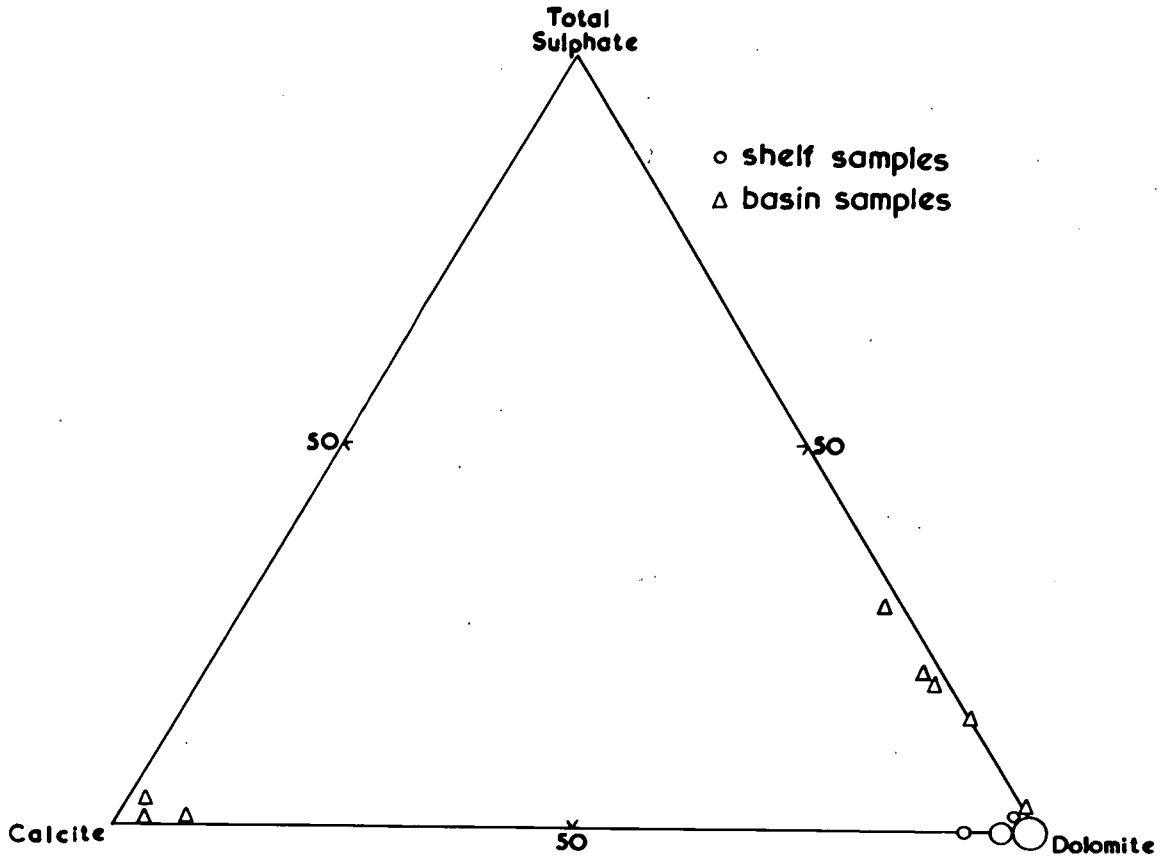

FIGURE 4–1. MINERALOGY OF THE SHELF AND BASIN FACIES OF THE LOWER MAGNESIAN LIMESTONE.

A larger symbol indicates the occurrence of several samples with similar compositions.

Other Components.

The non-carbonate/sulphate components reach a maximum recorded value of 8.55 per cent. in YG 4690, but as seen in Figure 4-2, values are most commonly below 1 per cent. The most important components are Fe_2O_3 and SiO_2. The Fe_2O_3 content is most commonly below 1 per cent. (Figure 4-3) with a maximum recorded value of 2.27 per cent. in K85. The sum of values for the components SiO_2, Al_2O_3, TiO_2, Na_2O and K_2O may be considered to give a crude indication of the quantity of inorganic detrital material in the samples. Figure 4-4 shows the variation in the quantity of detrital material in the facies. In borehole ML 2, the detrital content increases towards the base of the Lower Magnesian Limestone but in ML 11, the only other borehole in which the full thickness of shelf Lower Magnesian Limestone was sampled, the highest contents of detrital material are found near the middle of the division. In ML 13 and ML 14, the detrital material decreases in an upward direction, while in ML 7 and ML 8, there are no discernable consistent vertical changes. There is thus no consistent pattern in the distribution of detrital material which can be related to age.

LOWER MAGNESIAN LIMESTONE

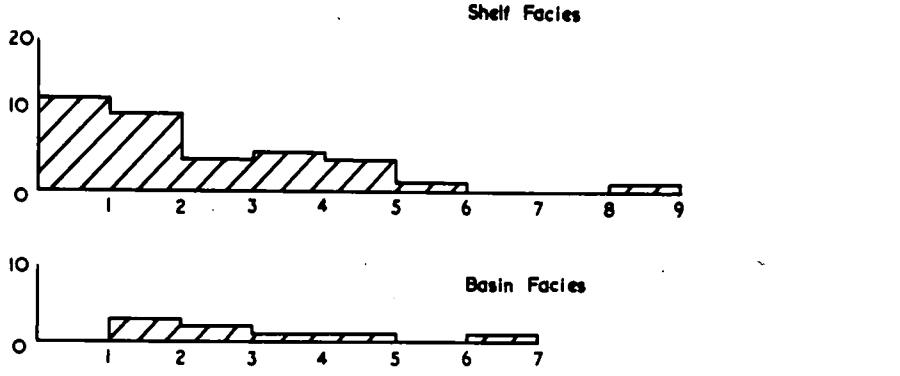

MIDDLE MAGNESIAN LIMESTONE

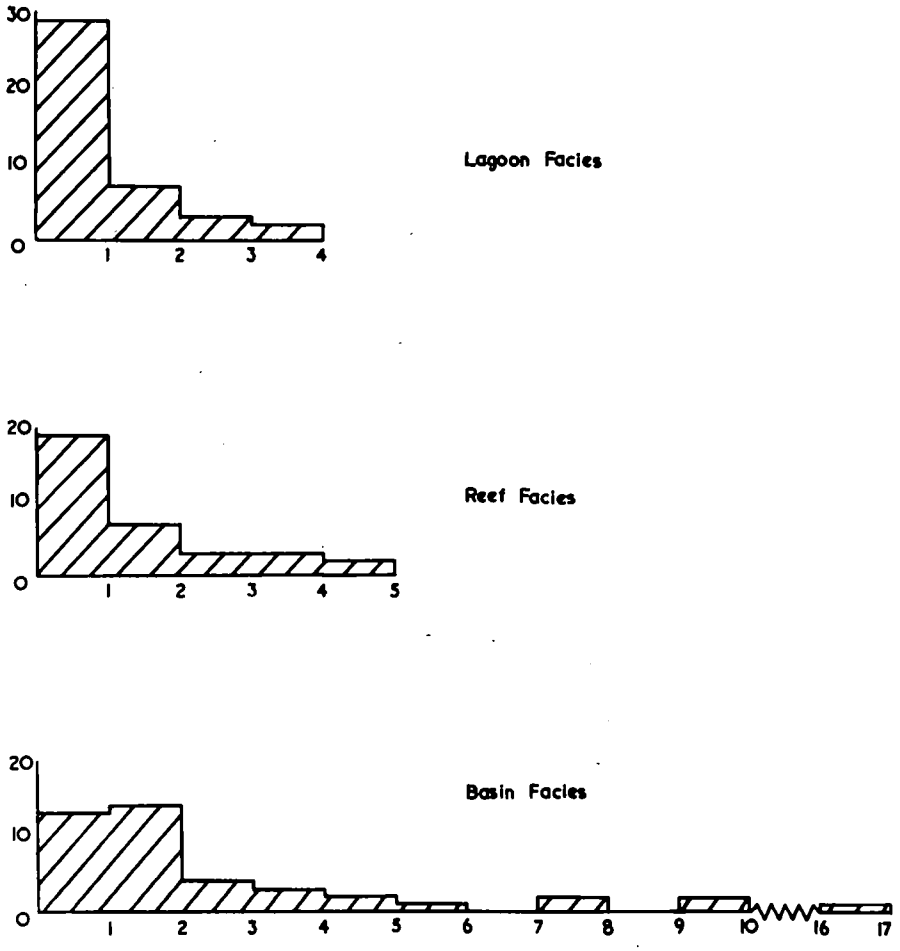

FIGURE 4–2. HISTOGRAMS SHOWING THE DISTRIBUTION OF NON–CARBONATE/SULPHATE MATERIAL.
Number of samples as the ordinate. Per cent. non-carbonate/sulphate material as the abscissa.

The highest contents of detrital material are found in boreholes ML 2, ML 11 and ML 13 and no evidence was found to support Trechmann's statement (1914, p. 258) that in the Lower Magnesian Limestone of Durham, the detrital residues increase towards the west, in the direction of the presumed Permian shoreline.

Lower Magnesian Limestone - Basin Facies.

This facies is very poorly represented as partial mineralogical analyses were obtained for only 8 samples taken from three boreholes. The Lower Magnesian Limestone was completely intersected in all three boreholes and the variation in thickness of the facies is recorded below:-

Borehole	ML 3	ML 6	ML 12
Thickness of Facies (ft in)	39 10	122 10½	18 6

The samples from borehole ML 3 were taken from the upper 27 ft of the division while those from ML 6 and ML 12 represent only the upper 11 ft of the division. In view of the difference

in total thickness of the division in the three boreholes, it is evident that the facies is only poorly represented by the samples taken from borehole ML 6.

Sulphates.

Gypsum is present in all 8 samples and ranges in concentration from 0.55 per cent. (YJ 1081) to 23.87 per cent. (YG 4400). Anhydrite was recorded in only 4 samples in which the content varies from 1 per cent. (B 50) to 15.08 per cent. (B 52); no anhydrite was recorded in samples from borehole ML 3. In all three boreholes, the gypsum content consistently increases upwards through the sequence, and in ML 12 there is a parallel decrease in the anhydrite content. In borehole ML 12 therefore, the gypsum:anhydrite ratio shows a marked increase towards the top of the division.

Smith (in Magraw et al., 1963, p. 172) has reported minor amounts of sulphate disseminated throughout the Lower Magnesian Limestone of the basin area. The logs of the boreholes from which the samples were taken record gypsum, and sometimes anhydrite, as small, acicular crystals and porphyroblastic blebs. Gypsum also occurs as thin, fibrous veins which are frequently sub-parallel to the bedding and which sometimes

brecciate the carbonate host-rock, apparently as a result of expansion following the hydration of anhydrite (Raymond, 1962). In some of the samples, particularly those from boreholes ML 6 and ML 12, sulphates, and especially gypsum, were visible under a hand lens. Unfortunately, the small size of the samples did not allow any thin sections to be taken and the textural relationships of the sulphate minerals could not be examined. However, Raymond (1962, p. 49) noted that in the "Lower Magnesian Limestone" of the Billingham area, anhydrite commonly occurs as corroded, relic crystals within the gypsum; the upwards increase in the gypsum:anhydrite ratio in borehole ML 12 shows how the hydration is related to depth from the surface.

Carbonates.

The relative proportions of calcite and dolomite vary remarkably in samples from this facies. In borehole ML 3, calcite is the predominant carbonate, having a concentration of 90 per cent. or more in the 3 samples examined. However, in samples from boreholes ML 6 and ML 12, the content of calcite is in every case less than 2 per cent. and dolomite is the predominant carbonate, ranging in concentration from 64.53 per cent. (YG 4400) to 96.09 per cent. (YG 4407). It is regrettable that no thin sections were available for the samples from

this facies as the calcite-dolomite relationship is obviously of great interest. Information bearing on this relationship must come indirectly from the Middle Magnesian Limestone basin facies which shows similar extremes in carbonate composition and for which some thin sections were available.

When expressed in terms of calcite, dolomite and total sulphate (Figure 4-1), the mineralogical analyses of samples from this facies contrast sharply with the neat cluster of analyses from the shelf facies of the Lower Magnesian Limestone. The basin samples fall naturally into two separate and contrasting groups. In one group, the calcite content is less than 2 per cent. and sulphate, which is present both as gypsum and anhydrite, reaches high values. The other group is characterized by very high calcite and low sulphate values entirely in the form of gypsum. The most obvious difference between the two groups is in the calcite content and the antipathetic relationship between calcite and sulphate is perhaps less obvious. No intermediate compositions exist with relatively high sulphate and calcite values. A similar phenomenon, believed to be due to the same cause, is observed in samples from the basin facies of the Middle Magnesian Limestone. The reason for the antipathetic relationship between calcite and sul-

phate is discussed later.

Other Components.

The non-carbonate/sulphate components reach a maximum recorded value of 6.92 per cent. in sample YG 4400 but are most commonly in the 1-2 per cent. range (see Figure 4-2). As in the shelf facies of the Lower Magnesian Limestone, Fe_2O_3 and SiO_2 are the most important components. Except for one value of 5.22 per cent. (YG 4400), the Fe_2O_3 values are all less than 1 per cent. (Figure 4-3). The content of inorganic detrital material, as indicated by the sum of values for the components SiO_2, Al_2O_3, TiO_2, Na_2O and K_2O, is most commonly in the 1-2 per cent. range (Figure 4-4), although the maximum recorded value is 4.05 per cent. in YJ 1072. Figure 4-4 shows that although higher values of inorganic detrital material occur in the shelf facies of the Lower Magnesian Limestone, the most common level in the basin facies is higher than in the shelf. In borehole ML 12, the content of detrital material increases downwards through the sequence, while the borehole log shows that the base of the Lower Magnesian Limestone is arenaceous and contains black, micaceous shaley partings. The increase in clastic material towards the base of the Magnesian Limestone in this borehole is almost certainly related to the presence of the underlying Carbon-

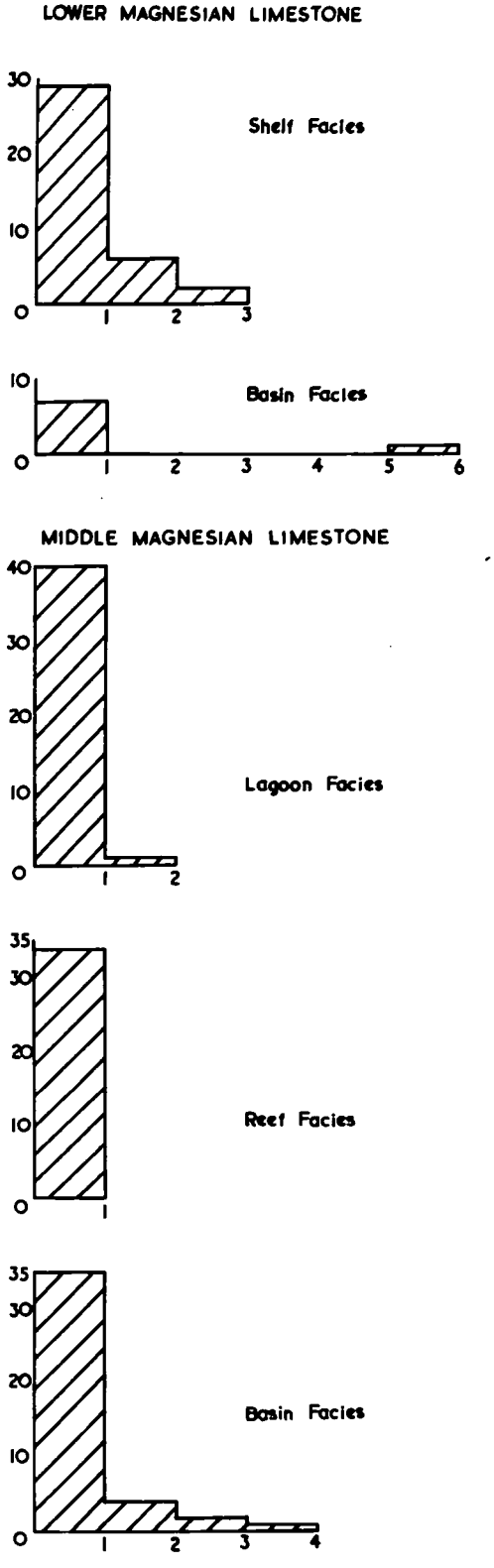

FIGURE 4–3. HISTOGRAMS SHOWING THE DISTRIBUTION OF Fe_2O_3. Number of samples as the ordinate. Per cent. Fe_2O_3 as the abscissa.

iferous basement "high". There does not appear to be any systematic lateral variation in the level of detrital material in the three boreholes.

Middle Magnesian Limestone - Lagoon Facies.

Partial mineralogical analyses were calculated for 41 samples taken from six boreholes which intersected beds of this facies. The thickness of the facies in each of the boreholes is given below:-

Borehole	ML 2	ML 7	ML 8	ML 11	ML 13	ML 15
Thickness of Facies (ft in)	184 (but top not seen)	298 6 (proved)	?41 (proved)	42 6 (proved)	c.52 7	168 (proved)

With the exception of ML 15, these boreholes were also used to furnish samples of shelf Lower Magnesian Limestone, and as in the case of the shelf facies of the Lower Magnesian Limestone, five of the sampling locations are situated south of the Butterknowle Fault.

The base of the division (i.e. the base of the transitional beds) is seen in all boreholes except ML 15, but the top of the division is seen only in ML 13 where it is overlain by the Middle Permian Marls. In ML 2, the uppermost part of the lagoonal beds is truncated by an interdigitation of the reef. The close proximity

of boreholes ML 2 and ML 7 to the reef would suggest that the greater part of the lagoonal Middle Magnesian Limestone is present in these two boreholes. In ML 8 and ML 11, only the lower part of the division is preserved, while in ML 15, the relative position of the intersection is uncertain as neither the top nor the bottom of the division is seen.

Sulphates.

Sulphates were recorded in the analyses of only 2 samples from this facies, UP 49 with 1.78 per cent. anhydrite and 0.09 per cent. gypsum and UP 21 with 0.24 per cent. anhydrite. No trace of either gypsum or anhydrite was observed in thin sections of these samples. The relatively shallow depth from which these samples were taken and the presence of pyrite and a comparatively high Fe_2O_3 content in UP 49 suggest that these sulphate values are a reflection of the amount of pyrite in the samples. Trechmann (1914, p. 246) however, recorded small, but consistent, quantities of sulphur trioxide, apparently attributable to traces of gypsum, in samples taken from this facies north of the Butterknowle Fault. In South Durham, the lagoonal facies is known to contain sulphates, particularly where it is overlain by the Middle Permian Marls/Lower Evaporites. Thus,

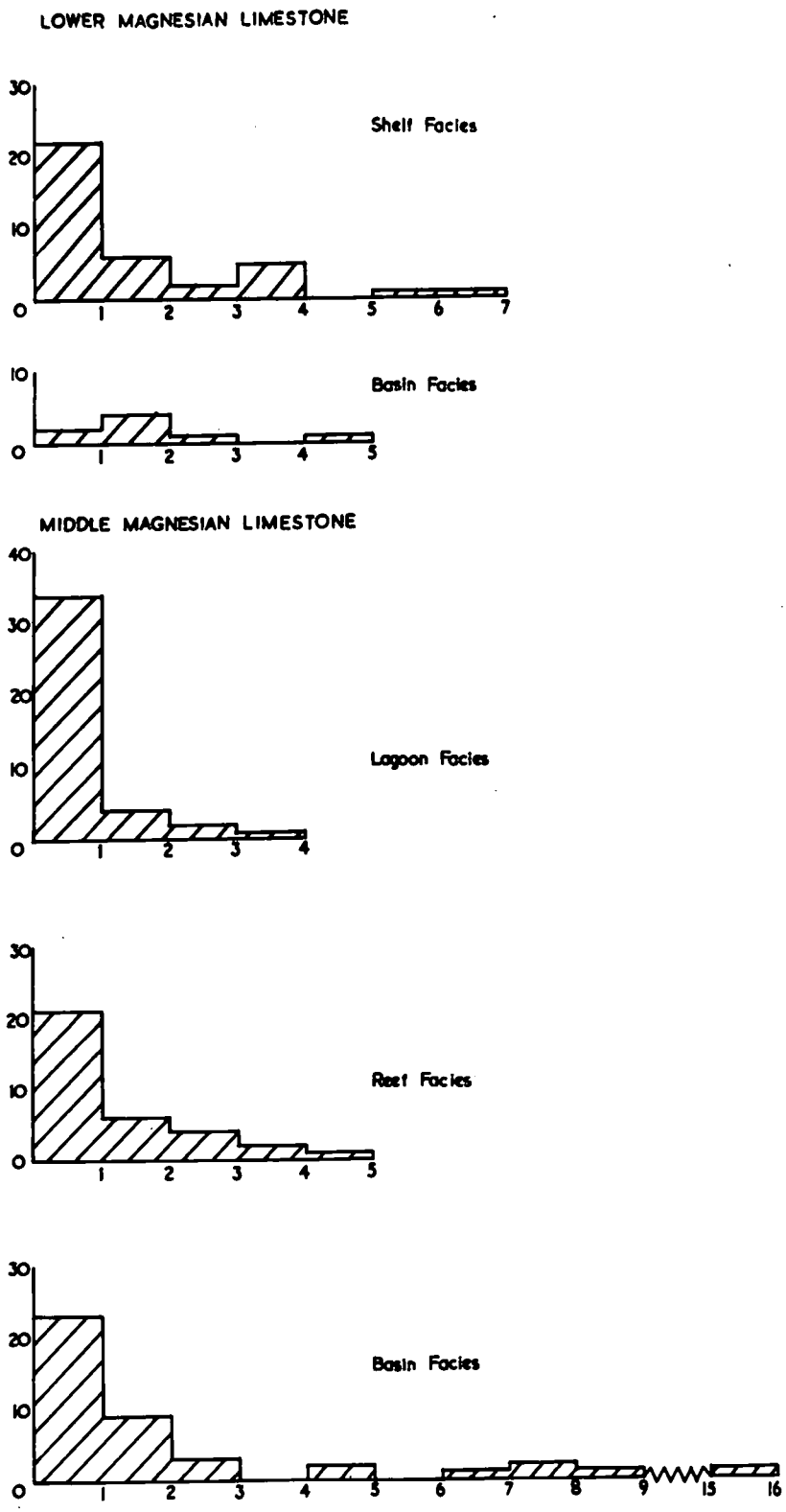

FIGURE 4–4. HISTOGRAMS SHOWING THE DISTRIBUTION OF INORGANIC DETRITAL MATERIAL.
Number of samples as the ordinate. Per cent. inorganic detrital material as the abscissa.

in a borehole at Wynyard (N.G.R. NZ 4166 2469), gypsum with minor anhydrite occurs as pore filling, porphyroblastic blebs, radiating clusters of "needles" and thin, fibrous veins within the dolomite host-rock. In borehole ML 13, small amounts of sulphate are known to occur in association with thin beds of mudstone which are occasionally intercalated with the beds of lagoonal dolomite.

Carbonates.

Dolomite is the predominant carbonate in all the samples analysed. The lowest recorded value is 59.56 per cent. in UP 21, but many samples contain in excess of 99 per cent. Calcite is present in 15 samples, the highest recorded value being 39.73 per cent. (UP 21) although 10 of the samples contain less than 10 per cent.; all six boreholes contain calcitic samples. In borehole ML 8, only samples from the transitional beds are calcitic, and in ML 11 and ML 13, slightly calcitic samples are found in the lower part of the division. However, calcite also occurs at higher levels, sometimes in considerable quantities, and no particular part of the succession appears to be constantly calcitic.

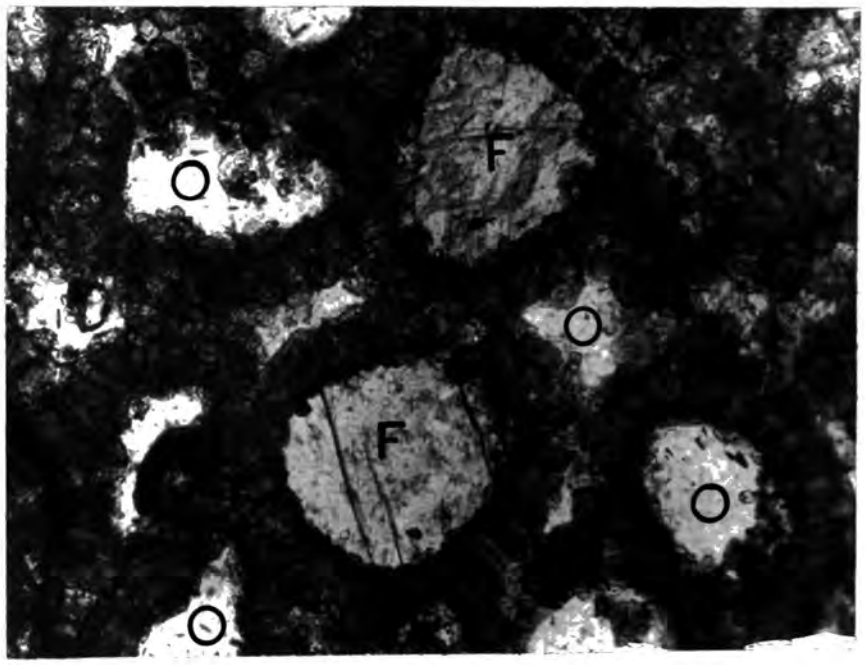

Plate 4-1. Highly porous, oolitic dolomite with some voids open (O) and others filled with calcite (F). Thin section, plane polarized light, X 160.

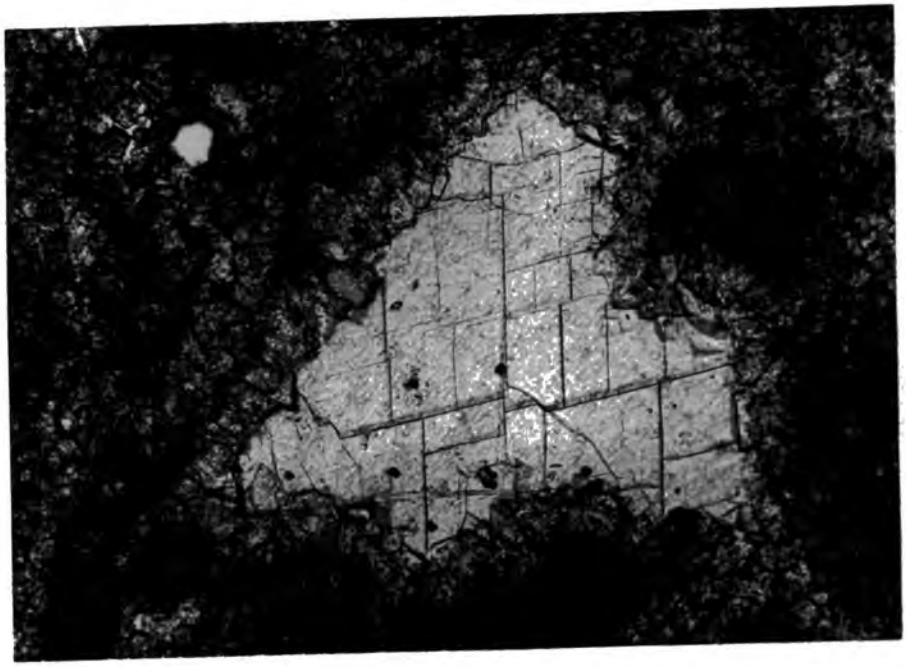

Plate 4-2. Calcite completely filling a cavity in reef dolomite. The calcite is separated from the dolomite matrix by a single layer of large dolomite crystals. Thin section, plane polarized light, X 100.

When the analyses are plotted on a triangular diagram in terms of calcite, dolomite and total sulphate (Figure 4-5), the two component mineralogical nature of the lagoonal samples is brought out. The analyses are scattered along the calcite-dolomite axis with only UP 49 showing the presence of a significant amount of sulphate. As discussed above, it seems certain that this sulphate value, together with that recorded for UP 21, is essentially a manifestation of the quantity of pyrite in the sample. This being the case, it is true to say that the samples of lagoonal Middle Magnesian Limestone investigated are all extremely pure carbonate rocks and that the analyses are in agreement with Smith and Francis (1967, p. 123) who report that the carbonate rocks of the lagoonal facies are almost universally dolomitic.

In thin section, the dolomite usually occurs as euhedral to subhedral rhombs 10-70 μ in diameter, although individual sections tend to show a uniform rhomb-size. In oolitic and pisolitic rocks, the dolomite rhombs are commonly loosely packed and this, together with the open texture usually associated with rocks composed of accretionary grains (see Plate 4-1), gives the rocks a high porosity. In finely granular rocks of the facies, the dolomite rhombs are frequently closely packed (see

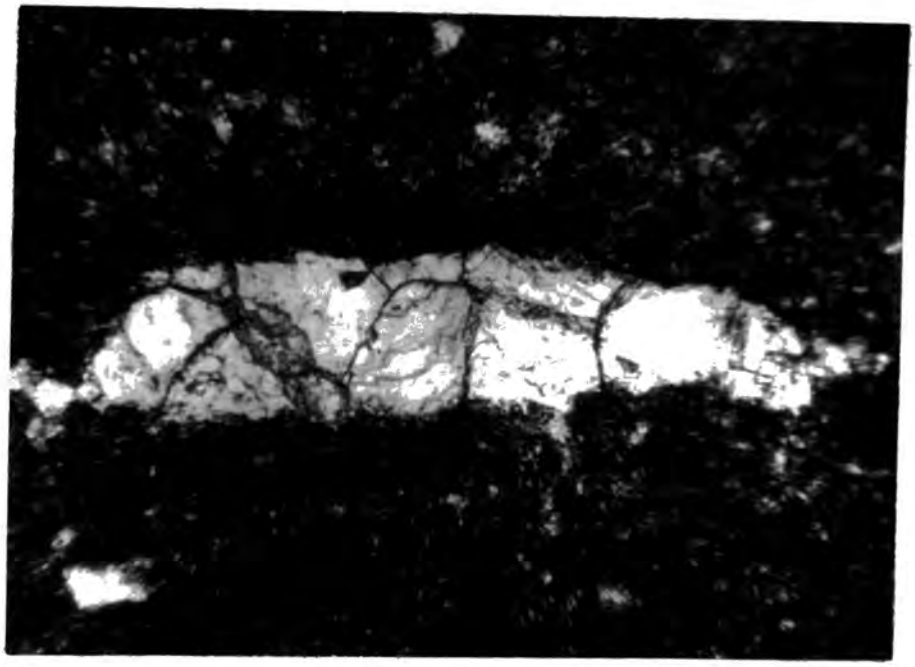

Plate 4-3. Calcite completely filling an elongate void in alga—laminated dolomite. Thin section, plane polarized light, X 200.

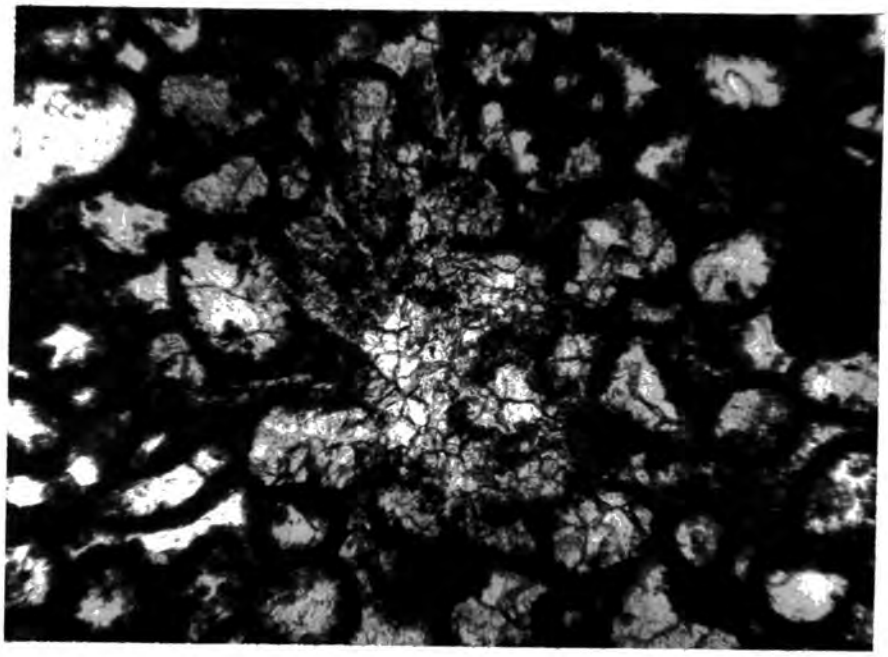

Plate 4-4. Calcite filling inter- and intra-accretionary grain voids and replacing the dolomite walls of some ooliths. Thin section, plane polarized light, X 50.

Plate 4-9) and usually show a uniform equigranular texture which gives these rocks a low porosity.

Although calcite appears to be the less common carbonate, thin sections taken from analysed samples, together with sections taken from representative lithologies at outcrop, show that this mineral becomes locally important. Calcite probably occurs most commonly as sparry crystals, interpreted as void filling. In oolitic and pisolitic rocks, the calcite infills both the interiors of the ooliths and pisoliths and the interstices between the individual accretionary grains (see Plates 4-1, 4-4). In some of the large pisoliths (0.5-1 cm in diameter), the calcite also occupies the elongate voids lying between the individual concentric layers of the pisoliths. In granular beds, the voids are usually in the form of cavities which cut across the original sedimentary fabric. Smaller cavities are usually completely filled with calcite (as in Plate 4-2), whereas the larger ones, clearly visible with the naked eye, only show a lining of dog-tooth crystals. Cavities of this type also occur in oolitic and pisolitic beds, but appear to be more common in the granular beds. Hairline fractures, which are present in many beds, are also often filled with sparry calcite.

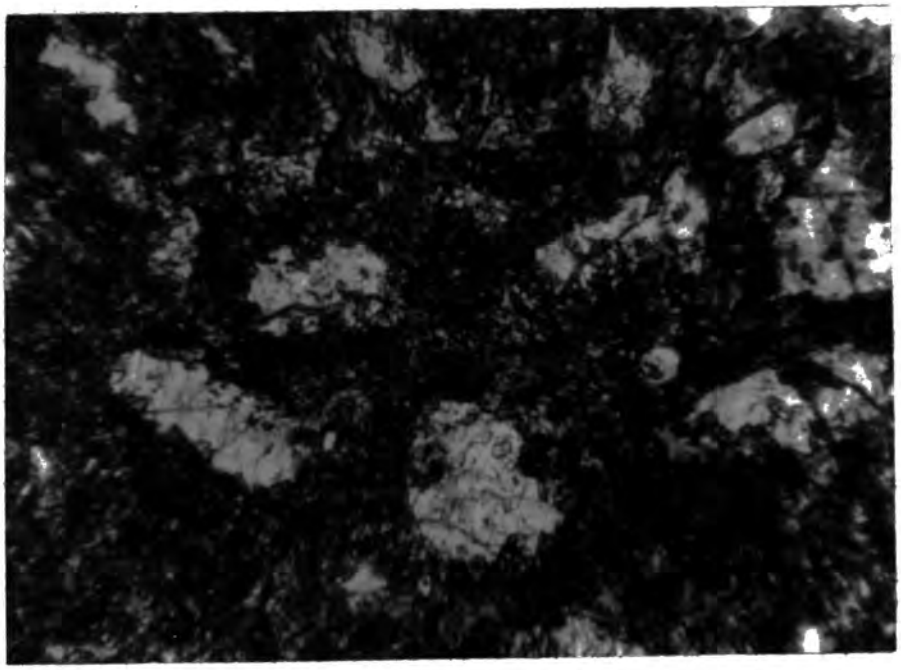

Plate 4-5. Thin section, plane polarized light, X 250.

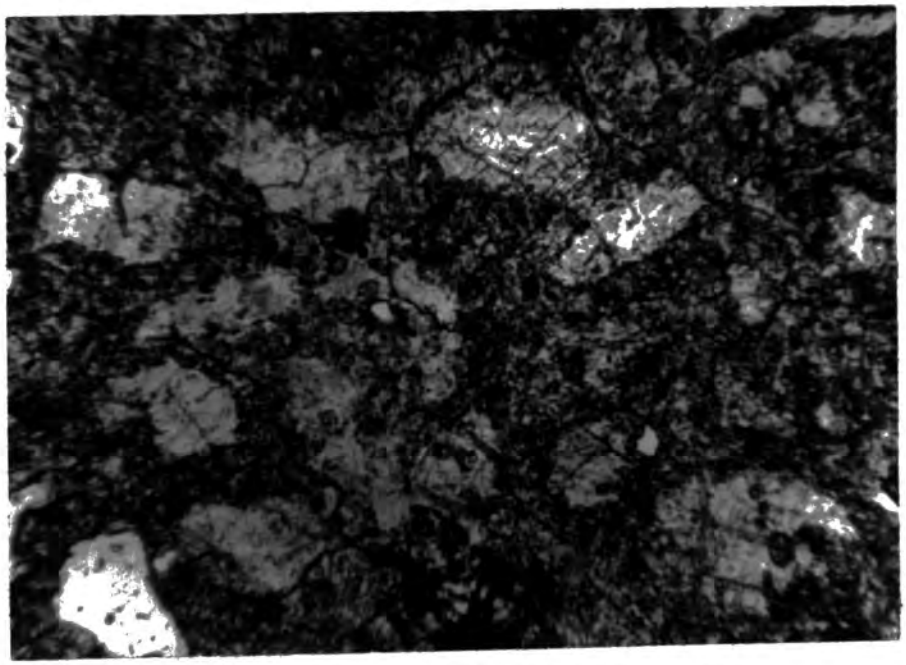

Plate 4-6. Thin section, plane polarized light, X 200.

Oolitic dolomite with void-filling calcite in inter- and intra-accretionary grain positions (Plate 4-5) passing into slightly dedolomitized oolitic rock (Plate 4-6).

In oolitic and pisolitic rocks, where both the accretionary grain interiors and adjacent interstices are infilled with calcite, the inter- and intra- accretionary grain calcite is sometimes seen to be continuous, and part or all of the grain wall is outlined by included trails of very small dolomite crystals (see Plates 4-4, 4-7). The dolomite inclusions appear to be too scattered to form a supporting framework; hence, the calcite is not simply cement. However, the dolomite does not appear to be replacing the sparry calcite because it does not have the large euhedral form characteristic of replacement dolomite. The texture is attributed to dedolomitization in which calcite has replaced dolomite by a centripetal process (Shearman et al., 1961). In most cases, the phenomenon appears to be developed only in isolated areas on a small scale. Occasionally, a very sharp transition may be observed within the area of one section, from oolitic or pisolitic dolomite with sparry calcite in inter- and intra- grain void-space to a mosaic of equigranular calcite crystals in which the outlines of the former accretionary grains are recognizable by the trains of dolomite inclusions (Plates 4-5, 4-6, 4-7), On fresh surfaces, such rocks show lustre mottling while differential weathering of the bands of dolomite and "dedolomite" gives rise to a ribbed surface. Sometimes, the dolomite bands are more resistant than the dedolomitized ones, but in other cases the reverse is true; possibly the original

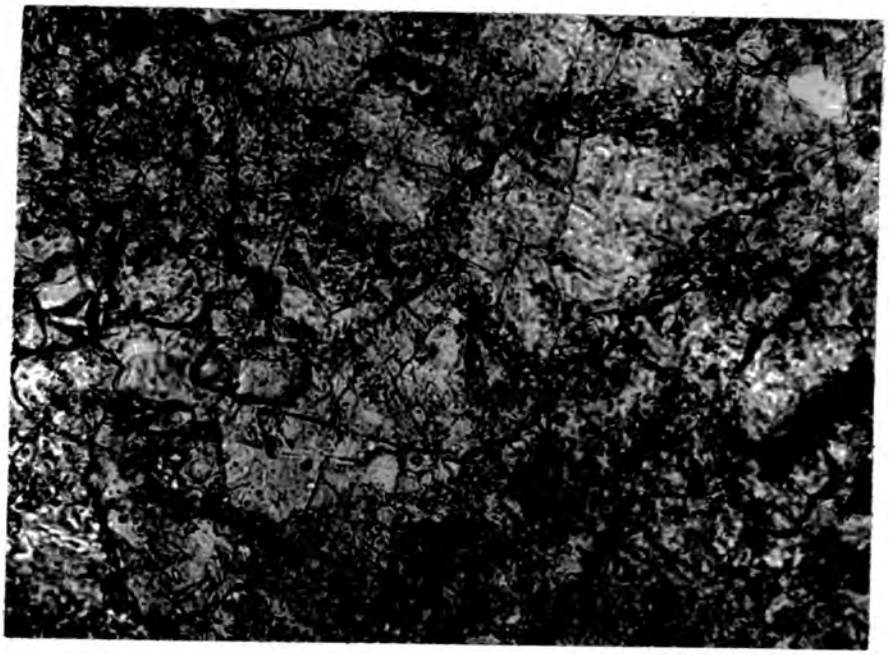

Plate 4-7. Almost completely dedolomitized rock in which outlines of former ooliths are preserved by trails of dolomite inclusions within replacement calcite (see Plates 4-5, 4-6). Thin section, plane polarized light, X 320.

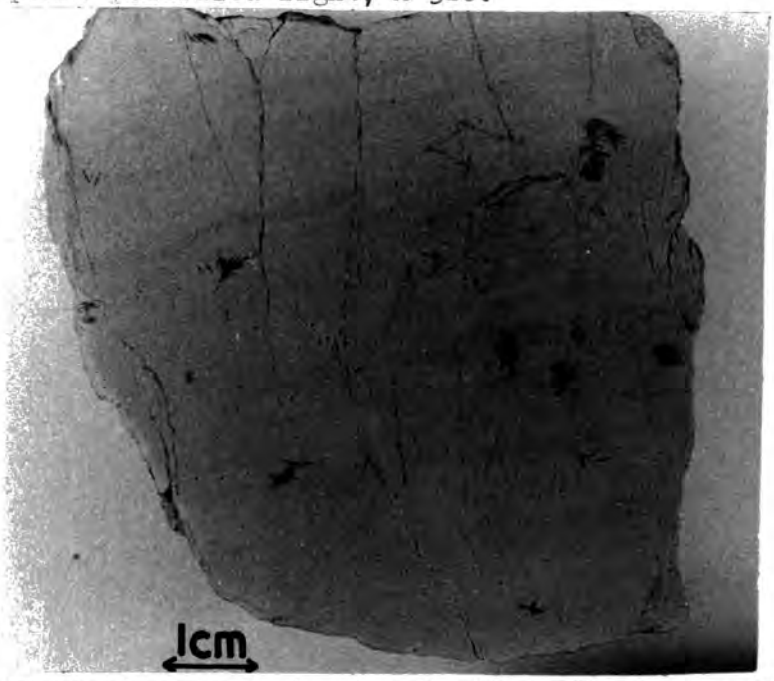

Plate 4-8. "Felted" texture developed within finely granular dolomite of the lagoon facies of the Middle Magnesian Limestone. Hand specimen.

texture is critical in determining resistance to weathering. This type of dedolomitization appears to occur often in the lagoonal rocks adjacent to fault zones. Dedolomitization which is apparently related to fault movement has also been noted by Trechmann (1914, p. 252, footnote 2) and Smith and Francis (1967).

Calcite occurs less commonly, but more conspicuously, as an equigranular crystal mosaic in laths up to 1 cm long. These composite calcite laths are arranged in sheath and radial forms (Plates 4-9, 4-10) to which Smith and Francis (1967, p. 123) have given the name "felted" texture. This texture is clearly visible with the naked eye (Plate 4-8) and is developed irregularly, but particularly in the finely granular dolomite beds with few oolitic and pisolitic remains. Smith and Francis (op. cit.) consider this texture to be virtually confined to the lagoonal beds and in this investigation, examples of "felted" texture were only seen once elsewhere - in a sample (UP 51) from the shelf facies of the Lower Magnesian Limestone. Smith and Francis also reported that the "felted" texture involved recrystallized dolomite, but in all the sections examined in this investigation, staining revealed that calcite, sometimes ferroan, was the only carbonate producing this texture. The individual

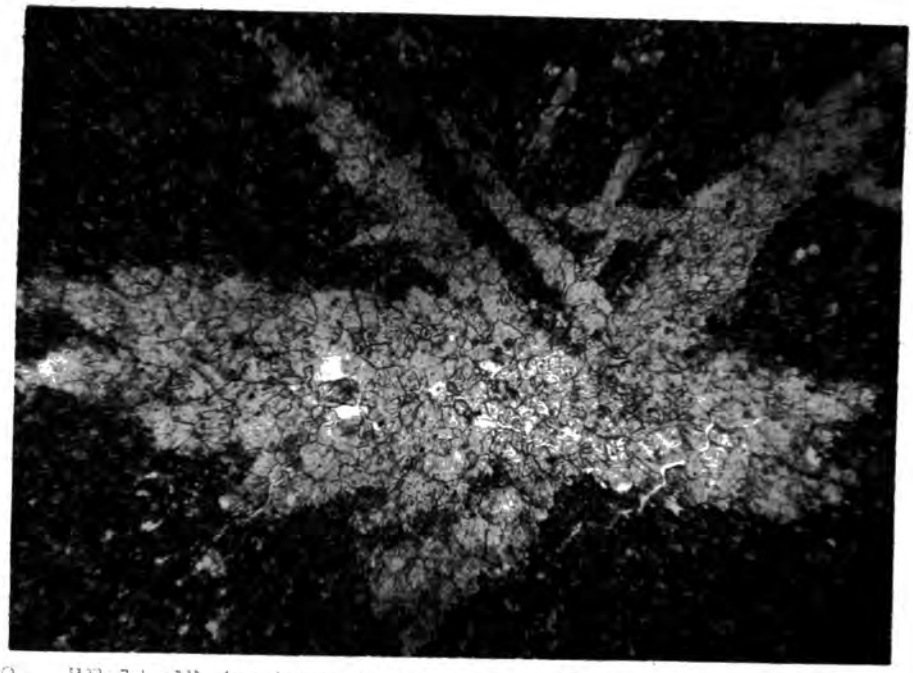

Plate 4-9. "Felted" texture developed within fine-grained equigranular dolomite. Composite calcite laths arranged in sheath and semi-radial form. Thin section, plane polarized light, X 50.

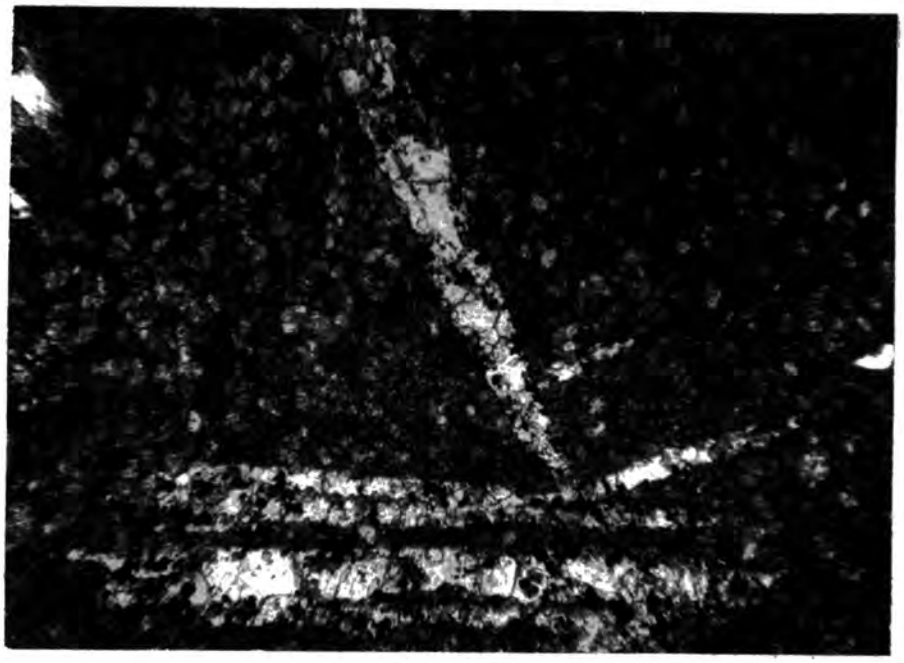

Plate 4-10. "Felted" texture with associated pyrite crystals developed within inequigranular dolomite. In some cases, individual composite calcite laths are separated by small dolomite rhombs but in other cases, they mutually interfere. Thin section, plane polarized light, X 50.

laths, where they do not mutually interfere, are often separated by small dolomite rhombs (Plate 4-10) and contain small, scattered dolomite inclusions. For reasons similar to those outlined above, the dolomite inclusions are considered to be relics left after replacement of the dolomite host-rock. However, while dolomite inclusions within calcite are characteristic of centripetal dedolomitization (Shearman et al., 1961), to the writer's knowledge the replacement calcite has never been reported to have taken a form similar to the "felted" texture.

Evidence for the origin of the texture comes from the sides of the composite calcite laths; they are straight, end abruptly against the dolomite host-rock (e.g. Plate 4-10) and sometimes show the development of rectangular re-entrants and projections (Plate 4-11). According to Murray (1960) and Lucia (1961), these features are characteristic of replacement anhydrite, and the "felted" texture is here considered to represent the former presence of replacement sulphate in the lagoonal facies of the Middle Magnesian Limestone. Samples taken from the lower part of the Middle Magnesian Limestone, intersected in a borehole in the Wynyard area (N.G.R. NZ 4166 2469), consist of oolitic dolomite and contain sulphate which, among

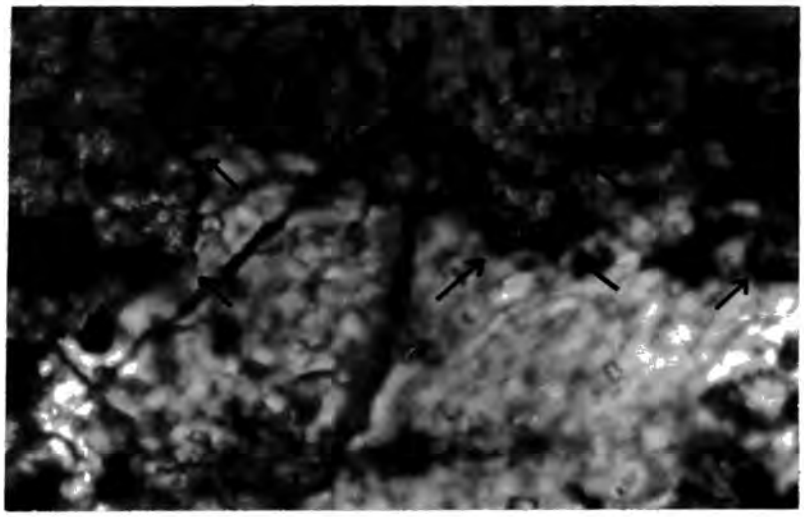

Plate 4-11. High magnification of the side of one of the composite calcite laths shown in Plate 4-10 showing the development of rectangular re-entrants and projections (indicated). Thin section, plane polarized light, X 320.

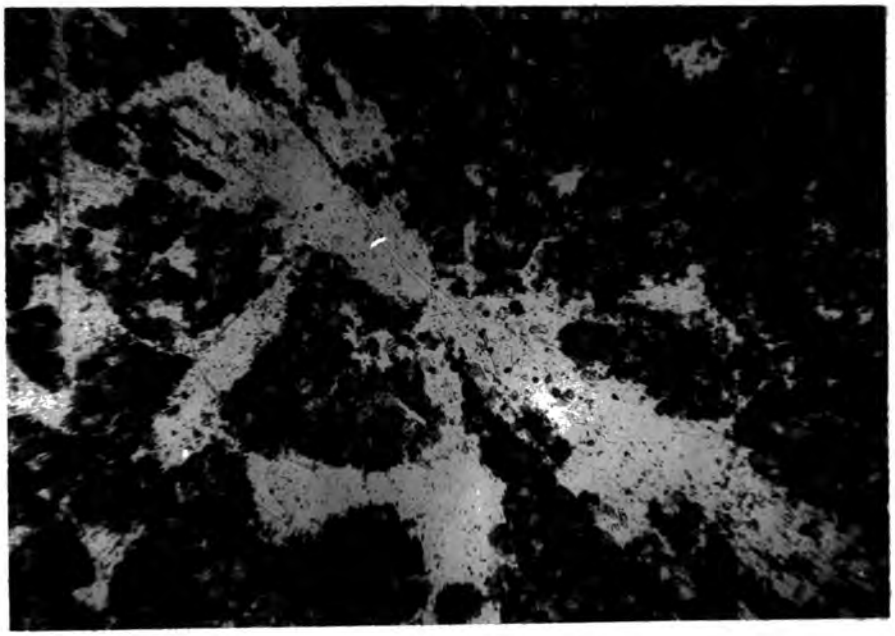

Plate 4-12. Semi-radial arrangement of replacement gypsum "needles" in dolomite from a borehole in South-East Durham. Thin section, plane polarized light, X 50.

other forms, occurs as sheath-like and radiating clusters of gypsum "needles" (Plate 4-12). These clusters cut across, and hence replace, the original sedimentary fabric, while individual "needles" have straight sides, rectangular re-entrants and contain scattered dolomite inclusions. Trechmann (1914, analysis XLIX and plate XXXVII, fig. 1) also recorded almost identical replacement sulphate, complete with dolomite inclusions, from basinal Middle Magnesian Limestone immediately below the Hartlepool Anhydrite. The similarity in form between the replacement sulphate clusters and the "felted" texture is further supported by the occurrence of pyrite crystals in association with some composite calcite laths of the "felted" texture (Plate 4-10). Raymond (1953, p. 287; 1962, p. 49) noted that in the Magnesian Limestone of South Durham and North Yorkshire, rims of small pyrite crystals are a characteristic feature of some sulphate "inclusions". The very delicate internal form of many of the sheaths and radiating clusters of the "felted" texture, together with the presence of dolomite inclusions within the calcite, suggests that the calcite actually replaced the replacement sulphate and did not simply fill the voids left after solution of the sulphate as described by Lucia (1961, p. 1107) in the Permian Tansill Formation. The calcite of the "felted" texture is often associated with limon-

ite and not pyrite, while the calcite itself is of the ferroan variety although adjacent void-filling calcite is not. This suggests that the pyrite rimming the sulphate may have become involved in the reactions leading to replacement by calcite.

The original form of the sulphate is problematical, although the straight sides and rectangular re-entrants observed in both the "felted" texture and the sulphate clusters from the Wynyard borehole are usually quoted as being characteristic of replacement anhydrite. The crystal form of gypsum, however, suggests that it could also develop similar features if it were the original replacement mineral; indeed, the sulphate clusters examined in the samples from the Wynyard borehole are all of gypsum, apparently free of anhydrite relics. Nevertheless, in the example described by Trechmann (q.v.), the sulphate was in the form of anhydrite, and all the evidence from the South Durham area suggests that while gypsum forms diagenetically by hydration of anhydrite, the reverse transition seldom, if ever, takes place. If alteration of anhydrite to gypsum occurred prior to replacement of the sulphate by calcite, it must have taken place on an equal-volume basis, as no fractures attributable to expansion following hydration (see Raymond, 1962) were observed radiating from any examples of the "felted" texture.

The textural relationships suggest that the following sequence of events led to the development of the "felted" texture. Formation of dolomite was followed by introduction of replacement sulphate, most probably in the form of anhydrite. Gypsum may possibly have been the original form of sulphate, or gypsum may have formed from original anhydrite by a process of constant-volume hydration. Finally, the replacement sulphate was in turn replaced by calcite.

The fact that the "felted" texture is especially characteristic of the lagoonal Middle Magnesian Limestone, together with the fact that the texture appears to represent the former presence of replacement sulphate, has further implications. It suggests that the lagoonal beds of Central Durham formerly contained sulphate in the form of sheaths and clusters of "needles" as the lagoonal beds of South Durham still do today. As the lagoonal Middle Magnesian Limestone of South Durham is overlain by the Lower Evaporites/Middle Permian Marls, the recognition of the former presence of sheaths and clusters of sulphate "needles" within equivalent beds in Central Durham lends support to the suggestion (see Chapter 2) that the Middle Permian Marls once extended much farther north. Indeed, the removal of these overlying evaporites and red beds may in some way be responsible for the further replacement of the sulphate

sheaths and clusters by calcite in Central Durham.

Other Components.

The non-carbonate/sulphate components in all samples from this facies are very low in quantity. The maximum recorded value is 3.53 per cent. (YG 4625) but the majority of samples contain less than 1 per cent. (Figure 4-2). The $Fe_2 O_3$ content (Figure 4-3) is less than 1 per cent. for all samples except UP 49 which contains 1.71 per cent. This comparatively high $Fe_2 O_3$ value is almost certainly due to the fact that the sample contains pyrite. Figure 4-4 shows that the content of inorganic detrital material is most commonly less than 1 per cent. Smith and Francis (1967, p. 126) have also noted the remarkably low level of detrital material in the lagoonal facies of the Middle Magnesian Limestone.

In borehole ML 8, the content of inorganic detrital material decreases in an upward direction, whereas in ML 2, the reverse trend is observed. The other boreholes show no apparent systematic vertical variation in the distribution of inorganic detrital material. Perhaps more surprisingly, the boreholes reveal no marked lateral variation in the content of detrital material within the facies. It might be expected

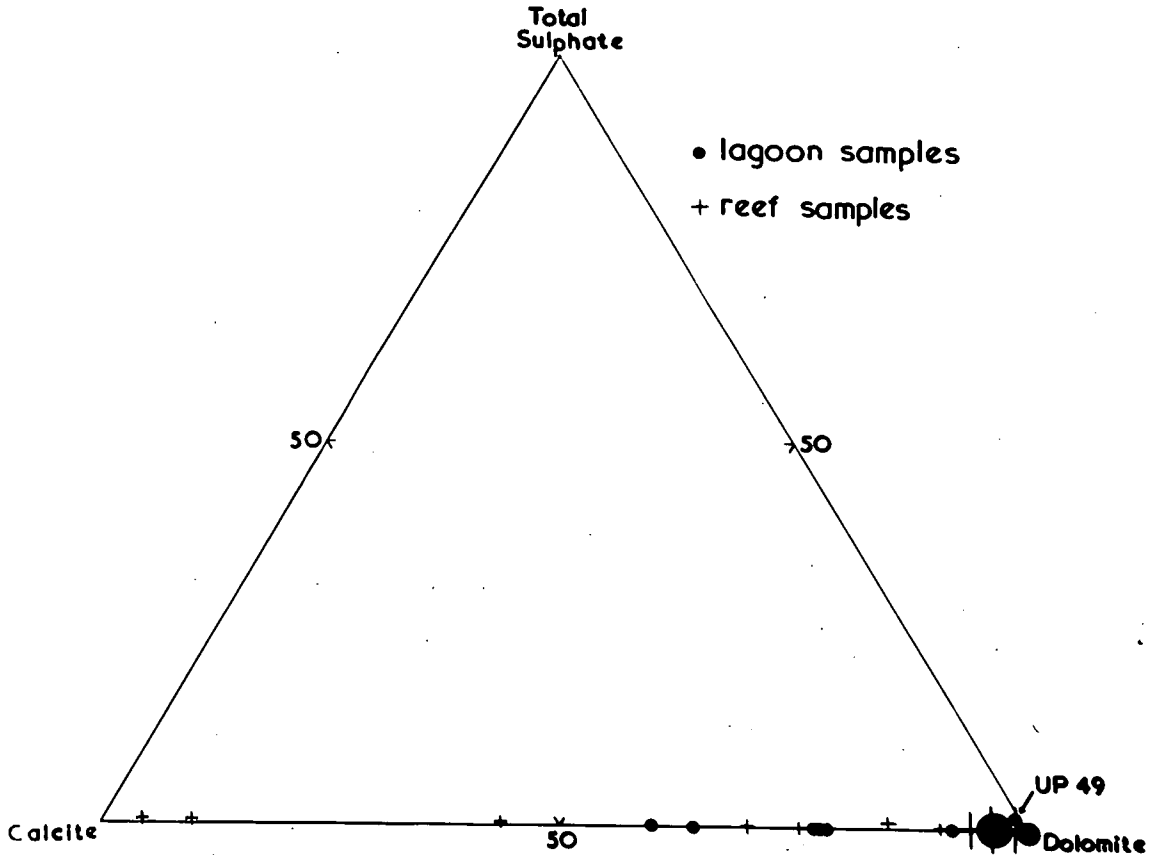

FIGURE 4-5. MINERALOGY OF THE LAGOON AND REEF FACIES OF THE MIDDLE MAGNESIAN LIMESTONE.

A larger symbol indicates the occurrence of several samples with similar compositions.

that a reef-bound, shallow-water, lagoonal environment would act as a very effective trap for land-derived material, even though the adjacent land is believed to have been of low-relief and the climate is considered to have been arid. The general low level of detrital material shows that this is not true. It is not even possible to detect a general increase in the content of detrital material going towards the west, in the direction of the presumed shore-line; in fact, borehole ML 2, which is closest to the reef, shows the highest general level of detrital material in the lagoonal facies.

Middle Magnesian Limestone - Reef Facies.

Partial mineralogical analyses were obtained for 34 samples taken from the inclined adit ML 1 and the two boreholes ML 2 and ML 5.

The inclined adit ML 1 gives an almost complete section through the reef, beginning in the transitional beds and ending in collapse-brecciated reef, and perhaps post-reef dolomite. In borehole ML 2, 32 ft 6 in of reef-rock is overlain by post-reef beds and underlain by beds of lagoonal facies; this development is believed to represent the last stages of reef formation near the edge of the lagoon. In ML 5, reef facies dolomites are interbedded with lagoonal beds in a presumed

zone of interdigitation on the landward side of the reef. In this borehole, 85 ft of reef-rock are separated by 12 ft of lagoonal beds from 68 ft of younger, alga-laminated reef dolomite. The upper reef-rocks are overlain by post-reef beds, while the lower reef-rocks are underlain by beds of lagoonal facies. The reef intersections in boreholes ML 2 and ML 5 must therefore be equivalent to the upper part of the reef section exposed in the inclined adit ML 1.

Sulphates.

Small quantities of sulphate were recorded in 5 samples from this facies. Gypsum is present in 3 samples from ML 1 and ranges in value from 0.33 per cent. (ED 31) to 0.82 per cent. (ED 33), while values of 0.19 per cent. and 0.76 per cent. anhydrite were recorded in the analyses of samples ED 17 and Y G F 1038 respectively. The shallow depth of the anhydrite-bearing samples suggests that the sulphur is actually present in some other form, perhaps as pyrite, although neither sample shows a relatively high $Fe_2 O_3$ content.

The presence of gypsum in 3 samples (ED 31, 33 and 35) from the adit ML 1 also requires comment. Samples ED 33 and 35 are taken from reef-rock which shows signs of collapse-

brecciation. Smith and Francis (1967, p. 137) have noted that fragments of soft red and green marl are incorporated in these breccias; from South Durham it is known that sulphates are usually associated with red and green Permian marls. However, all 3 samples were taken from near the top of the adit where they lay within a few feet of the surface. The preservation of gypsum under such conditions seems very unlikely. Consequently, these analyses are regarded with suspicion, with the possibility of error both in the method of analysis and in the recalculation procedure.

Carbonates.

Dolomite is the predominant carbonate in all the reef samples except ED 17, 33 and 35 which contain 55.58 per cent., 92.97 per cent.and 86.29 per cent. calcite respectively. Calcite occurs as the minor carbonate in 16 other samples, ranging in content from 0.16 per cent. to 29.54 per cent. In the adit ML 1, calcite is absent in the transitional and lower reef beds but becomes more important at higher levels; a similar trend is observed in borehole ML 5. Only the lowest sample of reef-rock from borehole ML 2 contains calcite. When plotted on a triangular diagram (Figure 4-5), the analyses of samples from this facies lie scattered along the calcite-dolomite axis and

differ from the lagoonal analyses only in showing a greater range of carbonate composition.

In thin section, dolomite forms two populations of euhedral to subhedral grains characterized by different diameters. Algal laminations and details of algal colonies and fossil walls are preserved by dolomite grains 10 - 15μ in diameter, while the remainder of the dolomite occurs as grains 25 - 50μ in diameter. The relative proportions of the two populations vary considerably, although the smaller dolomite grains are generally less common. Thin sections of rocks with a large proportion of the smaller grains have a characteristic opaque appearance at low magnifications.

Calcite has two basic modes of occurrence, one of which is very much more common than the other. In most sections, calcite occurs in cavities and sometimes in hairline fractures as sparry crystals which have all the characteristics of void filling. In cavities, the sparry calcite is often separated from the dolomite matrix by a single layer of large dolomite crystals up to 100μ in size (Plate 4-2). Smaller cavities are usually completely filled with calcite whereas the larger cavities, which are readily discernable with the naked eye, are often only partly filled. In rocks showing prominent algal lamination, elongate voids occurring in interlaminae positions

are common (Plate 4-3). Void-filling calcite also occupies intergranular pores as cement. The intergranular pores adjacent to larger voids and cavities are, in particular, frequently filled with calcite.

Sometimes, the calcite cement appears to have extended into the dolomite matrix by replacement as it encloses small dolomite crystals incapable of forming a supporting framework. This is particularly true when the dolomite inclusions are concentrated in the centre of calcite crystals (Plate 4-13) and give rise to a clotted or "grumeleuse" texture (see Shearman et al., 1961, p. 5; Lucia, 1961, p. 1108; Evamy, 1967, p. 1207). Calcite which replaces dolomite in this manner usually occurs only sporadically in reef-rocks; it is much less common than void-filling calcite, to which it appears to be related genetically. However, in beds overlying the massive reef dolomite in the adit ML 1, dedolomitization appears to be locally very important and accounts for the highly calcitic nature of some horizons.

Other Components.

The non-carbonate/sulphate components reach a maximum recorded value of 4.52 per cent. in sample YG 4562, although most samples contain less than 1 per cent. (Figure 4-2). The

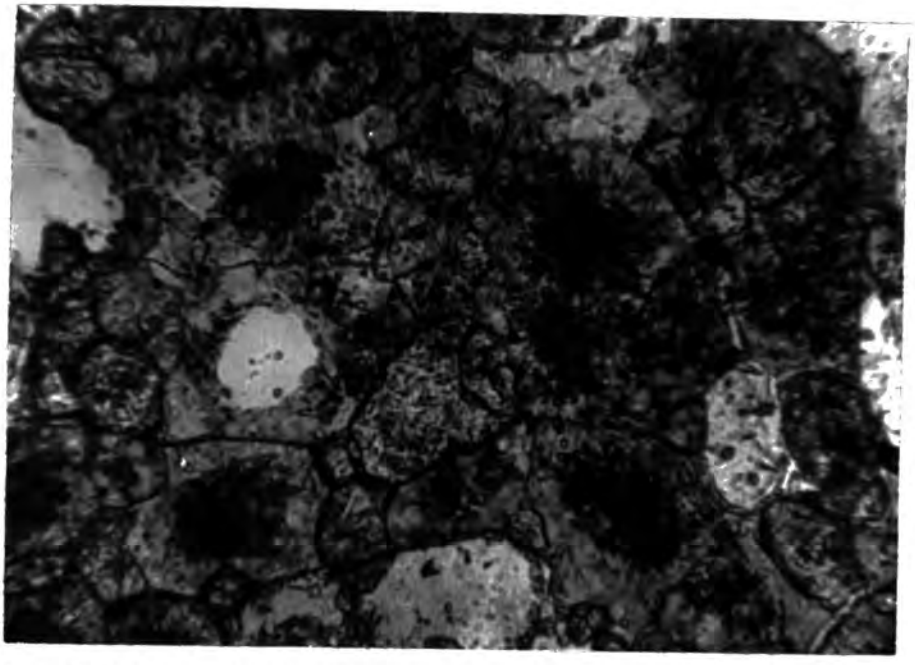

Plate 4-13. Dolomite inclusions concentrated near the centre of replacement calcite giving rise to a clotted or "grumeleuse" texture. Thin section, plane polarized light, X 250.

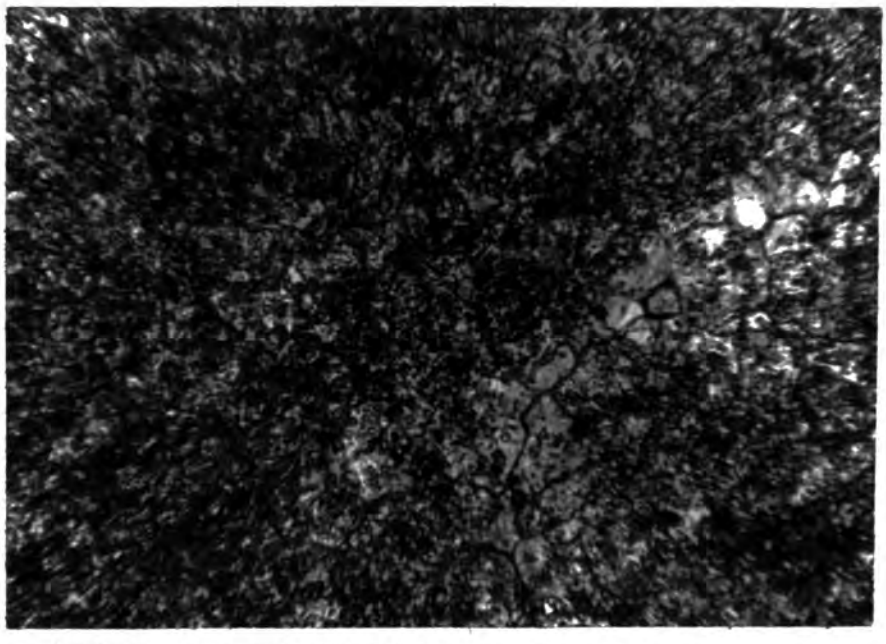

Plane 4-14. Replacement calcite which is cloudy in appearance due to the presence of densely packed dolomite inclusions. Thin section, plane polarized light, X 200.

reef is thus very pure and is similar to the lagoon facies of the Middle Magnesian Limestone. $Fe_2 O_3$ values are in every case less than 1 per cent. (Figure 4-3). The content of inorganic detrital material is most commonly less than 1 per cent. (Figure 4-4), although the maximum recorded value is 4.29 per cent. in sample YG 4562. In the adit ML 1, the highest contents of detrital material occur in samples ED 33 and 35 which were taken from the brecciated beds in which Smith and Francis (1967) recorded fragments of red and green marl.

Middle Magnesian Limestone - Basin Facies.

Partial mineralogical analyses were calculated for 42 samples taken from three boreholes in which the facies was completely intersected. The variation in the thickness of the facies in the boreholes is shown below:-

Borehole	ML 3	ML 6	ML 12
Thickness of Facies (ft in)	94	136 7	191 6 (but see Appendix 1)

In all three boreholes the facies is underlain by basinal Lower Magnesian Limestone. In ML 3 and ML 6, the facies is overlain

by the Hartlepool Anhydrite, while in ML 12 it is overlain by the Lower Evaporite Bed.

Sulphates.

Gypsum is present in all but one sample (YG 4397) and ranges in value from 0.05 per cent. in YG 4395 to 47.80 per cent. in B7. Boreholes ML 3 and ML 6 are characterized by low gypsum values which reach a maximum of 5.36 per cent. in sample YJ 1056. In contrast, in borehole ML 12 gypsum contents range from 5.99 per cent. in B 5 to 47.80 per cent. in B 7. In ML 3, there is a general increase in gypsum content towards the top of the sequence but no such trend is seen in ML 6, although the two lowest samples are effectively free of gypsum. In ML 12, several high gypsum values ($>$40 per cent.) were recorded in samples from the higher beds, but paradoxically, the two lowest gypsum values recorded in this borehole occur at the top of the sequence where anhydrite is the predominant form of sulphate.

Anhydrite was recorded in 16 samples, ranging from 0.03 per cent. in B 39 to 43.26 per cent. in B 5. In boreholes ML 3 and ML 6, low anhydrite values ($<$0.5 per cent.) occur only sporadically, but always in samples containing gypsum. In ML 12, anhydrite is present in small amounts in the samples

from the lower part of the sequence, but shows a general decrease in content from B 49 to B 31. This is a continuation of the trend noted in the underlying basin facies of the Lower Magnesian Limestone and is believed to be an effect of hydration. However, this marked trend is interrupted by the high levels of anhydrite (18.18 per cent. to 43.26 per cent.) in the 3 uppermost samples. These apparently anomalous values occur in dolomite interbedded with massive sulphate. The massive sulphate may have protected the interbedded dolomite with anhydrite from the action of circulating groundwater while hydration has proceeded in the relatively more permeable beds below.

In borehole ML 12, gypsum commonly occurs as colourless to black blebs and patches, although the borehole log records its occurrence as thin, fibrous, anastomosing veins which frequently cause brecciation of the surrounding dolomite. Anhydrite was only observed in samples B 5, 7 and 9 although petrographic studies by Raymond (1962, p. 48) record its presence in the "Lower Magnesian Limestone" of the Billingham area mainly as corroded relics within gypsum crystals. The small quantities of anhydrite recorded in the interval represented by samples B 49 to B 31 are thus probably real and not due to the presence

of pyrite which Raymond (op. cit.) has observed in association with some gypsum "inclusions".

Gypsum was also visible in many samples from boreholes ML 3 and ML 6, although mainly as small acicular crystals scattered throughout the carbonate host-rock and only occasionally as colourless blebs and patches. However, the borehole logs again show that gypsum takes the form of thin, fibrous veins, particularly in the lower part of the sequence, and sometimes lines rare joints and slickensides. Anhydrite was not observed under a hand lens in any specimens from these two boreholes although it is recorded in the log of ML 6 from the lower part of the sequence. A thin section of a sample from borehole ML 3 showed anhydrite as relic crystals concentrated in the centre of a gypsum bleb.

Carbonates.

The dolomite content varies remarkably and there is a complete range from YG 4397 with 99.61 per cent. to YG 4279 in which dolomite is absent. In borehole ML 12, dolomite is the predominant carbonate as it is in the underlying Lower Magnesian Limestone basin facies at this location. The lowest values in this borehole are 31.85 per cent. and 49.50 per cent. in B 7 and B 5 respectively; these samples contain no calcite and are

therefore not carbonate rocks according to the definition used in this investigation (viz. calcite plus dolomite $\geqslant$ 50 per cent.).

Calcite also shows extremes of value, being absent in 13 samples and reaching a maximum of 96.80 per cent. in YJ 1061. However, unlike dolomite, calcite does not show a range of values and the samples can be divided into two groups characterized respectively by low and high calcite values. In the low calcite group, values reach a maximum of 6.60 per cent.; the group includes all the samples from borehole ML 12, 3 samples from ML 3 and 2 from ML 6. In the high calcite group, the lowest recorded value is 56.11 per cent. but values are usually much higher than this and include 9 which are in excess of 90 per cent. This group is numerically inferior to the first group and is comprised of samples from boreholes ML 3 and ML 6. Except for the top 3 samples, calcite is the predominant carbonate in borehole ML 3. In this respect, the lower part of the Middle Magnesian Limestone basin facies in this borehole is similar to the underlying Lower Magnesian Limestone. In ML 6, calcite is the predominant carbonate in all but the top and bottom samples analysed. The decrease in the importance of calcite shown by the bottom sample is a trend which is maintained in the 2 samples from the underlying Lower Magnesian Limestone basin facies.

When plotted on a triangular diagram in terms of calcite, dolomite and total sulphate (Figure 4-6), the samples from the basin facies of the Middle Magnesian Limestone are seen to be very similar to the samples from the basin facies of the Lower Magnesian Limestone, with extremes of carbonate composition and with a marked antipathy between calcite and sulphate; there are no intermediate compositions in which relatively high sulphate and calcite values occur together.

Raymond (1962, p. 49) has reported that the dolomite in the "Lower Magnesian Limestone" of the Billingham area, including that in borehole ML 12, occurs mainly as equant grains between 10 and 20μ in diameter. However, in the soft, sugary part of the sequence which, according to the revised classification, lies near the base of the Middle Magnesian Limestone (see Appendix 1), he reported that the grains vary between 40 and 100μ . Raymond makes no mention of the small amount of calcite in the Billingham area.

The fine-grained dolomite beds from the top of the sequence in borehole ML 3 are seen in thin section to consist of closely packed, euhedral to subhedral dolomite grains about 30μ in diameter. In contrast, thin sections of samples from lower in the sequence are seen to be comprised of an approximately equigranular mosaic of calcite crystals which appear cloudy due to

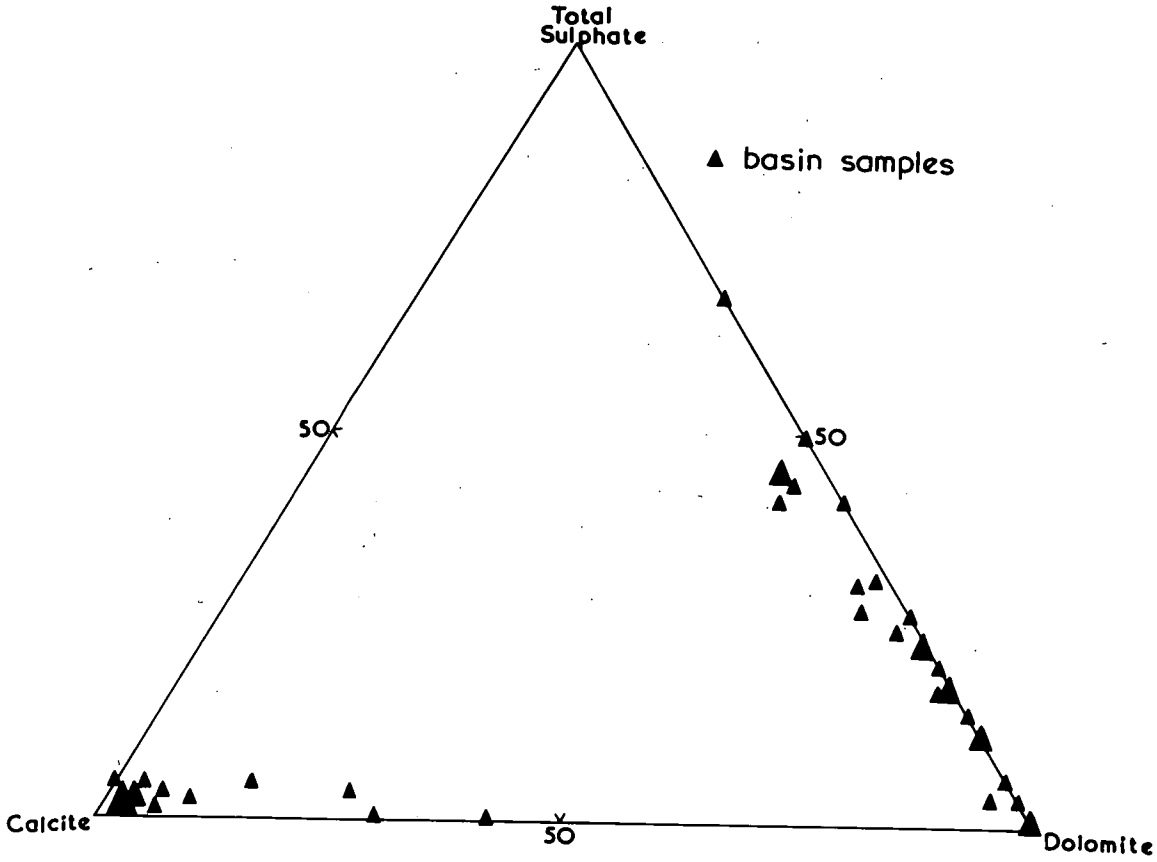

FIGURE 4–6. MINERALOGY OF THE BASIN FACIES OF THE MIDDLE MAGNESIAN LIMESTONE.

A larger symbol indicates the occurrence of several samples with similar compositions.

the presence of minute dolomite inclusions, similar to, but not as dense as, those shown in Plate 4-14. The inclusions could not have formed a supporting framework and are considered to be relic crystals remaining after the centripetal dedolomitization of fine-grained dolomite beds similar to those higher in the sequence.

In borehole ML 6, a similar dedolomitization texture is seen in the fine-grained beds which are interbedded with coarser, reef-derived material. The coarser beds themselves show a patchy development of this texture, together with the development of composite calcite rhombohedra (Plate 4-15), perhaps the most characteristic, and certainly the most easily recognizable, dedolomitization texture (Shearman et al., 1961; Evamy, 1967). In these beds, calcite also occurs very occasionally in discrete areas as sparry crystals (Plate 4-16) which contrast markedly with the surrounding cloudy calcite and composite calcite rhombohedra. This calcite has all the characteristics of void filling and usually contains clear dolomite euhedra, commonly 100μ in diameter (Plate 4-16). These dolomite euhedra do not contain cores of fine-grained calcite, which would be indicative of the beginning of centrifugal dedolomitization, nor do their faces show signs of corrosion, a feature which would suggest incipient centripetal

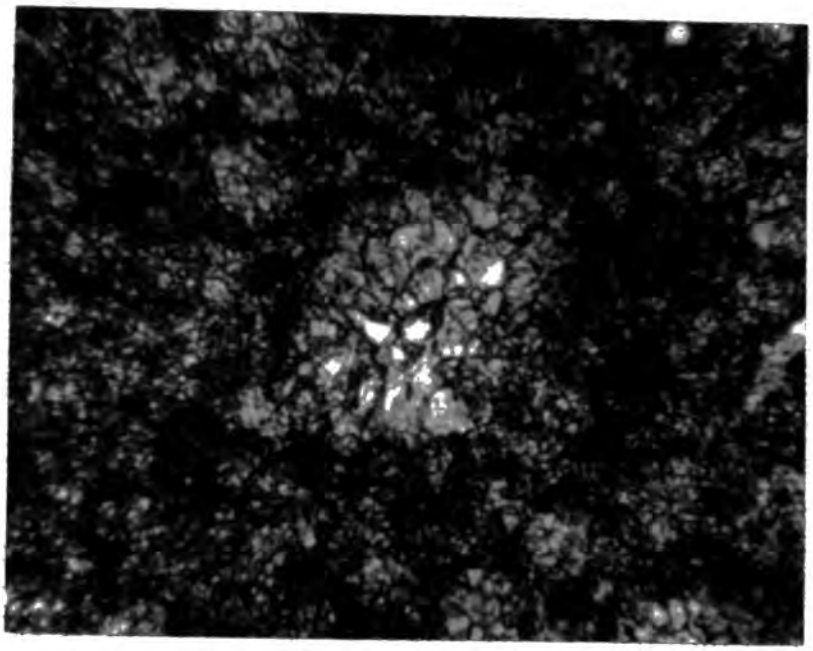

Plate 4-15. Composite calcite rhombohedron in a sample from a bioclastic bed of the Middle Magnesian Limestone basin facies close to the reef-front (borehole ML 6). Thin section, plane polarized light, X 275.

Plate 4-16. Sparry calcite containing clear dolomite euhedra in a sample from a bioclastic bed of the Middle Magnesian Limestone basin facies close to the reef-front (borehole ML 6). Thin section, plane polarized light, X 400.

dedolomitization (Shearman et al., op. cit.). It seems strange that dolomite rhombs developed in early void-filling calcite should completely escape dedolomitization, while adjacent dolomite rhombs in the matrix were completely replaced by calcite. This consideration tends to suggest that these dolomite euhedra represent a late development in the calcite-filled voids, after the dedolomitization of the matrix. It is not possible to say whether the apparent void-filling calcite was emplaced before or after dedolomitization of the matrix. Trechmann (1914, analysis L and plate XXXVI, fig. 1) recorded the presence of an apparently late generation of large, clear dolomite euhedra developed within patches of gypsum which are in turn enclosed by earlier, fine-grained dolomite. Raymond (1962, p. 57) has also recorded late dolomite within sulphate. These occurrences are distinct from the cases of "simultaneous precipitation" of dolomite and sulphate reported by Dunham (1948, pp. 219 - 221) and Raymond (op. cit., p. 58). Trechmann's sample comes from the Middle Magnesian Limestone beneath the Hartlepool Anhydrite, in an old borehole close to the site of ML 6. From his description, there does not appear to have been any dedolomitization and yet in ML 6, dedolomitization has taken place and the late dolomite euhedra are still present. This suggests that the generations of late dolomite euhedra in the

two boreholes from near Hartlepool are both of post-dedolomitization age, or that they are of different age (one pre-dedolomitization and one post-dedolomitization), or that they are both of pre-dedolomitization age. Consideration of the age of dedolomitization (see below) tends to suggest that the development of dolomite in the period since dedolomitization of the basin facies of the Lower and Middle Magnesian Limestone is extremely unlikely. This conclusion lends support to the suggestion that both generations of dolomite euhedra are of pre-dedolomitization age and implies that the dolomite euhedra in borehole ML 6 have escaped dedolomitization. If this interpretation is correct, the apparent void-filling calcite, in which the dolomite euhedra of ML 6 are developed, may in fact be replacing former sulphate patches, although there is no evidence for this.

Other Components.

The non-carbonate/sulphate components reach a maximum recorded value of 16.47 per cent., the highest value recorded from all the samples analysed in this investigation. This value is unusually high for the facies, being found in sample YJ 1053 B which is taken from the nodular bed directly underlying the Hartlepool Anhydrite in borehole ML 3. Apart from

this, values are less than 10 per cent. (Figure 4-2) with 1-2 per cent. being the most common range.

In all samples, the most important components are Fe_2O_3 and SiO_2, although occasionally Al_2O_3 becomes significant, reaching a maximum value of 2.94 per cent. in sample YJ 1053 B. Fe_2O_3 reaches 3.09 per cent. in YG 4366 but, as Figure 4-3 shows, most samples contain less than 1 per cent. Sample YJ 1053 B contains 15.39 per cent. inorganic detrital material, but this is clearly unusual (Figure 4-4) and the samples most commonly contain less than 1 per cent. No systematic variation in the content of detrital material is apparent, high values in particular samples can usually be attributed to the close proximity of black, shaley partings.

The Significance of the Calcite-Sulphate Antipathy.

The basin facies of the Lower and Middle Magnesian Limestone exhibit extremes of carbonate composition. Dolomite is the predominant carbonate in the majority of samples, while in the remainder, calcite is predominant. Petrographic evidence shows that the calcite of the Middle Magnesian Limestone basin facies is essentially in the form of "dedolomite". High values of calcite occur only in samples which contain very little sulphate, while high sulphate values are found only in rocks in

which dolomite is the predominant carbonate. This calcite-sulphate antipathy is marked in the basin facies of both divisions and suggests that the development of calcite by dedolomitization is related to the solution and removal of sulphate from within rocks which originally consisted almost entirely of dolomite and sulphate. The overall reaction can probably be represented by a reversal of von Morlot's reaction

$$Ca\ Mg\ (CO_3)_2 + Ca\ SO_4 \rightleftharpoons 2\ Ca\ CO_3 + Mg\ SO_4.$$

Replacement of dolomite by calcite appears to take place on an equal-volume basis, the highly soluble $Mg\ SO_4$ being removed in solution and the sites formerly occupied by calcium sulphate minerals being represented by voids. The formation of calcite from dolomite in this manner would cause the calcium sulphate to be "consumed" and thus account for the calcite-sulphate antipathy. A similar relationship has been noted by Krotov (1925, in Makhlaev, 1957), Makhlaev (1957) and Goldberg (1967).

It must be emphasized that although there is a calcite-sulphate antipathy in rocks from the basin facies, the development of calcite as "dedolomite" through removal of sulphate actually occurs on a regional basis. Thus, leaching of sulphate

and concomitant dedolomitization appears only to have occurred in the basin facies of the Lower and Middle Magnesian Limestone in boreholes ML 3 and ML 6. Even in these boreholes, dolomite is still the predominant carbonate at some horizons, particularly immediately beneath the Hartlepool Anhydrite. According to Smith (in press), boreholes ML 3 and ML 6 lie in a region where varying degrees of solution of the Hartlepool Anhydrite have occurred. The borehole logs, however, give no indication of any such solution. This evidence, together with the presence of dolomitic beds immediately beneath the Anhydrite, would appear to discount the possibility of downward percolation of sulphate solutions contributing significantly to the dedolomitization of the underlying strata.

Dedolomitization is often recorded as occurring in rocks which are exposed, or which lie at relatively shallow depths. Dedolomitization effects have also been reported at depth, but usually in rocks which lie beneath an unconformity (e.g. Schmidt, 1965) and which have therefore been at, or near, the earth's surface in the geological past. De Groot (1967), on the basis of experimental data, has indicated that dedolomitization must be a near-surface process as it can only take place at a relatively low temperature and carbon dioxide partial pressure and

requires a constant supply of Ca^{2+}-rich water. It does not seem likely that formation of calcite after dolomite by leaching of sulphate from dolomite-sulphate rocks under the conditions shown to be necessary by de Groot (op. cit.) can be an early diagenetic process (see Katz, 1968). For this reason, together with the reasons mentioned below, it is not considered that the leaching and concomitant dedolomitization of the basin facies of the Lower and Middle Magnesian Limestone occurred during the Permian. Formation of the Permian in North-East England was followed, apparently without major interruption, by deposition of Triassic, Jurassic and Cretaceous sediments. Eventually, the Permian in Durham must have lain at a depth comparable to that at which it is now found in East Yorkshire (see Raymond, 1953, table 1). Leaching of sulphate and concurrent dedolomitization seems even more unlikely under an increasing thickness of sediments than at any time during the Permian.

Smith (in press) has concluded that solution of the Hartlepool Anhydrite, which brought about collapse-brecciation and concomitant dedolomitization of the overlying Upper Magnesian Limestone, occurred at the end of the Mesozoic or early in the Tertiary, when Alpine uplift brought the Permian rocks within reach of freely circulating groundwater. He has indi-

cated that the main phase of solution of the Anhydrite was complete by the time Miocene earth movements affected the area. It seems logical that considerable leaching of disseminated sulphate and concomitant dedolomitization in the Lower and Middle Magnesian Limestone lying beneath the Hartlepool Anhydrite should take place at the same time as the main phase of solution of the Anhydrite itself. However, the presence of dissolved sulphate in water from springs in the offshore coal workings, and from wells at Sunderland and particularly in South-East Durham, suggests that slow solution of sulphate and possible concurrent dedolomitization is still proceeding.

If the late dolomite euhedra occasionally observed in samples from borehole ML 6 (Plate 4-16) are of post-dedolomitization age, they must therefore have been formed at some time since the early Tertiary. However, the physico-chemical conditions which must have existed within the Permian rocks since the early Tertiary would appear to preclude the formation of late dolomite during this period. This conclusion lends support to the suggestion (see above) that these clear and uncorroded dolomite euhedra are of pre-dedolomitization age but have escaped dedolomitization, although there is no obvious reason why this should have occurred when the surrounding dolomite has been replaced by calcite.

It seems strange that the Hartlepool Anhydrite, which is 429 ft and 360 ft respectively in boreholes ML 3 and ML 6, should have apparently escaped solution, while disseminated sulphates in the underlying Lower and Middle Magnesian Limestone have been leached and have brought about dedolomitization. The anomaly may be due to the fact that the sulphate-bearing carbonates were relatively more permeable to circulating groundwaters than the overlying massive Anhydrite. An analogous situation has been observed in borehole ML 12 where it is believed to have led to the preservation of anhydrite in dolomite interbedded with massive sulphate, while hydration of anhydrite to gypsum has occurred in the underlying and relatively more permeable carbonate beds.

Smith (in press) has concluded that dedolomitization of the collapse-brecciated Upper Magnesian Limestone in the Durham Province took place under more than 220 metres of cover. This conclusion is based on the occurrence in late-stage breccia-gashes of fragments of Bunter Sandstone which is believed to have been separated by at least 220 metres of strata from the underlying Hartlepool Anhydrite at the time of its solution. If this depth is correct, then the Lower and Middle Magnesian Limestone in boreholes ML 3 and ML 6 must have lain at even greater depths during the main phase of sulphate removal and contemporaneous dedolomitization. As

Smith (op. cit.) has noted, depths of this magnitude conflict with the findings of de Groot (1967). Nevertheless, if a late Mesozoic or early Tertiary age for the main phase of sulphate removal and dedolomitization is accepted, it must also be accepted that dedolomitization occurred at such depths. Other workers have also shown that dedolomitization by the "sulphate-agent" mechanism can apparently take place at considerable depth; in particular, Mattavelli et al. (1969, p. 79) have reported that dedolomitization by this process has occurred in the Triassic Taormina Formation of Sicily".....at a depth of several hundreds of metres".

The Non-Carbonate/Sulphate Material in the Magnesian Limestone.

From thin sections, it is known that limonite and quartz are the most common non-carbonate/sulphate minerals; this is reflected in the analyses by the fact that Fe_2O_3 and SiO_2 are the most important non-carbonate/sulphate components in all facies of the Lower and Middle Magnesian Limestone. However, as noted above, some Fe is associated with the clay minerals and also with sporadic occurrences of pyrite. The petrographic evidence from this investigation suggests that the quartz is detrital as it occurs as small, angular grains within the carbonate host-rock, but Trechmann (1914) and Raymond (1962,

p. 46) have reported euhedral (and hence authigenic) quartz from the Durham Magnesian Limestone.

X-ray diffraction reveals that illite is the predominant clay mineral in the Magnesian Limestone; Hirst and Dunham (1963) have shown that this is also true of the Marl Slate. The illite has a broad basal (10 Å) reflection which "tails-off" towards higher "d" spacings, characteristics which are usually considered to be indicative of small grain-size, poor crystallinity and some mixed layering (possibly with chlorite). The illitic clay material is considered to be the source of the Al_2O_3 in the samples. Table 4-1 shows how the relative amounts of the various inorganic detrital components in the Magnesian Limestone (calculated from the arithmetic mean values of the entire 162 samples analysed by X-ray fluorescence major element analysis) compare with equivalent values for other clay material.

Table 4-1.

Ratios of some components in the Magnesian Limestone compared with clay material.

	Al_2O_3 :	SiO_2 :	K_2O :	Na_2O :	TiO_2
Magnesian Limestone (Arithmetic Mean of 162 samples)	1	4.356	0.279	0.668	0.054
Pure Illitic Material (Grim et al., 1937, analysis 1)	1	1.994	0.276	0.002	0.020
Average Shale (Turekian and Wedepohl, 1961)	1	3.864	0.212	0.085	0.051

The presence of detrital quartz is the obvious cause of the large variance between the SiO_2 : Al_2O_3 ratio for the Magnesian Limestone and that for pure illitic material. The K_2O : Al_2O_3 ratio in the Magnesian Limestone is consistent with the K being present in interlayer positions in the illite structure. The ratio is 0.279, comparable with the mean value of 0.212 which may be obtained from the analyses of 8 samples of Durham Marl Slate (Hirst and Dunham, 1963, table VII). Sodium is also known to occur in the interlayer positions of illite, but to a lesser extent than K, and the cause of the high Na_2O : Al_2O_3 ratio is unknown. The comparatively high TiO_2 : Al_2O_3

ratio for the Magnesian Limestone suggests that as well as being held in the illite, Ti is present in other forms, possibly rutile and/or leucoxene, both of which have been identified in the heavy mineral fraction of the Basal Sands (Hodge, 1932).

CHAPTER 5.

POROSITY AND PERMEABILITY.

Effective porosity and effective permeability were determined for 26 samples of Magnesian Limestone.

Determination of Porosity and Permeability.

Sampling Scheme and Sample Preparation.

One inch diameter cores were taken from the sides of borehole coresusing a laboratory diamond drill. Owing to the relatively large initial sample size required, it was possible only to obtain laboratory cores at irregular intervals from seven boreholes situated mainly in the South Durham area. The samples represent the shelf facies of the Lower Magnesian Limestone and the lagoon and basin facies of the Middle Magnesian Limestone. The laboratory cores were cut into discs approximately 0.25 inches thick and polished with sand on a glass plate in order to make the faces approximately parallel and reasonably smooth. The diameter and thickness of the rock discs were measured with a micrometer screw gauge. The mean thickness of each disc was obtained from measurements made in at least three places. Both porosity and permeability were determined for each disc, although the porosity was determined first to

avoid the effects of any alteration to pore characteristics which might have occurred during the permeability determination. In the boreholes examined, the dip of the Magnesian Limestone is relatively low and the rock discs therefore enable the flow characteristics to be determined along a direction approximately parallel to the bedding.

As Chakrabarti and Taylor (1968) have pointed out, the possibility of mechanical injury to the cores during diamond drilling (both in the field and in the laboratory) cannot be excluded. However, in view of the relative constancy of the results obtained for several rock discs taken from the same borehole sample, it was assumed that such effects were negligible. During the coring of beds at depth, a certain amount of stress relief occurs. The confining pressures, even for the sample from the greatest depth here investigated (sample YJ 1057 from a depth of 1027 ft), will be relatively small and consequently errors arising from this source are considered to be small.

Effective Porosity.

Effective porosity is the portion of the total porosity which is capable of transmitting fluids and may be defined as:-

$$\frac{\text{volume of interconnected voids in the porous medium}}{\text{total volume of the porous medium}}$$

This property is directional as both the size and degree of interconnection between voids may vary in different directions. In this investigation, overall effective porosity was determined following the method outlined below.

The rock discs were suspended from threads in groups of 4 inside a beaker. The beaker was placed inside a dessicator in which a vacuum was maintained for 24 hours to remove the entrapped moisture and air from the pores of the specimens. After this period, distilled water was run into the beaker while still under vacuum, until the discs were covered completely. The vacuum was maintained for a further 24 hours to ensure complete saturation of the samples, after which, the beaker, with samples still submerged, was removed from the dessicator. Each disc was weighed twice:-

(1) while suspended in air after removal from the beaker and having had the excess water blotted from its surface; this gave the saturated weight in air, W_A gm.

(2) while suspended in air after drying in an oven maintained at 40°C for 3 days; this gave the oven-dry weight in air, W_B gm.

The weight of distilled water contained in the voids of a disc is $W_A - W_B$ gm. As the density of distilled water at room

temperature (20°C) is 1 gm/cm^3, the volume of distilled water filling the voids, and hence the volume of the voids, is $W_A - W_B$ cm^3. The total volume of a disc is given by $t \cdot \pi \cdot \frac{d^2}{4}$ where d is the diameter and t the mean thickness of the disc in cm. The effective porosity in per cent. is then given by:-

$$\frac{4\ (W_A - W_B)\quad 100}{\pi \cdot t. \cdot d^2} \qquad (5\text{-}1)$$

Jackson (1968) has summarized the main sources of error in this technique. They are:-

(1) Although coarse sand was used as a finishing abrasive in order to prevent blocking of the external pores, some blockage may have occurred in the highly porous samples resulting in low porosity values.

(2) Some pores may have been too small for water to penetrate. This would also produce a low porosity value.

(3) The external pores of some of the more porous samples may have been so large as to lose water during the first weighing. This would also produce a low porosity value.

(4) Minerals may hydrate, absorb water and so produce a high porosity value.

Effective Permeability.

The effective permeability of a medium gives a measure of the rate of diffusion of a fluid under a pressure gradient and depends both on the structure of the medium and also on the properties of the fluid being transmitted through the medium. In this investigation, effective permeability was determined by means of a high-pressure permeameter similar to that used by Ohle (1951), but modified as outlined by Chakrabarti and Taylor (1968). Distilled water, under pressure, was applied to one side of a rock disc enclosed in the stainless-steel permeameter, and the rate of discharge on the low-pressure side was measured. Each rock disc was first de-aired and saturated with distilled water following the procedure outlined above. To prevent leakage around the disc, two greased rubber sleeves were placed around its circumference; it was then sandwiched between two rubber retaining washers inside the permeameter by screwing in the plug which makes up the low-pressure side of the apparatus. The water pressure was applied by means of an automatic constant-pressure system consisting of one set of mercury dashpots giving a maximum pressure of 132 $lb/in.^2$ The water discharged from the low-pressure side of the apparatus was collected in a graduated tube over a given time interval.

The effective permeability is calculated by using Darcy's Law, from which it can be shown that:-

$$k = \frac{\eta . Q}{A . i . \gamma} \qquad (5\text{-}2)$$

where k = permeability (cm/sec)

η = the viscosity of water at the laboratory temperature (c P)

Q = the rate of flow of water through the disc (cm^3/sec)

A = the cross-sectional area of the water inlet and outlet (cm^2)

i = the hydraulic gradient (dimensionless) = $\frac{h}{t}$

h = the applied pressure expressed as head of water (cm)

t = the mean thickness of the disc (cm)

γ = the density of water at the laboratory temperature (gm/cm^3).

As the permeability determinations were carried out in a constant-temperature laboratory, η and γ remained constant throughout the investigation.

The main sources of error involved in this method of determination have been summarized by Jackson (1968) and are listed below:-

(1) Leakage around the specimen is potentially the most important source of error; however, duplication of results with a constant flow-rate indicated that no leakage occurred.

(2) Variation in the internal diameter of the retaining rubber washers, in response to the pressure applied to the permeameter, may occur. This variation should be small, however, at the applied pressures used. The measured diameter was used to derive the cross-sectional area of the water inlet and outlet needed for Equation (5-2).

(3) Air dissolved in the water may form bubbles as the pressure decreases during flow through a specimen. As distilled water was used throughout the investigation, errors from this source should be small.

Discussion of Results.

The porosity and permeability results obtained for the 26 samples are presented in Appendix 4. Both properties vary considerably, the porosity range being 5.0 - 34.9 per cent. and the permeability range being 1.0×10^{-9} - 2.0×10^{-5} cm/sec. The range and arithmetic mean values of porosity and permeability for each facies are presented in Table 5-1, together with equivalent data from Jackson (1968).

Table 5-1 indicates that the samples of shelf Lower Magnesian Limestone investigated here have a greater range of both porosity and permeability than those examined by Jackson. However, the arithmetic means of the porosity values from the two studies are comparable, although agreement between the arithmetic means of the permeability values is poor. The porosity and permeability values quoted by Jackson for one sample of lagoonal Middle Magnesian Limestone are higher than the respective arithmetic mean values for samples of the same facies examined here. However, the value of permeability quoted by Jackson lies within, although at the upper end of, the range of permeability values found in this investigation, while the porosity value is greater than, but comparable with, the upper limit of the porosity range. There is close agreement between the arithmetic mean porosity and permeability values for the samples of Middle Magnesian Limestone basin facies here investigated and the respective arithmetic mean values given by Jackson for samples of Middle Magnesian Limestone post-reef facies. It must be emphasized that the basin samples YJ 1056 and YJ 1057 have not been dedolomitized. In dedolomitized samples, it seems likely that the voids remaining after solution of sulphates will

give rise to a higher porosity and perhaps permeability than before. On the whole, agreement between the two sets of results is good, in spite of the fact that the permeability values compiled from Jackson's data were obtained from samples taken both parallel and normal to the bedding, and were determined by a different method (a falling-head technique) to that employed in this investigation.

Taken in conjunction with the results provided by Jackson, the data indicate that:-

(1) In the Middle Magnesian Limestone, the lagoon and reef facies are more porous and permeable than the non-dedolomitized basin facies.

(2) The lagoon and reef facies of the Middle Magnesian Limestone tend to be more porous and permeable than the shelf facies of the Lower Magnesian Limestone.

(3) There is much greater variation in the porosity and permeability of the shelf facies of the Lower Magnesian Limestone and the lagoon facies of the Middle Magnesian Limestone than there is in the reef facies of the Middle Magnesian Limestone.

	Porosity (%)		Permeability (cm/sec)	
	This Investigation	Jackson (1968)	This Investigation	Jackson (1968)
Lower Magnesian Limestone Shelf Facies	13 samples Range: 5.0 - 30.1 Arithmetic Mean: 18.8	20 samples Range: 10.6 - 25.4 Arithmetic Mean: 15.3	13 samples Range: 1.0×10^{-9} – 1.5×10^{-5} Arithmetic Mean: 2.4×10^{-6}	20 samples Range: 1.2×10^{-6} – 7.8×10^{-4} Arithmetic Mean: 7.0×10^{-5}
Middle Magnesian Limestone Lagoon Facies	11 samples Range: 9.9 - 34.9 Arithmetic Mean: 22.6	1 sample 38.6	11 samples Range: 3.3×10^{-8} – 2.0×10^{-5} Arithmetic Mean: 4.9×10^{-6}	1 sample 1.9×10^{-5}
Middle Magnesian Limestone Reef Facies	-	24 samples Range: 15.6 - 28.7 Arithmetic Mean: 21.4	-	24 samples Range: 5.6×10^{-6} – 2.5×10^{-3} Arithmetic Mean: 1.8×10^{-4}
Middle Magnesian Limestone Post-reef/Basin Facies	2 samples Range: 6.4 - 9.3 Arithmetic Mean: 7.9	8 samples Range: 3.4 - 10.4 Arithmetic Mean: 6.9	2 samples Range: 6.3×10^{-7} – 3.3×10^{-6} Arithmetic Mean: 1.9×10^{-6}	8 samples Range: 7.7×10^{-7} – 1.4×10^{-5} Arithmetic Mean: 5.8×10^{-6}
Upper Magnesian Limestone	-	1 sample 7.3	-	1 sample 1.4×10^{-6}

Table 5-1.

Summary of Porosity and Permeability Values for the Magnesian Limestone.

Factors Influencing Porosity and Permeability.

The petrophysical properties of sedimentary rocks have received a great deal of attention in recent years, owing to the importance of sedimentary rocks as reservoirs for the economically valuable hydrocarbons. The more important information has been extracted from the wealth of literature concerned with these properties in order to assess the factors which might influence the porosity and permeability of the Magnesian Limestone.

Griffiths (1952) has summarized the effects of textural properties on the porosity of various media and has shown that:-

(1) In most cases, porosity increases with decrease in grain-size, but in other instances, the reverse relationship holds. Sometimes porosity appears to be independent of grain-size.

(2) Invariably , poorly sorted mixtures of grain-sizes give the lowest porosities.

Griffiths concluded however, that no general statement could be made concerning the effects of grain-size and sorting on porosity and further, that the contradictory evidence allowed no general statement to be made about the effects of shape, grain-size or sorting on permeability.

Mineralogical composition can also influence porosity and permeability. The degree to which carbonate rocks are dolomitized is clearly important; Chilingar and Terry (1954) and Gaskell (in Chilingar et al., 1967, p. 288) have demonstrated a definite relationship between porosity and degree of dolomitization. However, this type of relationship could only exist if dolomitization has taken place by the molecular replacement of calcite, a process which involves a contraction of 12-13 per cent. with a resultant increase in porosity, and has not been followed either by the additional precipitation of carbonates in the pores or by subsequent compaction. Correlation between porosity and degree of dolomitization is thus unlikely in rocks which have been dolomitized early in diagenesis as subsequent compaction should appreciably reduce, or eliminate completely, any increase in porosity. No increase in porosity would be expected in those carbonates where replacement of calcite by dolomite has occurred on an equal-volume basis. Griffiths (1952) considers that permeability is very sensitive to minor changes in mineral composition; he appears to share the view of Archie (1950) that the presence of clay minerals in rocks might be particularly important, presumably because of the possibility of hydration of these minerals.

Archie (1950) considers that pore-size distribution is the principal factor controlling not only porosity and permeability, but also other petrophysical properties. Each rock-type is characterized by a particular pore-size distribution which is the result of conditions of deposition, subsequent compaction, mineralogical changes, cementation and re-solution. The pore-size distribution is therefore the end-product of the entire depositional and diagenetic history of a particular rock-type.

In the 26 samples of Magnesian Limestone investigated, there is no relationship between the quantity of dolomite and either porosity or permeability. Only 3 samples contain less than 90 per cent. dolomite and yet the porosity ranges from 5.0 - 34.9 per cent. and the permeability from 1.0×10^{-9} - 2.0×10^{-5} cm/sec. The grain-size of the dolomite (the principal mineral) does not appear to change significantly with either the porosity or the permeability. There is, however, a qualitative relationship between pore-size distribution and both porosity and permeability. In general, lower values of both porosity and permeability are associated with rocks which are uniform and dense and which appear to consist of closely packed, tightly interlocking dolomite grains. Higher values

of both properties are associated with loosely packed, oolitic or pisolitic rocks and with coarsely granular rocks which have obvious pores, clearly visible with the naked eye.

The Relationship between Porosity and Permeability.

Theoretical considerations of the structure of porous media indicate that a general relationship between porosity and permeability cannot exist (Scheidegger, 1960, p. 112). The influence of porosity on permeability has nevertheless provided the basis for much empirical work; many attempts have also been made to relate the two properties mathematically. Archie (1950) approached the problem from an empirical standpoint and showed that for a given rock-type, and therefore a particular pore-size distribution, there is a broad relationship between porosity and permeability. A mathematical treatment of the geometry of isotropic unconsolidated porous media by Kozeny (1927) has led to an equation relating permeability to porosity. The basic form of the equation is as follows (Scheidegger, 1960, p. 128):-

$$k = \frac{c.P^3}{S^2} \qquad (5\text{-}3)$$

where k is the permeability, P the porosity, S the surface area

per unit volume and c a constant, found to be of the order of 0.5 by Kozeny. Much attention has been given to developing this equation in an attempt to make it generally applicable to consolidated and non-isotropic porous media. Modifications have centred principally on the use of different values of c. However, it must be said that while it has not been possible to make this or any other equation generally applicable, a measure of success has been achieved with some rock-types.

Figure 5-1 shows the relationship between permeability and porosity for the 26 samples of Magnesian Limestone examined in this investigation. For 23 of the samples, which belong to the shelf facies of the Lower Magnesian Limestone and the lagoon facies of the Middle Magnesian Limestone, there is a clear positive trend between the two properties, an increase in porosity from 5 - 35 per cent. being matched by an increase in permeability from 1.0×10^{-9} - 1.0×10^{-5} cm/sec. Thus, an increase in porosity of about 8 per cent. produces a ten-fold increase in permeability. Following the interpretation of Archie (1950), the trend is not considered to be the manifestation of a strict mathematical relationship, but rather an indication that the rocks were deposited under generally similar conditions and have since undergone similar diagenetic changes. However, in

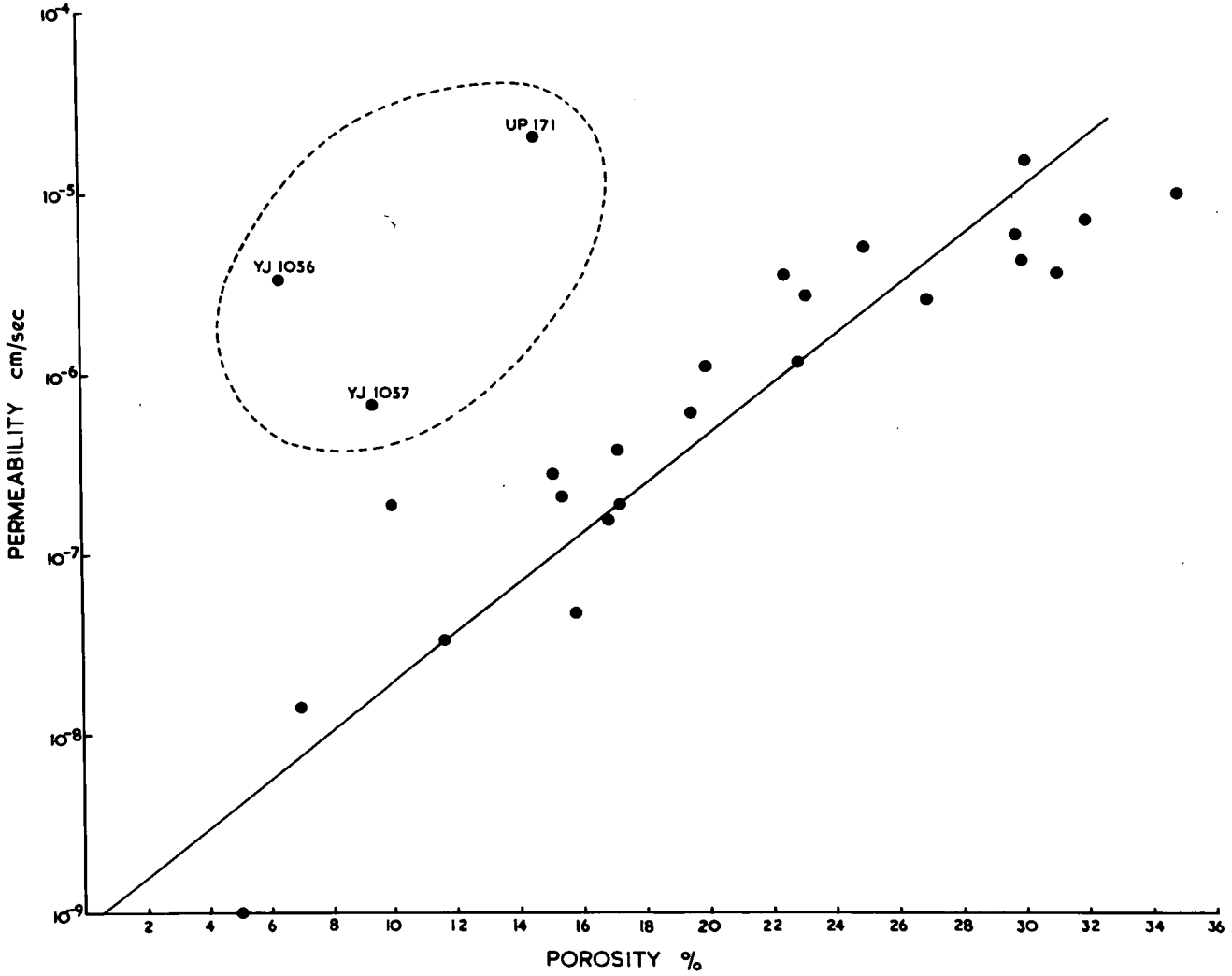

FIGURE 5-1. RELATIONSHIP BETWEEN PERMEABILITY AND POROSITY.

view of the general change in pore-size distribution which appears to influence the porosity and permeability of the samples, it is surprising to find only one clear trend (see Archie, 1950, p. 944).

It is perhaps significant that 2 of the 3 samples which lie well away from the positive trend in Figure 5-1 were derived from the basin facies of the Middle Magnesian Limestone. These samples have had a different depositional and probably diagenetic history to the samples from the shallow-water facies. According to Archie (op. cit.), the fact that these 2 samples have lower porosities than samples from the shallow-water facies with similar permeabilities should indicate that the basin samples have relatively large pores. This does not appear to be the case as thin sections of rocks from the basin facies indicate that the pores are essentially intergranular and small. The pore-size of these 2 samples would therefore appear to be at variance with the porosity values at the levels of permeability involved. However, Archie (op. cit.) has noted that re-deposition (cementation) and re-solution can alter the pore-structure and give rise to anomalous results. The 2 basin samples both contain significant quantities of gypsum and it is possible that cementation of the pores by this mineral has contributed to the apparently anomalous values for these samples.

Re-solution, producing larger pores, followed by re-deposition may help to explain the anomalous position of the third sample (UP 171) lying away from the positive trend in Figure 5-1. This sample shows the presence of small vugs lined with calcite and is obviously different from the rest of the samples from the lagoon facies of the Middle Magnesian Limestone to which it belongs. Archie (op. cit.) has noted that a porosity/permeability trend for a given formation or rock-type may not actually apply to a small integral part which has a markedly different pore-structure and which is not typical of the formation as a whole. However, it must also be mentioned that the anomalous position of this sample may be due, in part at least, to a low porosity value caused by the failure of water to remain in the vuggy external pores during the first weighing of the porosity determination.

CHAPTER 6.

MINOR AND TRACE ELEMENT GEOCHEMISTRY.

A total of 281 samples, taken from all fifteen sinkings, were analysed for the elements Ba, Sr, Rb, Pb, Zn, Cu, Ni and Mn by X-ray fluorescence spectrography. The analyses are presented in Appendix 5. Only 27 samples of Magnesian Limestone, taken from three sinkings, were analysed for boron by emission spectrography; these analyses are presented in Appendix 6. The minor and trace element analyses are used in conjunction with the partial mineralogical analyses of 162 samples taken from twelve sinkings and with the organic carbon analyses of 34 samples selected from various sinkings.

Correlation coefficients were calculated for all possible pairs of mineralogical components and elements. It must be emphasized that the calculation of correlation coefficients assumes a linear relationship between the various parameters, a condition which is not always true. Nevertheless, the use of correlation coefficients in conjunction with significance tests does help to identify the most likely geochemical associations.

Strontium.

Strontium is present in all the samples analysed, ranging in concentration from 77 ppm. to 4749 ppm., although no Sr minerals were observed or detected. The distribution of Sr in the various facies of the Lower and Middle Magnesian Limestone is shown in Figure 6-1 while the arithmetic mean Sr values for the facies are given in Table 6-1. Clearly, the basin facies of both the Lower and Middle Magnesian Limestone are characterized by higher values of Sr than the equivalent shallow - water facies.

Rankama and Sahama (1950) have reported that Sr is only occasionally present in sufficient abundance to form independent minerals. In both igneous and sedimentary rocks, Sr usually proxies for Ca in calcium-rich minerals because Sr^{2+} and Ca^{2+} are closely similar in ionic size. In the Magnesian Limestone, Sr will occur in a variety of forms, the most common of which will be as a solid-solution impurity in calcite and dolomite. In sulphate-rich samples, Sr may perhaps occur occasionally in celestite although in quantities below the detection limit of X-ray diffraction; more certainly it will substitute for Ca in gypsum and anhydrite. Strontium is also likely to occur in the clay minerals, especially illite, where it is known to proxy for K in the interlayer positions.

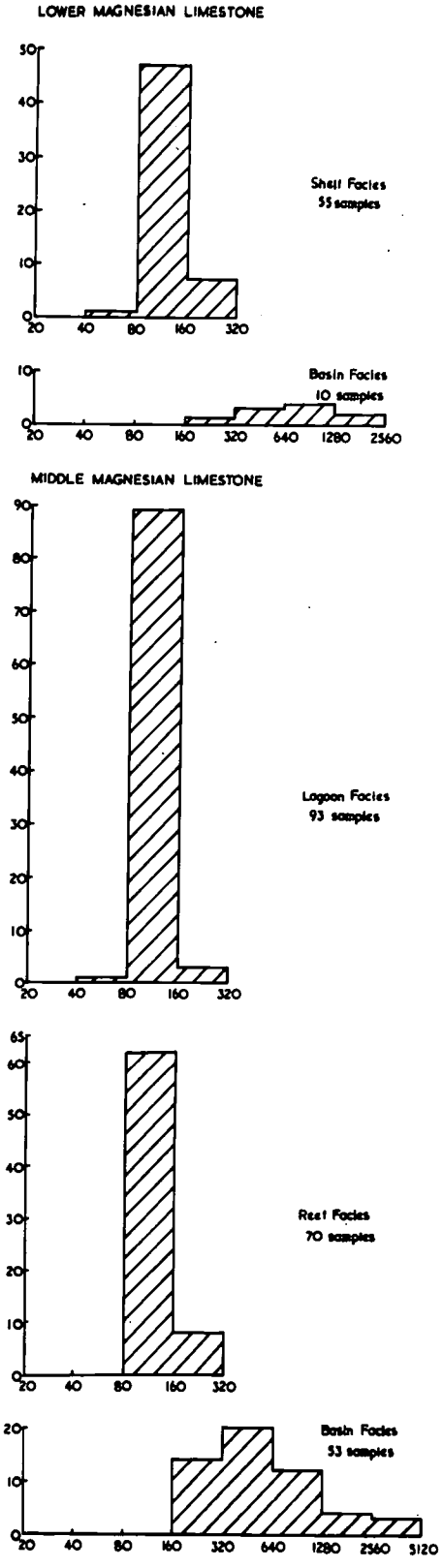

FIGURE 6-I. HISTOGRAMS SHOWING THE DISTRIBUTION OF STRONTIUM IN THE LOWER AND MIDDLE MAGNESIAN LIMESTONE. Number of samples as the ordinate. P.p.m. strontium as the abscissa.

Table 6-1.

Arithmetic mean Sr values for the various facies of the Lower and Middle Magnesian Limestone.

Lower Magnesian Limestone	Arithmetic mean Sr value (ppm.)	Middle Magnesian Limestone	Arithmetic mean Sr value (ppm.)
Shelf Facies	133	Lagoon Facies	117
		Reef Facies	124
Basin Facies	865	Basin Facies	770

Turekian and Wedepohl (1961) give the contents of Sr and Al in the average shale as 300 ppm. and 8 per cent. respectively, i.e. 19.8 ppm. Sr per 1 per cent. Al_2O_3. The mean contents of Al_2O_3 in the various facies of the Lower and Middle Magnesian Limestone are low and may be taken to represent the clay mineral contents of the sediments. Application of the data from Turekian and Wedepohl (op. cit.) allows calculation of the approximate amounts of Sr associated with clay minerals. Table 6-2 indicates the very small contribution to the total Sr content made by the clay minerals in the Magnesian Limestone.

Table 6-2.

Approximate quantities of Sr associated with clay minerals in the various facies of the Lower and Middle Magnesian Limestone, calculated using data from Turekian and Wedepohl (1961).

Lower Magnesian Limestone	Arithmetic mean Al_2O_3 Value (%)	Associated Sr (ppm.)	Middle Magnesian Limestone	Arithmetic mean Al_2O_3 Value (%)	Associated Sr (ppm.)
Shelf Facies	0.28	6	Lagoon Facies	0.07	1
			Reef Facies	0.17	3
Basin Facies	0.22	4	Basin Facies	0.29	6

The mineralogical analyses have revealed the presence of dolomite-rich rocks, calcite-rich rocks and rocks of intermediate composition in the shelf facies of the Lower Magnesian Limestone and the lagoon and reef facies of the Middle Magnesian Limestone. The sediments from these facies, with no recorded sulphate and less than 5 per cent. non-carbonate material, have been divided arbitrarily into those containing no calcite, those containing less than 20 per cent. calcite and those containing more than 20 per cent. calcite. The distribution of Sr within the three groups is shown in Figure 6-2. The 57 samples with no calcite have an arithmetic mean content of

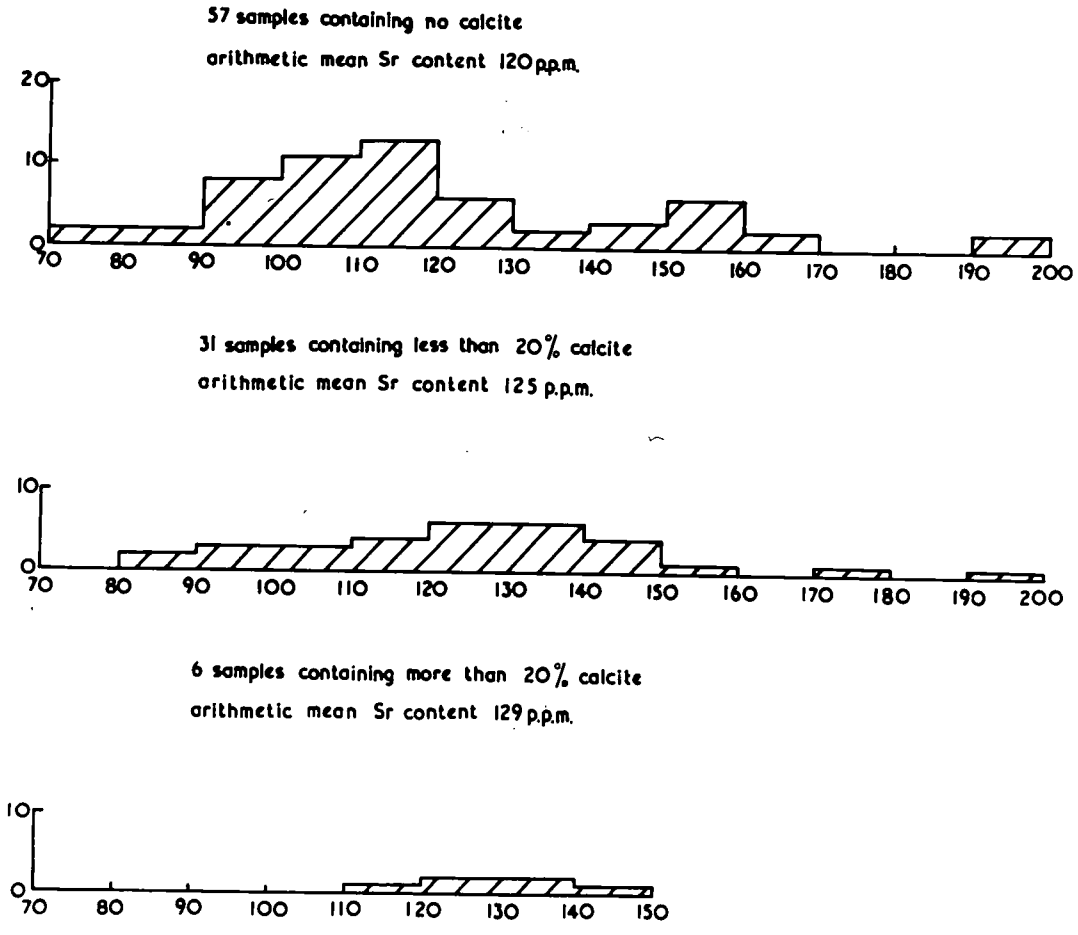

FIGURE 6–2. HISTOGRAMS SHOWING THE DISTRIBUTION OF STRONTIUM IN THREE GROUPS OF CARBONATE ROCKS WITH NO RECORDED SULPHATE AND LESS THAN 5% NON-CARBONATE MATERIAL. Number of samples as the ordinate. P.p.m. strontium as the abscissa.

120 ppm. Sr, closely similar to the arithmetic mean value of 105 ppm. Sr which may be obtained from the data of Mitchell (1956) for 15 dolomitic limestones with no recorded sulphur trioxide, less than 5 per cent. insoluble residue and more than 15 per cent. MgO. Noll (1934), Mitchell (1956), Atwood and Fry (1967) and Cameron (1969) have all shown that Sr is less abundant in dolomite than in calcite, the Sr^{2+} ion being less acceptable in the smaller dolomite lattice (Atwood and Fry, op. cit., p. 1533). A related suite of relatively pure carbonate rocks in which the proportion of dolomite to calcite gradually increases would thus be expected to show a concomitant decrease in total Sr content; such a relationship has been reported by Shearman and Shirmohammadi (1969) for a suite of related normal limestones and dolomites. There is, however, no marked trend in the arithmetic mean Sr contents of the three groups of analyses, presented in Figure 6-2, which might be related to a change in the proportions of calcite and dolomite.

In the samples investigated from all three shallow-water facies, calcite occurs most commonly as void filling, although in the lagoon facies of the Middle Magnesian Limestone it also appears to replace sulphate and sometimes appears to replace

dolomite in both the lagoon and reef facies of the Middle Magnesian Limestone. All the calcite recorded in samples from these facies is considered to be late-diagenetic and appears to be characterized by a low level of Sr, comparable to that in dolomite. By application of the mean value of 120 ppm. Sr (i.e. 1.2 ppm. per 1 per cent.) obtained for "pure" dolomite, it is possible to estimate a mean value of 1.6 ppm. Sr per 1 per cent. of late-diagenetic calcite for the 6 samples (Figure 6-2) containing in excess of 20 per cent. calcite. "Pure" late-diagenetic calcite would thus contain only 160 ppm. Sr, a significantly lower value than the 610 ppm. Sr given by Turekian and Kulp (1956) for "pure $CaCO_3$" limestones and the 640 ppm. Sr obtained by Cameron (1968, p. 299) from the data of Mitchell (1956) for 59 limestones containing less than 5 per cent. MgO and less than 5 per cent. insoluble residue. As the late-diagenetic calcite contains only slightly more Sr than dolomite, an increase in the proportion of calcite to dolomite therefore produces only a slight increase in the total Sr content.

It is interesting to consider why the late-diagenetic calcite is so low in Sr compared with the calcite of "pure" limestones. Void-filling calcite must form by precipitation

from circulating solutions, whereas much, if not most, of the calcite in limestones has been formed biogenically. Kulp et al. (1952) have shown that on average, fossils contain twice as much Sr as the adjacent calcite matrix which may have resulted from inorganic precipitation. The Sr : Ca ratio in carbonate skeletons is governed very strongly by the polymorph (calcite or aragonite) of which the shell is composed and the generic level of the organism; the temperature, salinity and Sr : Ca ratio of the environmental waters in which the organism lives have only minor influence (Turekian and Kulp, 1956; Turekian and Armstrong, 1961). The biogenic Sr contribution therefore gives ordinary limestones a relatively high overall Sr content. In contrast, the inorganic precipitation of calcite at low temperatures apparently does not lead to the incorporation of much Sr as a diadochic replacement for Ca, a conclusion already reached by Rankama and Sahama (1950).

The basin facies of both the Lower and Middle Magnesian Limestone are characterized by high values of Sr, due almost certainly to the presence of considerable quantities of calcium sulphate. The Sr contents of calcium sulphate minerals are known to be high; Goldschmidt (1958, p. 249) reported

1700 - 6900 ppm. SrO (c. 1440 - 5850 ppm. Sr) in anhydrite and up to 1300 ppm. SrO (c. 1100 ppm. Sr) in secondary gypsum formed by hydration of anhydrite. More recently, Dunham (1966, table 1) has recorded a range of 1120 - 6600 ppm. Sr for 5 samples of apparently primary anhydrite and a range of 390 - 1500 ppm. Sr for 3 samples of related secondary gypsum.

In Figure 6-3, Sr can be seen to vary with the total sulphate (gypsum plus anhydrite) content of samples from the basin facies of both the Lower and Middle Magnesian Limestone which have not been dedolomitized. There appears to be a relationship between Sr and total sulphate for samples containing less than 2000 ppm. Sr. The best-fit line calculated for the relationship has a gradient of 30.67 ppm. Sr per 1 per cent. total sulphate and a correlation coefficient of 0.65 (significant at the 0.1 per cent. level). The best-fit line indicates that between 100 and 200 ppm. Sr can be attributed to the non-sulphate material in these samples, essentially dolomite. This value agrees with the Sr content of similar sulphate-free dolomite from the shallow-water facies.

For the 3 samples B 5, 7 and 9, which contain more than 2000 ppm. Sr, there also appears to be a relationship between Sr and total sulphate, but the gradient of the best-fit line is calculated as 72.41 ppm. Sr per 1 per cent. of total sul-

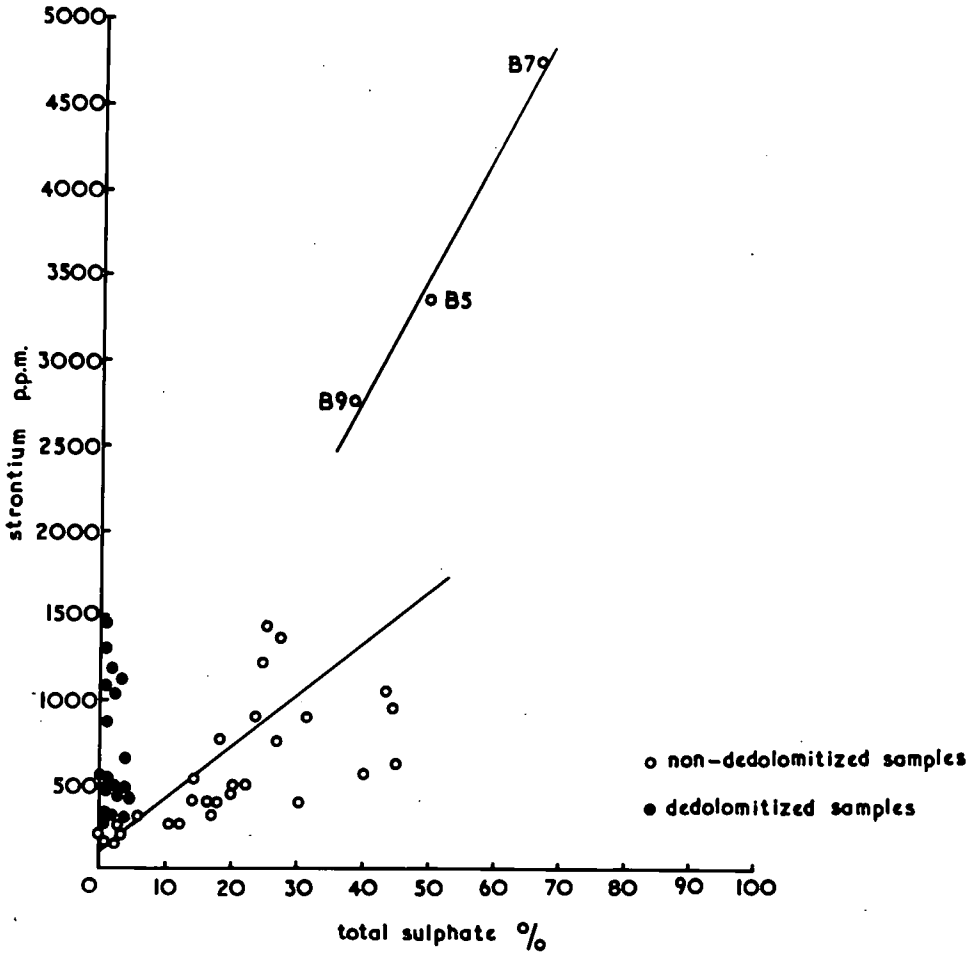

FIGURE 6-3. RELATIONSHIP BETWEEN STRONTIUM AND TOTAL SULPHATE CONTENT FOR SAMPLES FROM THE BASIN FACIES OF THE LOWER AND MIDDLE MAGNESIAN LIMESTONE. (Best-fit curves drawn for non-dedolomitized samples).

phate. These 3 samples were taken from dolomite interbedded with massive sulphate at the top of the sampled interval in borehole ML 12. All 3 samples contain large quantities of anhydrite which have escaped secondary hydration. Although anhydrite is known to contain more Sr than gypsum, this fact alone would not appear to explain the exceptionally high Sr contents of samples B5, 7 and 9. For instance, sample B 7 contains the least amount of anhydrite and yet actually contains most Sr. Also, other samples from the same borehole (e.g. B 51 and B 52) contain considerable anhydrite but do not show correspondingly large values of Sr. The anhydrite in samples B 5, 7 and 9 is believed to have been protected from solution and complete hydration by the massive sulphate beds which occur at the top of the Middle Magnesian Limestone sequence in borehole ML 12; any celestite separated during hydration (see Goldschmidt, 1958, p. 249) might also have been retained. The <u>total</u> Sr content of samples B 5, 7 and 9 might thus have changed very little, even though some hydration of anhydrite to gypsum has taken place. A value of 7241 ppm. Sr for "pure" anhydrite can therefore be obtained from the gradient of the best-fit line for samples B 5, 7 and 9; such a value is compatible with the upper limits of the range of Sr values given for "primary" anhydrite by both Goldschmidt and Dunham.

In the samples containing less than 2000 ppm. Sr, the sulphate is nearly all in the form of gypsum, although samples B 51 and B 52 form notable exceptions. The best-fit line to this data indicates that 100 per cent. gypsum would contain 3067 ppm. Sr, a considerably higher value than those given for gypsum by both Goldschmidt and Dunham. Nevertheless, the data suggests that Sr released during the hydration of anhydrite to gypsum has been removed from the system.

The Sr and total sulphate contents of the dedolomitized samples from the basin facies of the two divisions are also shown in Figure 6-3. The content of sulphate, predominantly gypsum, is less than 5 per cent. in every case, but Sr values vary over the range 280 - 1485 ppm. There is no reason to believe that the Sr : Ca ratio of the gypsum in these samples varies to this extent and it therefore seems unlikely that the entire Sr content can be attributed to the presence of sulphate minerals. However, the Sr in the dedolomitized samples does appear to be related to calcite, at least in a general sense - high values of Sr always being associated with highly calcitic samples. This evidence suggests that the late-diagenetic calcite replacing dolomite in these samples contains considerable Sr, in contrast to the late-diagenetic calcite which occurs mainly as void filling in the

shallow-water facies of the Lower and Middle Magnesian Limestone. This evidence is also in direct contrast to that of Shearman and Shirmohammadi (1969) who report low Sr contents in late-diagenetic calcite which has replaced dolomite. However, the dedolomitization described by these authors is considered to have been produced by near-surface leaching and is probably best considered as part of chemical weathering. Solution of calcium sulphate minerals and their involvement in dedolomitization reactions would thus appear to provide Sr which becomes incorporated in the newly formed "dedolomite". The overall sequence of events may perhaps be represented by the following, slightly modified, reversed form of von Morlot's equation:-

$$Ca\ Mg\ (CO_3)_2 + (Ca,\ Sr)\ SO_4 \longrightarrow 2\ (Ca,\ Sr)\ CO_3 + Mg\ SO_4$$

High Sr in "dedolomite" may therefore be indicative of dedolomitization by the "sulphate-agent" mechanism.

Manganese.

Manganese is present in all samples and ranges from 95 ppm. to 3154 ppm. The distribution of Mn in the five facies is shown in Figure 6-4 and the arithmetic mean Mn values for

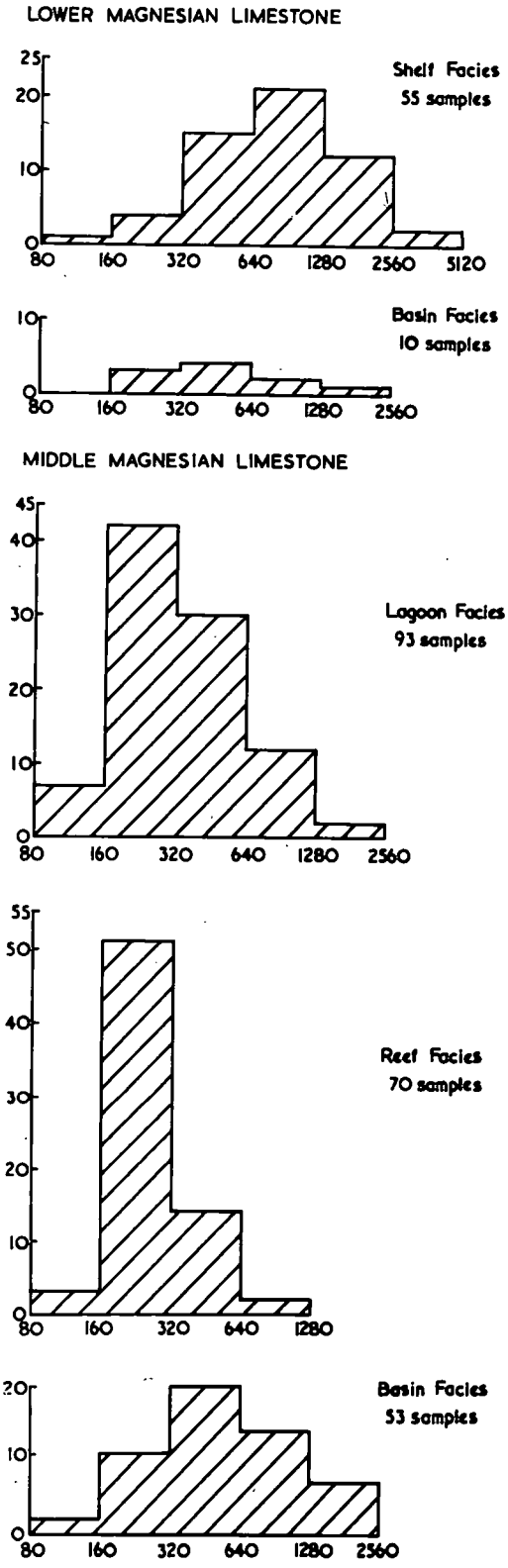

FIGURE 6–4. HISTOGRAMS SHOWING THE DISTRIBUTION OF MANGANESE IN THE LOWER AND MIDDLE MAGNESIAN LIMESTONE. Number of samples as the ordinate. P.p.m. manganese as the abscissa.

the facies are presented in Table 6-3. The shelf facies of the Lower Magnesian Limestone has the highest average Mn content, while the average Mn contents of the two basin facies are closely similar.

Table 6-3.

Arithmetic mean Mn values for the various facies of the Lower and Middle Magnesian Limestone.

Lower Magnesian Limestone	Arithmetic mean Mn value (ppm.)	Middle Magnesian Limestone	Arithmetic mean Mn value (ppm.)
Shelf Facies	870	Lagoon Facies	413
		Reef Facies	273
Basin Facies	615	Basin Facies	653

In sedimentary carbonate rocks, Mn occurs most commonly as a solid-solution impurity in the carbonate minerals, especially dolomite. According to Goldschmidt (1958), the quantity of Mn in the marine evaporite minerals is insignificant, while the small size of the clay fraction in the Magnesian Limestone rules out the clay minerals as important contributors to the total Mn content.

Figure 6-6 shows the relationship between log. Mn content and total sulphate for samples from the basin facies of the

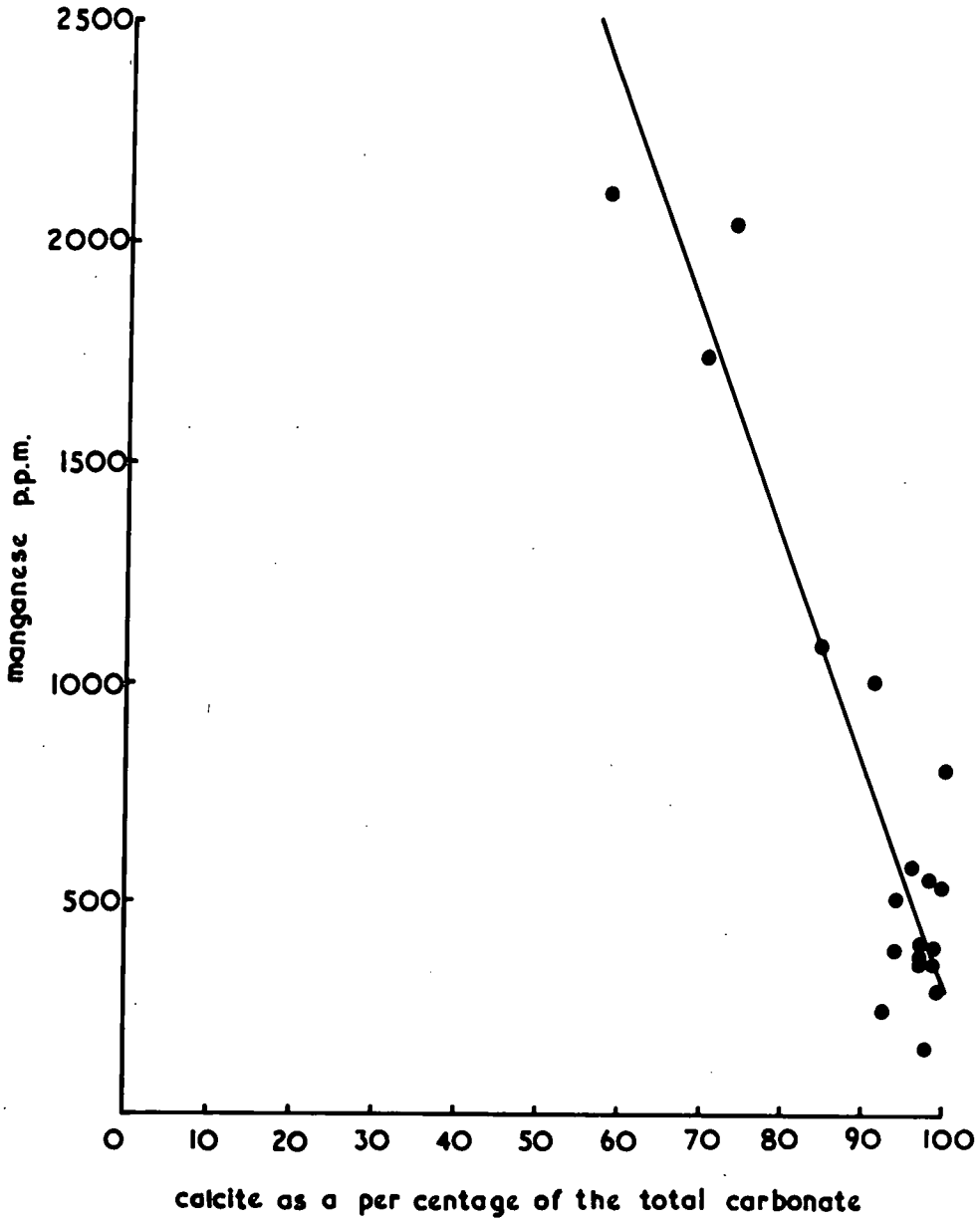

FIGURE 6-5. RELATIONSHIP BETWEEN MANGANESE AND DEGREE OF DEDOLOMITIZATION FOR BASIN SAMPLES FROM THE LOWER AND MIDDLE MAGNESIAN LIMESTONE.

Lower and Middle Magnesian Limestone. In the samples which have not been dedolomitized, there is a significant relationship between the two components, the Mn decreasing as the quantity of sulphate increases. Extrapolation of the best-fit line, drawn after visual inspection, suggests that "pure" sulphate would contain only 10 - 20 ppm. Mn and indicates that the sulphate-free carbonates, essentially dolomite, contain approximately 1100 ppm. Mn in solid solution. The latter value is in close agreement with the mean value of 1221 ppm. Mn obtained for 21 samples of dolomite separated from dolomitized limestone by Atwood and Fry (1967), but considerably higher than the mean values of 632 ppm. Mn and 402 ppm. Mn obtained by Weber (1964) for dolomite separated respectively from 59 samples of "secondary" and 84 samples of "primary" dolostone.*

Figure 6-6 indicates that there is no relationship between Mn and total sulphate in the dedolomitized samples from the two basin facies. These samples contain less than 5 per cent. sulphate in every case but Mn varies from 161 ppm. to 2116 ppm. However, the Mn content of the dedolomitized samples

---

* Weber defines a dolostone as a carbonate rock consisting mostly or wholly of the mineral dolomite.

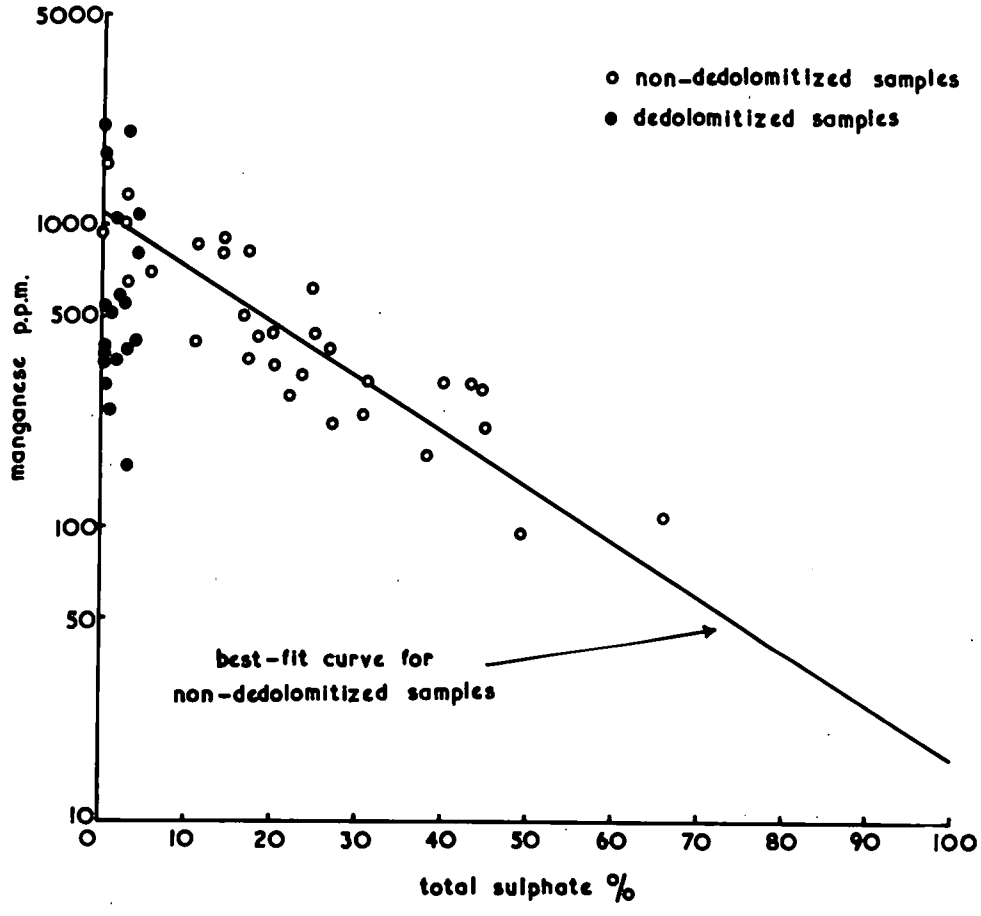

FIGURE 6-6. RELATIONSHIP BETWEEN MANGANESE AND TOTAL SULPHATE CONTENT FOR SAMPLES FROM THE BASIN FACIES OF THE LOWER AND MIDDLE MAGNESIAN LIMESTONE.

appears to be controlled by the degree to which calcite has replaced dolomite, as shown in Figure 6-5, the Mn content decreasing with increase in the degree of dedolomitization. The best-fit line calculated for the relationship has a gradient of -51.48 ppm. Mn per 1 per cent. of dedolomitization, a correlation coefficient of 0.93 (significant at the 0.1 per cent. level) and indicates that completely dedolomitized rocks should contain 284 ppm. Mn. After allowing for the small quantity of Mn likely to be held in both the sulphate and clay minerals, it is apparent that the Mn content of the late-diagenetic replacement calcite must be low. During dedolomitization by the "sulphate-agent" mechanism, therefore, Mn is removed from the system, presumably in solution.

The gradient of the best-fit line shown in Figure 6-5 indicates that pure dolomite contains 5148 ppm. Mn, a considerably higher content than the value of 1100 ppm. Mn obtained by extrapolation from Figure 6-6. The reason for the discrepancy between the two values is uncertain, but perhaps results from errors incurred in the extrapolations. Both values confirm the relatively high level of Mn held in solid solution by dolomite from the basin facies of the two divisions. Wedepohl (1964) has also recorded high Mn in dolomite from the Kupferschiefer of North-West Germany.

Although it is likely that Mn is also held in dolomite in the shallow-water facies of the Lower and Middle Magnesian Limestone, variation in Mn appears to be unrelated to dolomite, calcite or total carbonate (dolomite plus calcite). For instance, total carbonate only varies from 91.44 per cent. to 99.91 per cent. yet Mn ranges from 105 ppm. to 2861 ppm. The rocks from the shallow-water facies are frequently minutely speckled with a black substance, considered to be amorphous Mn O_2 by D. B. Smith (personal communication). This feature is not characteristic of the basin facies of the two divisions. The source of this Mn O_2 is problematical; it is possible that Mn has been leached from some rocks of the shallow-water facies by circulating groundwater and precipitated as Mn O_2 in other rocks of these facies, thus leading to wide variations in Mn content. It is also possible that some of the Mn removed during dedolomitization of the basin facies may have been carried in solution and precipitated in parts of the shallow-water facies.

Barium.

The Ba content of the samples examined varies from below the detection limit of 5 ppm. to 628 ppm. The distribution of Ba in the various facies is shown in Figure 6-7 while the

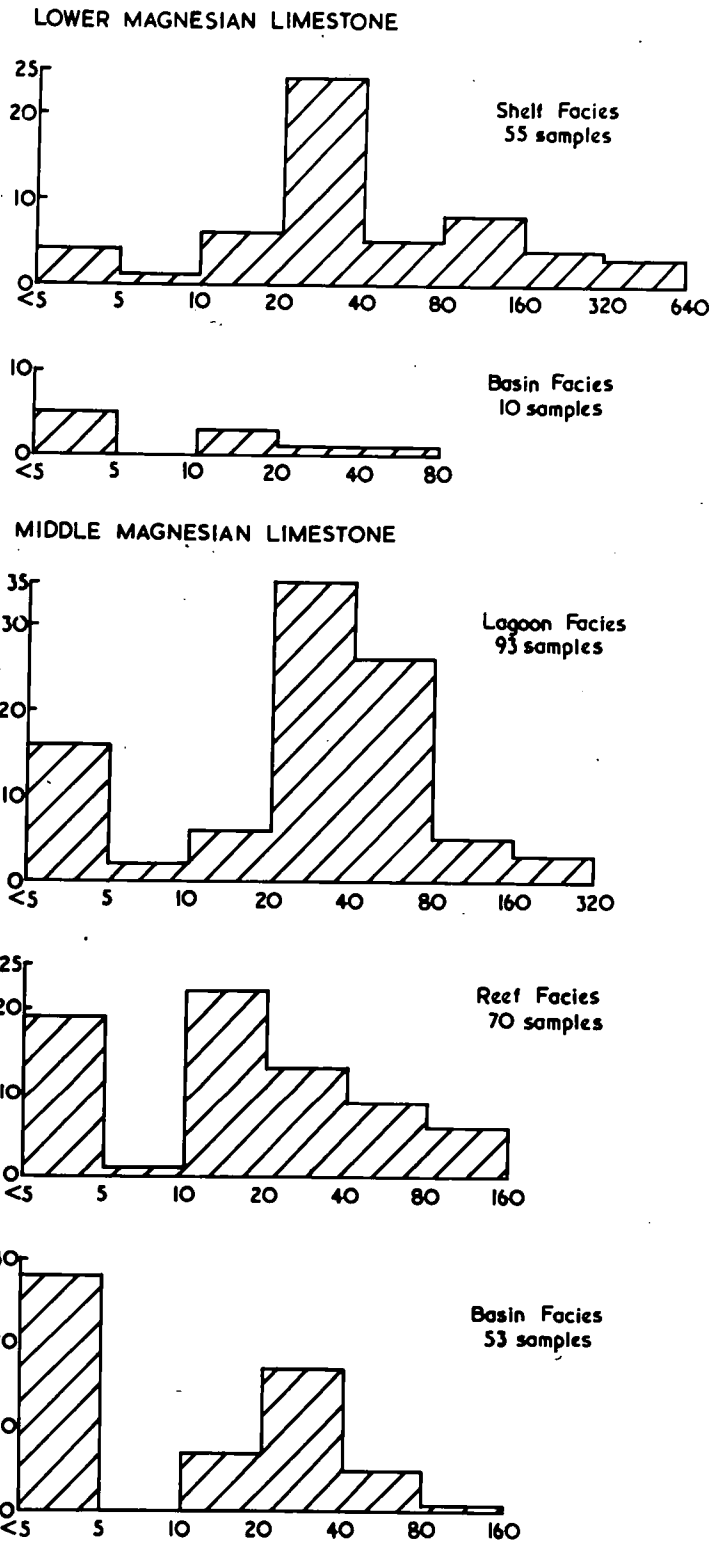

FIGURE 6-7. HISTOGRAMS SHOWING THE DISTRIBUTION OF BARIUM IN THE LOWER AND MIDDLE MAGNESIAN LIMESTONE. Number of samples as the ordinate. P.p.m. barium as the abscissa.

arithmetic mean Ba values for the facies are given in Table 6-4. All facies contain a number of samples in which Ba is below the detection limit of 5 ppm. They are particularly evident in the Middle Magnesian Limestone where their presence results in bimodal distributions of Ba in all three facies. However, at least some of the low Ba contents may be artificial, resulting from analytical error. In the analysis of Ba, the critical sample depth is greater than for other elements because of the short wavelength radiation required to excite the Ba Kα analytical line. Those samples for which there was very little powder available consistently gave a low count-rate during analysis for Ba. For these samples, it seems likely that there was insufficient powder to exceed the critical sample depth. The arithmetic mean Ba values for both basin facies are considerably lower than the means for the equivalent shallow-water facies. As Ba is most commonly below the detection limit in the basin facies, it is possible that their mean values are low due to analytical error. However, both basin facies show a comparatively close distribution of Ba values and contain no sample with Ba in excess of 100 ppm. Consequently, the differences between the levels of Ba in the basin and shallow-water facies of the Lower and Middle Magnesian Limestone are probably real.

Table 6-4.

Arithmetic mean* Ba values for the various facies of the Lower and Middle Magnesian Limestone.

Lower Magnesian Limestone	Arithmetic mean Ba value (ppm.)	Middle Magnesian Limestone	Arithmetic mean Ba value (ppm.)
Shelf Facies	83	Lagoon Facies	38
		Reef Facies	25
Basin Facies	13	Basin Facies	15

The Ba^{2+} ion is too big to replace the Ca^{2+} ion and consequently calcite, dolomite and low-temperature calcium sulphate minerals usually contain little Ba. Ba^{2+} often substitutes for K^{+} (which is of similar size) in micas and potash felspars ; in sediments, Ba is found in association with the silicate phase, either inherited from the source area or adsorbed from the overlying waters by clay minerals in shallow-water environments. In limestones, dolomites and evaporites, at least part of the Ba content can be attributed to the presence of admixed argillaceous material. Thus, Vinogradov et al. (1952) showed a direct relationship between the Ba content of limestone and the percentage of insoluble residue.

---

* In calculating the arithmetic mean values for the facies, a zero concentration is assumed for those samples which contain less than the detection limit of the element concerned. The true arithmetic mean value in such cases is therefore always slightly higher than that recorded.

Weaver (1968) has revealed a similar relationship in argillaceous limestones and calcareous shales and has also shown that more than 95 per cent. of the total Ba in the samples is associated with the insoluble residue.

Basin facies samples containing Ba in excess of 5 ppm. show a significant linear relationship between Ba and non-carbonate/sulphate material (Figure 6-8). The best-fit line calculated for the relationship has a gradient of 5 ppm. Ba per 1 per cent. of non-carbonate/sulphate material, intersects the Ba "axis" at 12 ppm. and has a correlation coefficient of 0.87 (significant at the 0.1 per cent. level). The Ba in these samples is probably associated with the clay minerals, chiefly illite. Turekian and Wedepohl (1961) quote values of 580 ppm. Ba and 8 per cent. Al for the average shale, that is, 38.6 ppm. Ba per 1 per cent. $Al_2 O_3$. The basin facies of the Lower and Middle Magnesian Limestone have arithmetic mean $Al_2 O_3$ contents of 0.22 per cent. and 0.29 per cent. respectively. By application of the data from Turekian and Wedepohl (op. cit.), it can be shown that approximately 8.5 ppm. and 11 ppm. Ba are associated with the mean $Al_2 O_3$ contents of the basinal Lower and Middle Magnesian Limestone respectively. The close similarity between these values and the arithmetic mean Ba contents is

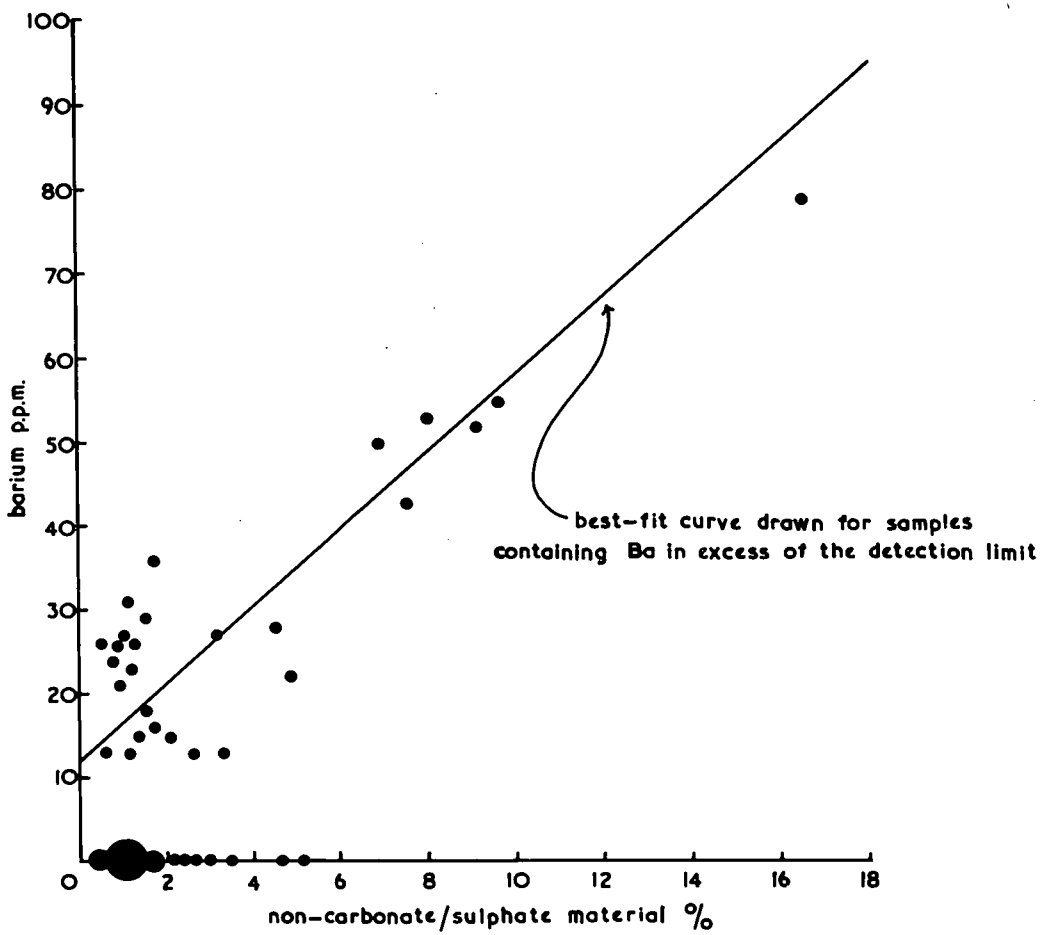

FIGURE 6-8. RELATIONSHIP BETWEEN BARIUM AND NON-CARBONATE/SULPHATE MATERIAL FOR SAMPLES FROM THE BASIN FACIES OF THE LOWER AND MIDDLE MAGNESIAN LIMESTONE. A larger symbol indicates the occurrence of several samples with similar values.

considered to confirm that the detrital clay minerals are the chief contributors of Ba in both basin facies. The positive intercept of 12 ppm. shown in Figure 6-8 suggests that some Ba is not associated with the non-carbonate/sulphate material. The intercept on the Ba "axis" would have been less if data for the samples in which Ba was not detected had been included in the calculations. However, it is possible that a small quantity of Ba is associated with the carbonates and/or sulphates in the basin facies of the two divisions; Weaver (1968) has reported that a small quantity of Ba is apparently associated with carbonate minerals, while Dunham (1966, table 1) has demonstrated low, but consistent, Ba in gypsum and anhydrite.

The Ba content of samples from the shelf facies of the Lower Magnesian Limestone and the lagoon and reef facies of the Middle Magnesian Limestone also varies with the content of non-carbonate/sulphate material. However, in these shallow-water facies the variation is more complex. After disregarding the samples which contain less than 5 ppm. Ba, it is possible to recognize two populations, each characterized by a different relationship between Ba and non-carbonate/sulphate material (Figure 6-9). For population 1, the relationship between Ba and non-carbonate/sulphate material is similar to

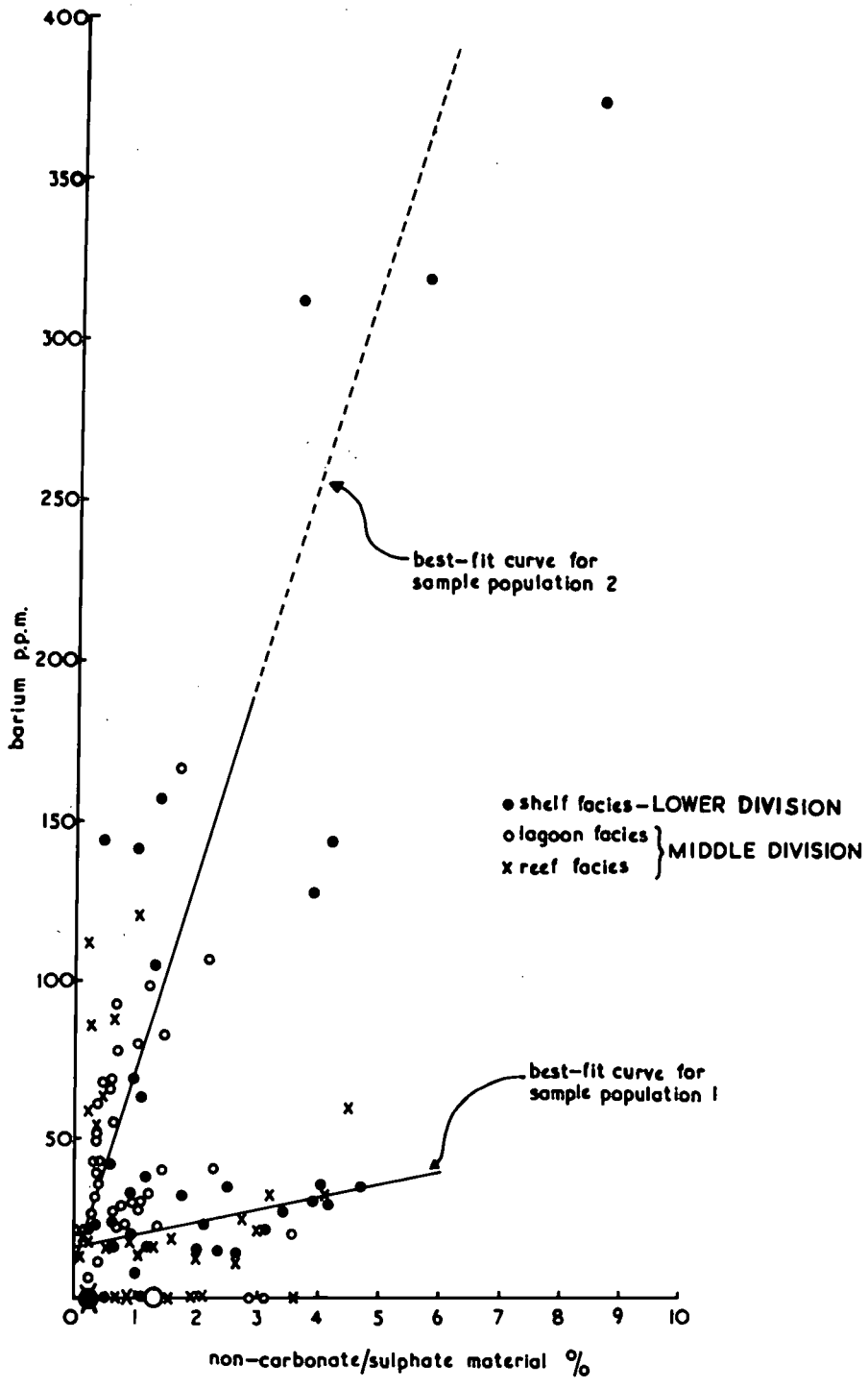

FIGURE 6–9. RELATIONSHIP BETWEEN BARIUM AND NON-CARBONATE/SULPHATE MATERIAL FOR SAMPLES FROM THE SHALLOW-WATER FACIES OF THE LOWER AND MIDDLE MAGNESIAN LIMESTONE. A larger symbol indicates the occurrence of several samples with similar values.

that for the basin facies. The gradient of the best-fit line (drawn after visual inspection) and its intercept on the Ba "axis" are comparable with those shown in Figure 6-8. The best-fit line drawn for population 2 intersects the Ba "axis" at approximately the same value but has a gradient of 60 - 70 ppm. per 1 per cent. non-carbonate/sulphate material. There is however, no apparent difference between the non-carbonate/sulphate material of the two sample populations.

The samples of population 2 are not confined to any one facies, although the 3 specimens containing more than 300 ppm. Ba shown in Figure 6-9 belong to the shelf facies of the Lower Magnesian Limestone. There may be some regional influence as all the samples from adit ML 1 and boreholes ML 8 and ML 15 belong to population 2. However, samples from the shelf Lower Magnesian Limestone in borehole ML 2 belong to population 2 while samples from the overlying lagoon and reef facies of the Middle Magnesian Limestone in the same borehole belong to population 1. In borehole ML 11, the reverse is seen. Samples from the remaining boreholes belong to population 1.

Coloured barite has been recorded in the borehole logs of ML 8 and ML 11 as occurring in occasional cavities and hairline veins in the Lower Magnesian Limestone. Barite has

also been reported from the Lower Magnesian Limestone near ML 1 and ML 2 (personal communication, Dr. D. Magraw); there is no information on the occurrence of this mineral in or near borehole ML 15. Thus, barite is known to occur in the vicinity of nearly all the boreholes from which samples belonging to population 2 were taken. However, the levels of barite which correspond with the Ba contents of samples from population 2 would be below the limit of detection of X-ray diffraction and would not contain sufficient sulphur to be detected by X-ray fluorescence spectrography. Consequently, the possibility that the samples of population 2 contain small quantities of barite cannot be ruled out. However, in view of the relationship between Ba and non-carbonate/sulphate material, it seems unlikely that the presence of barite can be entirely responsible for the enrichment of Ba in this group of samples.

There is no evidence to suggest that the level of detrital Ba in the clay minerals varies significantly in the Lower and Middle Magnesian Limestone. Thus, it could be argued that changes in the quantity of Ba associated with the clay fraction must result from adsorption by the clay minerals in the Zechstein Sea. If this were true, the general sympathetic relationship between the clay content of

the samples, as indicated by the Al_2O_3 content, and the content of non-carbonate/sulphate material, together with the linear relationship between Ba and non-carbonate/sulphate material in samples of population 2, would suggest that the uptake of extra Ba must have been approximately constant. The scattered and sporadic occurrences of the barium-rich sediments could be used to suggest that the adsorption of extra Ba did not occur everywhere and that the concentration of Ba in the overlying waters varied from locality to locality. A local enrichment of Ba by thermal springs in the Zechstein Sea has been suggested by Hirst and Dunham (1963) and recently reiterated by Dunham (1966, p. B228). As local enrichments in Ba are unlikely to have been of the same magnitude, the linear relationship between Ba and non-carbonate/sulphate material in samples of population 2 would suggest that the clays all reached equilibrium adsorption with respect to Ba. The enrichment of Ba in the samples of population 2 is, however, discussed further in conjunction with Pb and Zn.

Lead.

Lead ranges from below the detection limit of 10 ppm. to 207 ppm. The distribution and arithmetic mean values of Pb in the various facies are presented in Figure 6-10 and

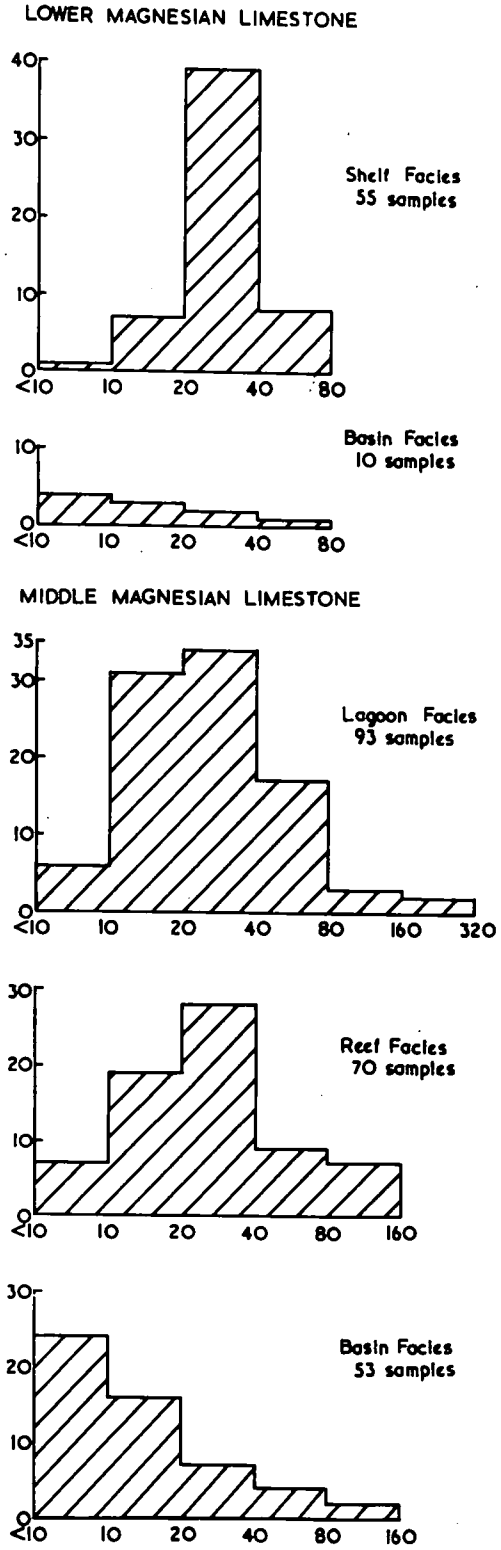

FIGURE 6-10. HISTOGRAMS SHOWING THE DISTRIBUTION OF LEAD IN THE LOWER AND MIDDLE MAGNESIAN LIMESTONE. Number of samples as the ordinate. P.p.m. lead as the abscissa.

Table 6-5 respectively. Clearly, the shallow-water facies of both divisions are characterized by higher levels of Pb than the equivalent basin facies.

Table 6-5.

Arithmetic mean Pb values for the various facies of the Lower and Middle Magnesian Limestone.

Lower Magnesian Limestone	Arithmetic mean Pb value (ppm.)	Middle Magnesian Limestone	Arithmetic mean Pb value (ppm.)
Shelf Facies	29	Lagoon Facies	34
		Reef Facies	32
Basin Facies	15	Basin Facies	19

The arithmetic mean Pb contents of the facies may be compared with the average values of 68.2 ppm. and 18.2 ppm. quoted by Weber (1964) respectively for 7 samples of "primary" and 4 samples of "secondary" dolostone. They are greater than the figure of 9 ppm. Pb given by Turekian and Wedepohl (1961) for the average carbonate rock and are considerably higher than the mean value of 4 ppm. Pb which may be obtained from the data of Mitchell (1956) for 15 samples of dolomite in which Mg O is more than 15 per cent. and the insoluble residue is less than 5 per cent.

Lead, like Ba, is related to the content of non-carbonate/sulphate material in the samples examined. Figure 6-11 shows the relationship for samples from the basin facies of the two divisions. The line of best fit (by calculation) has a gradient of 7 ppm. Pb per 1 per cent. non-carbonate/sulphate material, passes through the origin and has a correlation coefficient of 0.91 (significant at the 0.1 per cent. level). Pb also shows positive correlations, which are all significant at the 0.1 per cent. level, with SiO_2, Al_2O_3, K_2O and Rb. The above evidence suggests that Pb is associated with the detrital components, and, in particular, with the clay minerals. The association of Pb with clay minerals in sediments has already been noted (e.g. Wedepohl, 1956; Hirst, 1962). Gad *et al.* (1969) consider that approximately 70 per cent. of the total Pb in the Whitbian (Lower Jurassic) shales of North-East Yorkshire is detrital and situated in the clay minerals. These authors (*op. cit.*, table 3) give the arithmetic mean Pb and Al contents of 25 shales as 21 ppm. and 11 per cent, respectively and consider all the Al to be combined in the clay minerals. The figures show that approximately 0.7 ppm. detrital Pb is associated with each 1 per cent. of Al_2O_3 combined in the clay minerals. Using this figure to calculate the amount of detrital Pb associated

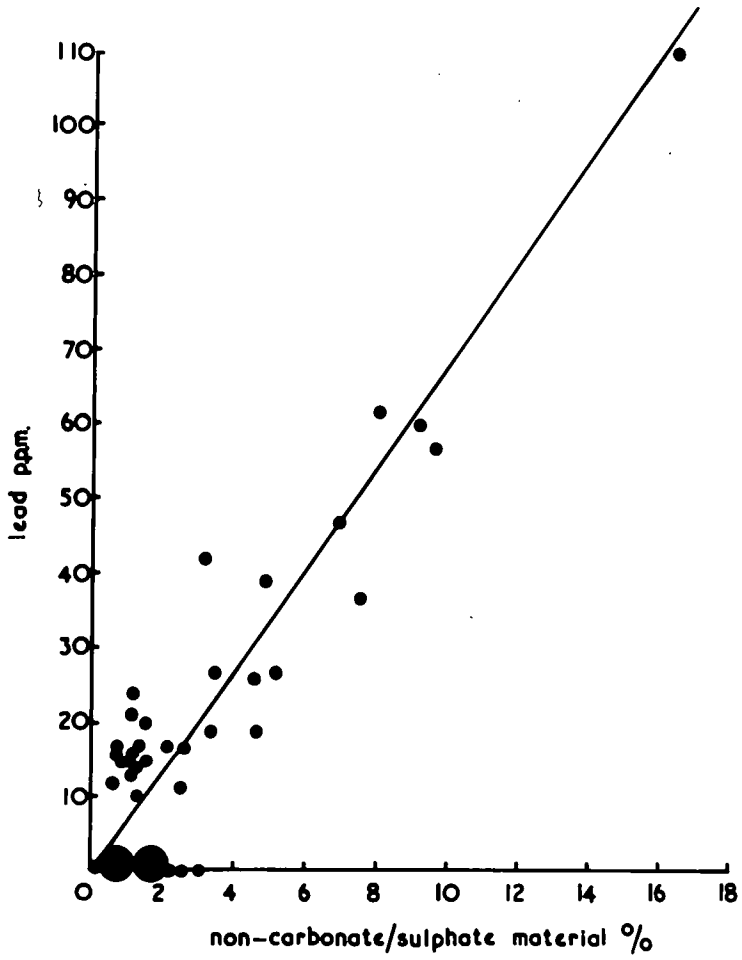

FIGURE 6-11. RELATIONSHIP BETWEEN LEAD AND NON-CARBONATE/SULPHATE MATERIAL FOR SAMPLES FROM THE BASIN FACIES OF THE LOWER AND MIDDLE MAGNESIAN LIMESTONE. A larger symbol indicates the occurrence of several samples with similar values.

with the mean Al_2O_3 contents of the basinal Lower and Middle Magnesian Limestone, 0.22 per cent. and 0.29 per cent. respectively, indicates that detrital Pb only accounts for a small proportion of the total Pb in the basin facies of either division. Thus, if all the Pb is associated with the clay minerals, their detrital Pb content must have been many times higher than 0.7 ppm. per 1 per cent. Al_2O_3, or substantial adsorption of Pb must have occurred in the Zechstein Sea. Krauskopf (1956) has shown that Pb is strongly adsorbed from sea-water by clay minerals, as well as other adsorbents.

The behaviour of Pb in the shelf facies of the Lower Magnesian Limestone and the lagoon and reef facies of the Middle Magnesian Limestone (Figure 6-12) is closely comparable to that of Ba in that there are two populations of samples, each characterized by an apparently different relationship between Pb and non-carbonate/sulphate material. The line of best fit (drawn after visual inspection) for sample population 1 has a gradient of approximately 8 ppm. Pb per 1 per cent. non-carbonate/sulphate material, passes near the origin and thus closely resembles the relationship for the basinal samples shown in Figure 6-11. Population 2 contains more samples while the relationship between Pb and non-carbonate/sulphate material is less pronounced. The

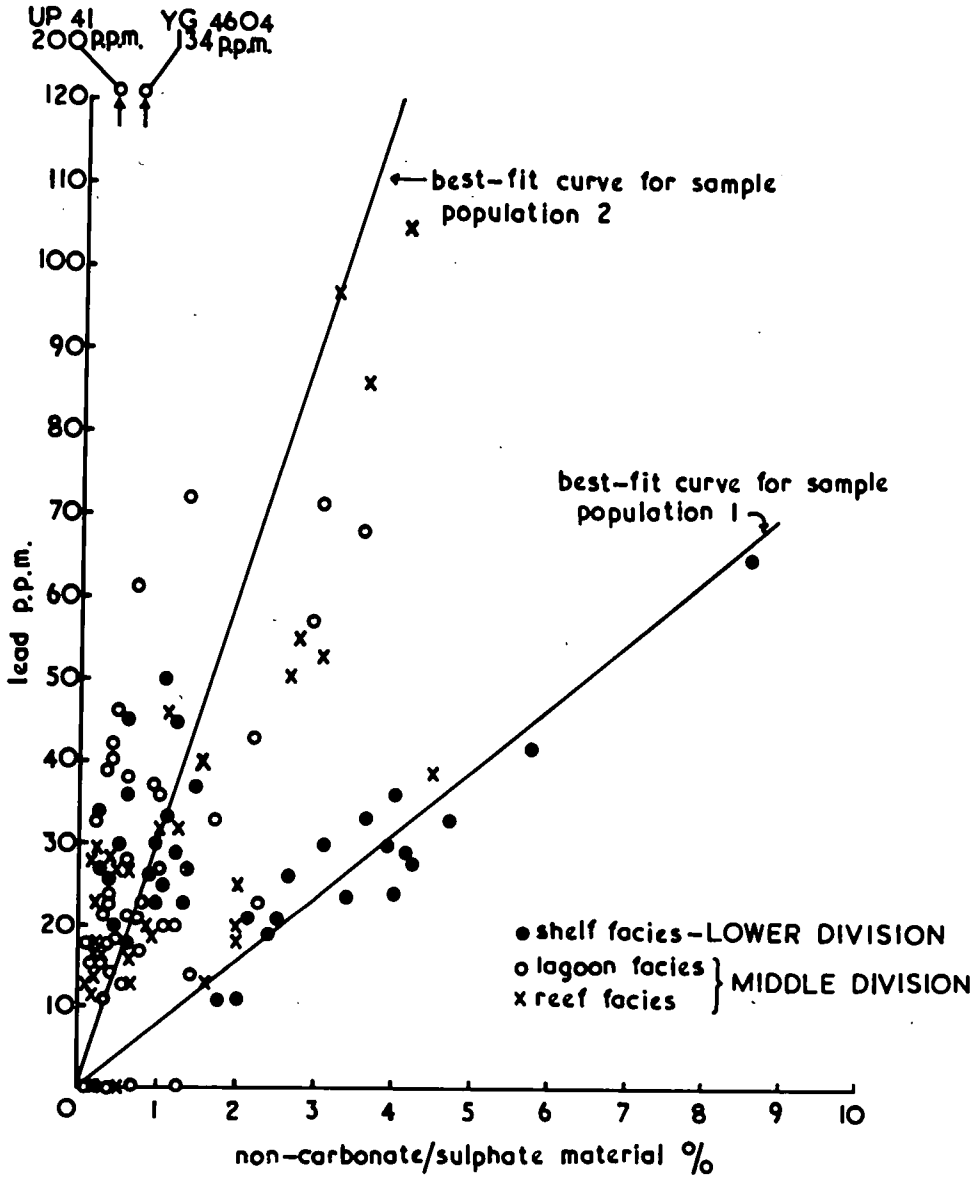

FIGURE 6-12. RELATIONSHIP BETWEEN LEAD AND NON-CARBONATE/SULPHATE MATERIAL FOR SAMPLES FROM THE SHALLOW-WATER FACIES OF THE LOWER AND MIDDLE MAGNESIAN LIMESTONE.

best-fit line (again drawn after visual inspection) passes near the origin and has a gradient of approximately 25 ppm. Pb per 1 per cent. non-carbonate/sulphate material. Samples UP 41 and YG 4604 have Pb contents which are anomalously high, even for the second relationship. As in the case of Ba, there is no apparent difference between the non-carbonate/sulphate material of the two sample populations.

Most of the samples from the lagoon and reef facies of the Middle Magnesian Limestone belong to population 2. In this population, it is only samples from these two facies which contain Pb in excess of 50 ppm. In this respect Pb contrasts with Ba, the higher values of which occur in samples from the shelf facies of the Lower Magnesian Limestone. Again, all the samples from the adit ML 1 and boreholes ML 8 and ML 15 belong to population 2 but in the other boreholes, there is no systematic variation in the occurrence of samples from the two populations.

Galena was not observed or detected in any specimens, and only 2 of the samples from the shallow-water facies which contain more than 50 ppm. Pb show the presence of any sulphur (recorded as 0.66 per cent. gypsum in ED 35 and as 0.76 per cent. anhydrite in YGF 1038). However, galena is known to occur sporadically at certain levels in the Magnesian Limestone and it is possible, therefore, that the Pb contents of

samples from population 2 could be due to the presence of small quantities of galena which would not be detectable by X-ray diffraction or contain sufficient sulphur to be detected by X-ray fluorescence. However, while the poorly defined relationship between Pb and non-carbonate/sulphate material for population 2 might suggest that some samples do contain galena, especially UP 41 and YG 4604 (see Figure 6-12), it seems unlikely that the presence of this mineral is responsible for the enrichment of Pb in all the samples.

The similarity in the relationship between Pb and non-carbonate/sulphate material for samples from the basin facies of the Lower and Middle Magnesian Limestone and for one population of samples from the corresponding shallow-water facies suggests that the mode of occurrence of the Pb in these samples is similar. However, it is necessary to invoke some additional process to explain the enrichment of Pb in the second population of samples from the shallow-water facies. While some, at least, of the extra Pb in these samples might be contributed by small quantities of galena, as with Ba, it could be postulated that the clay minerals adsorbed Pb to equilibrium from locally enriched waters in the shelf zone of the Zechstein Sea. However, it

has already been necessary to consider the possibility of adsorption of Pb by clay minerals in order to explain the content of Pb in samples from the basin facies and in some samples from the shallow-water facies of the two divisions. To invoke yet further adsorption of Pb by the clay minerals of samples from population 2 is even less satisfactory than suggesting a similar process for the enrichment of Ba, particularly in view of the less well-defined relationship between Pb and non-carbonate/sulphate material in these samples. The enrichment of Pb in sample population 2 is discussed further, in conjunction with Zn.

It is worthy of note that there is no apparent relationship between Pb and organic carbon in the 34 samples for which both analyses are available. This is perhaps surprising in view of the moderately good relationship between the two reported by Hirst and Dunham (1963) in the Marl Slate of Durham, although the low level of organic carbon in the Magnesian Limestone might obscure any relationship. Krauskopf (1956) reported that Pb is strongly adsorbed from sea-water by organic matter, but Nicholls and Loring (1962) found no relationship between Pb and organic carbon in a series of Carboniferous sediments.

Zinc.

The Zn content of the samples examined varies considerably; values range from below the detection limit of 5 ppm. to 566 ppm. The distribution of Zn in the various facies is shown in Figure 6-13 while the arithmetic mean Zn contents are given in Table 6-6. The basin facies of both divisions are clearly characterized by much lower Zn contents than the corresponding shallow-water facies. Of the latter, the reef facies of the Middle Magnesian Limestone has the highest mean Zn content. However, high Zn values are characteristic of all three shallow-water facies and it is the presence of samples with very low Zn contents, often below the detection limit, in the shelf and lagoon facies of the Lower and Middle Magnesian Limestone respectively, which reduces their mean Zn contents. All samples from these two facies in boreholes ML 7, 8 and 9 are characterized by Zn values below 20 ppm.; most other boreholes, however, also contain some samples with low Zn values in these facies.

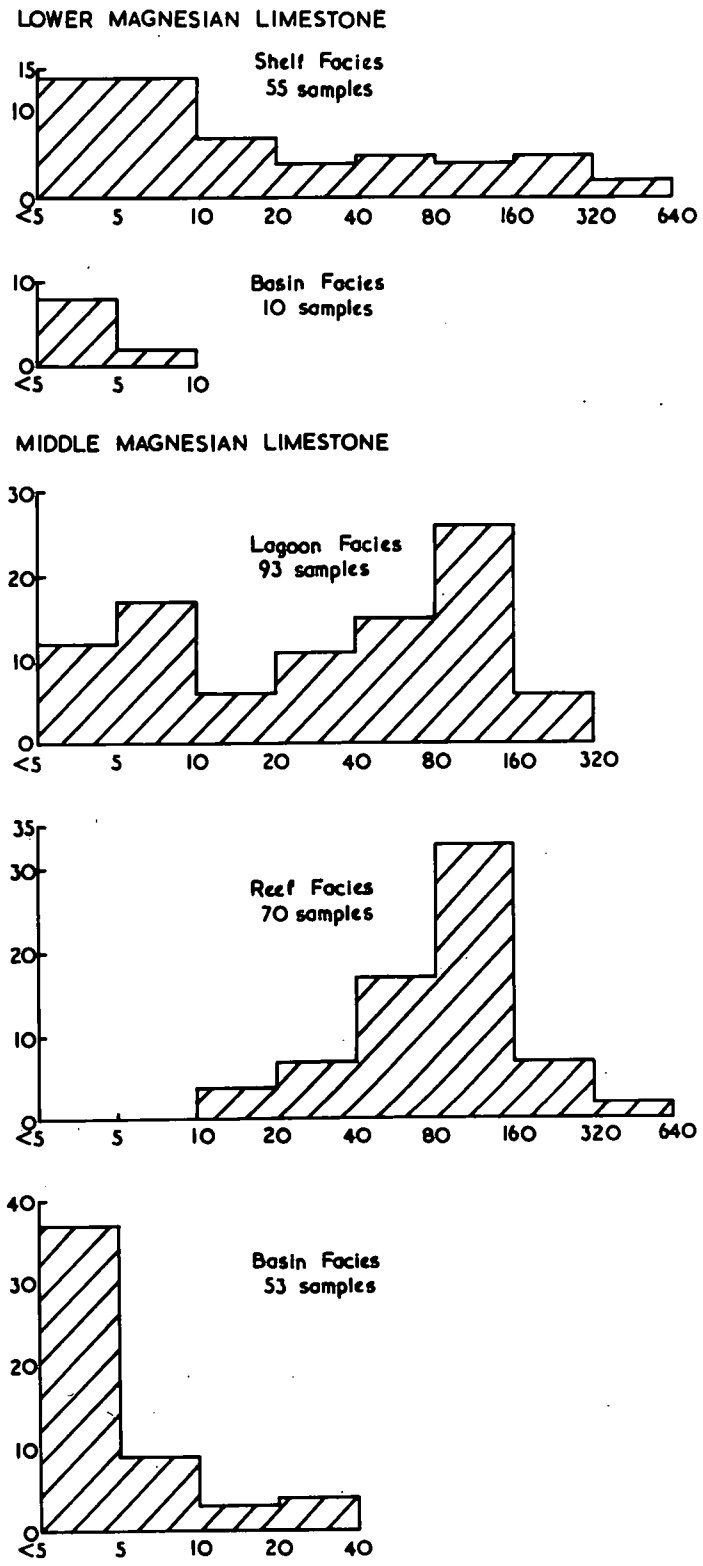

FIGURE 6–13. HISTOGRAMS SHOWING THE DISTRIBUTION OF ZINC IN THE LOWER AND MIDDLE MAGNESIAN LIMESTONE. Number of samples as the ordinate. P.p.m. zinc as the abscissa.

Table 6-6.

Arithmetic mean* Zn values for the various facies of the Lower and Middle Magnesian Limestone.

Lower Magnesian Limestone	Arithmetic mean Zn value (ppm.)	Middle Magnesian Limestone	Arithmetic mean Zn value (ppm.)
Shelf Facies	57	Lagoon Facies	61
		Reef Facies	102
Basin Facies	2	Basin Facies	4

The arithmetic mean Zn contents of the two basin facies are significantly lower than the value of 20 ppm. Zn quoted by Turekian and Wedepohl (1961) for the average carbonate rock; conversely the Zn contents of the shallow-water facies are considerably higher than this value. The Zn contents of all facies are lower than the mean value of 402 ppm. recorded by Cameron (1969) for 18 composite samples of dolomite and are even more at variance with the mean values of 1100 ppm. and 550 ppm. Zn reported by Weber (1964) for 51 samples of "primary" and 15 samples of "secondary" dolostone respectively.

---

* As a zero concentration is assumed for those samples containing less than the detection limit of the element concerned, it is possible to obtain an arithmetic mean value which is less than the detection limit.

Correlation tests carried out on the entire 162 samples for which both mineralogical and minor element analyses are available, and also on the 34 samples for which both Zn and organic carbon analyses are available, failed to reveal any significant relationships between Zn and other mineralogical or chemical components. The low values of Zn which characterize the basin facies of the two divisions suggest that the clay, carbonate and sulphate minerals of the basinal samples contain negligible Zn. The evidence available gives very little information on the mode of occurrence of Zn in the shallow-water facies. However, as carbonate rocks, and dolomites in particular, frequently act as host to sulphide minerals including sphalerite (see Cameron, 1969), it is possible that the considerable variation in the Zn content of samples from these facies is due to the sporadic occurrence of this mineral. Indeed, small quantities of sphalerite are known to occur scattered throughout the Magnesian Limestone, although according to Fowler (1943, 1957), the occurrences are most common in the (shelf) Lower Magnesian Limestone, in the beds immediately overlying the Marl Slate. Sphalerite has been recorded from joints and cavities in the Lower Magnesian Limestone of borehole ML 11 at a depth of 312 ft; a few possible crystals have also been reported from

the Lower Magnesian Limestone in borehole ML 7 at a depth of 476 ft. Sphalerite, however, was not observed or detected in any of the samples analysed, although this is hardly surprising in view of the relatively low levels of Zn involved.

In the 26 samples of Magnesian Limestone on which porosity and permeability were determined, Zn appears to be related to these petrophysical properties. The Zn content is plotted against porosity and permeability in Figures 6-14 and 6-15 respectively, from which it can be seen that all samples containing more than 30 ppm. Zn have a porosity in excess of 22 per cent. and a permeability greater than 2.5×10^{-6} cm/sec. Conversely, only one sample with less than 30 ppm. Zn has a porosity greater than 22 per cent. (UP 167) and only 2 samples with less than 30 ppm. Zn have a permeability in excess of 2.5×10^{-6} cm/sec (UP 171 and YJ 1056). It is worthy of note that sample UP 171 is considered to have an anomalous pore-structure (see p.151). The higher values of Zn are thus only found in the most porous and permeable samples.

The low arithmetic mean Zn contents of the basin facies of the two divisions are in accord with the above data as these facies are the least porous and permeable. Rocks of the reef facies of the Middle Magnesian Limestone are not only the most porous and permeable but also show a smaller

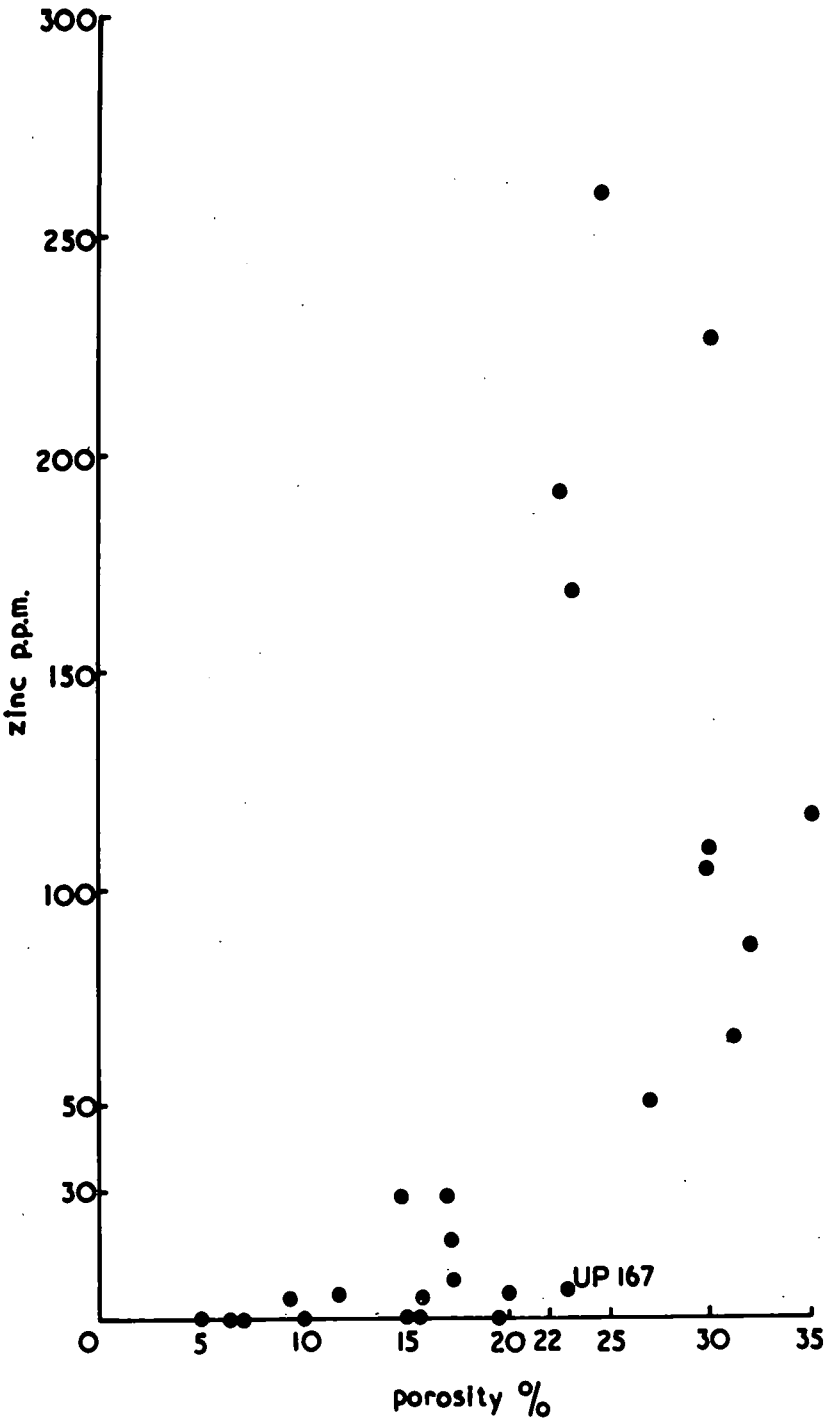

FIGURE 6-14. RELATIONSHIP BETWEEN ZINC AND POROSITY IN THE MAGNESIAN LIMESTONE.

range of porosity and permeability than rocks from either the lagoon facies of the Middle Magnesian Limestone or the shelf facies of the Lower Magnesian Limestone. The reef facies consequently shows a close distribution of relatively high Zn values in contrast to the lagoon and shelf facies which have a much wider range of Zn values.

In view of the linear trend between porosity and permeability (Figure 5-1), a relationship between Zn and one of these properties will automatically lead to a similar relationship between Zn and the other property. This accounts for the close similarity in the form of Figures 6-14 and 6-15. The relationship between Zn and permeability is considered to be most significant as it suggests that the Zn content of the samples is related to their capacity to transmit fluids. The change in the relationship between Zn and permeability which takes place at a permeability of about 2.5×10^{-6} cm/sec may thus be related to conditions of flow within the rocks, and in turn to the pore-structure. Below a permeability of about 2.5×10^{-6} cm/sec, conditions of intergranular flow probably prevail in rocks which are predominantly dense and closely packed. Above this permeability level, conditions of pipe flow may prevail, the rocks being predominantly loosely

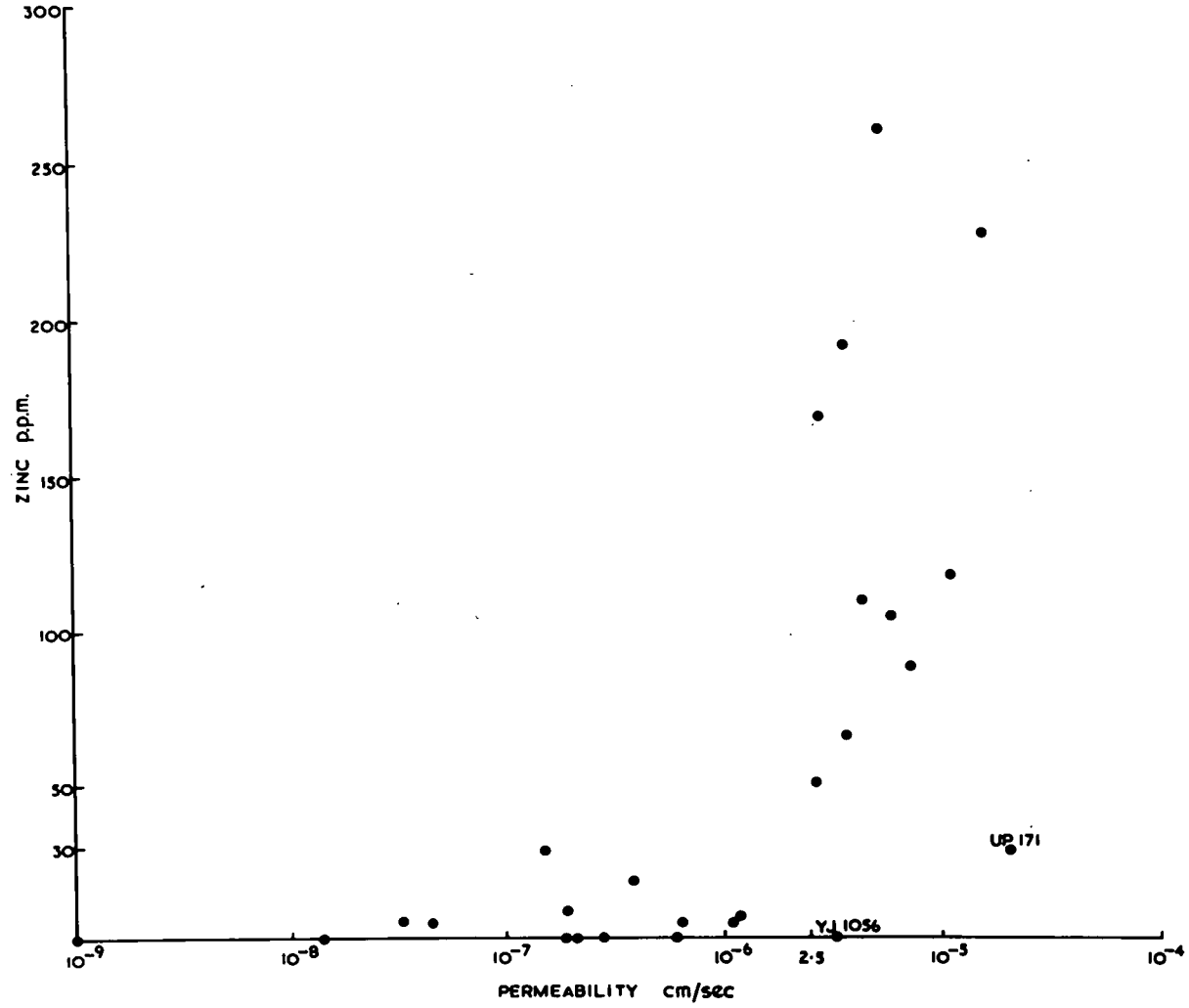

FIGURE 6–15. RELATIONSHIP BETWEEN ZINC AND PERMEABILITY IN THE MAGNESIAN LIMESTONE.

packed, oolitic, pisolitic or coarsely granular. High Zn values are thus only associated with rocks in which conditions of pipe flow prevail.

Ohle (1951), working on mineralized carbonate rocks from the East Tennessee Zinc District, also found that permeability strongly influenced the distribution of the disseminated sphalerite ore. He considered that the exclusive limitation of the mineralization to beds of "recrystallized" limestone, with relatively high permeability, was due to the relative ease of circulation of the mineralizing solutions in that rock-type. Interbedded dolomites were not mineralized because they were too "dense" to accommodate important solution flow. Without wishing to press the similarity between the East Tennessee Zinc District and the Magnesian Limestone too far, Ohle's work does support the contention that the freer circulation of solutions in the more permeable beds of the Magnesian Limestone has influenced the distribution of Zn.

In the East Tennessee Zinc District, the zinc takes the form of disseminated sphalerite. In the Magnesian Limestone, the form in which the Zn occurs is unknown, although its occurrence as sphalerite cannot be ruled out. It is possible, however, that Zn may also have been adsorbed, and later absorbed, by mineral grains, especially clay minerals, adja-

cent to pores. During the passage of a fluid through a porous medium, molecules may be adsorbed from the fluid on to the pore walls (Scheidegger, 1960). Ineson (1967) has shown that in the wall-rocks adjacent to hydrothermal mineral veins, certain elements can be "fixed" on the crystal faces of carbonate minerals, apparently by adsorption. The adsorptive capacity of any surface is influenced by the effective surface area, the amount of adsorption increasing as the surface area increases. Surface area increases with decrease in pore-size just as it increases with decrease in grain-size. It might therefore be expected that most Zn would be adsorbed by the small pores of the samples lying in the region of intergranular flow; this does not appear to have been the case. Carman (1939, p. 268) has indicated, however, that very small surface areas can hold a stationary film of water, thus reducing the effective pore-space and possibly removing these surfaces from the system as far as adsorption is concerned. The relatively low Zn contents in the region of intergranular flow may result from this effect.

As Zn, Pb and Ba are all enriched in the shallow-water facies of the Lower and Middle Magnesian Limestone, it is possible that the extra quantities of these elements share

a common origin. Thus, it could be argued that Pb and Ba might also have been adsorbed by mineral grains from circulating solutions. Indeed, the relationship between Pb, and Ba, and non-carbonate/sulphate material in the enriched samples could be taken to imply that the adsorption was effected by the clay minerals. There is, however, no apparent relationship between Pb or Ba, and porosity or permeability in the 26 samples on which these petrophysical properties were determined.

In summary, high Zn contents in the shallow-water facies of the Lower and Middle Magnesian are associated with rocks of relatively high permeability. The concentration of Zn in the Magnesian Limestone is therefore apparently related to the ease with which Zn-bearing solutions have been able to flow through the rocks. While some of the Zn could be attributed to the presence of sphalerite, some might possibly have been adsorbed by mineral grains from the circulating solutions. The distribution of some of the Pb and Ba in the shallow-water facies might also be attributable to a similar mechanism.

What then is the source of these solutions carrying Zn and possibly Pb and Ba? Hydrothermal mineralizing solutions

of the type believed to have formed the Hercynian North Pennine ore deposits are possible candidates. However, the enrichment of Zn, Pb and Ba in porous and permeable shallow-water carbonate facies adjacent to an evaporitic basin may be more than coincidental. Noble (1963) and Jackson and Beales (1967) have suggested that formation waters expelled from compacting sedimentary basins might play an important role in the location of ore-deposits, especially Mississippi Valley-type Pb-Zn deposits, in adjacent porous and permeable rocks. The formation waters expelled from a compacting evaporitic basin will be highly saline brines which may carry Zn, Pb and other elements in solution (Roedder, 1965). The levels of Zn, Pb and Ba in the basin carbonates and the reported levels of these elements in the evaporitic minerals (Goldschmidt, 1958) suggest that formation fluids expelled from these sediments would not carry significant quantities of heavy metals. However, it is important to realize that the present concentration of elements in the compacted rocks is likely to be different from the original metal content of the unconsolidated sediments. Calcareous and other algae are known to be able to concentrate Zn, Pb and other elements from the waters in which they live (see for example Wolf et al., 1967, table V). The Middle Magnesian Limestone reef is built largely of cal-

careous algae; algae flourished in the Middle Magnesian Limestone lagoon and also, perhaps, in the Lower Magnesian Limestone shelf. These rocks may thus have acted as a source for Zn, Pb and other elements, any metals concentrated by the algae being readily removed and redistributed by formation waters escaping laterally from the adjacent compacting evaporitic basin.

Noble (1963) considers that formation fluids, as well as moving upwards and laterally, can also move downwards with much greater ease than meteoric groundwater. It is therefore also possible that formation water moving downwards from the compacting Permian evaporitic basin picked up Zn, Pb and perhaps also Ba from the underlying Carboniferous sediments, which contain all three elements in epigenetic minerals, and eventually migrated to the shallow-water facies of the Magnesian Limestone. This hypothesis has the advantage of being able to explain the coincidence between the enrichments of Zn, Pb and Ba in the shallow-water facies of the Magnesian Limestone and the occurrence of epigenetic sphalerite, galena and barite in the underlying Carboniferous sediments and perhaps deserves most consideration.

Copper.

Copper ranges from below the detection limit of 8 ppm. to 89 ppm.; no Cu minerals were observed or detected in the samples under investigation. The distribution and arithmetic mean values of Cu in the various facies of the Lower and Middle Magnesian Limestone are presented in Figure 6-16 and Table 6-7 respectively. The basin facies of both the Lower and Middle Magnesian Limestone are slightly lower in Cu than the respective shallow-water facies although, paradoxically, sample B 9 from the basin facies of the Middle Magnesian Limestone contains the highest recorded value of Cu. Figure 6-16 shows that this value is clearly atypical of the facies. Comparison of the arithmetic mean Cu values given in Table 6-7 with the value of 4 ppm. given by Turekian and Wedepohl (1961) for the average carbonate rock and with the mean values of 5.72 ppm. and 6.74 ppm. given by Weber (1964) for 128 "primary" and 87 "secondary" dolostones respectively shows that the Lower and Middle Magnesian Limestone are, on the whole, enriched in Cu.

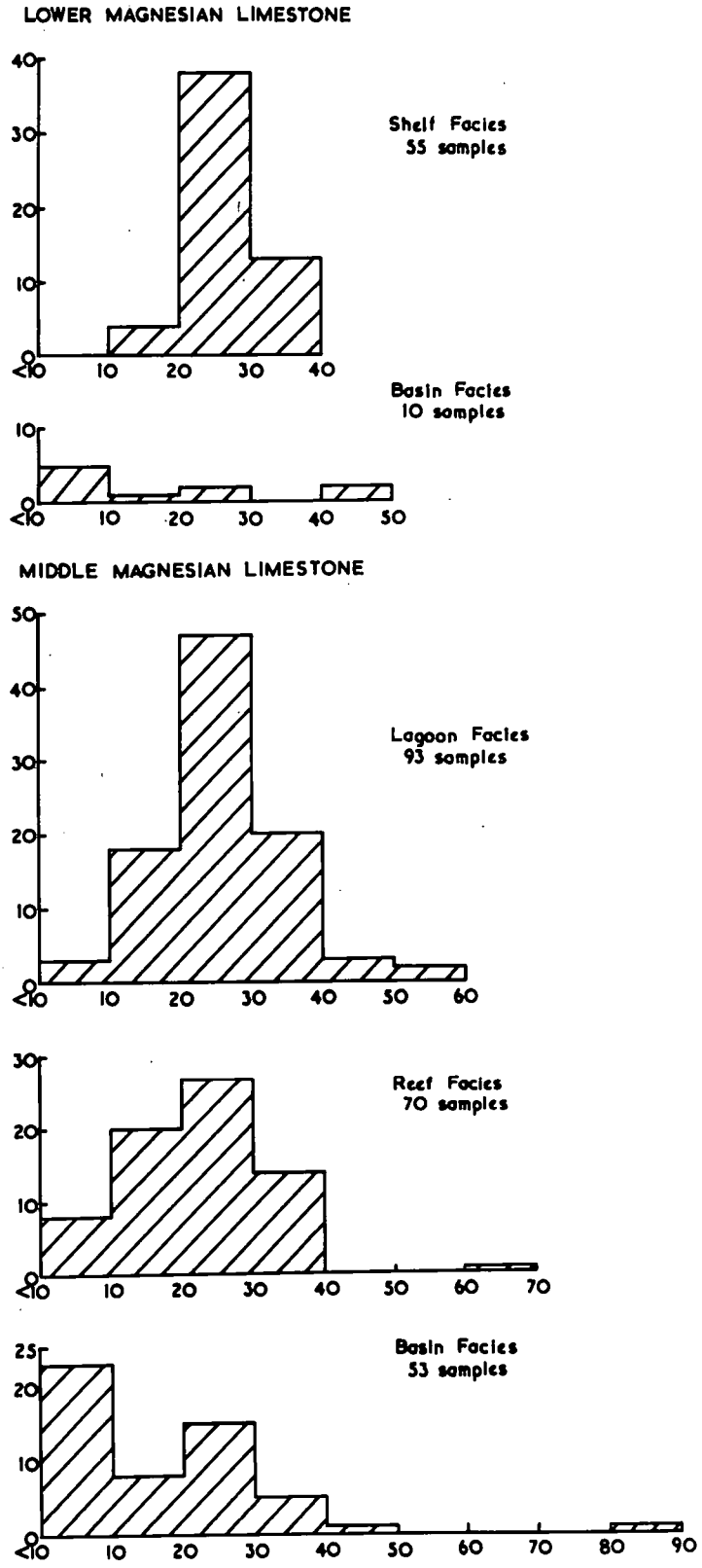

FIGURE 6-16. HISTOGRAMS SHOWING THE DISTRIBUTION OF COPPER IN THE LOWER AND MIDDLE MAGNESIAN LIMESTONE. Number of samples as the ordinate. P.p.m. copper as the abscissa.

Table 6-7.

Arithmetic mean Cu values for the various facies of the Lower and Middle Magnesian Limestone.

Lower Magnesian Limestone	Arithmetic mean Cu value (ppm.)	Middle Magnesian Limestone	Arithmetic mean Cu value (ppm.)
Shelf Facies	25	Lagoon Facies	25
		Reef Facies	21
Basin Facies	17	Basin Facies	15

In the Magnesian Limestone, Cu is controlled, in part at least, by organic carbon, as shown in Figure 6-17. The relationship between the two components is by no means perfect, but in spite of the relatively low concentrations of both Cu and carbon, the correlation coefficient is 0.73, significant at the 0.1 per cent. level. Hirst and Dunham (1963) noted a similar relationship in the Durham Marl Slate. The relationship suggests that at least part of the Cu incorporated in the sediments is related to the presence of organic matter. This may represent Cu originally concentrated in the living tissue of organisms (see Le Riche, 1959, p. 119) or Cu subsequently adsorbed on to the organic matter derived from it.

Figure 6-17 indicates that approximately 17 ppm. Cu is not associated with carbon. This observation is similar to that of Gad et al. (1969) who have reported that in the Whitbian shales of North-East Yorkshire, organic carbon only governs the concentration of Cu in excess of approximately 20 ppm. Gad et al. showed that this figure was similar to the Cu remaining in the shales after chemical extraction treatment and concluded that this Cu was detrital and situated in the clay minerals. The arithmetic mean Al content of 25 Whitbian shales is given as 11 per cent. (op. cit., table 3) which allows approximately 1 ppm. detrital Cu to each 1 per cent. of $Al_2 O_3$ combined in the clay minerals. The arithmetic mean $Al_2 O_3$ contents of each of the Lower and Middle Magnesian Limestone facies is below 0.3 per cent. It therefore seems very unlikely that as much as 17 ppm. detrital Cu could be associated with clay minerals, unless the clay minerals deposited in the Zechstein Sea contained an unusually high content of detrital Cu. Hirst and Dunham (1963), however, have shown that the clay minerals in the Marl Slate, underlying the Magnesian Limestone of Durham, contain insignificant quantities of Cu. It also seems unlikely that very much Cu is associated with the carbonate

and/or sulphate phases present in the Magnesian Limestone as carbonate and evaporite minerals are known to contain only low quantities of Cu (Rankama and Sahama, 1950; Stewart, 1963).

The analysis of Cu by X-ray fluorescence spectrography is complicated by the fact that Cu impurities in the X-ray tube filament cause contamination of the Cu Kα analytical line. The correction applied to eliminate this spectral contamination (see Chapter 3) may have been insufficient, resulting in a positive bias in the Cu analyses. In this respect, it is perhaps significant that the Cu determination on the Standard Diabase W-1 was higher by 25 ppm. than the value recommended by Fleischer (1965). However, this could be due to matrix differences between the Diabase and the Magnesian Limestone. The fact that a considerable number of samples of Magnesian Limestone were found to contain Cu in amounts less than the limit of detection of 8 ppm. suggests that any bias, if present at all, must be quite small.

In the absence of any further evidence, it must be assumed that small Cu contributions from the clay, carbonate and perhaps sulphate minerals, together with the effects of a possible slight positive bias in the Cu results, account for the Cu not associated with organic carbon.

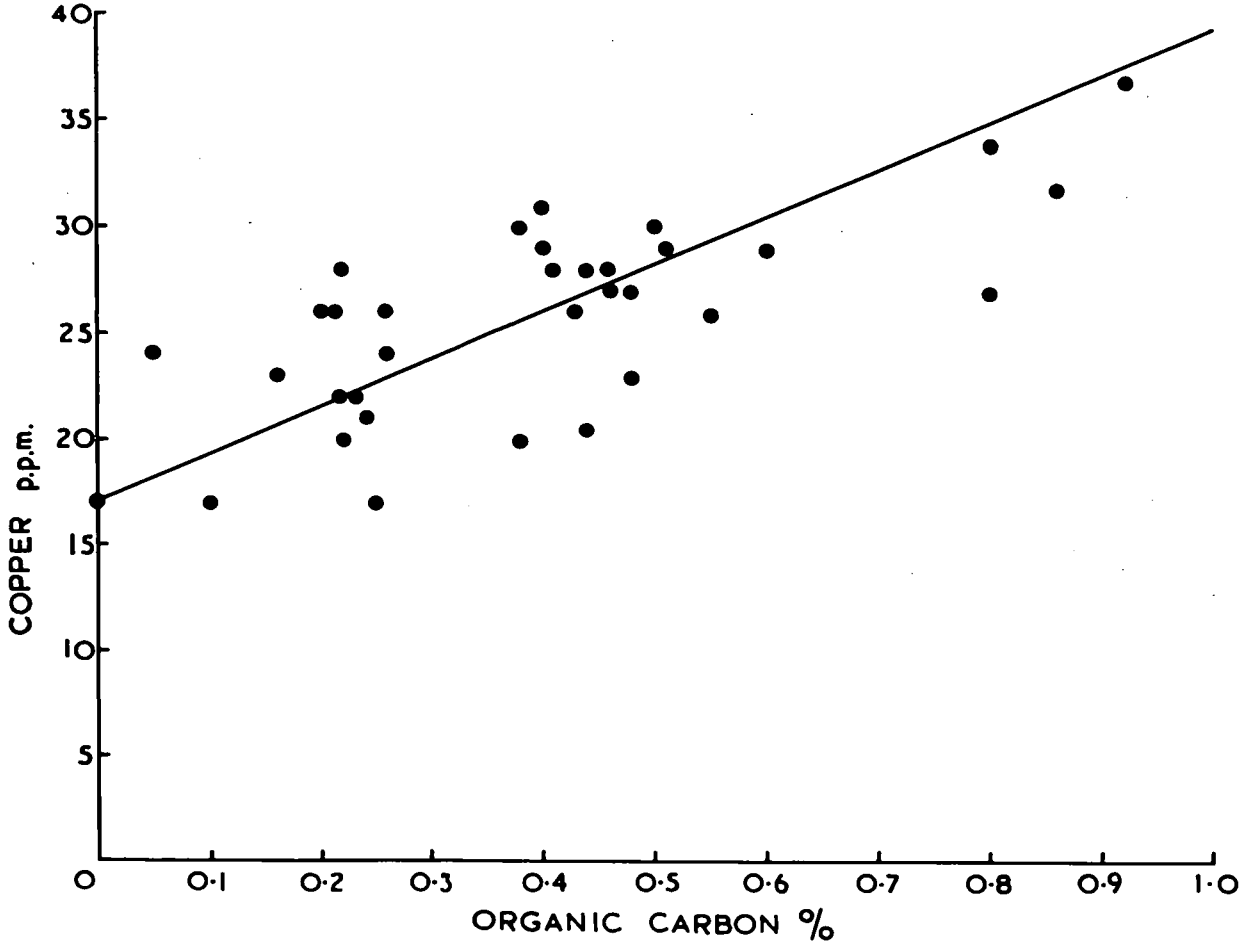

FIGURE 6–17. RELATIONSHIP BETWEEN COPPER AND ORGANIC CARBON.

Although relatively few organic carbon analyses are available, there is no evidence of any marked divergence from the relationship between Cu and organic carbon. Divergences from the Cu/carbon relationship in the Marl Slate led Hirst and Dunham (1963) to postulate a fluctuating source for at least part of the Cu in the Durham Zechstein. The lower arithmetic mean Cu values for the basin facies of the two divisions therefore suggest that the organic carbon contents of these facies are, in general, lower than in the equivalent shallow-water facies. However, extrapolation of the best-fit line in Figure 6-17 suggests that samples B 9 (with 89 ppm. Cu) and B 7 (with 67 ppm. Cu) must contain in excess of 3 per cent. and 2 per cent. organic carbon respectively. Organic carbon values of this magnitude are high for the Magnesian Limestone (see Appendix 2) and also for carbonate rocks in general (e.g. Gehman, 1962). Thus, in these 2 samples in particular, there may be evidence for an additional supply of Cu at the time of deposition or the values might result from subsequent diagenetic mobilization of this element.

Rubidium.

The concentration of Rb is usually near or below the detection limit of 3 ppm. Apart from samples UP 170, YJ 1053B and YG 4380 which contain respectively 78 ppm., 47 ppm. and 41 ppm., the Rb contents lie below 20 ppm. The arithmetic mean Rb values for the various facies, presented in Table 6-8, are closely similar to the value of 3 ppm. Rb given by Turekian and Wedepohl (1961) for the average carbonate rock but are considerably less than the mean values of 39.8 ppm. and 33.9 ppm. reported by Weber (1964) for 70 samples of "primary" and 26 samples of "secondary" dolostone respectively.

Table 6-8.

Arithmetic mean Rb values for the various facies of the Lower and Middle Magnesian Limestone and approximate quantities of Rb associated with clay minerals.

		Arithmetic mean Rb value (ppm.)	Rb associated with clay minerals (ppm.)
Lower Magnesian Limestone	Shelf Facies	3	2.6
	Basin Facies	2	2.0
Middle Magnesian Limestone	Lagoon Facies	1	0.6
	Reef Facies	2	1.6
	Basin Facies	3	2.7

The analyses of Mitchell (1956) clearly show that the Rb content of carbonate rocks of various age and provenance is related to the amount of insoluble residue; in particular, Rb is concentrated in the clay fraction. Data from Turekian and Wedepohl (1961) indicates that 9.3 ppm. Rb is associated with each 1 per cent. of Al_2O_3 in the average shale. Application of this figure to the arithmetic mean Al_2O_3 contents of the various facies gives a crude indication of the amounts of Rb likely to be associated with the clay minerals. The calculated values, presented in Table 6-8, are closely comparable with the arithmetic mean Rb contents for the facies, suggesting that this element is wholly contained in the clay minerals. This is confirmed by the correlation matrix for the entire 162 samples for which both Rb and major element analyses are available; Rb correlates positively with all the non-carbonate/sulphate components, in particular with SiO_2, Al_2O_3, TiO_2 and K_2O. The strongest correlation is with K_2O ($r = 0.90$, significant at the 0.1 per cent. level) and as the $K_2O : Al_2O_3$ ratio in the Magnesian Limestone is consistent with the K being held in the illite structure (see p.133), Rb must be associated with this mineral, most probably as a detrital constituent. An association between Rb and illite has also been demonstrated in the Marl Slate

of Durham by Hirst and Dunham (1963) and in the Kupferschiefer of North-West Germany by Wedepohl (1964).

The mean Rb : K_2O ratio for the Magnesian Limestone, calculated from the regression line, is 47.90, a value which is closely similar to the mean Rb : K_2O ratio of 49.42 which can be calculated from 8 analyses of Marl Slate presented by Hirst and Dunham (op. cit., tables IV and VII). The similarity in K_2O : Al_2O_3 and Rb : K_2O ratios of both the Marl Slate and Magnesian Limestone (see p.133) indicates that the composition of the illite deposited within the Zechstein Sea remained approximately constant and that there was no major change in provenance throughout the Lower Zechstein.

Nickel.

The Ni content ranges from below the detection limit of 3 ppm. to 97 ppm. although only 7 samples contain more than 20 ppm. Ni. The arithmetic mean Ni values for the various facies are given in Table 6-9, from which it can be seen that the basin facies of both divisions have slightly higher mean Ni contents than the corresponding shallow-water facies. However, although both basin facies contain samples with Ni contents in excess of 20 ppm., the Middle Magnesian Limestone lagoon facies also contains 3 samples with relatively high Ni contents.

Table 6-9.

Arithmetic mean Ni values for the various facies of the Lower and Middle Magnesian Limestone.

Lower Magnesian Limestone	Arithmetic mean Ni value (ppm.)	Middle Magnesian Limestone	Arithmetic mean Ni value (ppm.)
Shelf Facies	6	Lagoon Facies	4
		Reef Facies	4
Basin Facies	7	Basin Facies	7

The arithmetic mean Ni values presented in Table 6-9 agree closely with the average value of 7.5 ppm. quoted by Graf (1962) from 3067 analyses of carbonate rocks from the Russian Platform given by Ronov (1956). They also compare with the mean value of 12 ppm. Ni which may be obtained from the data of Mitchell (1956) for 183 sedimentary carbonate rocks from Scotland, but are considerably less than the mean values of 126 ppm. and 41 ppm. quoted by Weber (1964) for 22 samples of "primary" and 9 samples of "secondary" dolostone respectively.

Correlation tests on the 162 samples for which both major and minor element analyses are available reveal that Ni correlates positively with all the non-carbonate/sulphate components but shows the strongest correlations, all significant

at the 0.1 per cent. level, with Al_2O_3, TiO_2, K_2O and Rb. This evidence indicates that Ni is contained in the clay mineral illite. The occurrence of Ni in clay minerals has already been noted by Hirst (1962) and Nicholls and Loring (1962). Krauskopf (1956) has shown that the clay minerals are ineffective in removing Ni from sea-water. The Ni present in the clay minerals of the Magnesian Limestone may therefore very well be detrital.

The 34 samples for which organic carbon analyses are available reveal no significant relationship between Ni and carbon. This is in direct contrast to Hirst and Dunham (1963) and Wedepohl (1964) who demonstrated such a relationship in the Marl Slate of Durham and the Kupferschiefer of North-West Germany respectively. Gad et al. (1969) have also reported a significant relationship between Ni and organic carbon in Whitbian shales from North-East Yorkshire, although their data suggests that organic matter was responsible for the incorporation of Ni only in excess of about 50 ppm. (op. cit., p. 119). They consider this 50 ppm. to be detrital, and to be accommodated in clay minerals. As the arithmetic mean Al content of 25 Whitbian shales is 11 per cent., there is thus approximately 2.4 ppm. detrital Ni for each per cent. of Al_2O_3. Assuming this value to be a typical level of

detrital Ni in clay minerals and applying it to the mean Al_2O_3 values for the various facies (all $<$ 0.3 per cent.) accounts for only part of the mean Ni values for the facies. Some of the Ni in the Magnesian Limestone may therefore be associated with organic matter, the Ni-carbon relationship being obscured by the low level of both components.

Boron.

Boron was determined in 27 whole rock samples taken from the three sinkings ML 7, ML 1 and ML 3 which respectively intersected strata of the lagoon, reef and basin facies of the Middle Magnesian Limestone. Samples taken from the boreholes ML 3 and ML 7 include specimens from the underlying Lower Magnesian Limestone, although the sinkings were selected principally to investigate any variations in B within the three facies of the Middle Magnesian Limestone.

Boron is present in all 27 samples and ranges in concentration from 13 ppm. to 239 ppm. (see Appendix 6). The analyses are summarized in Table 6-10 in the form of arithmetic mean B values for the various facies. The comparatively high mean B value for the basin facies of the Middle Magnesian Limestone is caused by the high, and clearly atypical, value of 239 ppm. recorded in sample YJ 1053 B. The arithmetic mean

B contents for the facies are comparable with the mean B contents of 68.1 ppm. and 66.8 ppm. obtained respectively for 93 samples of "primary" and 30 samples of "secondary" dolostone by Weber (1964). The B content of sedimentary carbonate rocks, however, varies considerably due possibly to irregular disseminations of borate minerals, or more likely, to variations in the content of detrital clay minerals.

Table 6-10.

Summary of B analyses.

		Number of Samples	Arithmetic mean B value (ppm.)
Lower Magnesian Limestone	Shelf Facies	3	86
	Basin Facies	3	64
Middle Magnesian Limestone	Lagoon Facies	6	67
	Reef Facies	9	60
	Basin Facies	6	105

Borate minerals do not occur within the Lower and Middle Magnesian Limestone of Durham although, in the Whitby area, veatchite ($Sr\ B_6\ O_{10} \cdot 2H_2\ O$) has been recorded from the Lower Evaporites and boracite ($Mg_3\ B_7\ O_{13}\ Cl$) occurs in the Middle

and Upper Evaporites (Stewart, 1954, p. 228). However, small quantities of clay minerals, essentially illite, occur throughout the Magnesian Limestone. The B content of the 27 samples examined correlates positively with all the non-carbonate/sulphate components, but especially with K_2O ($r = 0.81$, significant at the 0.1 per cent. level). The relationship between B and K_2O is shown in Figure 6-18. The $K_2O : Al_2O_3$ ratio in the Magnesian Limestone is consistent with the K being held entirely in the illite (p.133); K_2O contents can thus be taken as a measure of the abundance of illite. The linear relationship between B and K_2O shows that the content of B is proportional to the content of illite, a situation which has also been demonstrated in the Kupferschiefer of North-West Germany by Wedepohl (1964). Harder (1959) appears to have been the first to show that much of the B in sediments is concentrated in illite although this conclusion has since been vindicated by many other workers.

Figure 6-18 shows that in the Magnesian Limestone, B is proportional to K_2O (and therefore illite) only in excess of about 50 ppm. This might indicate that some B is associated with components other than illite, such as organic carbon (Hirst, 1968) or detrital tourmaline (Walker, 1963). Samples for which both B and carbon analyses are available

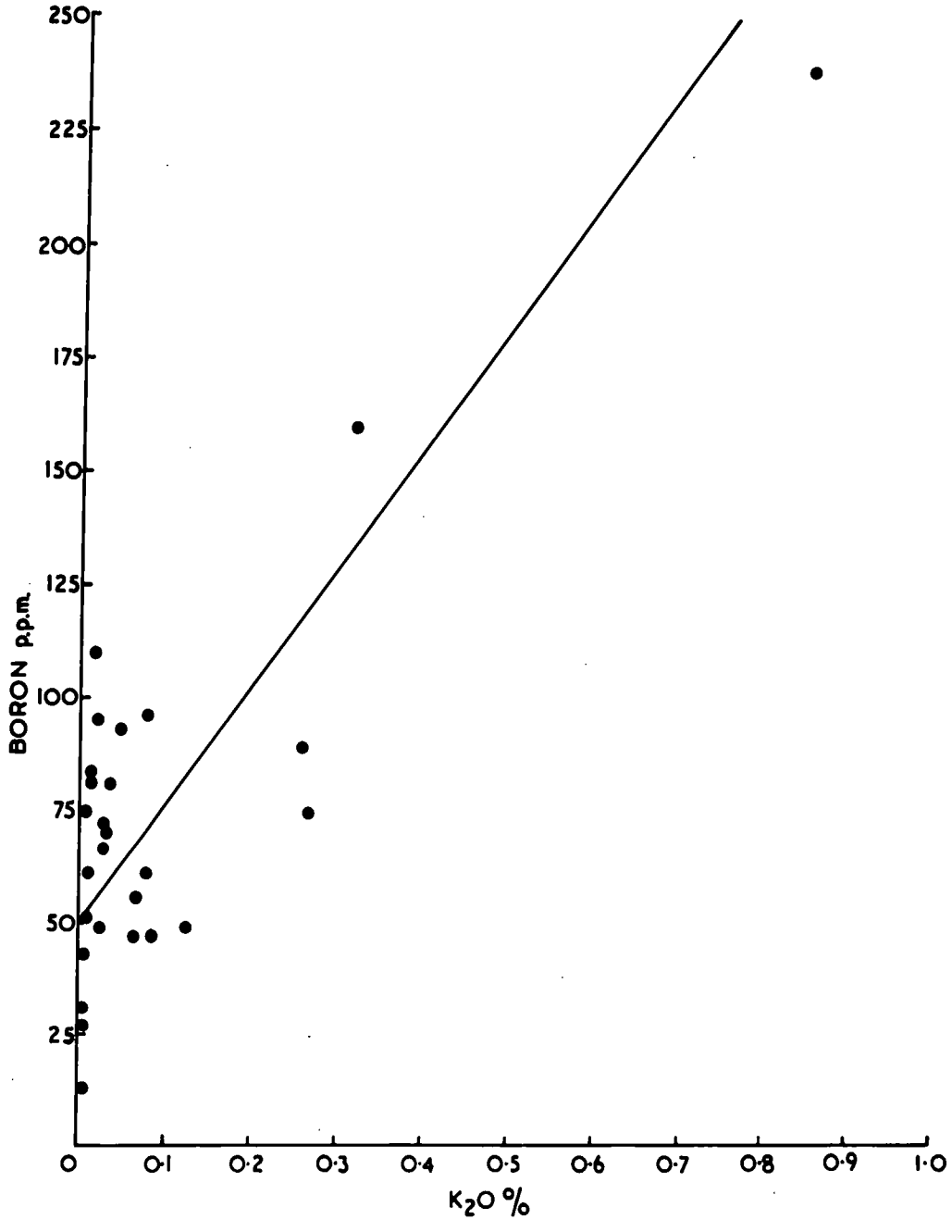

FIGURE 6–18. RELATIONSHIP BETWEEN BORON AND K_2O.

reveal no significant relationship between the two components and tourmaline was not detected, although the presence of small quantities of this mineral seems likely as it has been recorded from dolomite of reef facies by Trechmann (1914) and from the heavy mineral fraction of the Basal Sands by Hodge (1932). Small contributions from either or both of these sources, together with the low precision of both B and K_2O at the concentrations involved, might account for the positive intercept on the B "axis" in Figure 6-18.

From the gradient of the best-fit line shown in Figure 6-18, the mean B : K_2O ratio is 265. This value is greater than the B : K_2O ratios which may be obtained for Carboniferous rocks from data provided by Walker (1963; 1964) and Curtis (1964). It is also very much larger than the mean B : K_2O ratio of 87 which may be calculated from the data of Walker (1963, table 4) for illite separated from 3 samples of Yorkshire "Lower Magnesian Limestone". The B : K_2O ratio of illite from the Durham Magnesian Limestone therefore appears to be unusually high. Spears (1965) has indicated that the potassium content of illite decreases with degradation while the B content appears to be unaffected, i.e. the B : K_2O ratio in illite increases with degradation.

The correlation matrix for 162 samples of Magnesian Limestone shows that K_2O is very strongly correlated with Al_2O_3 ($r = 0.95$, significant at the 0.1 per cent. level). The $K_2O : Al_2O_3$ ratio, calculated from the arithmetic mean values for the same 162 samples, is 0.279, closely similar to the ratio of 0.276 for the typical illite analysed by Grim et al. (1937). This evidence indicates that the illite in the Magnesian Limestone is typical material and not severely degraded. Consequently, the high $B : K_2O$ ratio in the samples examined is taken to mean that the B content of the illite is high.

Work on Recent sediments indicates that detrital clay minerals, especially illite, deposited in a marine environment can take up B from the overlying waters. Frederickson and Reynolds (1960) showed that the amount of B taken up by illite is proportional to the salinity of the water in which the sediments are deposited. It might therefore be considered that the high salinity which is thought to have existed in the Zechstein Sea has resulted in the uptake of considerable quantities of B by detrital illite. However, without wishing to enter into the finer points of the "boron controversy", it must be said that although a relationship between the amount of B sorbed by detrital clay minerals and the salinity

of the overlying waters can be detected in some modern environments, other geological and geochemical processes can affect the relationship. Even assuming that these other processes were either inoperative or negligible in the case of the Magnesian Limestone, it does not seem likely that the type of salinity changes envisaged by Smith and Francis (1967) would give rise to the constant rate of B uptake which is necessary to explain the linear relationship shown in Figure 6-18.

In the absence of any other evidence, it can only be assumed that the B in the samples of Magnesian Limestone investigated is detrital and situated within the clay mineral illite; however, the possibility that some B is contained in components other than illite cannot be ruled out.

CHAPTER 7.

SUMMARY AND CONCLUSIONS.

The mineralogy and geochemistry of the Lower and Middle Magnesian Limestone of Co. Durham have been investigated. Analysis was carried out principally on carbonate material obtained from one adit and fourteen boreholes sunk in the central and southern parts of the Permian outcrop and in the adjacent offshore area. Insufficient palaeontological evidence and a lack of persistent "marker" horizons allow only a limited stratigraphic control over the mineralogical and geochemical data. Following the environmental scheme outlined by Smith and Francis (1967), the data for the Lower Magnesian Limestone is discussed in terms of shelf and basin facies and that for the Middle Magnesian Limestone in terms of lagoon, reef and basin facies.

Mineralogical and Textural Relationships.

Petrography and X-ray diffraction showed that the principal mineralogical components are calcite, dolomite, gypsum and anhydrite. The presence of gypsum in some samples rendered the use of a quantitative X-ray diffraction technique

unsuitable for modal analysis. Consequently, mineralogical composition was estimated by recalculation of the major element analyses obtained from a modified X-ray fluorescence method.

Gypsum and anhydrite were not detected in analysed samples from the shelf facies of the Lower Magnesian Limestone or the lagoon and reef facies of the Middle Magnesian Limestone, although small quantities of sulphate were occasionally recorded in the calculated mineralogical analyses. Some of the sulphate records probably represent minor amounts of gypsum but others certainly reflect the presence of small quantities of pyrite because all the sulphur was recalculated as sulphate. Gypsum and anhydrite, however, are known to occur interbedded with, and disseminated throughout, the carbonates of the shelf Lower Magnesian Limestone and lagoon Middle Magnesian Limestone in South-East Durham. Dolomite is the predominant carbonate in all but a few samples from the three shallow-water facies. Calcite occurs only sporadically, most commonly taking the form of void filling. In the lagoon and reef facies of the Middle Magnesian Limestone, void-filling calcite sometimes extends into the dolomite host-rock by a process of centripetal replacement. Such dedolomitization is found particularly in the beds adjacent to

fault zones. In the central part of the outcrop, calcite occurs in a "felted" texture in the lagoon facies of the Middle Magnesian Limestone and, rarely, in the immediately underlying beds of the shelf Lower Magnesian Limestone. The "felted" calcite is considered to have replaced sheaths and clusters of sulphate "needles" (probably originally in the form of anhydrite), similar to those now found in the Middle Magnesian Limestone beneath beds of the second cycle evaporite phase in South-East Durham. The recognition of former replacement sulphate sheaths and clusters in the lagoonal Middle Magnesian Limestone of Central Durham lends support to the contention that beds of Middle Permian Marl facies originally extended much farther north than their present position.

The relative proportions of calcite, dolomite, gypsum and anhydrite vary considerably in the basin facies of the Lower and Middle Magnesian Limestone. Sulphates were recorded in all but one of the samples analysed, although high contents are virtually confined to samples from borehole ML 12, near Billingham. Gypsum is present more commonly, and usually in greater abundance, than anhydrite. Both sulphate species occur as small acicular crystals, as porphyroblastic blebs and patches, and in occasional beds. Gypsum

also takes the form of thin, fibrous, anastomosing veins which sometimes brecciate the carbonate host-rock. The presence of corroded anhydrite relics within gypsum crystals, together with the tendency for the anhydrite : gypsum ratio to increase with depth as well as in dolomite interbedded with, and protected by, massive sulphate indicates that anhydrite is undergoing hydration to gypsum. Brecciation of the carbonate host-rock suggests that expansion has accompanied the hydration in some cases, but in other instances, the transition appears to have occurred on a constant-volume basis. Furthermore, the presence of sulphate-rich groundwaters in the coastal and offshore areas, and particularly in South-East Durham, suggests that some solution of sulphates is also occurring.

Dolomite is the predominant carbonate in all samples from borehole ML 12 but only in a few samples from boreholes ML 6 and ML 3, situated in the Hartlepool and offshore areas respectively. The samples in which calcite is the predominant carbonate are characterized by low sulphate contents; there are also no samples containing relatively high quantities of both sulphate and calcite. The marked antipathy between calcite and sulphate, taken in conjunction with the fact that calcite occurs almost entirely in

the form of "dedolomite", indicates that much of the basinal Lower and Middle Magnesian Limestone in boreholes ML 3 and ML 6 has been dedolomitized by reaction with sulphate-rich solutions derived locally from within the beds. This process might be termed "local source" dedolomitization. Most of the sulphate solution and concomitant dedolomitization is considered to have occurred at considerable depth and at approximately the same time as the main phase of solution of the Hartlepool Anhydrite - probably at the end of the Mesozoic or early in the Tertiary. However, the fact that slow solution of sulphates is taking place at the present day suggests that dedolomitization might still be occurring on a small scale.

In the absence of any evidence to the contrary, an early-diagenetic origin must be assumed for the dolomite in all facies, with the possible exception of the large, clear euhedra observed within the calcite which occasionally occurs as void filling or replacement after sulphate in coarse, reef-derived, basinal beds in borehole ML 6. All the calcite observed is clearly late-diagenetic; none is considered to represent original limestone which has escaped dolomitization. The origin of the sulphates appears to vary.

Limonite, quartz, pyrite and an illitic clay mineral are the principal minor mineralogical constituents of the Lower and Middle Magnesian Limestone. In all facies, the content of non-carbonate/sulphate material only occasionally exceeds 5 per cent. There are no systematic variations in the distribution of inorganic detrital material which can be attributed to age or to distance from the presumed Permian shoreline.

Porosity and Permeability.

Porosity and permeability in the Magnesian Limestone vary in a general sense with facies. Thus, although there is a considerable range in the porosity and permeability of both the shelf and lagoon facies of the Lower and Middle Magnesian Limestone respectively, the shallow-water facies on the whole appear to be more porous and permeable than the basin facies. However, it is likely that the removal of sulphates which accompanies "local source" dedolomitization will locally increase the porosity and perhaps also the permeability of the basin facies.

Pore-size distribution, which is the end-product of the entire depositional and diagenetic history of a particular rock-type, appears to be the main factor influencing porosity

and permeability rather than mineralogical composition or any specific textural property. The relationship which exists between porosity and permeability for samples from the shelf and lagoon facies of the Lower and Middle Magnesian Limestone respectively is not considered to be the manifestation of a strict mathematical relationship but rather an indication that the rocks of these facies were deposited under generally similar conditions and have since undergone similar diagenetic changes. It is pertinent, therefore, that samples from the basin facies are not included in this relationship, although cementation by gypsum might have altered the pore-structure of these samples.

Chemistry.

The distribution of Sr in the various facies of the Lower and Middle Magnesian Limestone can be attributed to variations in mineralogy. In the three shallow-water facies, Sr occurs almost entirely as a solid-solution impurity in the carbonate minerals - the dolomite and late-diagenetic calcite containing similar, relatively low levels of Sr. Strontium is enriched in the basin facies of the two divisions owing to the presence of gypsum and anhydrite. In rocks which have apparently been protected from the action of circulating groundwater, Sr released during the transition

of anhydrite to gypsum has been retained (most likely as celestite); elsewhere, Sr has been lost with the result that gypsum is characterized by a lower Sr content than anhydrite. The late-diagenetic calcite which has replaced dolomite in rocks of the basin facies contains considerable Sr, believed to have been incorporated in the calcite lattice during dedolomitization by the "sulphate-agent" mechanism.

Gypsum and anhydrite contain very little Mn so that in the two basin facies, the principal mode of occurrence of this element is as a solid-solution impurity in dolomite. During dedolomitization by the "sulphate-agent" mechanism, Mn originally held in the dolomite is to a large extent excluded from the lattice of the replacement calcite and removed from the system, presumably in solution. In the shallow-water facies, it is likely that Mn also occurs in dolomite but widespread MnO_2 speckling gives rise to sporadic variations in Mn content. Leaching of Mn from some rocks in these facies by circulating groundwater might have been followed by precipitation of MnO_2 elsewhere; the Mn released into solution during dedolomitization of the basin facies might also have been carried and precipitated in the shallow-water facies.

The basin facies of the two divisions are characterized by very low values of Zn, suggesting that the Zn contents of the clay, carbonate and sulphate minerals in basinal samples are very small. Zinc is enriched in the shallow-water facies, although the samples show a considerable variation in content. The location of Zn in rocks of the shallow-water facies is unknown, but high Zn values are only found in rocks of high porosity and permeability. This is considered to indicate that the enrichment of Zn is related to the ease with which Zn-bearing solutions have been able to move through the rocks. While some Zn probably occurs in the form of sphalerite, it seems unlikely that the presence of this mineral can entirely explain the enrichment of Zn throughout rocks of the shallow-water facies. In the absence of any other evidence, it is suggested that some Zn might therefore have been adsorbed, and perhaps later absorbed, by mineral grains.

Barium and Pb correlate with the non-carbonate/sulphate material in the Lower and Middle Magnesian Limestone. In all samples from the basin facies and in some from the shallow-water facies, the Ba and Pb appear to be associated almost entirely with the illitic clay material. The Ba and at least some of the Pb in these samples is considered to be

detrital; unless the clay minerals contain an unusually high level of detrital Pb, further Pb must have been adsorbed in the Zechstein Sea. In many (but not always the same) samples from the shallow-water facies, Ba and Pb are considerably enriched but still show a correlation with non-carbonate/sulphate material. It seems unlikely that small quantities of barite and galena undetected in the analyses can explain the enrichment in all of these samples. While it is possible that the clay minerals adsorbed Ba and Pb to equilibrium from locally enriched waters in the shelf zone of the Zechstein Sea, this hypothesis is not entirely satisfactory, especially with respect to Pb. As Zn, Pb and Ba are all enriched in the shallow-water facies, it is considered likely that the extra quantities of these elements share a similar origin. Thus, as in the case of Zn, Pb and Ba have probably been introduced into rocks of the shallow-water facies by circulating solutions; it is therefore possible that Pb and Ba were also removed from solution by adsorption on mineral grains, especially clay minerals.

The degree of coincidence between the enrichment of Zn, Pb and Ba in the porous and permeable rocks of the shelf zone adjacent to the Zechstein evaporite basin and the presence of sphalerite, galena and barite in the underlying Carboniferous

sediments is considered to be too high to be fortuitous. It is therefore suggested that highly saline formation waters expelled from the compacting evaporitic basin "scavenged" Zn, Pb and Ba from the underlying sediments and redeposited them in the porous and permeable shallow-water facies of the Lower and Middle Magnesian Limestone.

The Rb in the Magnesian Limestone is wholly contained in the illitic clay material where it is considered to be present as a detrital constituent. The similarity in Rb : K_2 O ratio in the Magnesian Limestone and in the underlying Marl Slate suggests that little change in the composition and provenance of the illitic clay material occurred in the Lower Zechstein. Boron and Ni are also considered to occur as detrital constituents within the illitic clay material. Some B might also be present in tourmaline or occur adsorbed on organic carbon. Similarly, unless the detrital Ni content of the clays is unusually high, some Ni may occur in association with organic matter.

Copper is related to organic carbon and was therefore at least partly accumulated by biological activity or adsorbed by organic matter derived from the soft parts of organisms. Some Cu might also be associated with the clay, carbonate and perhaps sulphate minerals.

In conclusion, it is hoped that the mineralogical and geochemical groundwork which has been undertaken in this investigation will provide the basis for more intensive examination of the Durham Magnesian Limestone in the future.

REFERENCES.

Abbot, T. G., 1903. The Cellular Magnesian Limestone of Durham. Quart. J. Geol. Soc., 59, pp. 51 - 52.

Ahrens, L. H., and Taylor, S. R., 1961. Spectrochemical Analysis. Addison-Wesley, Massachusetts, U.S.A., 454 p.

Andermann, G., and Kemp, J. W., 1958. Scattered X-rays as Internal Standards in X-ray Emission Spectroscopy. Anal. Chem., 30, pp. 1306 - 1309.

Anderson, W., and Dunham, K. C., 1953. Reddened Beds in the Coal Measures beneath the Permian of Durham and South Northumberland. Proc. Yorks, Geol. Soc., 29, pp. 21 - 32.

Archie, G. E., 1950. Introduction to Petrophysics of Reservoir Rocks. Am. Assoc. Petroleum Geol. Bull., 34, pp. 943 - 961.

Atwood, D. K., and Fry, H. M., 1967. Strontium and Manganese Content of some coexisting Calcites and Dolomites. Am. Mineralogist, 52, pp. 1530 - 1535.

Bathurst, R. G. C., 1958. Diagenetic Fabrics in some British Dinantian Limestones. Liverpool Manchester Geol. J., 2, pp. 11 - 36.

Bernstein, F., 1962. Application of X-ray Fluorescence Analysis to Process Control. Adv. X-ray Analysis, 5, pp. 486 - 499.

Bird, W. J., 1888. The South Durham Salt Bed and Associated Strata. Trans. Manchester Geol. Soc., 19, pp. 564 - 584.

Bromberger, S. H., and Hayes, J. B., 1966. Quantitative Determination of Calcite-Dolomite-Apatite Mixtures by X-ray Diffraction. J. Sediment. Petrol., 36, pp. 358 - 361.

Browell, E. J. J., and Kirkby, J. W., 1866. On the Chemical Composition of the Various Beds of the Magnesian Limestone and Associated Permian Rocks of Durham. Trans. Nat. Hist. Soc. Northumberland, Durham and Newcastle upon Tyne, 1, pp. 204 - 230.

Burton, R. C., 1911. Beds of Yellow Sands and Marl in the Magnesian Limestone of Durham. Geol. Mag., 8, pp. 299 - 306.

Cameron, E. M., 1966. Evaluation of Sampling and Analytical Methods for the Regional Geochemical Study of a Subsurface Carbonate Formation. J. Sediment. Petrol, 36, pp. 755 - 763.

Cameron, E. M., 1968. A Geochemical Profile of the Swan Hills Reef. Can. J. Earth Sci., 5, pp. 287 - 309.

Cameron, E. M., 1969. Regional Geochemical Study of the Slave Point Carbonates, Western Canada. Can. J. Earth Sci., 6, pp. 247 - 268.

Carman, P. C., 1939. Permeability of Saturated Sands, Soils and Clays. J. Agri. Sci., 29, pp. 262 - 273.

Chakrabarti, A. K., and Taylor, R. K., 1968. The Porosity and Permeability of the Zawar Dolomites. Int. J. Rock Mech. Min. Sci., 5, pp. 261 - 273.

Chave, K. E., 1954. Aspects of the Biogeochemistry of Magnesium. J. Geol., 62; Part 1: Calcareous Marine Organisms, pp. 266 - 283; Part 2: Calcareous Sediments and Rocks, pp. 587 - 599.

Chilingar, G. V., Bissell, H. J., and Wolf, K. H., 1967. Diagenesis of Carbonate Rocks. Chapter 5 of Diagenesis in Sediments, Volume 8 of Developments in Sedimentology. Elsevier, Amsterdam. 551 p.

Chilingar, G. V., and Terry, R. D., 1954. Relationship between Porosity and Chemical Composition of Carbonate Rocks. Petroleum Engr., B-54, pp. 341 - 342.

Curtis, C. D., 1964. Studies on the Use of Boron as a Palaeoenvironmental Indicator. Geochim. Cosmochim. Acta, 28, pp. 1125 - 1137.

Davies, T. A., 1958. The Effect of Variations in Ambient Temperature upon the Optical Alignment of an X-ray Fluorescence Spectrometer. J. Sci. Instr., 35, pp. 407 - 409.

Davies, W., and Rees, W. J., 1944. British Resources of Steel Moulding Sands. Part 5: The Permian Yellow Sands of Durham and Yorkshire. J. Iron and Steel Inst., No. 2 for 1943, pp. 104P - 111P.

Deans, T., 1950. The Kupferschiefer and the Associated Lead-Zinc Mineralization in the Permian of Silesia, Germany and England. Rept. XVIII Int. Geol. Congr. (London), 7, pp. 340 - 352.

Deer, W. A., Howie, R.A., and Zussman, J., 1962. Rock-Forming Minerals. Volume 5: Non-Silicates. Longmans, London. 371 p.

Dickson, J. A. D., 1965. A Modified Staining Technique for Carbonates in Thin Section. Nature, 205, p. 587.

Diebold, F. E., Lemish, J., and Hiltrop, C. L., 1963. Determination of Calcite, Dolomite, Quartz and Clay Content of Carbonate Rocks. J. Sediment. Petrol., 33, pp. 124 - 139.

Dunham, K. C., 1948. A Contribution to the Petrology of the Permian Evaporite Deposits of North-Eastern England. Proc. Yorks. Geol. Soc., 27, pp. 217 - 227.

Dunham, K. C., 1960. Syngenetic and Diagenetic Mineralization in Yorkshire. Proc. Yorks. Geol. Soc., 32, pp. 229 - 284.

Dunham, K. C., 1966. Role of Juvenile Solutions, Connate Waters and Evaporitic Brines in the Genesis of Lead-Zinc-Fluorine-Barium Deposits. Trans. Instn. Min. Metall. (Sect. B : Appl. Earth Sci.), 75, pp. B226 - B229.

Dunham, K. C., Claringbull, G. F., and Bannister, F. A., 1948. Dickite in the Magnesian Limestone of Durham. Mineral. Mag., 28, pp. 338 - 342.

Evamy, B. D., 1967. Dedolomitization and the Development of Rhombohedral Pores in Limestones. J. Sediment. Petrol., 37, pp. 1204 - 1215.

Fleischer, M., 1965. Summary of New Data on Rock Samples G-1 and W-1, 1962 - 1965. Geochim. Cosmochim. Acta, 29, pp. 1263 - 1283.

Fowler, A., 1943. On Fluorite and Other Minerals in Lower Permian Rocks of South Durham. Geol. Mag., 80, pp. 41 - 51.

Fowler, A., 1944. A Deep Bore in the Cleveland Hills. Geol. Mag., 81, pp. 193 - 206.

Fowler, A., 1945. Evidence for a New Major Fault in North-East England. Geol. Mag., 82, pp. 245 - 250.

Fowler, A., 1957. Minerals in the Permian and Trias of North-East England. Proc. Geol. Assoc., 67, pp. 251 - 265.

Frederickson, A.F., and Reynolds, R. C., 1960. Geochemical Methods for Determining Palaeo-salinity in Clays and Clay Minerals. 8th National Conf. Clays and Clay Minerals Proc., Pergamon Press, Oxford, pp. 203 - 213.

Gad, M. A., Catt, J. A., and Le Riche, H. H., 1969. Geochemistry of the Whitbian (Upper Lias) Sediments of the Yorkshire Coast. Proc. Yorks. Geol. Soc., 37, pp. 105 - 139.

Garwood, E. J., 1891. On the Origin and Mode of Formation of the Concretions in the Magnesian Limestone of Durham. Geol. Mag., 8, pp. 433 - 440.

Gehman, H. M., 1962. Organic Matter in Limestones. Geochim. Cosmochim. Acta., 26, pp. 885 - 897.

Goldberg, M., 1967. Supratidal Dolomitization and Dedolomitization in Jurassic Rocks of Hamakhtesh Haqatan, Israel. J. Sediment. Petrol., 37, pp. 760 - 773.

Goldschmidt, V. M., 1958. Geochemistry. Clarendon Press, Oxford, 730 p.

Goldsmith, J. R., Graf, D. L., and Joensu, O. I., 1955. The Occurrence of Magnesian Calcites in Nature. Geochim. Cosmochim. Acta, 7, pp. 212 - 230.

Graf, D. L., 1962. Minor Element Distribution in Sedimentary Carbonate Rocks. Geochim. Cosmochim. Acta, 26, pp. 849 - 856.

Griffiths, J. C., 1952. Grain-Size Distribution and Reservoir-Rock Characteristics. Am. Assoc. Petroleum Geol. Bull., 36, pp. 205 - 229.

Grim, R. E., Bray, R. H., and Bradley, W. F., 1937. The Mica in Argillaceous Sediments. Am. Mineralogist, 22, pp. 813 - 829.

Groot, K. de., 1967. Experimental Dedolomitization. J. Sediment. Petrol., 37, pp. 1216 - 1220.

Groves, A. W., 1951. Silicate Analysis. Allen and Unwin, London. 336 p.

Gülbrandsen, R. A., 1960. A Method of X-ray Analysis for Determining the Ratio of Calcite to Dolomite in Mineral Mixtures. U. S. Geol. Survey Bull. 1111-D, pp. 147 - 152.

Harder, H., 1959. Beitrag zur Geochemie des Bors. Nachr. Akad. Wiss. Göttingen, Math.-Phys. Klasse, 5, pp. 67 - 183.

Hickling, G., and Holmes, A., 1931. The Brecciation of the Permian Rocks. Proc. Geol. Assoc., 42, pp. 252 - 255.

Hirst, D. M., 1962. The Geochemistry of Modern Sediments from the Gulf of Paria. Part 2: The Location and Distribution of Trace Elements. Geochim. Cosmochim. Acta, 26, pp. 1147 - 1187.

Hirst, D. M., 1968. Relationships between Minor Elements, Mineralogy and Depositional Environment in Carboniferous Sedimentary Rocks from a Borehole at Rookhope, (Northern Pennines). Sediment. Geol., 2, pp. 5 - 12.

Hirst, D. M., and Dunham, K. C., 1963. Chemistry and Petrography of the Marl Slate of S. E. Durham, England. Econ. Geol., 58, pp. 912 - 940.

Hodge, M. B., 1932. The Permian Yellow Sands of North-East England. Proc. Univ. Durham Phil. Soc., 8, pp. 410 - 458.

Holland, J. G., and Brindle, D. W., 1966. A Self-Consistent Mass Absorption Correction for Silicate Analysis by X-ray Fluorescence. Spectrochim. Acta, 22, pp. 2083 - 2093.

Hollingworth, S. E., 1942. The Correlation of Gypsum-Anhydrite Deposits and the Associated Strata in the North of England. Proc. Geol. Assoc., 53, pp. 141 - 151.

Holmes, A., 1931. Concretionary and Oolitic Structures of the Permian Rocks. Proc. Geol. Assoc., 42, pp. 255 - 258.

Holtdahl, O., 1921. On the Occurrence of Structures like Walcott's Algonkian Algae in the Permian of England. Am. J. Sci., 201, pp. 195 - 206.

Howse, R., 1848. A Catalogue of the Fossils of the Permian System of the Counties of Northumberland and Durham. Trans. Tyneside Naturalists Field Club, 1, pp. 218 - 264.

Howse, R., 1857. Notes on the Permian System of the Counties of Northumberland and Durham. Ann. Mag. Nat. Hist. (2), 19, pp. 33 - 52, 304 - 312 and 463 - 473.

Howse, R., 1890. Note on the South Durham Salt Borings, with Remarks on the Fossils found in the Magnesian-Limestone Cores, and the Geological Position of the Salt. Trans. Nat. Hist. Soc. Northumberland, 10, pp. 220 - 226.

Imbrie, J., and Poldervaart, A., 1959. Mineral Compositions Calculated from Chemical Analyses of Sedimentary Rocks. J. Sediment. Petrol., 29, pp. 588 - 595.

Ineson, P. R., 1967. Trace Element Geochemistry of Wallrock Alteration in the Pennine Orefields and Cumberland Iron field. Unpublished Ph.D. Thesis, University of Durham, 286 p.

Jackson, R. S., 1968. Aquifer Studies in Co. Durham and in the Nairobi Area, Kenya. Unpublished M.Sc. Thesis, University of Durham. 184 p.

Jackson, S. A., and Beales, F. W., 1967. An Aspect of Sedimentary Basin Evolution: The Concentration of Mississippi-Valley-Type Ores during Late Stages of Diagenesis. Can. Petroleum Geol. Bull., 15, pp. 384 - 433.

Kalman, Z. H., and Heller, L., 1962. Theoretical Study of X-ray Fluorescent Determination of Traces of Heavy Elements in a Light Matrix: Application to rocks and soils. Anal. Chem., 34, pp. 946 - 951.

Katz, A., 1968. Calcian Dolomites and Dedolomitization. Nature, 217, pp. 439 - 440.

Kaye, M. J., Dunham, A. C., and Hirst, D. M., 1968. A Comparison of Two Methods of Quantitative Mineralogical Analysis of Sedimentary Rocks. J. Sediment. Petrol., 38, pp. 675 - 679.

Kennedy, G. C., 1947. Charts for Correlation of Optical Properties with Chemical Composition of Some Common Rock-Forming Minerals. Am. Mineralogist, 32, pp. 561 - 573.

King, W., 1850. A Monograph of the Permian Fossils of England. Palaeont. Soc.

Kirkby, J. W., 1860. On the Occurrence of Lingula Credneri Geinitz in the Coal Measures of Durham; and on the Claim of the Permian Rocks to be Entitled a System. Quart. J. Geol. Soc., 16, pp. 412 - 421.

Klug, H. P., and Alexander, L. E., 1954. X-ray Diffraction Procedures. Wiley, New York. 716 p.

Kozeny, J., 1927. Uber Kapillare Leitung des Wassers im Boden. Akad. Wiss. Wien, Math.-Naturw. Klasse, 136A, pp. 271 - 306.

Krauskopf, K. B., 1956. Factors Controlling the Concentration of 13 Rare Metals in Seawater. Geochim. Gosmochim.Acta, 9, pp. 1 - 32.

Kulp, J. L., Turekian, K. K., and Boyd, D. W., 1952. Strontium Content of Limestones and Fossils. Geol. Soc. America Bull., 63, pp. 701 - 716.

Le Riche, H. H., 1959. The Distribution of Certain Trace Elements in the Lower Lias of Southern England. Geochim.Cosmochim Acta, 16, pp. 101 - 122.

Lebour, G. A., 1884. On the "Breccia-Gashes" of the Durham Coast and Some Recent Earthshakes at Sunderland. Trans. N. Eng. Inst. Min. Eng., 23, pp. 165 - 177.

Lebour, G. A., 1887. On the Stratigraphical Position of the Salt Measures of South Durham. Geol. Mag. (iii), 4, p. 39.

Lebour, G. A., 1905. The Marl Slate and Yellow Sands of Northumberland and Durham. Trans. N. Eng. Inst. Min. Eng., 53, pp. 18 - 39.

Lees, G. M., and Taitt, A. H., 1946. The Geological Results of the Search for Oil-Fields in Great Britain. Quart. J. Geol. Soc., 101, pp. 255 - 317.

Liebhafsky, H. A., and Winslow, E. H., 1958. X-ray Absorption and Emission. Anal. Chem., 30, pp. 580 - 589.

Liebhafsky, H. A., Pfeiffer, H. G., Winslow, E. H., and Zemany, P. D., 1960. X-ray Absorption and Emission in Analytical Chemistry. Wiley, New York. 357 p.

Logan, A., 1962. A Revision of the Palaeontology of the Permian Limestones of County Durham. Unpublished Ph.D. Thesis, King's College, University of Durham. 2 Vols.

Love, L. G., 1962. Biogenic Primary Sulphide of the Permian Kupferschiefer and Marl Slate. Econ. Geol., 57, pp. 350 - 366.

Lucia, F. J., 1961. Dedolomitization in the Tansill (Permian) Formation. Geol. Soc. America Bull., 72, pp. 1107 - 1110.

Magraw, D., Clarke, A. M., and Smith, D. B., 1963. The Stratigraphy and Structure of Part of the South-East Durham Coalfield, Proc. Yorks. Geol. Soc., 34, pp. 153 - 208.

Makhlaev, V. G., 1957. Dedolomitized Rocks in the Dankovo-Lebedynsk Beds. Acad. Sci. USSR. Proc., 117, No. 1 - 6, pp. 1011 - 1014. (English Translation by Consultants Bureau, Inc.)

Marley, J., 1892. On the Cleveland and South Durham Salt Industry. Trans. N. Eng. Inst. Min. Eng., 39, pp. 91 - 125.

Mattavelli, L., Chilingar, G. V., and Storer, D., 1969. Petrography and Diagenesis of the Taormina Formation, Gela Oil Field, Sicily (Italy). Sediment. Geol., 3, pp. 59 - 86.

Meyer, H. O. A., 1965. Revision of the Stratigraphy of the Permian Evaporites and Associated Strata in North-Western England. Proc. Yorks. Geol. Soc., 35, pp. 71 - 89.

Miesch, A. T., 1962. Computing Mineral Compositions of Sedimentary Rocks from Chemical Analyses. J. Sediment. Petrol., 32, pp. 217 - 225.

Mitchell, R. L., 1956. The Limestones of Scotland. Chemical Analyses and Petrography. Part B: Spectrographic Determinations. Mem. Geol. Surv. Gt. Brit., Spec. Rept. Mineral Resources, 37, 150 p.

Moseley, F., and Ahmed, S. M., 1967. Carboniferous Joints in the North of England and their Relation to Earlier and Later Structures. Proc. Yorks. Geol. Soc., 36, pp. 61 - 90.

Murray, R. C., 1960. Origin of Porosity in Carbonate Rocks. J. Sediment. Petrol., 30, pp. 59 - 84.

Napier, E., 1948. The Lower Anhydrite Seams of the Tees Area. Proc. Yorks. Geol. Soc., 27, pp. 210 - 216.

Newell, N. D., Rigby, J. K., Fischer, A. G., Whiteman, A. J., Hickox, J. E., and Bradley, J. S., 1953. The Permian Reef Complex of the Guadalupe Mountains Region, Texas and New Mexico: A Study in Palaeoecology. Freeman, San Francisco. 236 p.

Nicholls, G. D., 1962. A Scheme for Recalculating the Chemical Analyses of Argillaceous Rocks for Comparative Purposes. Am. Mineralogist, 47, pp. 34 - 46.

Nicholls, G. D., and Loring, D. H., 1962. The Geochemistry of Some British Carboniferous Sediments. Geochim. Cosmochim. Acta, 26, pp. 181 - 223.

Noble, E. A., 1963. Formation of Ore Deposits by Water of Compaction. Econ. Geol., 58, pp. 1145 - 1156.

Noll, W., 1934. Geochemie des Strontiums. Chem. Erde, 8, pp. 507 - 600.

Oelsner, O., 1959. Bemerkungen zur Herkunft der Metalle im Kupferschiefer. Freiberger Forsch., 58, pp. 106 - 113.

Ohle, E. L., 1951. The Influence of Permeability on Ore Distribution in Limestone and Dolomite. Econ. Geol., 46, pp. 667 - 706 and 871 - 908.

Rankama, K., and Sahama, T. G., 1950. Geochemistry. University of Chicago Press, Chicago, Illinois, 912 p.

Raymond, L. R., 1953. Some Geological Results from the Exploration for Potash in North-East Yorkshire. Quart. J. Geol. Soc., 108, pp. 283 - 306.

Raymond, L. R., 1960. The Pre-Permian Floor beneath Billingham, Co. Durham, and Structures in Overlying Permian Sediments. Quart. J. Geol. Soc., 116, pp. 297 - 313.

Raymond, L. R., 1962. The Petrology of the Lower Magnesian Limestone of North-East Yorkshire and South-East Durham. Quart. J. Geol. Soc., 118, pp. 39 - 64.

Robertson, T.,1948. The Permian Sequence of South-East Durham and North-East Yorkshire. Proc. Yorks. Geol. Soc., 27, pp. 199 - 205.

Roedder, E., 1965. Report on S.E.G. Symposium on the Chemistry of Ore-Forming Fluids, August-September, 1964. Econ. Geol, 60, pp. 1380 - 1403.

Ronov, A. B., 1956. The Chemical Composition and the Conditions of Formation of Palaeozoic Carbonate Layers of the Russian Platform, based on the Data of Lithologic-Geochemical Maps. Trud. Geol. Inst. Akad. Nauk SSSR No. 4, pp. 256 - 343.

Scheidegger, A. E., 1960. The Physics of Flow through Porous Media. University of Toronto Press. 313 p.

Schmidt, V., 1965. Facies, Diagenesis and Related Reservoir Properties in the Gigas Beds (Upper Jurassic), North-Western Germany. Dolomitization and Limestone Genesis, A Symposium. Eds. Pray, L. C., and Murray, R.C.; Soc. Econ. Palaeontol. Mineral., Spec. Pubn. No. 13, pp. 124 - 168.

Sedgwick, A., 1835. On the Geological Relations and Internal Structure of the Magnesian Limestone, and the Lower Portions of the New Red Sandstone Series in Their Range through Nottinghamshire, Derbyshire, Yorkshire and Durham to the Southern Extremity of Northumberland. Trans. Geol. Soc., 3, pp. 37 - 124.

Shapiro, L., and Brannock, W. W., 1962. Rapid Analysis of Silicate, Carbonate and Phosphate Rocks. U.S. Geol. Survey Bull. 1144-A, 56 p.

Shearman, D. J., Khouri, J., and Taha, S., 1961. On the Replacement of Dolomite by Calcite in Some Mesozoic Limestones from the French Jura. Proc. Geol. Assoc., 72, pp. 1 - 12.

Shearman, D. J., and Shirmohammadi, N. H., 1969. Distribution of Strontium in Dedolomites from the French Jura. Nature, 223, pp. 606 - 608.

Sherlock, R. L., 1921. Rock Salt and Brine. Mem. Geol. Surv. Gt. Brit., Spec. Rept. Mineral Resources, 18, 123 p.

Sherlock, R. L., 1926. A Correlation of British Permo-Triassic Rocks. Part 1: North England, Scotland and Ireland. Proc. Geol. Assoc., 37, pp. 1 - 72.

Sherlock, R. L., 1948. The Permo-Triassic Formations. Hutchinson, London. 367 p.

Sherlock, R. L., and Hollingworth, S. E., 1938. Gypsum and Anhydrite and Celestine and Strontianite. Mem. Geol. Surv. Gt. Brit., Spec. Rept. Mineral Resources, 3, 98 p.

Smith, D. B., 1958. Observations on the Magnesian Limestone Reefs of North-Eastern Durham. Geol. Surv. Gt. Brit. Bull., No. 15, pp. 71 - 84.

Smith, D. B., 1968. The Hampole Beds - A Significant Marker in the Lower Magnesian Limestone of Yorkshire, Derbyshire and Nottinghamshire. Proc. Yorks. Geol. Soc., 36, pp. 463 - 477.

Smith, D. B., in press. Foundered Strata, Collapse-Breccias and Subsidence Features of the English Zechstein. Report on Symposium on the Geology of Saline Deposits, Hanover, 1968.

Smith, D. B., and Francis, E. A., 1967. Geology of the Country between Durham and West Hartlepool. Mem. Geol. Surv. Gt. Brit., 354 p.

Smythe, J. A., and Dunham, K. C., 1947. Ankerites and Chalybites from the Northern Pennine Ore- Field and the North-East Coalfield. Mineral. Mag., 28, pp. 53 - 74.

Spears, D. A., 1961. Joints in the Whin Sill and Associated Sediments in Upper Teesdale, Northern Pennines. Proc. Yorks. Geol. Soc., 33, pp. 21 - 30.

Spears, D. A., 1965. Boron in Some British Carboniferous Sedimentary Rocks. Geochim. Cosmochim. Acta, 29, pp. 315 - 328.

Stewart, F. H., 1954. Permian Evaporites and Associated Rocks in Texas and New Mexico Compared with Those in Northern England. Proc. Yorks. Geol. Soc., 29, pp. 185 - 235.

Stewart, F. H., 1963. Marine Evaporites in Data of Geochemistry, 6th edition (M. Fleischer, ed.). U.S. Geol. Surv. Prof. Paper 440-Y, 53 p.

Stoneley, H. M. M., 1958. The Upper Permian Flora of England. Bull. Brit. Mus. (Nat. Hist.) Geology, 3, pp. 295 - 337.

Tennant, C. B., and Berger, R. W., 1957. X-ray Determination of the Dolomite-Calcite Ratio of a Carbonate Rock. Am. Mineralogist, 42, pp. 23 - 29.

Thomas, H. H., Hallimond, A. F., and Radley, E.G., 1920. Refractory Materials: Ganister and Silica-Rock—Sand for Open-Hearth Steel Furnaces - Dolomite. Petrography and Chemistry. Mem. Geol. Surv. Gt. Brit., Spec. Rept. Mineral Resources, 16.

Trechmann, C. T., 1913. On a Mass of Anhydrite in the Magnesian Limestone at Hartlepool and on the Permian of South-Eastern Durham. Quart. J. Geol. Soc., 69, pp. 184 - 218.

Trechmann, C. T., 1914. On the Lithology and Composition of Durham Magnesian Limestones. Quart. J. Geol. Soc., 70, pp. 232 - 265.

Trechmann, C. T., 1921. Some Remarkably Preserved Brachiopods from the Lower Magnesian Limestone of Durham. Geol. Mag., 58, pp. 538 - 543.

Trechmann, C. T., 1925. The Permian Formation in Durham. Proc. Geol. Assoc., 36, pp. 135 - 145.

Trechmann, C. T., 1930. The Relations of the Permian and Trias in North-East England. Proc. Geol. Assoc., 41, pp. 323 - 335.

Trechmann, C. T., 1931. The Permian. Proc. Geol. Assoc., 42, pp. 246 - 252.

Trechmann, C. T., 1932. The Permian Shell-Limestone Reef beneath Hartlepool. Geol. Mag., 59, pp. 166 - 175.

Trechmann, C. T., 1942. Borings in the Permian and Coal Measures around Hartlepool. Proc. Yorks. Geol. Soc., 24, pp. 313 - 327.

Trechmann, C. T., 1954. Thrusting and Other Movements in the Durham Permian. Geol. Mag., 91, pp. 193 - 208.

Turekian, K. K., and Kulp, J. L., 1956. The Geochemistry of Strontium. Geochim. Cosmochim. Acta, 10, pp. 245 - 296.

Turekian, K. K., and Armstrong, R. L., 1961. The Composition of Fossil Shells from the Fox Hills Formation, South Dakota. Geol. Soc. America Bull., 72, pp. 1817 - 1828.

Turekian, K. K., and Wedepohl, K. H., 1961. Distribution of the Elements in Some Major Units of the Earth's Crust. Geol. Soc. America Bull., 72, pp. 175 - 192.

Vinogradov, A. P., Ronov, A. B., and Ratynskii, V. M., 1952. Variation in Chemical Composition of Carbonate Rocks of the Russian Platform (with time). Izvest. Akad. Nauk SSSR (Geol. Ser.) 1961, pp. 33 - 50. Abstract by Chilingar, G. V., 1957. Geochim. Cosmochim. Acta, 12, pp. 273 - 276.

Walker, C. T., 1963. Size Fractionation Applied to Geochemical Studies of Boron in Sedimentary Rocks. J. Sediment. Petrol., 33, pp. 694 - 702.

Walker, C. T., 1964. Palaeosalinity in Upper Viséan Yoredale Formation of England - Geochemical Method for Locating Porosity. Am. Assoc. Petroleum Geol. Bull., 48, pp. 207 - 220.

Weaver, C. E., 1968. Geochemical Study of a Reef Complex. Am. Assoc. Petroleum Geol. Bull., 52, pp. 2153 - 2169.

Weber, J. N., 1964. Trace Element Composition of Dolostones and Dolomites and Its Bearing on the Dolomite Problem. Geochim. Cosmochim. Acta, 28, pp. 1817 - 1868.

Weber, J. N., and Smith, F. G., 1961. Rapid Determination of Calcite-Dolomite Ratios in Sedimentary Rocks. J. Sediment. Petrol., 31, pp. 130 - 131.

Wedepohl, K. H., 1956. Untersuchungen zur Geochemie des Bleis. Geochim. Cosmochim. Acta, 10 pp. 69 - 148.

Wedepohl, K. H., 1964. Untersuchungen am Kupferschiefer in Nordwestdeutschland; Ein Beitrag zur Deutung der Genese Bituminöser Sedimente. Geochim. Cosmochim. Acta, 28, pp. 305 - 364.

Westoll, T. S., 1941. The Permian Fishes Dorypterus and Lekanichthys. Proc. Zoo. Soc., 111, pp. 39 - 58.

Westoll, T. S., 1943. Mineralization of Permian Rocks of South Durham. Geol. Mag., 80, pp. 119 - 120.

White, M. F., 1966. The Behaviour of Strontium in Sedimentary Carbonates and Sulphates. Unpublished M.Sc. Project Report, University of Leeds.

Wilson, E., 1881. The Permian Formation in the North-East of England. Midland Nat., 4, pp. 97 - 101, 121 - 124, 187 - 191 and 201 - 208.

Wilson, E., 1888. On the Durham Salt District. Quart. J. Geol. Soc., 44, pp. 761 - 782.

Winch, N. J., 1817. Observations on the Geology of Northumberland and Durham. Trans. Geol. Soc., 4, pp. 1- 101.

Wolf, K. H., Chilingar, G. V., and Beales, F. W., 1967. Elemental Composition of Carbonate Skeletons, Minerals and Sediments. Chapter 2 of Carbonate Rocks, Volume 9B of Developments in Sedimentology. Elsevier, Amsterdam. 413 p.

Wood, F. W., 1950. Recent Information Concerning the Evaporites and the Pre-Permian Floor of South-East Durham. Quart. J. Geol. Soc., 105, pp. 327 - 346.

Woolacott, D., 1909. A Case of Thrust and Crush-Brecciation in the Magnesian Limestone, County Durham. Univ. Durham. Phil. Soc. Mem., No. 1, 16 p.

Woolacott, D., 1912. The Stratigraphy and Tectonics of the Permian of Durham (Northern Area). Proc. Univ. Durham. Phil. Soc., 4, pp. 241 - 311.

Woolacott, D., 1919(A). Borings at Cotefold Close and Sheraton, Durham. Geol. Mag., 56, pp. 163 - 170.

Woolacott, D., 1919(B). The Magnesian Limestone of Durham. Geol. Mag., 56, pp. 452 - 465 and 485 - 498.

APPENDIX 1.

ABRIDGED GEOLOGICAL SECTIONS.

Adit ML 1 Easington Colliery West Drift.

Site of entrance NZ 4357 4418

Level of entrance 239.8 ft O.D.
Level of bottom 14.4 ft O.D.
Approximate length 730 ft

Reference Smith and Francis, 1967, pp. 136 - 137.

Middle Magnesian Limestone - Reef Facies.	Distance from adit bottom (ft)
Massive dolomite, collapse-brecciated in parts with included fragments of soft, red and green marl	730
Hard, slightly fossiliferous dolomite with thin, steeply-dipping, alga-laminated sheets	674
Unbedded, hard, fossiliferous dolomite	367
Vaguely bedded, very fossiliferous, friable dolomite	286
Thinly bedded, bioclastic, dolomitic calcarenite	235
Poorly bedded, friable, dolomitic coquina	184
Transitional beds - soft, bedded dolomite	143

Borehole ML 2 Mill Hill Bore, Easington.

Site NZ 4122 4248

Starting level 509 ft O.D.
Depth of hole 646 ft

Reference Smith and Francis, 1967, pp. 113, 125, 137 - 138.

	Depth (ft in)
Drift	35
Middle Magnesian Limestone	
Barren post-reef beds	48 6
Reef-top facies dolomite	69
Massive reef dolomite	81
Reef-lagoon "transitional beds"	90
Lagoonal dolomite deposited close to reef	120
Interbedded, granular and oolitic lagoonal dolomite	165
Fine, saccharoidal lagoonal dolomite	243
Transitional beds	265
Lower Magnesian Limestone	511
Marl Slate	513
Basal Sands	598
Coal Measures to bottom at	646

Borehole ML 3 Offshore Borehole No. 1.

Site NZ 5334 4043

Level of drilling platform 66.1 ft O.D.
Depth of hole 2157 ft 6 in

Reference Magraw et al., 1963, pp. 201 - 202

Sea-bed at	172 8
Drift	245 5
Upper Magnesian Limestone	591 3

	Depth (ft in)
Middle Magnesian Limestone	
Hartlepool Anhydrite	1020
Basinal equivalents of the reef — fine-grained, calcareous dolomite	1114
Lower Magnesian Limestone	1153 10
Basal Sands	1164 2
Coal Measures to bottom at	2157 6

Borehole ML 4 Hesleden Dene No. 1 (1940) Bore.

Site NZ 4672 3697

Starting level c. 60 ft O.D.
Depth of hole 230 ft

Reference Trechmann, 1942, p. 323.

Drift	36
Upper Magnesian Limestone	58
Middle Magnesian Limestone	
Reef dolomite to bottom at	230

Borehole ML 5 Naisberry Waterworks No. 1 Bore.

Site NZ 4662 3363

Starting level 384.2 ft O.D.
Depth of hole 500 ft

Reference Smith and Francis, 1967, pp. 132, 144, 151

	Depth (ft in)
Drift	30
?Upper Magnesian Limestone	?60
Middle Magnesian Limestone	
Post-reef beds	80
Reef beds - finely laminated, granular dolomite of algal origin	148
Lagoonal beds - bedded, granular and oolitic dolomite	160
Reef beds — thickly-bedded dolomite	190
Massive reef dolomite - very fossiliferous	245
Reef-lagoon "transitional beds"	248
Lagoonal beds — cross-bedded, granular, oolitic and pisolitic dolomite	c.400
Transitional beds	c.445
Lower Magnesian Limestone to bottom at	500

Borehole ML 6 Hartlepool Lighthouse Bore.

Site NZ 5319 3387

Starting level 25.5 ft O.D.
Depth of hole 1287 ft 10 in

Reference Magraw et al., 1963, pp. 199 - 200.

Drift	22
Upper Magnesian Limestone	238 7
Middle Magnesian Limestone	

	Depth (ft in)
Hartlepool Anhydrite	596 5
Fine-grained, shelly dolomite interbedded with off-reef breccias and bioclastic calcarenites	667
Finely crystalline dolomite with some bioclastic debris	733
Lower Magnesian Limestone	
Dolomitic breccia	737
Very finely crystalline dolomite with dolomitic limestone near base	855 10½
Marl Slate	856
Basal Breccia	862
Coal Measures to bottom at	1287 10

Borehole ML 7 Pudding Poke Farm Borehole.

Site NZ 4313 3280

Starting level c. 335 ft O.D.
Depth of hole 500 ft

Drift	125
Middle Magnesian Limestone	
Lagoonal beds	423 6
Lower Magnesian Limestone to bottom at	500

	Depth (ft in)
Borehole ML 8 Surtees Arms Borehole.	
Site NZ 3030 3091	
Starting level 311.5 ft O.D. Depth of hole 223 ft	
Drift	19
Middle Magnesian Limestone	
Lagoonal beds	?30
Transitional beds	?60
Lower Magnesian Limestone	189 10
"Transitional bed"	195 3
Marl Slate	203
Basal Sands	203 6
Coal Measures to bottom at	223
Borehole ML 9 Fishburn 'D' Bore.	
Site NZ 3567 3106	
Surface level 318 ft O.D. Depth of hole 687 ft	
Drift	36
Middle Magnesian Limestone	
Lagoonal beds	?183 1
Transitional beds	?203 3
Lower Magnesian Limestone	352

	Depth (ft in)
Marl Slate	353
Basal Sands	354
Coal Measures to bottom at	687

Borehole ML 10 Butterwick No. 1 Bore.

Site NZ 3777 2983

Surface level 310 ft O.D.
Depth of hole 350 ft

Drift	85
Middle Magnesian Limestone	
Lagoonal beds	120
Transitional beds	?165
Lower Magnesian Limestone	?330
Marl Slate	?335
Basal Sands	340
Basal Breccia	348
Carboniferous to bottom at	350

Borehole ML 11 Hope House Borehole.

Site NZ 3395 2541

Surface level 242.1 ft O.D.
Depth of hole 348 ft 9 in

	Depth (ft in)
Drift	223
Middle Magnesian Limestone	
Lagoonal beds	265 6
Lower Magnesian Limestone	327 5
Marl Slate	335 2
Basal Breccia	344 10
Carboniferous to bottom at	348 9

Borehole ML 12 Borehole B 18.

Site (approximately) NZ 470 238

Surface level 40 ft O.D.
Depth of hole 922 ft

Reference Raymond, 1962.

Drift	86
Bunter Sandstone, Upper Permian Marls and Upper Magnesian Limestone	622
Lower Evaporite Bed	655 6
Middle Magnesian Limestone	
Pale grey, anhydritic dolomite with fibrous gypsum veins	668
Massive gypsum with anhydrite and small dolomite stringers	669
Fine-grained, buff dolomite with black, shaley partings	673

	Depth (ft in)
Pale-grey anhydrite becoming gypsiferous towards the base	678 11 *
Fine, buff coloured bituminous dolomite containing irregular sulphate "inclusions" and black, shaley partings	690 10
Massive gypsum with thin dolomite bands	692
Pale cream coloured dolomite brecciated by veins of fibrous gypsum and containing sulphate porphyroblasts	788
Grey-black dolomite "marlstone" with veins and "inclusions" of gypsum	794
Buff dolomite with veins and inclusions of gypsum becoming very fossiliferous towards the base	813
Soft, sugary dolomite with bands of fine, buff dolomite and gypsum porphyroblasts	847
Lower Magnesian Limestone	
Fine-grained, buff dolomite with gypsum inclusions. Towards the base, the rock becomes arenaceous and contains many black, irregular, micaceous shaley partings	865 6
Basal deposits	888
Carboniferous to bottom at	922

* Raymond (1962) places the base of the Lower Evaporites at this depth, but see Chapter 3, pp. 51-52.

Borehole ML 13 Mount Pleasant Farm Borehole

Site NZ 3292 2064

Surface level 248.6 ft O.D.
Depth of hole 432 ft 2 in

	Depth (ft in)
Drift	201
Upper Magnesian Limestone	237
Middle Permian Marls	343 5
Middle Magnesian Limestone	
Lagoonal beds	c.396
Lower Magnesian Limestone to bottom at	432 2

Borehole ML 14 Mowden Bridge Borehole.

Site NZ 2608 1566

Surface level 160.2 ft O.D.
Depth of hole 130 ft

Drift	70
Middle Magnesian Limestone	
Lagoonal beds	c.85
Lower Magnesian Limestone to bottom at	130

Borehole ML 15 Broken Scar East No. 1 Borehole.

Site NZ 2568 1423

Surface level c.165 ft O.D.
Depth of hole 298 ft

Drift	130
Middle Magnesian Limestone	
Lagoonal beds to end of core at	220
Core disaggregated to dolomite sand to bottom of hole at	298

APPENDIX 2.

ORGANIC CARBON ANALYSES.

		Sample	Sinking	Depth (ft in)	Organic Carbon (%)
Lower Magnesian Limestone	Shelf Facies	UP 30	ML 14	100-110	0.46
		UP 31	"	110-113	0.46
		UP 33	"	120	0.51
		UP 34	"	124	0.40
		UP 51A	ML 7	429	0.21
		UP 55	"	472	0.44
		K 81	ML 8	99	0.05
		K 84A	"	75	0.60
		K 85	"	67	0.10
		UP 155	ML 11	271	0.16
		UP 157	"	281	0.38
		UP 160	"	296	0.86
		UP 162	"	307	0.80
		UP 164	"	316 6	0.50
		UP 167	"	323	0.41
		UP 182	ML 13	402 11	0.48
		UP 185	"	432	0.22

		Sample	Sinking	Depth (ft in)	Organic Carbon (%)
Middle Magnesian Limestone	Lagoon Facies	UP 23A	ML 15	174 2	0.92
		UP 23B	"	174 4	0.55
		UP 25	"	186	0.24
		UP 41	ML 7	304	0.43
		UP 42	"	324 6	0.22
		UP 44	"	361	0.22
		UP 48	"	396 6	0.38
		UP 61	ML 10	100	0.48
		K 87	ML 8	53 6	0.40
		K 91	"	33 6	0.26
		UP 141	ML 11	239 9	not detected
		UP 147	"	245	0.23
		UP 171	ML 13	357	0.25
	Reef Facies	ED 25	ML 1	520*	0.20
	Basin Facies	YJ 1056	ML 3	1022	0.44
		YJ 1057	"	1027	0.26
		B 37	ML 12	800	0.80

* For ML 1, figure refers to distance from bottom of adit

APPENDIX 3.

PARTIAL MINERALOGICAL ANALYSES.

Values in Weight Per Cent.

Sample	Sinking	Depth (ft in)	Gypsum	Anhydrite	Calcite	Dolomite	Fe_2O_3	SiO_2	Al_2O_3	TiO_2	Na_2O	K_2O
Lower Magnesian Limestone - Shelf Facies.												
YG 4666	ML 2	296	-	-	-	99.82	0.11	0.04	-	-	0.02	0.01
YG 4670	"	304	-	-	-	99.76	0.14	0.09	-	-	0.01	0.02
YG 4675	"	313	-	-	-	99.51	0.32	0.09	0.02	-	0.09	0.02
YG 4678	"	318	-	-	-	99.74	0.27	0.02	-	-	0.04	0.01
YG 4681	"	373	-	-	-	99.74	0.12	0.10	0.03	0.01	0.04	0.02
YG 4683	"	420	-	-	-	99.44	0.19	0.27	0.10	0.01	0.01	0.04
YG 4684	"	429	-	-	-	98.93	0.22	0.58	0.22	0.01	0.04	0.06
YG 4685	"	440	-	-	-	99.09	0.33	0.42	0.12	0.01	0.01	0.05
YG 4686	"	483	-	-	-	96.12	0.58	2.43	0.68	0.03	0.01	0.19
YG 4688	"	492	-	-	-	94.27	0.56	3.60	1.16	0.05	0.10	0.27
YG 4690	"	506	-	-	3.22	88.22	1.93	4.76	1.37	0.06	0.08	0.35
YG 4691	"	510	-	-	-	95.82	0.59	2.56	0.77	0.04	0.08	0.21
UP 30	ML 14	100-110	-	-	-	98.79	0.32	0.08	-	-	0.80	0.02
UP 31	"	110-113	-	-	-	99.43	0.34	0.07	-	-	0.13	0.01
UP 32	"	115	-	-	-	98.92	0.34	0.41	0.07	0.01	0.21	0.03
UP 33	"	120	-	-	0.14	97.49	0.67	1.12	0.35	0.01	0.09	0.09
UP 34	"	124	-	0.34	0.17	96.97	0.60	1.32	0.44	0.01	0.05	0.09
UP 35	"	130	0.05	0.33	0.82	96.14	0.72	1.24	0.50	0.01	0.09	0.09

Lower Magnesian Limestone - Shelf Facies (Continued).

Sample	Sinking	Depth (ft in)	Gypsum	Anhydrite	Calcite	Dolomite	Fe_2O_3	SiO_2	Al_2O_3	TiO_2	Na_2O	K_2O
UP 51A	ML 7	429	-	0.19	0.97	97.09	1.44	0.20	0.02	-	0.07	0.02
UP 53	"	451	-	0.92	0.66	95.31	2.16	0.63	0.15	0.01	0.13	0.05
UP 55	"	472	0.82	1.21	0.87	95.11	1.52	0.30	0.08	0.01	0.04	0.03
K 85	ML 8	67	-	-	7.50	88.88	2.27	0.90	0.21	0.02	0.15	0.05
K 84A	"	75	-	-	0.88	97.69	0.75	0.42	0.14	0.01	0.05	0.03
K 81	"	99	-	-	0.94	97.99	0.85	0.05	0.01	0.01	0.09	0.02
K 80	"	108	-	-	-	99.54	0.34	0.01	-	0.01	0.07	0.01
K 76	"	123	-	-	4.03	95.02	0.52	0.28	0.09	0.01	0.05	0.03
K 75	"	141	-	-	2.87	95.83	0.82	0.31	0.09	0.01	0.01	0.03
UP 155	ML 11	271	-	0.11	3.58	94.98	0.22	0.68	0.25	0.01	0.14	0.05
UP 157	"	281	-	-	-	98.86	0.53	0.48	0.12	-	0.01	0.03
UP 160	"	296	0.35	-	-	96.27	1.27	1.47	0.51	0.02	0.01	0.12
UP 162	"	307	0.65	-	0.13	94.54	1.23	2.32	0.87	0.02	0.09	0.15
UP 163	"	311 5	0.75	-	0.70	94.39	0.92	2.05	0.89	0.02	0.16	0.12
UP 164	"	316 6	-	-	-	99.39	0.47	0.07	-	-	0.11	0.01
UP 167	"	323	-	-	-	99.09	0.76	0.15	0.01	-	0.01	0.02
UP 182	ML 13	402 11	-	0.12	-	97.75	0.81	0.90	0.18	0.01	0.19	0.05
UP 183	"	410 8	-	-	1.20	94.90	1.26	2.09	0.40	0.01	0.12	0.08
UP 185	"	432	-	-	7.52	88.41	0.93	2.46	0.52	0.01	0.08	0.09

Lower Magnesian Limestone - Basin Facies.

Sample	Sinking	Depth (ft in)	Gypsum	Anhydrite	Calcite	Dolomite	Fe_2O_3	SiO_2	Al_2O_3	TiO_2	Na_2O	K_2O
YG 4400	ML 6	733 3	23.87	3.07	1.62	64.53	5.22	0.86	0.52	0.03	0.16	0.13
YG 4407	"	744	2.71	-	-	96.09	0.99	0.05	-	-	0.16	0.02
B 50	ML 12	850	13.22	1.00	-	83.63	0.65	1.29	-	0.01	0.17	0.02
B 51	"	854	11.08	8.81	1.96	75.64	0.68	1.51	0.06	0.01	0.20	0.04
B 52	"	858	3.12	15.08	1.90	76.54	0.83	2.15	0.08	0.01	0.24	0.04
YJ 1072	ML 3	1115	3.10	-	90.58	1.77	0.51	2.76	0.79	0.04	0.20	0.26
YJ 1078	"	1134	0.93	-	90.00	7.33	0.34	0.69	0.20	0.02	0.40	0.09
YJ 1081	"	1141	0.55	-	95.36	2.87	0.30	0.52	0.14	0.02	0.17	0.07
Middle Magnesian Limestone - Lagoon Facies.												
UP 20	ML 15	133-135 4	-	-	-	99.64	0.20	0.03	-	-	0.07	0.02
UP 21	"	135 4-145 4	-	0.24	39.73	59.56	0.19	0.19	0.05	0.01	0.01	0.03
UP 22	"	0.152	-	-	22.43	76.95	0.14	0.08	0.02	0.01	0.27	0.02
UP 23A	"	174 2	-	-	-	99.67	0.17	0.04	0.01	-	0.08	0.02
UP 23B	"	174 4	-	-	-	99.65	0.18	0.05	0.01	-	0.10	0.02
UP 24	"	178	-	-	-	99.60	0.26	0.02	0.01	-	0.12	0.02
UP 25	"	186	-	-	0.03	99.60	0.22	0.02	0.01	-	0.06	0.02
UP 26	"	186-220	-	-	3.08	96.53	0.17	-	-	-	0.19	0.01
UP 40	ML 7	283	-	-	0.12	96.60	0.26	0.02	-	-	0.01	0.01
UP 41	"	304	-	-	-	99.67	0.25	0.03	-	-	0.04	0.01

Sample	Sinking	Depth (ft in)	Gypsum	Anhydrite	Calcite	Dolomite	Fe_2O_3	SiO_2	Al_2O_3	TiO_2	Na_2O	K_2O
UP 42	ML 7	324 6	-	-	-	99.27	0.21	0.04	-	-	0.57	0.01
UP 44	"	361	-	-	-	99.64	0.33	0.07	-	-	0.01	0.01
UP 45	"	370	-	-	-	99.81	0.15	0.02	-	-	0.01	0.01
UP 48	"	396 6	-	-	-	99.39	0.49	0.16	0.01	-	0.02	0.02
UP 49	"	406 6	0.09	1.78	-	95.88	1.71	0.38	0.09	0.01	0.03	0.03
K 94	ML 8	21	-	-	-	99.56	0.30	0.04	0.03	0.01	0.10	0.02
K 93	"	23	-	-	-	99.62	0.23	-	-	-	0.16	0.01
K 91	"	33 6	-	-	4.84	93.96	0.51	0.46	0.17	0.01	0.06	0.04
K 89A	"	37 5	-	-	21.86	76.44	0.67	0.62	0.22	0.01	0.13	0.04
K 87	"	53 6	-	-	3.30	94.52	0.75	1.04	0.34	0.01	0.01	0.06
UP 141	ML 11	239 9	-	-	-	99.38	0.20	0.12	0.03	-	0.27	0.02
UP 147	"	245	-	-	-	99.43	0.27	0.13	0.03	-	0.11	0.02
UP 150	"	249	-	-	-	99.33	0.23	0.15	0.04	-	0.23	0.02
UP 154	"	255	-	-	2.10	96.89	0.43	0.39	0.11	0.01	0.06	0.04
UP 171	ML 13	357	-	-	21.68	76.90	0.28	0.10	0.18	-	0.78	0.01
UP 173	"	367	-	-	-	99.29	0.66	0.09	-	-	0.01	0.01
UP 175	"	375	-	-	-	99.21	0.61	0.06	-	-	0.13	0.01
UP 176	"	376	-	-	-	98.78	0.77	0.12	-	-	0.26	0.01
UP 178	"	385	-	-	-	99.05	0.67	0.21	-	-	0.07	0.01
UP 179	"	388 6	-	-	0.14	98.81	0.59	0.16	-	-	0.23	0.01
UP 180	"	392 6	-	-	1.78	97.24	0.72	0.23	-	-	0.01	0.01

Sample	Sinking	Depth (ft in)	Gypsum	Anhydrite	Calcite	Dolomite	Fe_2O_3	SiO_2	Al_2O_3	TiO_2	Na_2O	K_2O
YG 4604	ML 2	83 6	-	-	35.50	63.84	0.21	0.19	0.01	0.01	0.07	0.02
YG 4625	"	92 6	-	-	-	96.47	0.33	2.36	0.60	0.03	0.02	0.19
YG 4629	"	99 6	-	-	-	96.87	0.26	2.25	0.51	0.02	0.09	0.16
YG 4631	"	108	-	-	-	97.08	0.25	2.15	0.48	0.02	0.07	0.15
YG 4635	"	124	-	-	8.42	91.37	0.09	-	-	-	0.10	0.01
YG 4637	"	149 9	-	-	-	98.65	0.16	1.24	0.09	0.01	-	0.05
YG 4642	"	164	-	-	-	99.78	0.13	-	-	-	0.08	0.01
YG 4646	"	171 3	-	-	-	99.80	0.12	0.02	-	-	0.04	0.01
YG 4650	"	206	-	-	2.97	96.78	0.15	0.09	-	-	-	0.02
YG 4652	"	251	-	-	-	99.83	0.07	0.09	-	-	-	0.01
<u>Middle Magnesian Limestone - Reef Facies</u>.												
YGF 1036	ML 5	100 3	-	-	6.53	92.59	0.34	0.30	0.04	-	0.17	0.03
YGF 1037	"	109 6	-	-	23.97	74.41	0.33	0.83	0.18	0.01	0.17	0.05
YGF 1038	"	144	-	0.76	13.70	82.33	0.35	1.92	0.59	0.02	0.13	0.20
YGF 1039	"	168	-	-	2.41	94.94	0.29	1.49	0.47	0.02	0.19	0.14
YGF 1041	"	174	-	-	0.31	98.43	0.22	0.71	0.19	0.01	0.07	0.08
YGF 1045	"	177	-	-	1.88	95.37	0.33	1.63	0.50	0.02	0.09	0.16
YGF 1049	"	184	-	-	3.23	92.68	0.32	2.52	0.87	0.04	0.05	0.29
YGF 1048	"	188	-	-	1.83	95.14	0.40	1.66	0.52	0.02	0.21	0.18
YGF 1050	"	190	-	-	5.05	93.94	0.13	0.58	0.16	0.01	0.03	0.07

Sample	Sinking	Depth (ft in)	Gypsum	Anhydrite	Calcite	Dolomite	Fe_2O_3	SiO_2	Al_2O_3	TiO_2	Na_2O	K_2O
YGF 1058	ML 5	c. 200	-	-	-	98.01	0.18	1.20	0.38	0.01	0.17	0.13
YGF 1067	"	c. 205	-	-	-	99.40	0.13	0.05	-	-	0.40	0.02
ED 1	ML 1	* 40	-	-	-	99.63	0.19	0.07	-	-	0.10	0.01
ED 3	"	80	-	-	-	99.59	0.16	0.08	-	-	0.15	0.02
ED 5	"	120	-	-	-	99.74	0.17	0.04	-	-	0.04	0.01
ED 7	"	160	-	-	-	99.91	0.07	-	-	-	0.30	0.01
ED 9	"	200	-	-	-	99.75	0.09	-	-	-	0.13	0.01
ED 10	"	220	-	-	0.16	98.29	0.15	0.99	0.32	0.02	0.01	0.08
ED 11	"	240	-	-	-	99.37	0.12	0.49	0.08	0.01	0.09	0.03
ED 13	"	280	-	-	8.77	90.75	0.10	0.34	0.05	0.01	0.11	0.03
ED 15	"	320	-	-	-	99.80	0.12	-	-	-	0.06	0.01
ED 17	"	360	-	0.19	55.58	43.61	0.13	0.24	0.05	0.01	0.17	0.02
ED 19	"	400	-	-	0.76	98.99	0.13	-	-	-	0.05	0.01
ED 21	"	440	-	-	-	99.81	0.14	-	-	-	-	0.01
ED 23	"	480	-	-	3.18	96.66	0.08	-	-	-	0.05	0.01
ED 25	"	520	-	-	-	99.76	0.12	-	-	-	0.11	0.01
ED 27	"	560	-	-	4.52	95.36	0.11	-	-	-	-	0.01
ED 29	"	600	-	-	-	99.82	0.04	-	-	-	0.13	0.01

Sample	Sinking	Depth (ft in)	Gypsum	Anhydrite	Calcite	Dolomite	Fe_2O_3	SiO_2	Al_2O_3	TiO_2	Na_2O	K_2O
ED 31	ML 1	640	0.33	-	-	99.44	0.05	-	-	-	0.18	0.01
ED 33	"	680	0.82	-	92.97	4.20	0.23	1.58	0.14	0.02	-	0.04
ED 34	"	706	-	-	6.69	92.23	0.23	0.51	0.12	0.01	0.12	0.03
ED 35	"	720	0.66	-	86.29	9.44	0.31	2.92	0.27	0.02	0.06	0.04
YG 4552	ML 2	56 6	-	-	-	98.01	0.17	1.53	0.20	0.01	0.14	0.09
YG 4562	"	63 6	-	-	-	95.48	0.23	3.24	0.73	0.03	0.05	0.24
YG 4581	"	73 9	-	-	29.54	69.63	0.19	0.12	-	0.01	0.12	0.02
Middle Magnesian Limestone - Basin Facies.						* For ML 1, figures refer to distance from bottom of adit						
YG 4276	ML 6	597 8	0.26	0.36	-	97.67	1.40	0.18	0.06	-	0.05	0.02
YG 4279	"	602	4.08	-	94.39	-	0.35	0.60	0.29	0.02	0.32	0.05
YG 4282	"	616	1.59	0.25	93.84	2.97	0.47	0.50	0.30	0.02	0.02	0.05
YG 4284	"	626 3	3.92	-	79.11	14.50	1.42	0.68	0.30	0.02	-	0.06
YG 4287	"	636	1.00	-	88.18	5.66	0.55	3.25	0.80	0.04	0.36	0.16
YG 4297	"	647 3	0.46	-	96.26	1.50	0.20	1.24	0.21	0.01	0.08	0.03
YG 4317	"	656	1.97	-	80.57	8.35	1.16	5.15	2.12	0.06	0.32	0.31
YG 4366	"	662	2.60	0.44	67.59	24.73	3.09	0.92	0.27	0.02	0.27	0.06
YG 4387	"	667 6	1.63	-	95.23	1.55	0.23	0.77	0.25	0.02	0.27	0.05
YG 4388	"	689	2.49	-	93.83	2.24	0.30	0.51	0.21	0.02	0.36	0.04
YG 4391	"	701	4.09	-	92.01	3.01	0.31	0.26	0.17	0.01	0.09	0.04

Sample	Sinking	Depth (ft in)	Gypsum	Anhydrite	Calcite	Dolomite	Fe_2O_3	SiO_2	Al_2O_3	TiO_2	Na_2O	K_2O
YG 4393	ML 6	707 6	0.28	-	67.77	29.37	2.39	0.08	0.09	0.01	-	0.02
YG 4395	"	717 6	0.05	-	56.11	40.82	2.72	0.09	0.09	0.01	0.13	0.03
YG 4397	"	725	-	-	-	99.61	0.26	-	0.01	-	0.11	0.01
YJ 1053B	ML 3	1020	2.54	-	-	80.99	1.08	11.17	2.94	0.13	0.30	0.85
YJ 1056	"	1022	5.36	0.40	-	91.10	0.77	1.73	0.35	0.02	0.15	0.13
YJ 1057	"	1027	2.64	0.21	2.76	86.94	0.74	4.68	1.24	0.04	0.43	0.31
YJ 1060	"	1034	3.09	-	86.72	5.35	0.57	2.84	0.75	0.04	0.38	0.27
YJ 1061	"	1061	0.62	-	96.80	1.60	0.22	0.33	0.08	0.02	0.27	0.07
YJ 1066	"	1072	0.36	-	96.39	2.05	0.29	0.33	0.08	0.02	0.42	0.07
YJ 1071	"	1074	0.35	-	95.65	2.84	0.23	0.39	0.10	0.02	0.34	0.08
B 5	ML 12	660	5.99	43.26	-	49.50	0.10	0.66	0.09	0.01	0.38	0.02
B 7	"	666	47.80	18.18	-	31.85	0.13	1.78	0.20	0.01	-	0.05
B 9	"	671	7.77	30.19	-	54.05	0.13	7.52	0.05	0.01	0.23	0.03
B 14	"	689	24.94	-	4.26	61.18	0.65	7.78	0.63	0.03	0.36	0.16
B 16	"	700	44.37	-	5.04	50.07	0.41	0.08	-	-	0.09	0.02
B 18	"	710	23.24	-	0.17	75.73	0.39	0.26	-	-	0.11	0.02
B 20	"	720	44.82	-	4.33	50.13	0.26	0.42	0.01	0.01	-	0.03
B 23	"	730	26.61	-	-	72.51	0.49	0.20	-	-	0.18	0.02
B 25	"	740	31.05	-	1.57	66.98	0.32	-	-	-	0.11	0.01

Sample	Sinking	Depth (ft in)	Gypsum	Anhydrite	Calcite	Dolomite	Fe_2O_3	SiO_2	Al_2O_3	TiO_2	Na_2O	K_2O
B 27	ML 12	750	43.14	-	4.42	51.94	0.39	0.13	-	-	-	0.02
B 29	"	760	16.66	-	-	82.42	0.47	0.12	-	-	0.33	0.02
B 31	"	770	20.07	0.10	-	78.96	0.45	0.23	0.01	0.01	0.15	0.03
B 33	"	780	39.25	0.68	6.60	50.02	0.45	2.10	0.49	0.03	0.21	0.16
B 37	"	800	23.80	0.69	2.44	72.32	0.70	-	-	-	0.08	0.01
B 39	"	810	10.95	0.03	-	88.45	0.47	-	-	-	0.16	0.01
B 41	"	819	16.01	0.88	1.22	79.75	0.85	0.97	-	0.01	0.29	0.02
B 44	"	830	11.03	-	-	87.44	0.74	0.62	-	-	0.19	0.02
B 46	"	835	12.62	1.26	-	84.56	0.56	0.72	-	-	0.27	0.02
B 47	"	838	16.93	-	0.11	81.66	0.54	0.48	-	-	0.30	0.02
B 48	"	842	28.48	1.83	3.75	64.79	0.54	0.35	-	-	0.29	0.02
B 49	"	847	16.97	4.86	0.90	75.73	0.57	0.86	-	-	0.09	0.02

APPENDIX 4.

POROSITY AND PERMEABILITY RESULTS.

		Sample	Sinking	Depth (ft in)	Porosity (%)	Permeability (cm/sec)
Lower Magnesian Limestone	Shelf Facies	UP 30	ML 14	100-110	24.5	5.0×10^{-6}
		UP 31	"	110-113	22.5	3.5×10^{-6}
		UP 34	"	124	23.2	2.7×10^{-6}
		K 81	ML 8	99	7.0	1.4×10^{-8}
		K 84A	"	75	5.0	1.0×10^{-9}
		K 85	"	67	15.4	2.1×10^{-7}
		UP 155	ML 11	271	17.2	3.7×10^{-7}
		UP 157	"	281	16.9	1.5×10^{-7}
		UP 160	"	296	15.8	4.6×10^{-8}
		UP 162	"	307	17.3	1.9×10^{-7}
		UP 164	"	316 6	27.0	2.6×10^{-6}
		UP 167	"	323	22.9	1.1×10^{-6}
		UP 182	ML 13	402 11	30.1	1.5×10^{-5}

		Sample	Sinking	Depth (ft in)	Porosity (%)	Permeability (cm/sec)
Middle Magnesian Limestone	Lagoon Facies	UP 23A	ML 15	174 2	29.8	5.7×10^{-6}
		UP 23B	"	174 4	29.9	4.3×10^{-6}
		UP 25	"	186	34.9	1.0×10^{-5}
		UP 41	ML 7	304	19.5	6.1×10^{-7}
		UP 44	"	361	19.9	1.1×10^{-6}
		UP 48	"	396 6	9.9	1.8×10^{-7}
		K 87	ML 8	53 6	11.7	3.3×10^{-8}
		K 91	"	33 6	15.1	2.8×10^{-7}
		UP 141	ML 11	239 9	31.1	3.6×10^{-6}
		UP 147	"	245	32.0	7.0×10^{-6}
		UP 171	ML 13	357	14.6	2.0×10^{-5}
	Basin Facies	YJ 1056	ML 3	1022	6.4	3.3×10^{-6}
		YJ 1057	"	1027	9.3	6.3×10^{-7}

APPENDIX 5.

MINOR AND TRACE ELEMENT ANALYSES.

Values in ppm.

ND = not detected.

Sample	Sinking	Depth (ft in)	Ba	Sr	Rb	Pb	Zn	Cu	Ni	Mn
Lower Magnesian Limestone - Shelf Facies.										
YG 4664	ML 2	280	ND	89	ND	19	43	34	ND	106
YG 4666	"	296	22	143	ND	ND	67	24	4	178
YG 4670	"	304	ND	101	ND	34	52	31	7	199
YG 4675	"	313	ND	96	ND	30	135	20	8	286
YG 4678	"	318	23	77	ND	26	89	33	6	519
YG 4681	"	373	ND	156	ND	27	55	30	4	209
YG 4683	"	420	42	148	ND	36	14	29	4	346
YG 4684	"	429	63	140	3	33	12	21	ND	375
YG 4685	"	440	33	93	ND	23	8	36	ND	509
YG 4686	"	483	128	106	11	30	28	26	8	718
YG 4688	"	492	319	131	11	42	21	24	15	923
YG 4690	"	506	375	156	17	65	13	31	14	1383
YG 4691	"	510	144	119	7	28	25	35	8	743
UP 51A	ML 7	429	32	146	4	11	5	26	5	1803
UP 52	"	439	39	113	5	25	5	12	3	3154
UP 53	"	451	22	84	6	30	ND	20	7	2525

Sample	Sinking	Depth (ft in)	Ba	Sr	Rb	Pb	Zn	Cu	Ni	Mn
UP 54	ML 7	461	26	83	3	20	ND	17	ND	1914
UP 55	"	472	15	122	ND	11	ND	21	6	1652
UP 56	"	484	33	118	ND	23	ND	21	4	1284
UP 57	"	492	29	107	3	28	5	26	6	1383
K 85	ML 8	67	312	105	3	33	ND	17	9	2861
K 84A	"	75	86	132	4	37	ND	29	5	1172
K 83	"	89	178	166	ND	30	6	20	18	878
K 81	"	99	141	143	ND	25	ND	24	4	1464
K 80	"	108	144	169	ND	20	5	28	10	642
K 77	"	115	164	145	ND	23	ND	25	4	808
K 76	"	123	69	137	ND	30	ND	26	6	931
K 74	"	135	475	116	4	44	9	13	18	1838
K 75	"	141	105	135	ND	23	ND	23	6	1434
UP 30	ML 14	100-110	16	157	ND	29	261	27	ND	398
UP 31	"	110-113	16	156	ND	45	192	28	ND	354
UP 32	"	115	8	197	ND	50	481	25	3	462
UP 33	"	120	15	127	5	18	566	29	3	855
UP 34	"	124	35	164	ND	21	169	29	6	701
UP 35	"	130	14	144	5	26	95	24	8	782
F 1143	ML 9	216	41	158	ND	23	5	20	ND	527

Sample	Sinking	Depth (ft in)	Ba	Sr	Rb	Pb	Zn	Cu	Ni	Mn
F 1384	ML 9	255	21	157	3	29	ND	23	5	1454
UP 155	ML 11	271	157	146	3	27	19	23	7	369
UP 156	"	277	48	122	ND	67	5	26	3	361
UP 157	"	281	38	116	4	45	29	30	6	699
UP 158A	"	286 6	27	193	4	24	12	26	8	429
UP 159	"	291 6	131	137	3	27	9	30	11	890
UP 160	"	296	27	143	7	24	5	32	13	1128
UP 161	"	301	34	123	9	23	6	29	5	1355
UP 162	"	307	35	159	7	33	9	34	14	1079
UP 163	"	311 5	29	169	7	29	ND	25	16	857
UP 164	"	316 6	24	150	ND	18	51	30	5	407
UP 165	"	319	19	114	ND	14	ND	ND	ND	655
UP 166	"	320 11	25	121	ND	13	ND	20	ND	625
UP 167	"	323	20	125	ND	26	7	28	ND	706
UP 168A	"	327	628	176	3	42	17	26	ND	510
UP 182	ML 13	402 11	23	98	ND	21	228	23	7	641
UP 183	"	410 8	30	111	3	36	179	20	9	707
UP 184	"	416 9	30	124	4	33	156	30	8	586
UP 185	"	432	36	142	3	24	14	22	8	722
<u>Lower Magnesian Limestone - Basin Facies</u>.										
YG 4400	ML 6	733 3	50	1375	ND	47	ND	27	28	220

Sample	Sinking	Depth (ft in)	Ba	Sr	Rb	Pb	Zn	Cu	Ni	Mn
YG 4401	ML 6	739	15	332	ND	ND	ND	ND	3	1621
YG 4407	"	744	ND	273	ND	24	ND	ND	4	1239
YG 4409	"	746 3	ND	1845	ND	ND	ND	28	5	597
YJ 1072	ML 3	1115	28	1125	8	26	5	ND	11	161
YJ 1078	"	1134	16	874	ND	ND	5	ND	9	244
YJ 1081	"	1141	ND	1079	ND	ND	ND	ND	5	386
B 50	ML 12	850	ND	531	ND	17	ND	43	ND	905
B 51	"	854	ND	453	ND	11	ND	19	ND	348
B 52	"	858	13	768	ND	19	ND	42	ND	427
Middle Magnesian Limestone - Lagoon Facies.										
YG 4598	ML 2	82	13	143	ND	74	150	16	ND	240
YG 4601	"	83	ND	146	ND	102	158	31	ND	247
YG 4604	"	83 6	ND	136	ND	134	165	9	ND	267
YG 4605	"	86 6	ND	140	ND	55	125	31	ND	212
YG 4608	"	87	33	129	ND	41	96	26	ND	197
YG 4616	"	88	48	134	ND	39	108	32	ND	222
YG 4622	"	90	70	135	ND	41	110	33	ND	197
YG 4624	ML 2	91	11	150	ND	39	94	27	ND	176
YG 4625	"	92 6	20	112	3	68	173	26	19	265
YG 4626	"	94	ND	121	15	60	204	42	54	262
YG 4627	"	96	ND	119	7	92	137	53	29	251
YG 4628	"	98 6	15	110	4	67	137	30	ND	250

Sample	Sinking	Depth (ft in)	Ba	Sr	Rb	Pb	Zn	Cu	Ni	Mn
YG 4629	ML 2	99 6	ND	114	3	71	150	30	3	254
YG 4630	"	104	ND	117	ND	59	134	36	ND	251
YG 4631	"	108	ND	118	3	57	132	59	18	200
YG 4633	"	116	ND	159	6	33	196	44	28	221
YG 4635	"	124	7	106	ND	16	161	22	ND	135
YG 4637	"	149 9	22	108	ND	72	145	17	ND	367
YG 4638	"	160	ND	113	ND	18	67	48	ND	149
YG 4642	"	164	ND	88	ND	ND	95	29	ND	149
YG 4646	"	171 3	ND	92	ND	ND	110	ND	13	196
YG 4648	"	204	59	89	ND	15	46	15	3	128
YG 4650	"	206	ND	134	ND	16	111	12	5	216
YG 4652	"	251	ND	100	ND	33	18	21	ND	105
YG 4658	"	263	ND	196	3	ND	52	34	10	169
UP 40	ML 7	283	25	86	ND	11	5	23	ND	251
UP 41	"	304	32	88	ND	200	ND	26	ND	410
UP 42	"	324 6	29	93	ND	17	20	20	3	191
UP 43	"	348	42	84	ND	18	9	22	ND	579
UP 44	"	361	43	116	ND	22	6	28	11	580
UP 45	"	370	22	104	ND	18	9	34	ND	390
UP 46	"	378	50	114	ND	18	6	25	ND	557

Sample	Sinking	Depth (ft in)	Ba	Sr	Rb	Pb	Zn	Cu	Ni	Mn
UP 47	ML 7	388	45	88	ND	23	ND	22	3	574
UP 48	"	396 6	27	163	ND	21	ND	20	3	671
UP 49	"	406 6	41	86	ND	23	ND	29	ND	1786
UP 50	"	418	55	105	ND	24	ND	26	7	887
K 94	ML 8	21	68	128	ND	18	11	28	ND	607
K 93	"	23	36	117	ND	14	14	31	3	561
K 92	"	28	43	138	3	16	ND	30	3	553
K 91	"	33 6	99	96	4	20	ND	24	ND	702
K 89A	"	37 5	167	126	3	33	5	16	ND	849
K 90	"	39	62	87	ND	207	9	25	ND	1135
K 88	"	44	163	82	ND	15	5	24	5	903
K 87	"	53 6	107	119	ND	43	6	31	6	961
K 86	"	58	198	88	ND	33	5	23	ND	1450
UP 20	ML 15	133-135 4	52	92	ND	18	113	25	ND	322
UP 21	"	135 4-145 4	66	148	5	46	124	17	3	215
UP 22	"	c. 152	55	132	ND	38	107	15	ND	138
UP 23A	"	174 2	61	94	ND	22	105	37	ND	345
UP 23B	"	174 4	51	100	ND	39	110	26	ND	378
UP 24	"	178	43	79	ND	40	115	26	ND	415
UP 25	"	186	39	90	ND	23	118	21	ND	352
UP 26	"	186-220	11	129	ND	42	80	26	ND	238

Sample	Sinking	Depth (ft in)	Ba	Sr	Rb	Pb	Zn	Cu	Ni	Mn
UP 140	ML 11	238 9	26	131	ND	20	51	26	3	208
UP 141	"	239 9	93	121	ND	13	66	17	3	221
UP 142	"	241	63	128	3	22	59	16	ND	213
UP 144	"	243 3	92	124	ND	29	51	22	ND	230
UP 147	"	245	69	126	ND	27	88	22	ND	253
UP 149	"	247 3	47	125	ND	37	43	21	4	241
UP 150	"	249	78	115	ND	61	32	31	3	222
UP 154	"	255	80	128	ND	36	124	28	3	282
UP 170	ML 13	352 8	70	161	78	12	31	34	20	901
UP 171	"	357	40	143	4	14	29	17	ND	423
UP 172	"	362	29	130	ND	19	33	23	3	378
UP 173	"	367	22	106	ND	ND	7	25	4	458
UP 174	"	372 1	23	114	ND	17	5	24	ND	399
UP 175	"	375	22	127	3	23	ND	10	ND	501
UP 176	"	376	33	115	ND	ND	5	14	3	641
UP 177	"	382	21	124	ND	19	12	11	ND	668
UP 178	"	385	30	112	ND	26	13	12	ND	604
UP 179	"	388 6	28	117	ND	20	22	23	4	511
UP 180	"	392 6	30	120	ND	37	106	28	3	613
UP 181	"	396	29	113	ND	27	211	29	4	693
UP 60	ML 10	95 6	ND	104	ND	16	62	23	3	156

Sample	Sinking	Depth (ft in)	Ba	Sr	Rb	Pb	Zn	Cu	Ni	Mn
UP 61	ML 10	100	28	115	ND	16	51	27	ND	203
UP 62	"	105	33	101	ND	13	74	15	4	249
UP 63	"	110	14	128	ND	ND	32	30	ND	269
UP 64	"	115	25	115	ND	18	21	34	4	278
UP 65	"	120	9	111	3	22	71	36	ND	215
UP 66	"	122	31	109	ND	19	48	30	ND	222
UP 67	"	138 6	35	118	ND	16	25	26	ND	305
UP 68	"	141	13	117	ND	27	17	24	ND	275
UP 69	"	146	38	90	ND	26	38	18	4	207
UP 70	"	151	34	103	ND	41	67	27	ND	288
UP 71	"	157	28	108	ND	10	31	27	ND	309
F 1155	ML 9	99	37	91	ND	14	6	14	ND	537
F 1157	"	117	27	87	ND	14	ND	17	ND	544
F 1141	"	120	24	152	ND	22	7	ND	ND	563
F 1159	"	129	40	145	ND	15	ND	24	ND	560
F 1126	"	134 6	31	134	ND	26	7	30	4	426
F 1160	"	140	38	119	ND	32	ND	23	ND	610
F 1154	"	147	41	115	ND	36	ND	20	4	536
F 1151	"	152	29	131	ND	16	6	23	4	697
<u>Middle Magnesian Limestone - Reef Facies.</u> * For ML 1, figures refer to distance from bottom of adit.										
ED 1	ML 1	*40	53	102	ND	28	128	14	6	257

Sample	Sinking	Depth (ft in)	Ba	Sr	Rb	Pb	Zn	Cu	Ni	Mn
ED 2	ML 1	60	68	84	ND	34	143	25	6	245
ED 3	"	80	112	92	ND	28	106	23	6	273
ED 4	"	100	13	98	ND	29	64	13	6	223
ED 5	"	120	86	105	ND	17	102	12	7	177
ED 6	"	140	ND	133	ND	22	44	22	ND	150
ED 7	"	160	13	117	ND	13	44	22	4	154
ED 8	"	180	26	140	ND	16	37	11	3	170
ED 9	"	200	18	154	ND	29	45	28	4	178
ED 10	"	220	ND	117	ND	40	112	36	7	277
ED 11	"	240	ND	115	ND	16	65	14	8	199
ED 12	"	260	59	105	ND	26	65	19	4	159
ED 13	"	280	64	105	ND	27	112	21	3	214
ED 14	"	300	40	94	ND	27	127	17	ND	215
ED 15	"	320	20	92	ND	18	61	31	4	243
ED 16	"	340	86	116	ND	25	107	12	ND	194
ED 17	"	360	88	168	ND	13	29	ND	ND	320
ED 18	"	380	ND	91	ND	15	85	33	5	265
ED 19	"	400	ND	124	ND	ND	70	18	ND	275
ED 20	"	420	42	93	ND	18	34	30	ND	282
ED 21	"	440	ND	158	ND	14	78	ND	3	470
ED 22	"	460	ND	259	ND	ND	36	20	3	178

Sample	Sinking	Depth (ft in)	Ba	Sr	Rb	Pb	Zn	Cu	Ni	Mn
ED 23	ML 1	480	ND	89	ND	12	90	21	ND	215
ED 24	"	500	11	200	ND	ND	111	18	3	235
ED 25	"	520	ND	124	ND	26	115	26	7	261
ED 26	"	540	15	95	ND	12	35	11	5	261
ED 27	"	560	ND	139	ND	ND	16	8	ND	357
ED 28	"	580	13	106	ND	ND	11	11	ND	189
ED 29	"	600	22	101	ND	23	11	16	4	171
ED 30	"	620	88	111	ND	ND	12	20	ND	183
ED 31	"	640	59	109	ND	17	22	24	6	209
ED 32	"	660	11	109	ND	18	40	17	ND	205
ED 33	"	680	ND	183	ND	19	84	ND	3	344
ED 34	"	706	121	96	ND	46	193	34	8	346
ED 35	"	720	ND	150	ND	86	72	ND	ND	344
YGF 1036	ML 5	100 3	18	121	4	19	99	25	3	807
YGF 1037	"	109 6	18	121	ND	13	84	ND	ND	663
YGF 1038	"	144	33	213	3	97	133	26	ND	588
YGF 1039	"	168	12	191	6	51	112	28	4	317
YGF 1041	"	174	16	140	4	32	92	27	4	305
YGF 1045	"	177	25	157	7	55	124	31	4	364
YGF 1049	"	184	33	148	13	105	135	33	3	312
YGF 1048	"	188	22	138	6	53	132	33	7	442
YGF 1050	"	190	14	176	4	32	83	21	ND	270

Sample	Sinking	Depth (ft in)	Ba	Sr	Rb	Pb	Zn	Cu	Ni	Mn
YGF 1058	ML 5	c. 200	13	111	4	25	66	16	15	388
YGF 1067	"	c. 205	16	136	ND	27	52	14	5	223
YG 4548	ML 2	53	ND	130	ND	38	80	28	ND	236
YG 4552	"	56 6	ND	133	4	20	153	32	ND	229
YG 4556	"	58	33	84	ND	43	349	11	6	227
YG 4559	"	61 3	29	89	ND	99	215	14	ND	254
YG 4562	"	63 6	59	102	ND	39	193	23	7	214
YG 4566	"	69 9	53	95	ND	13	100	29	ND	233
YG 4567	"	70 6	ND	109	ND	13	92	30	ND	345
YG 4569	"	71 6	18	122	ND	32	126	24	ND	246
YG 4575	"	72 6	24	115	ND	22	123	9	ND	226
YG 4581	"	73 9	ND	116	ND	20	190	ND	ND	246
YG 4586	"	75	ND	114	ND	ND	106	35	ND	269
YG 4590	"	76	ND	122	ND	29	69	34	ND	161
YG 4591	"	77	9	150	ND	46	134	26	ND	207
YG 4592	"	78	ND	139	ND	27	103	28	ND	236
YG 4594	"	79	31	145	ND	41	162	12	ND	196
Bu 4815	ML 4	90	10	83	4	95	136	26	ND	397
Bu 4817	"	100	25	84	7	100	353	67	7	320
Bu 4819	"	129	19	103	ND	65	315	31	5	222
Bu 4822	"	160	15	181	6	97	227	30	16	417

Sample	Sinking	Depth (ft in)	Ba	Sr	Rb	Pb	Zn	Cu	Ni	Mn
F 766	ML 4	176	28	111	5	30	74	28	6	203
F 767	"	180	19	113	ND	29	54	27	3	199
F 769	"	190	14	91	ND	33	93	26	5	287
F 771	"	228	15	101	ND	25	45	25	ND	197
F 770	"	230	13	94	ND	18	21	15	4	218
Middle Magnesian Limestone - Basin Facies.										
YG 4276	ML 6	597 8	36	174	ND	ND	ND	29	3	1590
YG 4279	"	602	18	657	ND	ND	ND	ND	3	803
YG 4280	"	613	ND	567	ND	ND	24	10	ND	681
YG 4282	"	616	15	485	ND	17	5	ND	ND	585
YG 4284	"	626 3	ND	480	4	ND	ND	ND	7	1083
YG 4287	"	636	ND	469	4	27	ND	ND	16	508
YG 4294	"	638	ND	844	ND	14	ND	12	ND	523
YG 4295	"	641 2	ND	1165	ND	14	ND	ND	ND	395
YG 4297	"	647 3	ND	1294	ND	ND	ND	ND	3	396
YG 4303	"	648 9	ND	1048	ND	ND	ND	ND	6	297
YG 4305	"	651	ND	455	ND	ND	24	ND	9	867
YG 4317	"	656	52	304	6	60	25	19	17	1005
YG 4333	"	658 1	ND	340	ND	38	ND	ND	10	1005
YG 4351	"	659	ND	224	ND	ND	20	ND	4	1516
YG 4366	"	662	ND	280	ND	19	10	ND	10	2042

Sample	Sinking	Depth (ft in)	Ba	Sr	Rb	Pb	Zn	Cu	Ni	Mn
YG 4380	ML 6	664 3	92	218	41	125	9	15	49	1917
YG 4387	"	667 6	ND	1189	ND	ND	6	ND	9	358
YG 4388	"	689	ND	1037	ND	ND	ND	ND	97	555
YG 4389	"	693 6	ND	1391	4	ND	ND	ND	5	515
YG 4391	"	701	ND	414	3	ND	ND	ND	ND	407
YG 4392	"	703	13	444	ND	ND	ND	ND	4	720
YG 4393	"	707 6	13	289	ND	17	ND	ND	6	1742
YG 4394	"	710	ND	161	ND	12	ND	ND	5	1730
YG 4395	"	717 6	ND	324	ND	ND	ND	ND	ND	2116
YG 4397	"	725	ND	190	ND	ND	ND	16	ND	942
YJ 1053B	ML 3	1020	79	167	47	110	12	35	38	1033
YJ 1056	"	1022	27	315	3	42	ND	28	11	699
YJ 1057	"	1027	43	209	8	37	5	26	13	649
YJ 1060	"	1034	22	419	8	39	6	ND	14	387
YJ 1061	"	1061	27	1485	3	15	ND	ND	ND	295
YJ 1066	"	1072	23	539	ND	13	7	ND	ND	536
YJ 1071	"	1074	13	540	5	16	ND	ND	ND	368
B 5	ML 12	660	26	3361	ND	14	ND	40	ND	95
B 7	"	666	ND	4749	ND	ND	ND	36	ND	109
B 9	"	671	53	2762	ND	62	13	89	3	174
B 14	"	689	55	1436	4	57	ND	38	ND	442
B 16	"	700	ND	945	ND	ND	ND	18	4	282

Sample	Sinking	Depth (ft in)	Ba	Sr	Rb	Pb	Zn	Cu	Ni	Mn
B 18	ML 12	710	ND	913	ND	ND	ND	33	ND	321
B 20	"	720	ND	639	ND	16	ND	24	3	213
B 23	"	730	ND	754	ND	ND	ND	24	ND	392
B 25	"	740	ND	892	ND	ND	ND	23	ND	306
B 27	"	750	26	1051	ND	ND	ND	22	ND	295
B 29	"	760	26	393	ND	15	ND	29	ND	497
B 31	"	770	21	478	ND	ND	ND	24	ND	442
B 33	"	780	ND	567	7	27	ND	34	ND	298
B 37	"	800	24	1226	ND	17	5	27	10	620
B 39	"	810	13	270	ND	12	ND	21	ND	863
B 41	"	819	15	316	ND	ND	6	24	ND	361
B 44	"	830	ND	268	ND	15	ND	24	3	410
B 46	"	835	ND	407	ND	ND	ND	26	ND	811
B 47	"	838	ND	392	ND	10	ND	16	ND	819
B 48	"	842	31	396	ND	21	ND	19	ND	231
B 49	"	847	29	489	ND	20	6	25	5	272

APPENDIX 6.

BORON ANALYSES.

		Sample	Sinking	Depth (ft in)	Boron Content+ (ppm.)
Lower Magnesian Limestone	Shelf Facies	UP 51A	ML 7	429	95
		UP 53	"	451	93
		UP 55	"	472	71
	Basin Facies	YJ 1072	ML 3	1115	89
		YJ 1078	"	1134	47
		YJ 1081	"	1141	55
Middle Magnesian Limestone	Lagoon Facies	UP 41	ML 7	304	31
		UP 42	"	324 6	51
		UP 44	"	361	83
		UP 45	"	370	61
		UP 48	"	396 6	110
		UP 49	"	406 6	67
	Reef Facies	ED 1	ML 1	*40	82
		ED 5	"	120	13
		ED 10	"	220	96
		ED 13	"	280	72
		ED 17	"	360	49
		ED 21	"	440	75
		ED 25	"	520	27
		ED 29	"	600	43
		ED 34	"	706	81
	Basin Facies	YJ 1053 B	ML 3	1020	239
		YJ 1056	"	1022	49
		YJ 1057	"	1027	160
		YJ 1060	"	1034	75
		YJ 1061	"	1061	47
		YJ 1071	"	1074	61

* For ML 1, figures refer to distance from bottom of adit.

\+ The limit of detection for boron is 5 ppm.